

T ✓ INVESTIGATION OF 2:1 LAYER SILICATE CLAYS

IN SELECTED SOUTHERN AFRICAN SOILS /

SR by

A
CHRISTL BÜHMANN .

Diplom Vorprüfung, Geology (University of Munich)

Diplom Hauptprüfung, Mineralogy (University of Göttingen)

NT Thesis (Ph.D.; Soil Science and Agrometeorology) - University of Natal
Pietermaritzburg, 1986.

Submitted in partial fulfilment

of the requirements for

the degree of

DOCTOR OF PHILOSOPHY

in

Department of Soil Science and Agrometeorology

University of Natal, P

PIETERMARITZBURG; PP

NATAL

FEBRUARY 1986
D

DECLARATION

I declare that the results contained in
this thesis are from my own original work
except where acknowledged.

C BÜHMANN

FEBRUARY 1986

Acknowledgements

I wish to express my sincere gratitude to :

Dr M V Fey, Senior lecturer in the Department of Soil Science and Agrometeorology and Supervisor of this thesis for his continued keen interest during this investigation, for his encouragement and guidance and countless interesting discussions. His enthusiasm in the art of scientific investigation will always be remembered. Professor J M de Villiers, Head of the Department of Soil Science and Agrometeorology, Dean of the Faculty and Co-supervisor, for his encouragement and advice, especially in preparing the final draft. It was a privilege to work with him and gain access to his wide knowledge of clays in soils.

Staff members of the Department of Soil Science and Agrometeorology especially Dr A Cass, Dr J C Hughes for their advice and Mr I Hunsraj and Mary Clark for assistance with the IR investigations. Mr P Evers and Mr A Bruton of the Electron Microscopy units in Durban and Pietermaritzburg for assistance with SEM and TEM and chemical analyses.

Mr B Martin, Department of Geography, for his help in the preparation of maps and figures.

Mrs P Collingwood for typing this thesis. Her patience and friendliness are appreciated.

The research was supported in part by a CSIR postgraduate research bursary and by the University of Natal Research Fund.

Financial support to complete and type this thesis was generously provided by the Internat. Potash Institute. Mr A. Cohen's help in arranging the support and his interest in the subject of K-fixation will always be remembered.

Permission to collect samples at Melody Ranch and at the Tutuka power station was kindly granted by Masonite SA (Pty) Ltd and the Electricity Supply Commission, respectively.

The author is greatly indebted to Dr A.A.B. Williams, CSIR, Pretoria, for kindly providing samples and scientific literature for Chapter 6, and to Dr R.A. Wood of the S.A. Sugar Association Research Station Mt. Edgecombe, and to Dr G.C.H. Venter, Director of the Fertilizer Society of S.A., for providing the samples for Chapter 5.

		iv
	CONTENTS	
Chapter		page
	DECLARATION	i
	ACKNOWLEDGEMENTS	ii
	LIST OF APPENDICES	ix
	LIST OF FIGURES	x
	LIST OF TABLES	xxiii
	ABSTRACT	xxv
	INTRODUCTION	1
1	AN ASSESSMENT OF CERTAIN DIFFICULTIES IN THE X-RAY IDENTIFICATION OF 2:1 LAYER SILICATES	6
	1.1 Introduction	6
	1.2 Factors influencing X-ray diffraction line broadening	7
	1.2.1 Crystallite size	8
	1.2.2 Defect broadening	9
	1.2.2.1 Crystal defects	9
	1.2.2.2 Substitutions	9
	1.2.2.3 Stacking disorder	9
	1.2.2.4 Site occupancy disorder	11
	1.2.3 Instrumental factors and specimen preparation	12
	1.2.4 Interstratifications	12
	1.2.4.1 Constituted by members of the same mineral group	13
	1.2.4.2 Constituted by members of different mineral groups	13
1.3	Some difficulties in the identification of discrete clay minerals	14

Chapter		page
1.3.1	Differentiation between vermiculite and smectite	15
1.3.2	Subgroup and species identification	17
1.3.3	Mixed-layer formation of smectites upon potassium saturation	21
1.4	The analysis of interstratified clay minerals	22
1.4.1	Assumptions in the use of computer-calculated diffractograms and their limitations	23
1.4.1.1	K-saturated samples	23
1.4.1.2	Mg-saturated samples	24
1.4.1.3	Non-uniform interlayer distance	24
1.4.2	Analysis and interpretation of diffractograms for particular types of interstratifications	25
1.4.2.1	Two component interstratifications	25
1.4.2.2	Three- or multicomponent interstratifications	35
1.5	Interstratified clay minerals: A new structural model based on charge consideration of interlayers	38
1.5.1	The classical concept	39
1.5.2	A proposed revised concept	41
1.6	Summary and discussion	46
2	MINERALOGICAL STUDY OF DOLERITE-DERIVED SOILS FROM THE IXOPO DISTRICT OF NATAL	48
2.1	Introduction	48
2.2	Materials and methods	49

Chapter	page
2.3 Results and discussion	56
2.3.1 XRD investigation	56
2.3.1.1 Smectite dominated soil	57
2.3.1.2 Soils with co-dominant kaolinite and smectite	61
2.3.1.3 kaolinite dominated soils	76
2.3.2 Electron microscopy	82
2.4 Conclusions	
3 MINERALOGICAL ASPECTS OF THE GENESIS OF SWELLING SOILS OF THE HIGHVELD NEAR STANDERTON	87
3.1 Introduction	87
3.2 Materials and methods	88
3.3 Results and discussion	91
3.3.1 X-ray diffractometry	91
3.3.1.1 Whole soil mineralogy	91
3.3.1.2 Mineralogy of the clay fraction	95
3.3.1.2.1 Group I profiles (pit 12-25) derived from dolerite	95
3.3.1.2.2 Group II profiles (pit 1-8) derived from shale	105
3.3.1.2.3 Group III profiles (pit 26-30)	116
3.3.2 Exchangeable cations and the "degree of crystallinity"	121

Chapter		page
	3.3.3 Electron microscopy	125
	3.3.4 Total chemical analysis	127
	3.4 Heavy mineral investigation with special reference to group III soils and the prevalence of quartz	130
	3.5 Summary and discussion	133
4	THE OCCURRENCE OF FE-RICH TALC IN A PEDOGENIC ENVIRONMENT	138
	4.1 Introduction	138
	4.2 Materials and methods	140
	4.3 Results and discussion	140
	4.3.1 Soil mineral composition	140
	4.3.2 Investigation of the talc concentrate	145
	4.3.2.1 XRD data	145
	4.3.2.2 Infrared spectroscopy	147
	4.3.2.3 Electron microscopy	151
	4.3.2.4 Chemical composition	151
	4.4 Conclusions	152
	4.5 General discussion of phyllosilicate clay formation at Melody Ranch and Tutuka	154
5	THE MINERALOGY OF POTASSIUM FIXATION IN SOILS	164
	5.1 Introduction	164
	5.2 The problem of the relationship between layer charge density and XRD spacings for smectite-vermiculite series	172
	5.3 Materials and methods	177
	5.4 Results and discussion	179
	5.4.1 XRD investigation	179
	5.4.2 Chemical analysis	205

Chapter	page
5.5 Discussion and conclusions	207
6 MINERALOGICAL FACTORS ASSOCIATED WITH STRONG SWELLING IN SOILS AND CLAYS	212
6.1 Introduction	212
6.2 Materials and methods	220
6.3 Results and discussion	224
6.3.1 XRD results	224
6.3.1.1 Smectite dominated soil profiles	225
6.3.1.2 Soils with mica-smectite inter- stratifications as the swelling component	240
6.3.2 Major element chemical analysis	255
6.3.3 Measure of expansiveness	258
6.3.4 Infrared spectroscopy	260
6.4 Conclusions	260
REFERENCES	264

Appendix	LIST OF APPENDICES	Page
1	Exchangeable Ca and Mg values, exchangeable acidity and grain size distribution of Melody Ranch samples	289
2 - 17	Field descriptions of soil profiles along the transect T ₁ (Figure 3.1) at the Tutuka power station	291
18	Analytical data for ten profiles selected from the T ₁ transect	302
19	Exchangeable cations, iron and manganese oxyhydroxides and grain size analysis of highly swelling soils (Chapter 6)	303

LIST OF FIGURES

x

Figure		Page
1.1	Dependence of apparent basal spacings of kaolinite on the number of layers (N) in a crystallite (after Trunz, 1976)	8
1.2	Variations in relative intensities as a function of layer shift (a) and rotational stacking faults (w) for kaolinite (after Ray <u>et al.</u> , 1980)	10
1.3	Characteristic migration of subsequent smectite peaks (\bar{A}) (Mg-saturated, ethylene glycol solvated), when interstratified with mica or kaolinite. Basal spacings are taken from Srodon (1984) for mica and from Novich and Martin (1983) for expanded smectite	26
1.4	Comparison of (a) calculated diffraction profile with (b) X-ray pattern of ethylene glycol treated mica-smectite from Two Medicine clay with 35% smectite layers and a maximum degree of ordering (after Reynolds and Hower, 1970)	28
1.5	Characteristic migration of subsequent rectorite peaks (\bar{A}), when interstratified with mica or smectite (Mg-saturated, ethylene glycol solvated)	28
1.6	XRD trace of an ordered interstratification of 82% mica and 18% ethylene glycol expanded smectite (after Huff and Turkmenoglu, 1981)	29
1.7	Calculated diffraction profiles assuming maximum rectorite-like ordered interstratification of 10 \bar{A} and 16,9 \bar{A} layers. Fractions of smectite layers are 0,8, 0,6 and 0,4 (after Reynolds and Hower, 1970)	31

Figure		Page
1.8	Computer-calculated diffraction patterns of Mg-saturated, ethylene glycol treated samples of smectite, mica and randomly interstratified mica-smectite (modified after Reynolds and Hower, 1970)	32
1.9	Peak migration curves for kaolinite-smectite interstratifications (a) kaolinite with glycol expanded smectite; (b) kaolinite with collapsed smectite (after Cradwick and Wilson, 1972)	35
1.10	Calculated XRD patterns for a three-component interstratification with 60% mica, 20% vermiculite and 20% smectite (glycol). The various probability coefficients are given as p_{AA} for mica, p_{BB} for vermiculite and p_{CC} for glycolated smectite. Spacings corresponding to peak positions are marked in Å (after Cradwick and Wilson, 1978)	36
1.11	Aliettite structure : the classical concept	40
1.12a	Revised concept of a regular mica-beidellite interstratification	42
1.12b	Revised concept of an ordered mica ($p = 0,6$) beidellite ($p = 0,33$) interstratification	42
1.12c	Revised concept of an ordered mica ($p = 0,75$) beidellite ($p = 0,25$) interstratification	43
2.1	Location of sampling sites on Melody Ranch	52
2.2	Whole-soil mineral distribution in the profile of the Rensburg soil constructed from relative XRD peak heights	58

Figure

2.3	XRD traces of the clay fraction (oriented preparations) from horizons of the Rensburg soil profile (a) Mg-saturated, air-dried; (b) Mg-saturated, ethylene glycol solvated; (c) Mg-saturated, glycerol solvated	59
2.4	XRD traces of the clay fraction (oriented preparation) from horizons of the Rensburg soil profile after dodecylammonium-chloride intercalation	60
2.5	XRD traces of the clay fraction (oriented preparation) from horizons of the Rensburg soil profile (a) K-saturated, air-dried; (b) K-saturated, 110°C; (c) K-saturated, 500°C	62
2.6	XRD trace of the clay fraction (oriented preparation) from the Rensburg G ₂ horizon after formamide intercalation	64
2.7	Whole-soil mineral distribution in the profile of the Mayo soil	64
2.8	XRD powder pattern of hand-picked white grains (plagioclase) from the Mayo B horizon	66
2.9	XRD powder pattern of hand-picked black grains (pyroxene orh) from the Mayo B horizon	66
2.10	XRD traces of the clay fraction (oriented preparation) from horizons of the Mayo soil profile (a) Mg-saturated, air-dried; (b) Mg-saturated, ethylene glycol solvated; (c) Mg-saturated, glycerol solvated	67
2.11	XRD traces of the clay fraction (oriented preparation) from horizons of the Mayo soil profile (a) Li-saturated, air-dried; (b) Li-saturated, 290°C, ethylene glycol solvated	69

Figure		Page
2.12	XRD traces of the clay fraction (oriented preparation) from horizons of the Mayo soil profile (a) K-saturated, air-dried; (b) K-saturated, 500°C	71
2.13	XRD traces of the clay fraction (oriented preparation) from horizons of the Mayo soil profile (a) Mg-saturated, air-dried; (a ₀) Mg-saturated, 110°C; (b) Mg-saturated, formamide intercalated	72
2.14	Whole soil mineral distribution in the profile of the Arcadia soil (constructed from relative XRD peak heights)	74
2.15	XRD traces of the two horizons of the Arcadia soil profile (oriented clay) (a) Mg-saturated, air-dried; (b) Mg-saturated, ethylene glycol solvated; (c) Mg-saturated, glycerol solvated	75
2.16	XRD traces of the two horizons of the Arcadia soil profile (oriented clay) (a) Li-saturated, air-dried; (b) Li-saturated, 290°C, ethylene glycol solvated	77
2.17	XRD traces of the two horizons of the Arcadia soil profile (oriented clay) (a) K-saturated, air-dried; (b) K-saturated, 500°C	78
2.18	XRD traces of the two horizons of the Arcadia soil profile (oriented clay) (a) Mg-saturated, air-dried; (b) Mg-saturated, formamide intercalated	79
2.19	Whole soil mineral distribution in the profile of the Hutton soil (constructed from relative XRD peak heights)	80
2.20	Whole soil mineral distribution in the profile of the Shortlands soil (constructed from relative XRD peak heights)	80

Figure		Page
2.21	XRD traces of the B ₁ horizon of the Hutton (Balmoral) profile (oriented clay) (a) Mg-saturated, air-dried; (b) Mg-saturated, ethylene glycol solvated; (c) Mg-saturated, glycerol solvated	82
2.22	XRD traces of the B ₁ horizon of the Hutton (Balmoral) profile (oriented clay) (a) K-saturated, air-dried; (b) K-saturated, 300°C; (c) K-saturated, 500°C	83
2.23	Scanning electron micrograph of a hand-picked plagioclase particle from the Mayo B horizon (magnification 1:3000)	84
2.24	Scanning electron micrograph of a hand-picked pyroxene particle from the Mayo B horizon (magnification 1:5500)	85
3.1	Soil map of Tutuka power station (modified after Fey and Cass, 1983)	89
3.2	Slope profile of transect T ₁ from which soils were sampled at 100 m intervals. Vertical scale exaggerated x 20 (after Snyman <u>et al.</u> , 1985)	90
3.3	X-ray diffraction patterns of two saprolite horizons (a) pit 3 : shale saprolite; (b) pit 30 : dolerite saprolite (random powder mounts, whole-soil)	93
3.4	XRD pattern of hand-picked shale fragments from the saprolite of pit 1 (random powder mounts)	94
3.5	X-ray diffraction patterns for whole soil from horizons of pit 25 (random powder mounts)	96
3.6	XRD traces of the < 2 um fraction of the surface horizon of pit 17 (oriented specimen)	97

Figure		Page
3.7	XRD traces of selected clay fractions (oriented specimen, Li-saturated, glycolated) without (a) and with (b) heating at 290 °C, illustrating variations in shape of the first reflection and position of the second with increasing amount of collapsed (montmorillonite) layers, randomly stacked with expanded (beidellite) layers	101
3.8	XRD traces of the clay fraction of pit 14 (oriented specimen)	103
3.9	XRD pattern of the K-saturated, 500°C heated clay fraction from different horizons of pit 2	107
3.10	XRD traces of the clay fraction of the C horizon of pit 4 (oriented specimen) (a) Mg-saturated; (b) Li-saturated; (c) K-saturated	109
3.11a	XRD traces of the < 2 μ m fraction of the C and G horizons of pit 2 (oriented specimen, Mg-saturated) : (a) air-dried; (b) ethylene glycol solvated	112
3.11b	XRD traces of the < 2 μ m fraction of the two A horizons of pit 2 (oriented specimen, Mg-saturated) as Figure 3.11a	113
3.12	XRD pattern of the clay fraction of pit 1, G ₂ horizon	114
3.13	XRD traces of the clay fraction of the various horizons of pit 27 (oriented specimen, Mg-saturated) : (a) air-dried; (b) ethylene glycol solvated	119
3.14	XRD pattern of the clay fraction of the A horizon of pit 30 (oriented specimen, Mg-saturated, air dried)	120
3.15	XRD traces of a random kaolinite-smectite interstratification with approximately 70% kaolinite (Schultz <u>et al.</u> , 1971)	121

Figure		Page
3.16	XRD pattern of the < 2 um fraction of two top horizons (oriented specimen, K-saturated, 300°C, glycolated) (a) pit 29 (dolerite saprolite); (b) pit 1 (shale saprolite)	122
3.17	Relationship of total extractable bases to indices of crystallinity (a) peak intensity, and (b) angle of deviation of peak shoulder from the vertical, for the 001 reflection of swelling layer silicates in clay fractions from soil profiles on the Tutuka transect	124
3.18	Transmission electron micrograph of the clay fraction of pit 17 A ₁ (print magnification 1:15000)	126
3.19	Transmission electron micrograph of the clay fraction of pit 2 A ₁ (print magnification 1:15000)	127
4.1a	Stanger Soil Series : X-ray traces of the < 2 um fraction of the untreated sample (oriented specimen)	143
4.1b	Msinsini Soil Series : X-ray traces of the < 2 um fraction of the untreated sample (oriented specimen)	143
4.1c	Phoenix Soil Series : XRD traces of the < 2 um fraction of the untreated sample (oriented specimen)	144
4.2	Oriented specimen of the Stanger A horizon, heated to 510°C for 4 hours	145
4.3	XRD pattern of oriented specimen of talc, (a) concentrated from the Stanger clay and (b) of commercial talc	146
4.4	Infrared absorption spectra of (a) talc concentrate, (b) commercial talc. Range : 4 000 - 3 000 cm ⁻¹	149
4.5	Infrared absorption spectra of (a) talc concentrate, (b) commercial talc. Range : 3 000 - 200 cm ⁻¹	150

Figure		Page
4.6	Scanning electron micrograph of the talc concentrate	151
4.7	Alteration products derived from weathering of pyroxenes (Pion, 1979)	157
5.1	Effects of segregation of illite and of montmorillonite on calculated diffractometer (Cu K) of interstratified illite- montmorillonites with 70% illite; the bottom pattern is for random interstratification (no tendency for segregation defined by $P_{M.I} = 0,7$). Curves with smaller $P_{M.I}$ represent increasing segregation. Values in A corresponding to positions of maxima are also given (from Reynolds, 1980)	178
5.2	Whole soil XRD patterns of samples, containing plagioclase as the only feldspar variety besides quartz	181
5.3	Whole soil XRD patterns of samples, containing K-feldspar + plagioclase besides quartz	182
5.4	Whole soil XRD patterns of K-fixing samples from Germany	183
5.5	XRD traces of the < 2 um fraction of the Vimy sample (oriented specimen)	185
5.6	XRD traces of the < 2 um fraction of the Phoenix sample (oriented specimen)	186
5.7	X-ray diffraction pattern of the Phoenix sample (< 2 um fraction, oriented specimen) with dodecylammoniumchloride as interlayer cation complex	188
5.8	XRD traces of the < 2 um fraction of Boden 5 K_0 (oriented specimen); Mg-saturated	189
5.9	XRD traces of the < 2 um fraction of Boden 5 K_0 (oriented specimen); K-saturated	190

Figure		Page
5.10	XRD traces of the < 2 um fraction of Boden 3 K ₀ (oriented specimen)	191
5.11	XRD traces of the < 2 um fraction of Boden 5, K ₂ after the equivalent of 150 K ₂ O ha ⁻¹ has been added	193
5.12	XRD traces of the Kwezi soil sample (oriented clay)	195
5.13	XRD traces of the Arcadia soil sample (oriented clay)	196
5.14	XRD pattern of the Arcadia soil sample (< 2 um fraction, oriented specimen)	198
5.15	Calculated X-ray diffraction curves for interstratifications of mica and smectite for different stacking arrangements (from Cradwick and Wilson, 1978)	199
5.16	XRD pattern of the < 2 um fraction of the Arcadia sample (oriented specimen) after solvation with dodecylammonium-chloride	201
5.17	XRD traces of the < 2 um fraction of sample MIS 8492 Sucoma (oriented specimen).	203
5.18	XRD traces of the Milkwood soil sample < 2 um fraction, oriented specimen	204
5.19	X-ray diffraction pattern of (a) the "high-charged" smectite of Egashira <u>et al.</u> (1982) Mg-saturated, glycerol solvated, compared with (b) the calculated pattern of a randomly inter-stratified mica/smectite (glycolated) with 50% mica layers (Reynolds and Hower, 1970)	209

Figure

- 5.20 (a) X-ray traces of a K-fixing soil (glycerol solvated) (Niederbudde and Fischer, 1980); (b) calculated diffractometer patterns of interstratified illite-(glycol) montmorillonite with 70% illite and with increasing tendency for illite segregation from bottom to top (Reynolds, 1980) 210
- 6.1 Change of approximate mean spacing between layers of montmorillonite with reciprocal of square root of concentration (c) for Na-saturated clay (after Norrish, 1954) x in NaCl solution, 0 in NaSO₄ solution 214
- 6.2 Variations of the electrical potential with distance from the surface according to Stern (1924) and Grahame (1947) (Theng, 1979) 216
- 6.3 Diagram showing the energy of double layer repulsion (V_R) and of Van der Waals' attraction (V_A), together with the net or total interaction energy (V_T) for parallel flat plates, as a function of particle (plate) separation. The interaction curve shows a deep (primary) minimum at close separations. V_m is the energy barrier to particle coagulation and V_b is the barrier to redispersion (Theng, 1979) 217
- 6.4 XRD traces of the various horizons of the Onderstepoort soil profile (oriented clay) (a) Mg-saturated, air-dried; (b) Mg-saturated, ethylene glycol solvated; (c) Mg-saturated, glycerol solvated 227
- 6.5 XRD traces of the various horizons of the Onderstepoort soil profile after dodecylammoniumchloride intercalation (oriented clay) 228

Figure

Page

- 6.6 XRD traces of the various horizons of the Onderstepoort soil profile (oriented clay) (a) Li-saturated, air-dried; (b) Li-saturated, 290°C, ethylene glycol solvated 229
- 6.7 XRD traces of the various horizons of the Onderstepoort soil profile (oriented clay) (a) K-saturated, air-dried; (b) K-saturated, 300°C, ethylene glycol solvated 231
- (c) XRD traces of the various horizons of the Onderstepoort soil profile (oriented clay), K-saturated and heated to 500°C 232
- 6.8 XRD traces of the Vereeniging, Civic Centre (V_{CC2}) soil sample (oriented clay) (a) Mg-saturated, air-dried; (b) Mg-saturated, ethylene glycol solvated; (c) Mg-saturated, glycerol solvated 233
- 6.9 XRD traces of the Vereeniging, Civic Centre (V_{CC2}) soil sample (oriented clay) (a) K-saturated, air-dried; (b) K-saturated, 300°C, ethylene glycol solvated; (c) K-saturated, 500°C 233
- 6.10 XRD traces of the Vereeniging V_{CC2} soil sample (oriented clay) (a) Li-saturated, air-dried; (b) Li-saturated, 290°C; (c) Li-saturated 290°C, ethylene glycol solvated 235
- 6.11 XRD traces of the Vereeniging V_{CC2} soil sample (oriented clay) dodecylammoniumchloride intercalated 235
- 6.12 XRD traces of the Vredefort sample (oriented clay) (a) Mg-saturated, air-dried; (b) Mg-saturated, ethylene glycol solvated; (c) Mg-saturated, glycerol solvated 237
- 6.13 XRD traces of the Vredefort sample (oriented clay) (a) K-saturated, air-dried; (b) K-saturated, 300°C, ethylene glycol solvated; (c) K-saturated, 500°C 238

Figure		Page
6.14	XRD traces of the Vredefort sample (oriented clay) (a) Li-saturated, air-dried; (b) Li-saturated, 290°C; (c) Li-saturated, 290°C, ethylene glycol solvated	239
6.15	XRD trace of the Vredefort sample, intercalated with dodecylammoniumchloride (oriented clay)	240
6.16	XRD traces of the red varve material from Kimberley (oriented clay)	242
6.17	XRD traces of the Kimberley soil (i) varves, red (3,50 - 3,75 m); (ii) varves, grey (3,50 - 3,75 m); (iii) 10,50 - 10,75 m; (a) Mg-saturated, air-dried; (b) Mg-saturated, ethylene glycol solvated; (c) Mg-saturated, glycerol solvated	244
6.18	XRD traces of the Kimberley soil (i) varves, red (3,50 - 3,75 m); (ii) varves, grey (3,50 - 3,75 m); (ii) 10,50 - 10,75 m); (a) K-saturated, air-dried; (b) K-saturated, 300°C, ethylene glycol solvated; (c) K-saturated, 500°C	245
6.19	XRD traces of the Kimberley soil (oriented clay) (i) varves, red (3,50 - 3,75 m); (ii) varves, grey (3,50 - 3,75 m); (iii) 10,50 - 10,75 m; (a) Li-saturated, air-dried; (b) Li-saturated, 290°C, ethylene glycol solvated	246
6.20	XRD trace of the Kimberley red varves, dodecylammoniumchloride intercalated (oriented clay)	247
6.21	XRD traces of the soil sample from Kriel (oriented specimen) (a) Mg-saturated, air-dried; (b) Mg-saturated, ethylene glycol solvated; (c) Mg-saturated, glycerol solvated	249
6.22	XRD traces of the soil sample from Kriel (oriented clay) (a) K-saturated, air-dried; (b) K-saturated, 500°C	250

Figure	Page
6.23	XRD traces of the soil sample from Kriel (oriented clay) (a) Li-saturated, air-dried; (b) Li-saturated, 290°C; (c) Li-saturated, 290°C, ethylene glycol solvated 250
6.24	XRD traces of the soil sample from Kriel (oriented clay) after dodecylammoniumchloride intercalation 251
6.25	XRD traces of the soil sample from Cape Town (whole soil smear) 253
6.26	XRD traces of the soil sample from Cape Town (oriented clay) 255

LIST OF TABLES

xxiii

Table		Page
1.1	Relationship between compositions and peak positions for ordered mica-smectite (glycol) interstratifications	30
1.2	Relationship between compositions and peak positions for random mica-smectite (glycol) interstratifications	33
2.1	Soil profile characteristics for Melody Ranch samples	51
3.1	Percentage of montmorillonite layers in the smectite crystallites	100
3.2	Peak positions (\AA) of high-charge corrensite from pit 4, C horizon	108
3.3	Spacings and composition of the pit 2 clay	115
3.4	Chemical composition of the clay fraction from representative profiles of each of the 3 groups : pit 1 (shale-derived), pit 17 (dolerite-derived) and pit 30 (possible shale colluviation)	129
4.1	Relative clay mineral composition of the soil clay fractions, based on XRD peak areas	142
4.2	Comparison of XRD data for the enriched talc with those of pure talc, minnesotaite and ferripyrophyllite	148
4.3	Five analyses by EDX of separate particles observed by SEM in the soil talc concentrate	152
4.4	Alteration products derived from weathering of plagioclase as reported by the various authors	156

Table

Page

5.1	Probability coefficients for the 10 Å, 14,2 Å and 16,9 Å layers of potassium-saturated, ethylene glycol solvated montmorillonites from various parts of the world and the corresponding peak positions after air-drying and ethylene glycol solvation as well as the total layer charge, calculated for 0 (OH) (modified after Cicel and Machajdik, 1981)	175
5.2	Local charge density calculations (Machajdik and Cicel, 1981)	176
5.3	Selected properties of K-fixing surface soils	179
5.4	Chemical composition of some of the K-fixing samples (< 2 µm fraction, deferrated; Li-saturated)	206
6.1	001 spacing (Å) of water solvation complexes of smectites and vermiculites (after Suquet <u>et al.</u> , 1975)	219
6.2	Clay mineral and solution characteristics that influence the osmotic/intracrystalline swelling ratio of smectites	221
6.3	Sample localities, parent materials and sample donators	223
6.4	Total chemical analyses of the < 2 µm fraction (deferrated, Li-saturated) of soils which exhibit a strong swelling capacity	257
6.5	Plasticity index values	258
6.6	Magnitude of expansion	259

ABSTRACT

As very little detailed X-ray diffraction investigations have been carried out in South Africa on 2:1 phyllosilicates in soils, the aim of the present study was to contribute to the knowledge of soil genesis, as well as K-fixation and swelling, by investigation of the clay fraction of selected soils known to be rich in these minerals. X-ray diffraction analysis has been used almost exclusively as the investigative technique.

In Chapter 1 a literature review is presented on the reasons for X-ray diffraction peak broadening and the problems encountered in the identification of swelling clay minerals. For interstratifications, the concept of an ABAB layer sequence, considered as having an abab interlayer space, is questioned. It is suggested that the X-ray diffraction data from which the ABAB arrangement is inferred can as well be explained in terms of an alternative AAAB layer sequence, having an aabb interlayer arrangement.

Chapters 2, 3 and 4 deal with layer silicate formation/alteration in the course of soil development in dolerite and shale-derived profiles. Dolerite-derived pedons could be characterized by one of the following layer silicate suites :

suite i : discrete smectite (Fe-containing beidellite-montmorillonite) with or without traces of kaolinite and talc (Vertisol)

suite ii : smectite-kaolinite interstratification (Vertisol)

suite iii : 14 Δ minerals (vermiculite, beidellite, montmorillonite, chlorite) and 7 Δ minerals (halloysite, kaolinite) in about equal proportions (Vertisol and Mollisol)

suite iv : kaolinite with subordinate chlorite and traces of talc (Oxisol, Ultisol).

Ecca shale-derived Vertisols are dominated by mica-smectite interstratifications.

The occurrence of an iron-rich pedogenic talc is discussed in Chapter 4. X-ray and chemical data suggest 30 - 50 mole percent substitutions of iron for magnesium.

The mineralogical basis for K-fixation has been established in Chapter 5. Two K-fixing components could be identified : dioctahedral high-charge vermiculite as a discrete mineral and random mica-smectite interstratifications with 20 - 60% mica.

In Chapter 6, some of the most expansive soils in South Africa have been investigated. They can be subdivided into two groups denoted by the swelling component as follows :

- (a) smectite-dominated (the smectite species involved being most probably beidellite with a heterogeneous charge distribution);
- (b) mica-smectite interstratification with random or ordered stacking arrangement.

INTRODUCTION

The mineralogical composition of the clay fraction of a soil is one of the critical factors determining soil chemical and physical properties. Not only is there a close interrelationship between the criteria used for differentiating and classifying soils (colour, structure, consistency) and the amount and nature of the clay minerals, but other soil characteristics like K-fixation and base status are also closely linked to the presence or absence of certain clay minerals.

The aim of this study was to investigate the nature and relative abundance of 2 : 1 layer silicates, especially the swelling clays, in relation to certain soil properties which are important either to an understanding of soil genesis and classification or to prediction of physical and chemical behaviour. This task is especially interesting as very little detailed X-ray diffraction investigation has been carried out in South Africa on 2 : 1 phyllosilicates in soils since the advent of more recent intercalation methods for the differentiation of the swelling clay minerals compared to the considerable amount of research devoted to the sesquioxide components of soil materials at a relatively more advanced stage of weathering (van der Merwe and Heystek, 1952; MacVicar, 1965a,b; le Roux, 1972; Fey, 1974; Fitzpatrick, 1978). This general problem has been tackled by way of several facets, and these are briefly introduced as follows.

Clay mineral formation/transformation processes are best studied in soil pedons, in which changes in soil mineralogy can be attributed to variations in only one or two of the major soil forming factors (parent material, climate, topography, time, vegetation). The restriction of the source material to two localities and two parent materials has therefore been given preference to the collection of random samples from a variety of areas in the investigation of the genesis of 2 : 1 phyllosilicates reported in Chapters 2 and 3. In Chapter 2 the dependence of the clay mineral suite on climate and internal drainage as dominant soil forming factors has been investigated on samples from Melody Ranch, Natal. Here dolerite constitutes the parent material of soil profiles, which vary greatly with respect to soil chemical and physical properties. The influence of parent material on the clay mineralogy of soil pedons has been followed up in detail in Chapter 3 on samples from the Tutuka power station in the Transvaal Highveld, where dolerite and upper Ecca shale weather to Vertisols with very similar soil properties. In this area the parent material varies while other soil forming factors remain largely constant or show variations which may be considered insignificant beside that of the major factor. The Tutuka and Melody Ranch localities have been chosen as basic igneous rocks and shale/mudstone sediments are representative of large parts of South Africa. The mineralogy of the two parent materials differs significantly. Dolerite is reported to have a very uniform mineral assemblage with plagioclase and pyroxene (mkl and orh) as the dominant components. Quartz may occur in trace amounts. Phyllosilicates are absent in this type of basic

igneous rock (Deer, Howie and Zussman, 1962). The clay suite developed from doleritic parent material must therefore have formed by topotactic transformation inside the altering crystal or by precipitation/crystallisation out of solution.

Ecca shales contain feldspar (K-feldspar with or without plagioclase) as dominant non-clay mineral besides larger amounts of quartz. Mica and chlorite (Fe-rich) are reported as the main clay constituents of Ecca shale (Drennan, 1964). The clay mineral assemblage formed from Ecca parent material may be composed of feldspar-derived neoformed components as well as transformed or neoformed minerals from weathered phyllosilicates.

Talc was found in the Melody Ranch soils. As this is one of the few reports on pedogenic talc in South Africa (Hahne and Fitzpatrick, 1984), and as the basal spacing of this mineral is slightly higher than that reported for talc, more attention has been given to this clay mineral, and Chapter 4 is devoted to the results of this subsidiary investigation.

2 : 1 phyllosilicates, especially swelling clays, are known to influence a number of soil characteristics, swelling and K-fixation being probably the most important ones from an economic point of view. Having examined clay formation in smectite-rich soils, this study of 2 : 1 phyllosilicates was then pursued in a somewhat more applied direction in an attempt to establish a mineralogical basis for K-fixation and marked swelling for soils in southern Africa (Chapters 5 and 6).

For this investigation random samples from a variety of areas have been taken in order to obtain material exhibiting these properties to a greater or lesser degree.

K-fixation is generally linked to the presence of discrete minerals with a high layer charge: illite and vermiculite. There also exist a number of reports on smectite as a K-fixing component. A study of this clay characteristic is of special interest as mineralogical information on K-fixation by local soils is scarce (Bredell and Coleman, 1968; le Roux and Rich, 1969; le Roux and Sumner, 1969; le Roux, Rich and Ribbe, 1970).

Expansive or "active" soils are generally reported to contain large amounts of smectite or montmorillonite as discrete minerals, and clay mineral analysis is therefore an important approach for the study of expansive soils. As highly swelling soils in South Africa are not restricted to basic parent materials (du Plessis, 1969) but are also causing problems when shale is the weathering substrate (de Bruijn, Collins and Williams, 1957), a more detailed investigation into the swelling component seemed justified. The diverse nature of the mineral assemblage of the two parent materials may be expected to result in considerable differences in the nature of the weathering product.

Throughout the investigations which have formed the basis of this thesis and which have employed X-ray diffraction almost exclusively as the investigative technique special emphasis has

been placed on the differentiation between species of the 14 Å phyllosilicate group (montmorillonite, beidellite, vermiculite, chlorite) and on the nature of interstratifications.

Before reporting the results from the several facets of this study, a brief review has been presented (Chapter 1) of the literature concerning two aspects which were crucial for interpretation of XRD data, namely the degree of crystallinity (or the broadening of peaks) and the problems encountered in the identification and classification of interstratifications involving smectite species.

CHAPTER 1

AN ASSESSMENT OF CERTAIN DIFFICULTIES IN THE X-RAY IDENTIFICATION OF 2:1 LAYER SILICATES

1.1 Introduction

The most common analytical technique employed in the identification of clay minerals is X-ray diffraction analysis. Orientation of the sheet-like particles enhances the d_{001} diffraction maxima, thus resolving the diagnostic c dimension of the various clay minerals. Saturation, solvation and heating procedures permit differentiation of the clay minerals into groups and species.

It is important to stress, however, that the differentiation between the various 2:1 layer silicates must be made on the basis of layer charge. Problems arise in that the definition boundary is in certain cases not in line with XRD characteristics.

It is generally assumed that the same value of layer charge results in the same interlayer spacing. A great number of data, however, indicate that there exist fundamental differences between expansion characteristics and the absolute value of layer charge.

Controversy also arises from the relationship between the shape and intensity of the XRD maxima and clay characteristics, such as site occupancy, crystallite size or mixed layer formation.

For interstratified clays many different stacking sequences have been demonstrated and computer calculated patterns exist for comparison purposes with experimentally recorded ones.

The purposes of this first chapter are to present a literature review on the reasons for line broadening, point out the problems encountered in the identification of discrete clay minerals and report on the identification and analysis of interstratifications. The problem of whether an interstratification should be regarded as a stacking of layers or of interlayers is also discussed.

1.2 Factors influencing X-ray diffraction line broadening

Numerous publications on clay minerals have shown that the degree of crystallinity of soil clays, as inferred from the reduced X-ray diffraction peaks, is relatively low compared with that of clays of hydrothermal or diagenetic origin. There is also a persistent inadequacy inherent in many calculated patterns in that, generally, the calculated traces have sharper reflections than corresponding experimental profiles.

The theory of X-ray diffraction by crystals treats a crystal as a regular three-dimensional array of identical unit cells, all scattering X-rays with the same amplitude in any particular direction. In practice many kinds of structural disorder can occur in clay minerals and their recognition is an integral part in the process of identification and characterization. The

purpose of this introductory chapter is to develop a perspective of X-ray diffraction line broadening and to establish the extent to which it needs to be taken into account in clay mineralogical analysis.

1.2.1 Crystallite size

A crystal lattice is defined as an homogeneous distribution of points, and to be homogeneous, the point distribution must be infinite. When a crystal is less than 100 Å, i.e. when a real sample is composed of crystallites, in which the number of unit cells, stacked normal to the ab-plane, is less than 10 (for mica), peaks will become broadened and also measurably displaced from their nominal positions (Reynolds, 1968; Klug and Alexander, 1974; Trunz, 1976). The relationship between peak positions and the number of kaolinite layers, stacked along c, is shown in Figure 1.1.

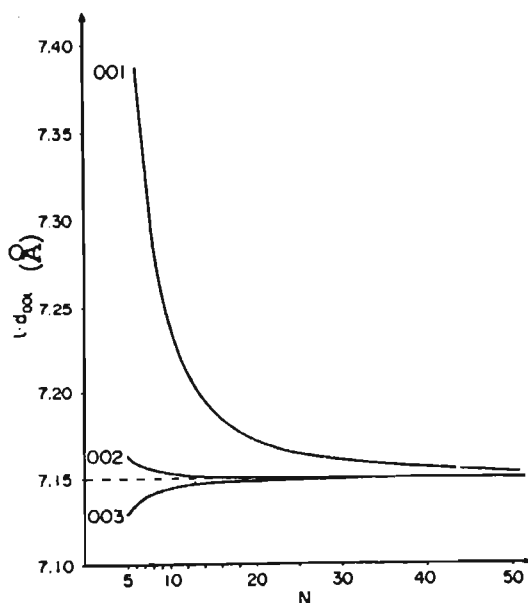


Figure 1.1 Dependence of apparent basal spacings of kaolinite on the number of layers (N) in a crystallite (after Trunz, 1976)

1.2.2 Defect broadening

- a) Crystal defects
- b) Substitutions
- c) Stacking disorder
- d) Site occupancy

1.2.2.1 Crystal defects

The effect of statistically arrayed defects in the crystal structure on the line broadening has been demonstrated by Ergun (1970) for graphite. So far, no attempt has been made to apply this treatment to clays, if indeed such is possible (Reynolds, 1980).

1.2.2.2 Substitutions

The influence of substitutions on the degree of crystallinity has been demonstrated for the case of Al substituting for Fe in iron oxide structures (Taylor and Schwertmann, 1980).

Substitutions in clay structures, which may vary in extent and nature of the cation between the various layers and sites, must be expected to result in a broadening of peaks as well (Brindley, 1980).

1.2.2.3 Stacking disorder

It is well known that layer lattices are highly prone to stacking

disorder due to their weak interlayer forces. Indeed, this type of disorder is almost universal among clay minerals (Plancon and Tchoubar, 1977).

Stacking order improves with increase in tetrahedral charge and the radius of the interlayer cation (Besson, Glaeser and Tchoubar, 1983). The influence of stacking disorder on the peak intensities (Ray, De and Bachatterjee, 1980) is shown in Figure 1.2.

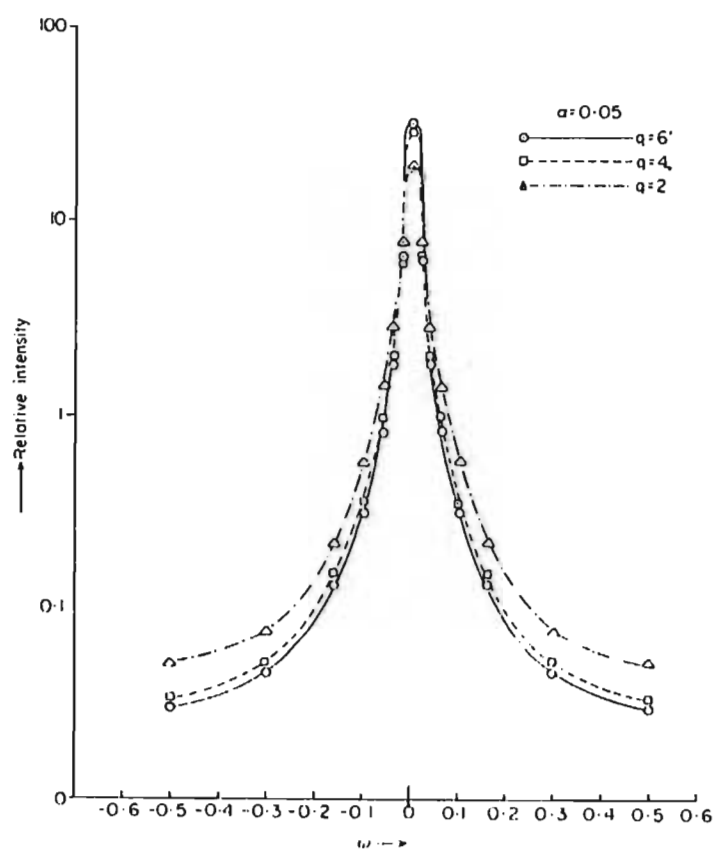


Figure 1.2 Variations in relative intensities as a function of layer shift (α) and rotational stacking faults (ω) for kaolinite (after Ray et al., 1980)
 q = fractional displacement of layers

Drits et al. (1984) have differentiated between translational and rotational stacking faults in smectites. The presence of $b/3$ stacking faults (translation) leads to an increase in the thickness of the interlayer space, the value also depending on the chemical composition of the smectite. Generally, the presence of translational stacking faults in smectites is accompanied by the appearance of several interlayer distances leading to a distribution of intensities as in mixed layer structures. Defects of rotation of layers of 120 degrees preserves the usual coordination of the interlayer cations. In the case of 60, 180 and 300 degrees of rotation of adjacent layers, interlayer cations appear to have a different coordination (in the case of potassium in the interlayer space, the coordination changes from octahedral to prismatic). Differences in coordination ultimately result in differences in interlayer spacings.

1.2.2.4 Site occupancy

When ionic substitutions occur in a smectite, the possibility exists that the different cations that occupy a given type of structural site may do so in a regular or irregular manner.

Tsipursky and Drits (1984) showed that for dioctahedral smectites, there are cases in which (i) the trans positions are vacant (all nontronites, some montmorillonites); (ii) one of the two cis positions are vacant (most montmorillonites, some beidellites); and (iii) all octahedral positions are occupied

with a 2/3 probability (some beidellites). In addition, some intermediate cases for cis and trans occupation were found (some montmorillonites).

Mössbauer data indicate that in many dioctahedral 14 Å species formed at or near 25°C, both tetrahedral and octahedral layers are completely disordered (Bagin, Gendler, Dainyak and Kuznin, 1980). This disorder in site occupancy can be expected to result in weak and/or broadened X-ray reflections.

1.2.3 Instrumental factors and specimen preparation

This category of broadening is controllable (Rich, 1975; Klug and Alexander, 1975; Brindley and Brown, 1980) provided that all samples are prepared the same way and all patterns run using the same instrument with a narrow range of settings. Possible broadening factors such as cracks in the clay material of the oriented specimen have been found by the author not to influence the degree of broadening in the case of well ordered smectites and can thus be assumed to have a negligible effect upon peak broadening in general.

1.2.4 Interstratifications

Two types of mixed-layer systems, each giving rise to line broadening effects may be considered.

1.2.4.1 Constituted by members of the same mineral group

With polar organic or inorganic molecules (water, ethylene glycol, glycerol) or charged organic molecules (alkylammonium-chloride) in the interlayer space of smectites, interlayer spacings may vary throughout individual crystallites due to charge heterogeneities, and expansion and collapse do not take place equally between all interlayers under the same conditions. In the case of monovalent ions and water, for example, monolayer and bilayer complexes may be formed at the same relative humidity and stacked in an ordered, random or segregated fashion, giving rise to 12,4 - 15,2 Å interstratifications (Cicel and Machajdik, 1981) and to line broadening. In a similar way, glycol, glycerol and alkylammoniumchloride molecules may be arranged in mono- and bilayers, giving rise to mixed-layer structures and consequent line broadening (Lagaly, Gonzales and Weiss, 1976; Cicel and Machajdik, 1981). This aspect is dealt with in more detail in the section below.

1.2.4.2 Constituted by members of different mineral groups

It is now generally accepted (Srodon, 1984) that the concept of "illite crystallinity", which was originally based on the sharpness of the 10,0 Å reflection and which is extensively used for studying deep diagenesis and low grade metamorphism, represents nothing else but the extent of smectite prevalence in a mica-

smectite interstratification. It has also been demonstrated that random stackings of clay components with different basal spacings can result in marked line broadening (Reynolds and Hower, 1970; Cradwick and Wilson, 1978) and the computer calculated patterns of three component interstratifications are sometimes characterized by very broad peaks or even the elimination of peaks with d -spacings $> 4,5 \text{ \AA}$. As random stacking of clay minerals with different basal spacings does not only result in a possible line broadening but also in a characteristic irrationality of higher order reflections, the reason for broadening can be established by exact measurement of as many peak positions as possible.

1.3 Some difficulties in the identification of discrete clay minerals

The identification of various clay minerals is normally based on the position and possible shift of a series of basal reflections, applying auxiliary tests. Generally, a discrete mineral must give a rational series of basal reflections with $d_{005} \times 5 = d_{004} \times 4 = d_{003} \times 3 = d_{002} \times 2 = d_{001} \text{ (\AA)}$ with a low background to both sides of the peak maximum. In the case of smectite this applies to the saturation with divalent ions only.

The identification of discrete kaolinite, mica and chlorite is relatively straightforward, by inspection of subsequent order reflections. Formamide treatment provides information on halloysite (7 \AA), while hydrazine treatment may be used

to identify kaolinite in the presence of chlorite (Churchman and Theng, 1984).

1.3.1 Differentiation between vermiculite and smectite

The positive identification of the 14 Å minerals smectite and vermiculite remains on the other hand, a subject which is beset with some uncertainty. It is important to stress that the differentiation between vermiculite and smectite must be made on the basis of layer charge, the boundary being tentatively defined as $0,60/O_{10}(OH)_2$ unit cell (Bailey, 1980), and not on the basis of peak positions. In practice, however, the differentiation between vermiculite and smectite is normally based on the 14 Å X-ray diffraction peak of vermiculite and the 16,9 and 17,9 Å line of smectite, when ethylene glycol or glycerol liquid are added to a Mg-saturated clay (Brindley, 1966; Harward, Carstea and Sayegh, 1969). The difficulty here lies in the fact that neither the glycol- nor the glycerol-determined smectite-vermiculite boundary coincides with the AIPEA definition (Bailey, 1980), the ethylene glycol test tending to overestimate smectite and the glycerol test to underestimate it (Suquet, de la Call and Pezerat, 1975; Srodon and Eberl, 1980).

By contrast, Egashira, Dixon and Hossner (1982) have described a "high charge" smectite with a "vermiculitic" layer charge of $0,8/O_{10}(OH)_2$ unit cell, which expands to 18 Å upon glycerol solvation.

The use of alkylammoniumchloride ions of appropriate number of

carbon atoms allows more exact characterization of swelling 14 Å minerals in terms of layer charge. But here too, problems are experienced. Lagaly (1982) reported a "low charge" vermiculite with a layer charge of $0,5/O_{10}(OH)_2$ unit cell and Malla and Douglas (1984) described a 14 Å mineral, which expanded to 18 Å upon glycerol solvation (smectite), but exhibited paraffin-type intercalation with alkylammoniumchloride ions (vermiculite). From these findings it must be concluded that the absolute value of the layer charge is not the only influencing factor for swelling characteristics (see also section 1.4).

The contraction of the basal spacing induced by potassium saturation seems to be the only consistent reaction characteristic of vermiculite (Harward et al., 1969; Douglas, 1977; MacEwan and Wilson, 1980). For soil vermiculite an additional heat treatment at 110°C is suggested (Alexiades and Jackson, 1965). According to Cicel and Machajdik (1981) both 10 Å and 12,4 Å peak positions are possible for vermiculite after K-saturation and air drying.

Similarly unresolved is the question concerning possible re-expansion of the K-saturated 10 Å lattice upon glycol solvation. Collapse without further expansion (Egashira et al., 1982) or formation of a glycol monolayer (Cicel and Machajdik, 1981) are both possible.

Additional difficulties arise in that "pure" minerals are very rare.

1.3.2 Subgroup and species identification

Any attempt to characterize 2:1 layer silicates should include the subgroup and/or species, especially in the case of swelling clay minerals.

The distinguishing factor between di- and trioctahedral minerals is the value of the b-parameter, which can be estimated from the 060 reflection. It should be remembered, however, that basal reflections may have peak positions in this range as well (d_{0010} for smectite = 1,52 Å).

Two smectite sub-groups are recognized on the basis of the trivalent and divalent occupancy of the octahedral sheet : the trioctahedral or saponite subgroup consists of saponite, hectorite, stevensite and sauconite, while montmorillonite, beidellite, nontronite and volkhonskoite make up the montmorillonite subgroup, which is dioctahedral.

Complete species identification consists of two main operations: analysis for chemical composition (all 2:1 layer silicates) and determination of the seat of the layer charge (smectite only).

Species within the saponite subgroup are distinguished primarily according to the dominant seat of the layer charge. In saponite this is tetrahedral whereas in hectorite and stevensite it is predominantly octahedral. Sauconite is distinguished chemically as the Zn-substituted variant of saponite (sensu stricto).

In the montmorillonite subgroup, montmorillonite has a layer

charge arising mainly from octahedral substitutions, whereas the beidellite layer charge is due mainly to tetrahedral substitutions. Nontronite (Fe-rich) and volkhonskoite (Cr-rich) are distinguished compositionally. Pure species are extremely rare and the three commonest species (montmorillonite, nontronite and beidellite) are often depicted as forming a continuous series.

There are three main approaches to identification on the basis of layer charge characteristics :

(i) Chemical analysis

It is necessary to note that the determination of the tetrahedral charge from chemical analysis of smectite requires a monomineralic composition, which is rare in soil environment. According to mathematical analysis by Cicel (1974) the effect of impurities on the determination of tetrahedral charge is critical. The presence of a hardly detectable 3% of free silica, for example, changes a calculated tetrahedral charge of $0,14/O_{10}(OH)_2$ to 0,02, whereas 3% of free alumina changes it in the opposite direction to $0,35/O_{10}(OH)_2$. The results lead to the conclusion that the plotting of any property of montmorillonite as a function of the tetrahedral charge (derived from chemical analysis) is hardly reliable. On the other hand, these impurities do not influence to such an extent the value of the total charge, derived from chemical analysis.

(ii) Greene-Kelly test (Greene-Kelly, 1953)

The test is based on the observation (Hoffmann and Klemen, 1949) that small ions such as Li^+ will migrate from interlayer positions towards octahedral vacancies when the Li-saturated smectite is heated to 200-290°C, thereby neutralizing the charge arising from ionic substitutions in this sheet and rendering the clay non-expansible (9,7 Å). The charge arising from substitutions in the tetrahedral sheet is not modified by this treatment and species with a high tetrahedral charge will therefore retain their expansibility. This test can only be applied to dioctahedral smectites and stevensite, since only these minerals possess vacant octahedral sites. Care must be taken to avoid any contact of the Li-saturated smectite with other metal cations, especially during the heating process. Heating the clay on a soda-lime glass, for example, leads to exchange of Na^+ from the glass for Li^+ , which results in an incomplete neutralization and thus an overestimation of the amount of tetrahedral substitution (Byström Brusewitz, 1975).

It must be emphasized that the test does not distinguish montmorillonite (with octahedral charge > tetrahedral charge) from beidellite (tetrahedral charge > octahedral charge). Assuming a smectite with a total layer charge of $0,5/\text{O}_{10}(\text{OH})_2$ and 60% charge arising from octahedral substitutions, i.e. a montmorillonite per definition, the complete neutralization of the octahedral sheet by Li^+ would leave a layer charge of $0,2/\text{O}_{10}(\text{OH})_2$, arising in the tetrahedral sheet, which is enough

to fully re-expand each interlayer, and identification as beidellite will result. In accordance with international practice, however, the smectite species, which re-expands after application of the Greene-Kelly test, will be termed beidellite.

A second problem arises from charge heterogeneities within the smectite crystallite, which is the rule in natural smectites. As soon as the smectite is composed of beidellitic charged units and montmorillonitic charged units within the same crystallite, the heat-treatment of the Li-saturated smectite will result in a (probably random) interstratification of irreversibly and reversibly collapsed units, that is an interstratification of 9,7 Å and 17 Å units upon glycolation. This type of interstratification must give the same irrational basal reflections as a mica-smectite (glycol) mixed-layer mineral and the same peak migration curves and tables can be used for their interpretation (see section 1.3.2.1).

(iii) Adsorption of alkylammoniumchloride

The third approach for identification based on layer charge is the alkylammoniumchloride method (Lagaly and Weiss, 1969; Lagaly, Gonzales and Weiss, 1976), by which it is possible to discern charge heterogeneity and estimate upper and lower limits of the layer charge of smectite.

An abbreviated form of the alkylammoniumchloride method is useful for diagnostic purposes. Using dodecylammoniumchloride, for example, all vermiculites give spacings > 20 Å, all beidellites form a bilayer complex (17,7 Å), while montmorillonites develop spacings characteristic of either a monolayer (13,6 Å) or are

characterized by monolayer-bilayer interstratification ($d_{001} < 17,7 \text{ \AA}$) (Bühmann, Fey and de Villiers, 1985). This procedure may also be applied to those trioctahedral species for which the Greene-Kelly test cannot be employed.

1.3.3 Mixed-layer formation of smectites upon K-saturation

By K-saturation of montmorillonites, which give with Mg saturation a rational series of basal reflections in both the air dried as well as the glycol and glycerol solvated states, mixed-layer structures may be formed (Muravyev and Sakharov, 1970; Cicel and Machajdik, 1981) in which the following layer structures can be found to exist in the air dried state : (a) a non-expanded layer (10 \AA ; vermiculite); (b) a structure with one interlayer of water molecules ($12,4 \text{ \AA}$; low-charge vermiculite and/or beidellite); (c) a structure with two interlayers of water molecules ($15,2 \text{ \AA}$; low charge smectite); and the following layer structures after ethylene glycol solvation; (d) a non-expanded layer (10 \AA ; high charge vermiculite); (e) a structure with a mono-interlayer of ethylene glycol ($14,2 \text{ \AA}$; low charge vermiculite, high charge smectite); (f) a structure with a duo-interlayer of ethylene glycol ($16,9 \text{ \AA}$; low charge smectite). Any peak position other than those above is the result of interstratifications of two or even three different layer types (Cicel and Machajdik, 1981). These authors found air-dried K-montmorillonites to contain all three types of layers, while ethylene glycol-solvated montmorillonites were composed of at least two, and mostly three, different layer types, type (f)

being the most common. Generally the air-dried samples contained more 10 Å layers than those solvated with ethylene glycol. This is evidently caused by the fact that the dipole moment of ethylene glycol is greater than that of water (Weast and Astle, 1978). Machajdik and Cicel (1981) also found excellent agreement between the local charge densities of the unit structures (d) - (f) with the layer charge and expansibility of mica, vermiculite and smectite.

Thus the position of the diffraction peaks of a K-saturated smectite provides valuable information on the proportions of local charge densities, both in the air-dried and especially in the glycolated state and is an indicator of charge heterogeneities of smectites.

1.4 The analysis of interstratified clay minerals

Detailed analysis of a mixed-layer clay diffraction pattern involves many variables, from the stacking arrangement to the degree of segregation and the involvement of more than two components (Tettenhorst and Grim, 1975). For many purposes satisfactory results may be obtained by matching the experimental pattern against a series of computer-calculated patterns. Migration curves constructed for several peaks can be used to refine estimates of layer-type composition. If similar compositions are obtained from more than one peak, small particle size may probably be discounted as being responsible for peak shift. For a complete analysis the total diffraction profile

must be clearly identifiable as representing either random or ordered, or perhaps even regular interstratifications (see page 27 for detail).

1.4.1 Assumptions in the use of computer-calculated diffractograms and their limitations

The use of computer-calculated patterns and migration curves and tables in determining the nature and amount of components in an interstratification unfortunately is affected by a number of serious limitations since the method is based on assumptions which are not necessarily valid.

1.4.1.1 K-saturated samples

The assumption of a 12,4 Å spacing for K-saturated air-dry smectites (Cradwick and Wilson, 1972) is erroneous in most of the cases. Cicel and Machajdik (1981) clearly demonstrated that any spacing between a water monolayer (12,4 Å) and a water duolayer (15,2 Å) is possible (see also 1.2.2). Results for the majority of smectites reported later in this present study show spacings between 13,4 and 14,5 Å.

The assumption of a 16,9 Å spacing for K-saturated, ethylene glycol solvated smectite (Cradwick and Wilson, 1972) is also incorrect; any peak position between an ethylene glycol monolayer and duolayer with values between 14,2 and 16,8 Å having been reported (Machajdik and Cicel, 1981) (see also 1.2.2).

1.4.1.2 Mg-saturated samples

The assumption of an ethylene glycol monolayer (14,2 Å) in the case of Mg-saturated vermiculite (Cradwick and Wilson, 1978) is an oversimplification, since the spacings of pure glycol-solvated vermiculites, even when Mg-saturated, vary between 14,2 and 16 Å (MacEwan and Wilson, 1980). The reason for this ambiguity lies in the fact that the smectite-vermiculite boundary is defined in terms of layer charge and not peak positions, as discussed earlier (section 1.2.1).

The assumption of a water duolayer for Mg-saturated smectites with a spacing of 15,2 Å (Cradwick and Wilson, 1972) is similarly tenuous, since this spacing is strongly dependent on relative humidity, so that variations between 14,2 and 15,2 Å are possible (MacEwan and Wilson, 1980).

Generally, the pattern of a Mg-saturated, ethylene glycol-solvated smectite is best suited for the measurement of peak migrations in smectites, as in all cases an ethylene glycol duolayer is formed with spacings ranging from 16,88 to 17,0 Å (Novich and Martin, 1983; Srodon, 1984). Other saturation and solvation tests remain necessary, however, in order to obtain an indication of the nature and number of 14 Å components.

1.4.1.3 Non-uniform interlayer distances

The assumption of a uniform interlayer space between two layers

may well be incorrect. Frayed crystal edges and wedge zones (Schroeder, 1979) were not included into any of the computer-calculated patterns but may well exert some influence on line broadening and peak positions.

1.4.2 Analysis and interpretation of diffractograms for particular types of interstratifications

Difficulties in the interpretation of XRD patterns arise when the clay fraction is composed of a two- or even multi-component interstratification. A peak position of 14,5 Å in the Mg-saturated, air-dried state, and expansion to 17,5 Å upon glycol solvation, can be characteristic for an interstratification with as much as 60% mica and 40% smectite as well as an interstratification with 20% mica, 20% vermiculite and 60% smectite (Cradwick and Wilson, 1978). Generally, interstratifications are indicated by the non-integral nature of higher order reflections, though small particle size may very occasionally be responsible for irrational peak positions.

1.4.2.1 Two component interstratifications

Interpretation of the nature and the amount of two minerals in a two-component interstratification is possible with the aid of tables and curves which show how the combined peak migrates as the relative proportions of the different layers change (Reynolds and Hower, 1970; Cradwick and Wilson, 1972; Cradwick and Wilson, 1978; Reynolds, 1980). Use of these tables and curves

is limited, however, by the fact that peak positions also depend on the stacking arrangement and tend to migrate in response to segregation. In all cases, ordered and random interstratifications have to be treated separately, as the migration curves differ in each case. The characteristic migration of smectite peaks with increasing mica or kaolinite content is demonstrated in Figure 1.3.

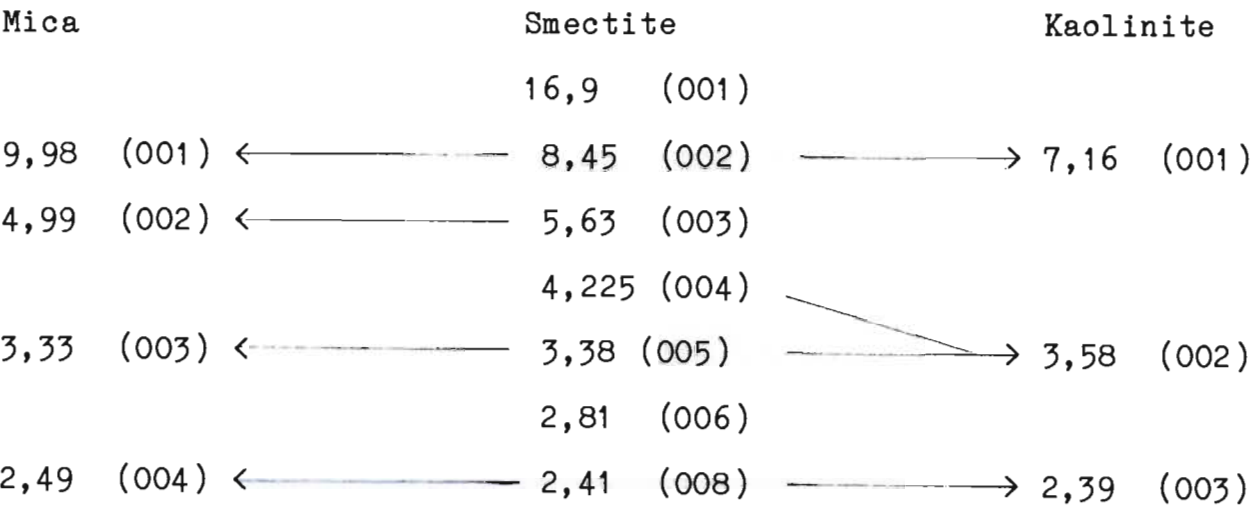


Figure 1.3 Characteristic migration of subsequent smectite peaks (Å) (Mg-saturated, ethylene glycol solvated), when inter-stratified with mica or kaolinite. Basal spacings are taken from Srodon (1984) for mica and from Novich and Martin (1983) for expanded smectite.

Mica-smectite

Mica-smectite interstratifications are undoubtedly the most interesting mixed-layer clays for they are ubiquitous, best known

chemically, show variations in response to pressure-temperature changes and are common in soil environments, where mica may weather to smectite through a series of interstratification steps. NB

Regular mica-smectite interstratifications are easy to identify by spacings which are the sum of the spacings of the two components, with the secondary reflections showing a regular sequence. The regular interstratification of mica-smectite is given the name rectorite (Bailey, 1982).

Ordered interstratifications in which the amount of each component is not equal may give a first basal spacing above 20 Å, but peaks are characterized by non-integral second order reflections (Figure 1.4) and the stacking is therefore often mistakenly assumed to be random.

While a peak position above 20 Å is an indication of ordering, the absence of such a peak does not necessarily indicate random stacking arrangements. Generally the ordering of a structure is indicated by peak positions which are the combined peaks of the regular mineral with those of one component (Figure 1.5).

Thus in an ordered structure with a mica content of more than 50%, a peak will be observed which migrates between 13,5 and 10 Å, depending on the amounts of mica, while the subsequent peaks will migrate between 8,97 Å and 10 Å, and 5,38 Å and 5,0 Å, respectively (Figure 1.5 and Table 1.1). A pattern for mica-

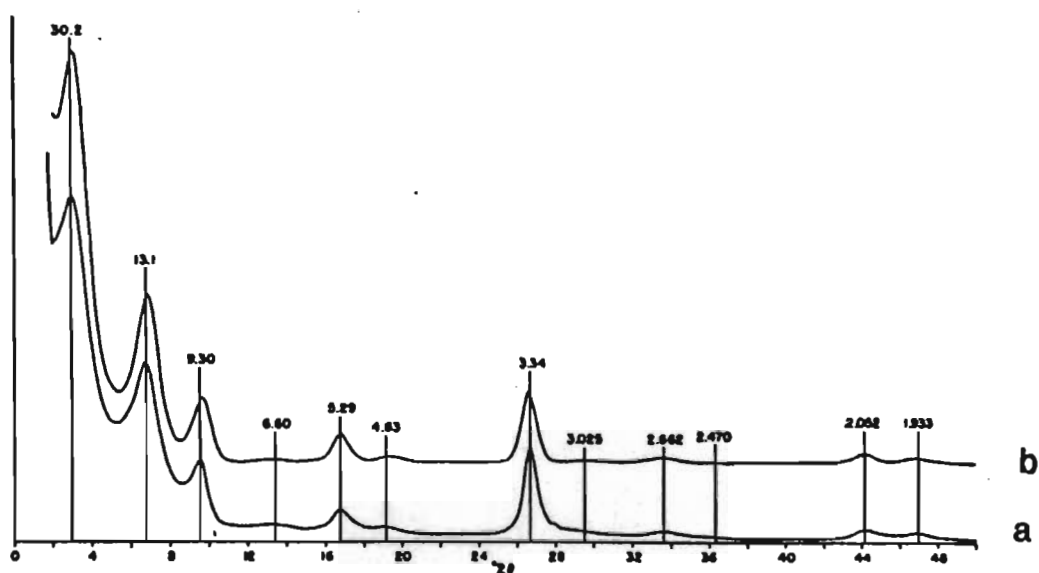


Figure 1.4 Comparison of (a) calculated diffraction profile with (b) X-ray pattern of ethylene glycol treated mica-smectite from Two Medicine clay with 35% smectite layers and a maximum degree of ordering (after Reynolds and Hower, 1970).

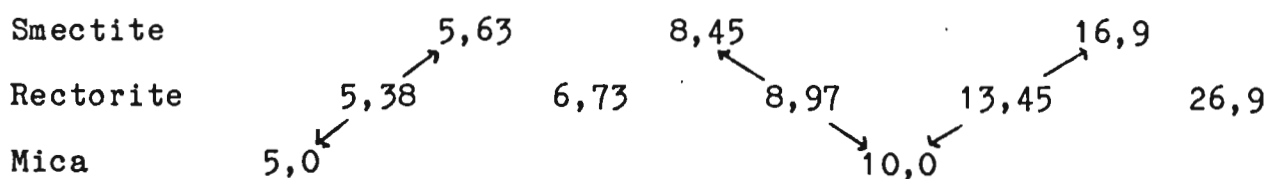


Figure 1.5 Characteristic migration of subsequent rectorite peaks (Å), when interstratified with mica or smectite (Mg-saturated, ethylene glycol solvated).

smectite interstratification with 18% smectite and a maximum degree of ordering (Mg-saturated, ethylene glycol solvated) is presented in Figure 1.6.

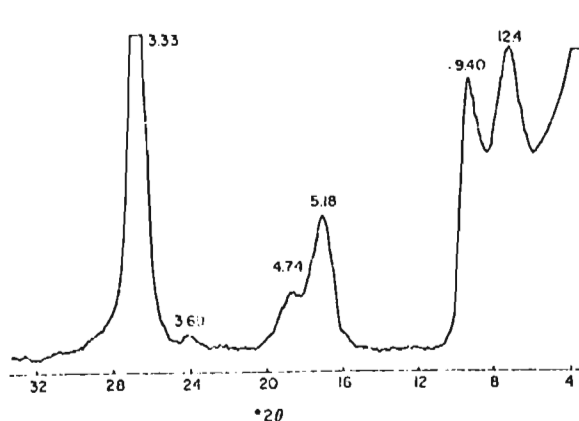


Figure 1.6 XRD trace of an ordered interstratification of 82% mica and 18% ethylene glycol expanded smectite (after Huff and Turkmenoglu, 1981).

When the smectite content exceeds 50%, the peak will migrate between 13,45 Å and 16,9 Å (the combined peak of the $001_{\text{smectite}}/002_{\text{rectorite}}$), between 8,97 Å and 8,45 Å (the combined $003_{\text{rectorite}}/002_{\text{smectite}}$), between 5,38 Å and 5,63 Å (the combined $005_{\text{rectorite}}/003_{\text{smectite}}$), etc., when the sample is Mg-saturated and glycolated (Table 1.1). Generally the peak positions of ordered structures are always those of the regular mineral with either one of the components. Three patterns of ordered structures are illustrated in Figure 1.7.

The most noteworthy feature of a randomly interstratified mica-smectite pattern is the extent to which it resembles smectite upon casual examination when the mica content is less than 50%. At a mica content of more than 80% the pattern resembles mica (Figure 1.8). No reflection is found for any composition in the range between mica 001 and smectite 001, as is the case in ordered structures. Instead, increasing proportions of mica

Table 1.1 Relationship between compositions and peak positions for ordered mica-smectite (glycol) interstratifications, spacings in Å.

% mica	d	d
	$002_{\text{smectite}}/003_{\text{rectorite}}$	$003_{\text{smectite}}/005_{\text{rectorite}}$
0	8,45	5,63
10	8,59	5,59
20	8,70	5,55
30	8,82	5,50
40	8,91	5,44
	$003_{\text{rectorite}}$	$005_{\text{rectorite}}$
50 (rectorite)	8,97	5,38
	$001_{\text{mica}}/003_{\text{rectorite}}$	$002_{\text{mica}}/005_{\text{rectorite}}$
60	9,20	5,34
70	9,40	5,28
80	9,64	5,22
90	9,96	5,09
100	9,99	5,00

cause an increase in intensity near the smectite 001 reflection, which is indicated by a shoulder at the lower angle side of the smectite 001 reflection (Figure 1.8). The spacings of the higher order reflections indicate interstratification components, for they have the characteristic irrationality that signifies interstratifications, i.e. the spacing of the second peak (the

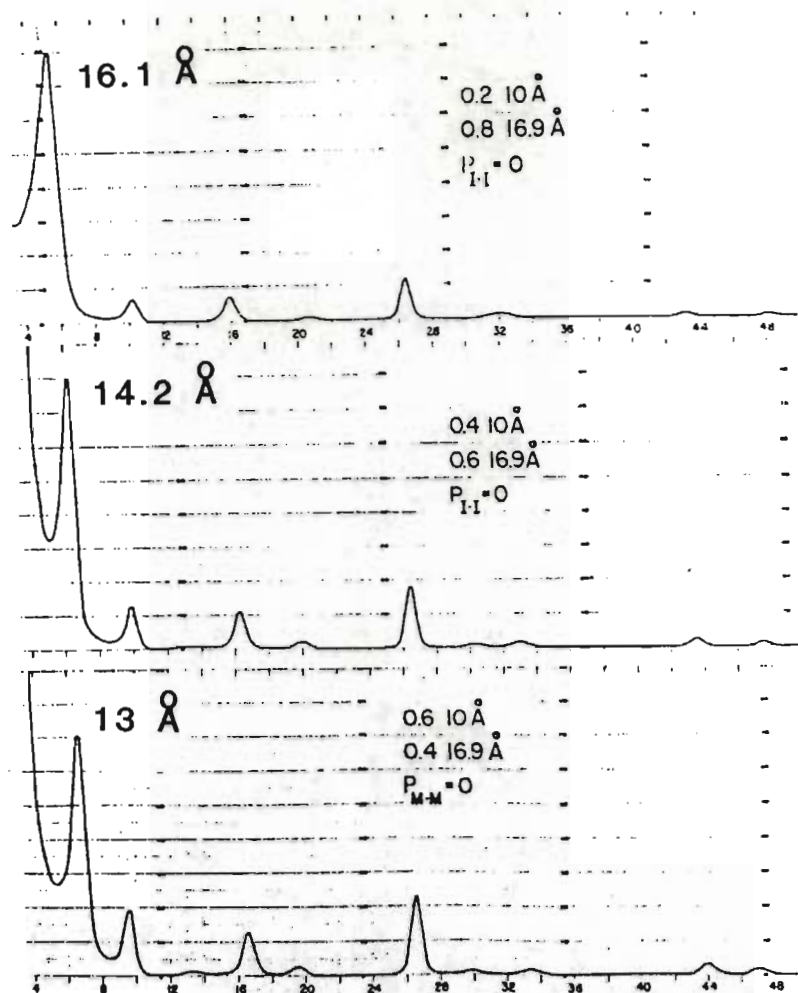


Figure 1.7 Calculated diffraction profiles assuming maximum rectorite-like ordered interstratification of 10 Å and 16,9 Å layers. Fractions of smectite layers are 0,8, 0,6 and 0,4 (after Reynolds and Hower, 1970).

combined $002_{\text{smectite}}/001_{\text{mica}}$) increases in Å value with increasing mica content, while the values of the third and all following reflections decrease (Figure 1.8).

The relationship between peak positions and composition for mica-smectite interstratifications (Mg-saturated, ethylene glycol solvated) is given in Table 1.2 for the random cases (spacings in Å).

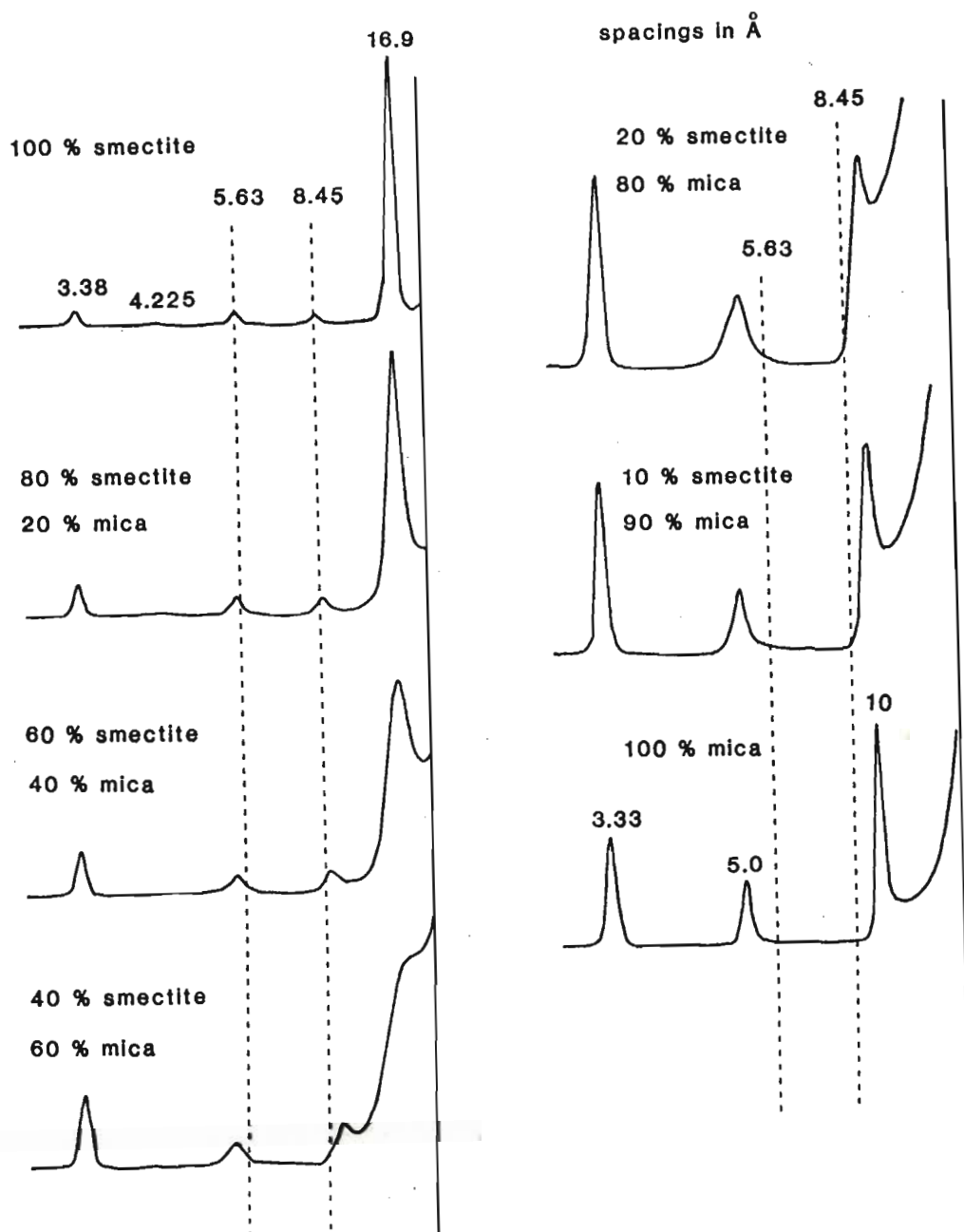


Figure 1.8 Computer-calculated diffraction patterns of Mg-saturated, ethylene glycol treated samples of smectite, mica and randomly interstratified mica-smectite (modified after Reynolds and Hower, 1970).

Table 1.2 Relationship between compositions and peak positions for random mica-smectite (glycol) interstratifications, spacings in Å.

% mica	d	d
	$002_{\text{smectite}}/001_{\text{mica}}$	$003_{\text{smectite}}/002_{\text{mica}}$
0	8,45	5,63
10	8,58	5,57
20	8,67	5,57
30	8,76	5,54
40	8,90	5,50
50	9,06	5,44
60	9,26	5,37
70	9,50	5,28
80	9,81	5,16
90	9,92	5,07
100	10,00	5,00

There are, however, certain problems attached to the identification of interstratifications in the presence of discrete minerals. If a sample contains large amounts of discrete mica additional to a mica-smectite interstratification, the $001_{\text{mica}}/002_{\text{smectite}}$ peak is not resolved, merging with the mica peak, and the $002_{\text{mica}}/003_{\text{smectite}}$ peak is also seriously interfered with by discrete mica as is the peak between 3,33 Å and 3,38 Å. In such a case, recognition of an interstratification and the conclusion as to the proportions of the components is restricted

to a comparison of the first order reflection with that of the calculated pattern, and must therefore be regarded as qualitative only. Similar problems arise in an assemblage of mica-smectite interstratifications with larger amounts of discrete smectite.

Generally, "broad shoulders" must always be regarded as an indication of an interstratification as must peak positions other than 16,9 Å after glycol solvation, when an interstratification with smectite as a major component can be assumed (Mills and Zwarich, 1972).

Kaolinite-smectite

So far, no ordered smectite-kaolinite mixed-layer mineral has been found (Reynolds, 1980). In the case of random kaolinite-smectite interstratifications the bases for identification are the $001_{\text{kaolinite}}/002_{\text{smectite}}$ and the $002_{\text{kaolinite}}/005_{\text{smectite}}$ reflections (Figure 1.3.). At higher smectite contents (more than 30%), a combined $002_{\text{kaolinite}}/004_{\text{smectite}}$ of low intensity appears as well (Cradwick and Wilson, 1972). An important feature of a kaolinite-smectite interstratification is the absence of any peak in the 5 Å region except for high smectite values of more than 75% and a high degree of smectite segregation. Characteristic migration curves for kaolinite-smectite interstratifications are presented in Figure 1.9.

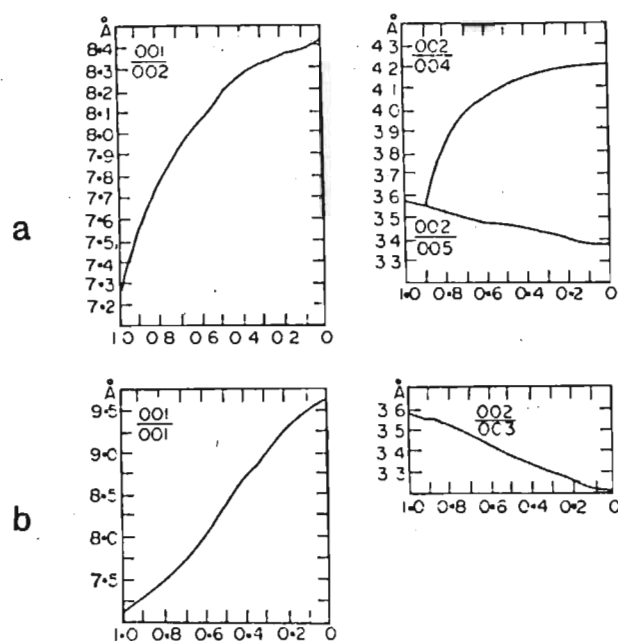


Figure 1.9 Peak migration curves for kaolinite-smectite interstratifications (a) kaolinite with glycol expanded smectite; (b) kaolinite with collapsed smectite (after Cradwick and Wilson, 1972).

1.4.2.2 Three- or multi-component interstratifications

XRD patterns of multicomponent systems are more difficult to interpret than those of two component interstratifications. While increased randomisation leads to peaks of reduced intensities in the case of a two-component system, it can lead to their effective extinction in the case of a three-component interstratification (Figure 1.10).

This is unfortunate, since multicomponent interstratifications can be assumed to be common in pedogenic environments where, for example, micaceous and/or chloritic parent materials may weather to smectite via mica-vermiculite-smectite or chlorite-

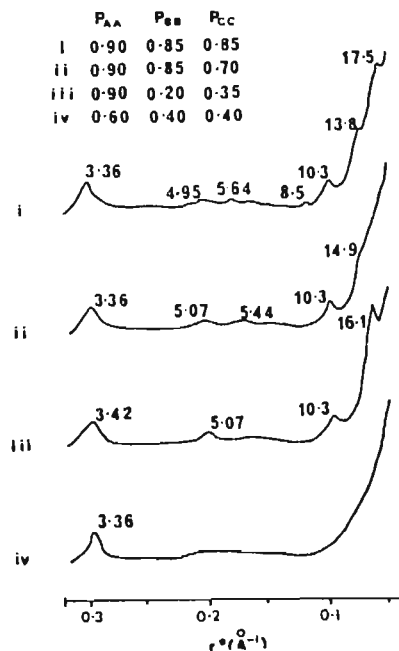


Figure 1.10 Calculated XRD patterns for a three-component interstratification with 60% mica, 20% vermiculite and 20% smectite (glycol). The various probability coefficients are given as p_{AA} for mica, p_{BB} for vermiculite and p_{CC} for glycolated smectite. Spacings corresponding to peak positions are marked in Å (after Cradwick and Wilson, 1978).

vermiculite-smectite intermediates, or where interstratified mica-smectite at the base of a pedon is converted to a mica-smectite-chlorite interstratification due to hydroxy aluminium interlayering. Thus Kodama and Brydon (1968) reported a mica-vermiculite-smectite interstratification in the A horizon from a Canadian podzol, while Cradwick and Wilson (1978) have published

the XRD pattern of a mica-vermiculite-smectite interstratification from a loessial soil from Poland.

The analytical system suggests that, for random interstratifications, mixed-layer maxima will appear intermediate to positions that would produce strong maxima from each of the components involved in the interstratification. This principle is correct generally, except for the case of components with primary maxima that are widely separated, i.e. the combined basal reflections of certain interstratifications. If the primary maxima are of great differences in \AA spacings, the first peak may not shift but will be strongly diminished in intensity or even eliminated. From this must follow that, whenever peaks are strongly decreased in intensity or eliminated, the interstratification is composed of components whose 001 peak positions are widely separated (kaolinite-smectite; mica-(glycol) smectite, etc.). Combined second order reflections are hardly affected by this type of intensity decrease, and the nature and proportions of the various components may be worked out from higher peak orders.

Methods may be applied of treating a three component interstratification in various ways to reduce it to a two-component system (K-saturation of a mica-vermiculite-chlorite interstratification will result in a two-component 10 \AA -14 \AA mixed-layer mineral). This procedure is essential in the recognition of a three component system, but it provides little information on the arrangement of the components.

1.5 Interstratified clay minerals : a new structural model based on charge consideration of interlayers.

The international (AIPEA) group definitions for 2:1 layer silicates are based upon differences in layer charge : smectite 0,2 - 0,6, vermiculite 0,6 - 0,9, illite 0,6 - 0,8, mica 1 and brittle mica 2 per $O_{10}(OH)_2$ (Bailey, 1980; 1982). A further differentiation into species is based on the seat of this charge (predominantly the tetrahedral or the octahedral sheet) and on chemical composition (see section 1.3). However, it is the spacing between layers which permits identification by means of XRD, since the layer itself has a very similar thickness in all 2:1 layer silicates. In fact, a layer can contribute to the XRD characteristics of a clay mineral only inasmuch as it is the seat of a charge deficit, which is balanced by counterions in the interlayer space. The nature of this charge (magnitude, distribution) determines whether or not interlayer spaces can be induced to expand or contract by the application of a number of standard treatments. The resultant shifts, if any, in the d-spacing are measured by X-ray diffractometry. The occurrence and extent of these shifts are governed by Coulombic attraction forces which may be modified by cation valency, radius and hydration, as well as by the polar nature and molecular size of compounds which are used to intercalate the stacked layers. X-ray identification is therefore based on differences in the interlayer charge density which emanates in turn from the layer charge. Despite the existence of a number of ancillary techniques (i.e. infrared spectroscopy, electron microscopy,

thermal and chemical analysis), the X-ray method remains a sine qua non for unambiguous clay mineral identification.

In this communication the classical structural models for interstratified (mixed layer) 2:1 phyllosilicates, formulated on the basis of X-ray diffraction data are questioned and an alternative model is presented which implies different stacking arrangements and may account more satisfactorily for certain observations relating to the genesis and behaviour of this family of clay minerals.

1.5.1 The classical concept

Reynolds (1980) defines interstratifications as "phyllosilicate structures in which two or more kinds of layers occur in a vertical stacking sequence, that is, along c." The stacking sequence may be either ordered or random. The classical view of the simplest possibility - an ordered two-component interstratification - can be illustrated by reference to aliettite, in which saponite layers are presumed to alternate regularly with talc layers (Alietti and Mejsner, 1980). The unit cell has a c dimension of 24,8 Å which is explained as the combined spacing of talc and saponite (Figure 1.11). Pure saponite has interlayer cations balancing the predominantly tetrahedral layer charge, whereas pure talc has no layer charge and no interlayer cations. The model in Figure 1.11 therefore represents an arbitrary assignment of one of the interlayers to the saponite layer and the other to talc in the aliettite unit cell. It is quite

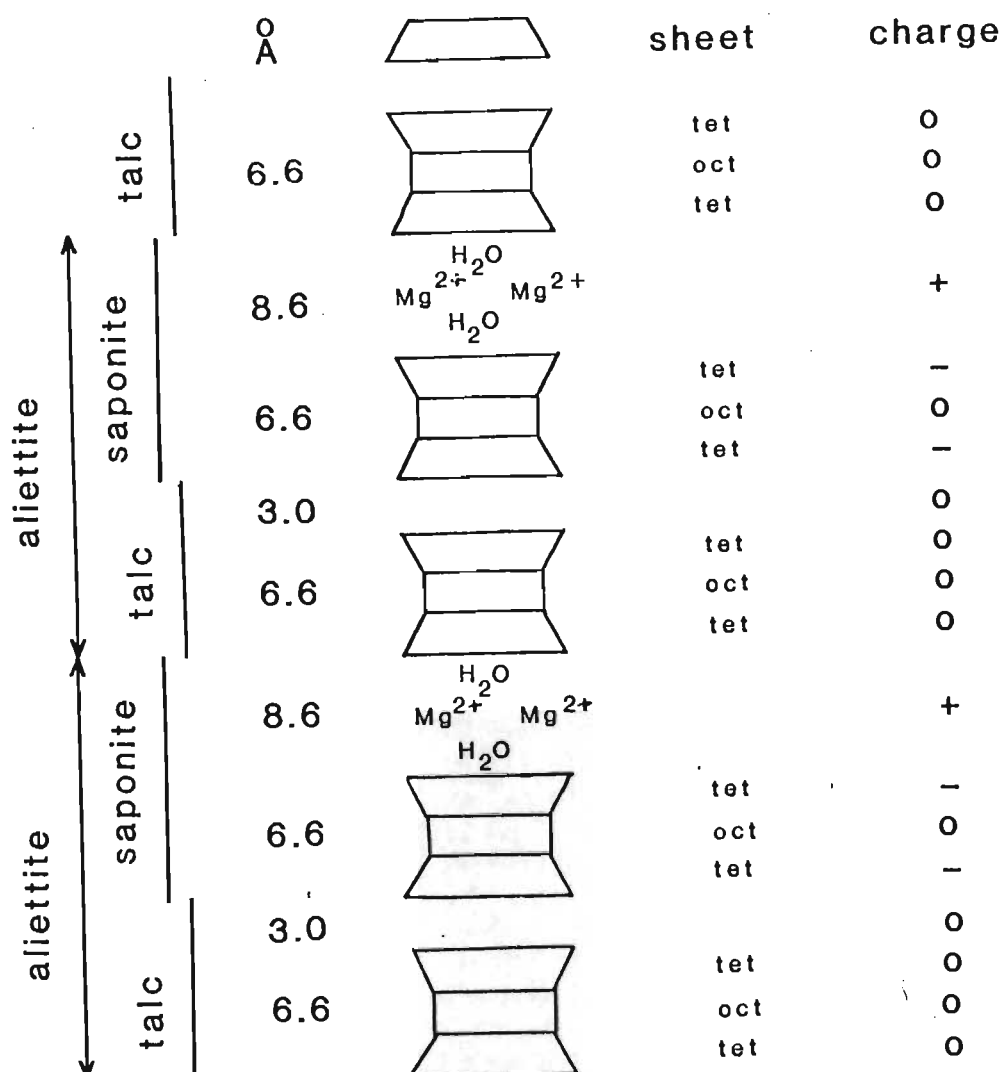


Figure 1.11 Aliettite structure : the classical concept.

clear, however, that the two interlayer spaces are different from their respective counterparts in pure saponite and talc. The "saponite" interlayer of aliettitite cannot have a charge density which is any different from that of the following "talc" interlayer.

Consequently there can be no sound reason for assuming that interlayer cations are confined to only one of the two aliettite interlayer spaces in the unit cell (Figure 1.11). Homogeneous cation distribution would necessitate a larger c dimension (about 30 Å). Thus the classical model fails, unless it is assumed that the layer charge of saponite is confined (or at least concentrated) in only one of the two tetrahedral sheets. This possibility cannot be easily demonstrated.

1.5.2 A proposed revised concept

The same consideration will apply to any other 1:1 interstratification. In order to demonstrate how this impasse may be overcome, various layer stacking arrangements (1:1, 2:1, 3:1) are presented for an ordered mica-smectite interstratification (visualized in this example as a pedogenic weathering product of mica in which the smectite component is beidellite rather than montmorillonite) in Figure 1.12. If the mica (M) and beidellite (B) layers are assumed to have charge densities of 1,0 and $0,4/0_{10}(\text{OH})_2$, respectively, then in the regular 1:1 stacking in Figure 1.12a, each interlayer space should possess a charge density of $(1 + 0,4)/2 = 0,7/0_{10}(\text{OH})_2$, equivalent to that of vermiculite (v). The X-ray diffraction pattern of this type of mixed layer should be that of a discrete vermiculite, the layer-interlayer sequence being MvBv. Thus a 1:1 stacking of different layers produces a 1:1 arrangement of identical interlayers. Since it is the properties of the interlayer which govern XRD identification, the c dimension of the unit cell in

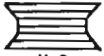
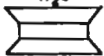
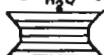
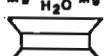
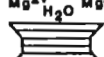
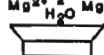
		charge / sheet or interlayer	unit cell Å
mica		-0.6	<div style="display: flex; align-items: center;"> <div style="border-left: 1px solid black; border-right: 1px solid black; height: 100px; position: relative;"> <div style="position: absolute; top: 0; right: 0; left: 0; bottom: 0; border-left: 1px solid black; border-right: 1px solid black;"></div> <div style="position: absolute; top: 15%; right: 0; left: 0; border-left: 1px solid black; border-right: 1px solid black;"></div> <div style="position: absolute; top: 30%; right: 0; left: 0; border-left: 1px solid black; border-right: 1px solid black;"></div> <div style="position: absolute; top: 45%; right: 0; left: 0; border-left: 1px solid black; border-right: 1px solid black;"></div> <div style="position: absolute; top: 60%; right: 0; left: 0; border-left: 1px solid black; border-right: 1px solid black;"></div> <div style="position: absolute; top: 75%; right: 0; left: 0; border-left: 1px solid black; border-right: 1px solid black;"></div> <div style="position: absolute; top: 90%; right: 0; left: 0; border-left: 1px solid black; border-right: 1px solid black;"></div> </div> <div style="margin: 0 10px;"> <div style="border-left: 1px solid black; border-right: 1px solid black; height: 15px; width: 10px; margin: 0 auto;"></div> <div style="border-left: 1px solid black; border-right: 1px solid black; height: 15px; width: 10px; margin: 0 auto;"></div> <div style="border-left: 1px solid black; border-right: 1px solid black; height: 15px; width: 10px; margin: 0 auto;"></div> <div style="border-left: 1px solid black; border-right: 1px solid black; height: 15px; width: 10px; margin: 0 auto;"></div> <div style="border-left: 1px solid black; border-right: 1px solid black; height: 15px; width: 10px; margin: 0 auto;"></div> <div style="border-left: 1px solid black; border-right: 1px solid black; height: 15px; width: 10px; margin: 0 auto;"></div> <div style="border-left: 1px solid black; border-right: 1px solid black; height: 15px; width: 10px; margin: 0 auto;"></div> </div> </div>
	Mg ²⁺ H ₂ O Mg ²⁺	+0.7	
beidellite		-0.2	
	Mg ²⁺ H ₂ O Mg ²⁺	+0.7	
mica		-0.6	
	Mg ²⁺ H ₂ O Mg ²⁺	+0.7	
beidellite		-0.2	
	Mg ²⁺ H ₂ O Mg ²⁺	+0.7	
mica		-0.6	
	Mg ²⁺ H ₂ O Mg ²⁺	+0.7	
beidellite		-0.2	
		-0.2	

Figure 1.12a Revised concept of a regular mica-beidellite interstratification


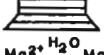
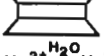

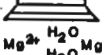
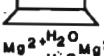
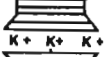
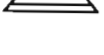
		charge / sheet or interlayer	unit cell Å
mica		-0.6	<div style="display: flex; align-items: center;"> <div style="border-left: 1px solid black; border-right: 1px solid black; height: 100px; position: relative;"> <div style="position: absolute; top: 0; right: 0; left: 0; bottom: 0; border-left: 1px solid black; border-right: 1px solid black;"></div> <div style="position: absolute; top: 15%; right: 0; left: 0; border-left: 1px solid black; border-right: 1px solid black;"></div> <div style="position: absolute; top: 30%; right: 0; left: 0; border-left: 1px solid black; border-right: 1px solid black;"></div> <div style="position: absolute; top: 45%; right: 0; left: 0; border-left: 1px solid black; border-right: 1px solid black;"></div> <div style="position: absolute; top: 60%; right: 0; left: 0; border-left: 1px solid black; border-right: 1px solid black;"></div> <div style="position: absolute; top: 75%; right: 0; left: 0; border-left: 1px solid black; border-right: 1px solid black;"></div> <div style="position: absolute; top: 90%; right: 0; left: 0; border-left: 1px solid black; border-right: 1px solid black;"></div> </div> <div style="margin: 0 10px;"> <div style="border-left: 1px solid black; border-right: 1px solid black; height: 15px; width: 10px; margin: 0 auto;"></div> <div style="border-left: 1px solid black; border-right: 1px solid black; height: 15px; width: 10px; margin: 0 auto;"></div> <div style="border-left: 1px solid black; border-right: 1px solid black; height: 15px; width: 10px; margin: 0 auto;"></div> <div style="border-left: 1px solid black; border-right: 1px solid black; height: 15px; width: 10px; margin: 0 auto;"></div> <div style="border-left: 1px solid black; border-right: 1px solid black; height: 15px; width: 10px; margin: 0 auto;"></div> <div style="border-left: 1px solid black; border-right: 1px solid black; height: 15px; width: 10px; margin: 0 auto;"></div> <div style="border-left: 1px solid black; border-right: 1px solid black; height: 15px; width: 10px; margin: 0 auto;"></div> </div> </div>
	K ⁺ K ⁺ K ⁺	+1.0	
mica		-0.6	
	Mg ²⁺ H ₂ O Mg ²⁺	+0.7	
beidellite		-0.2	
	Mg ²⁺ H ₂ O Mg ²⁺	+0.7	
mica		-0.6	
	K ⁺ K ⁺ K ⁺	+1.0	
mica		-0.6	
	Mg ²⁺ H ₂ O Mg ²⁺	+0.7	
beidellite		-0.2	
	Mg ²⁺ H ₂ O Mg ²⁺	+0.7	
mica		-0.6	
	K ⁺ K ⁺ K ⁺	+1.0	
mica		-0.6	
		-0.6	

Figure 1.12b Revised concept of an ordered mica (p = 0,66) beidellite (p = 0,33) interstratification

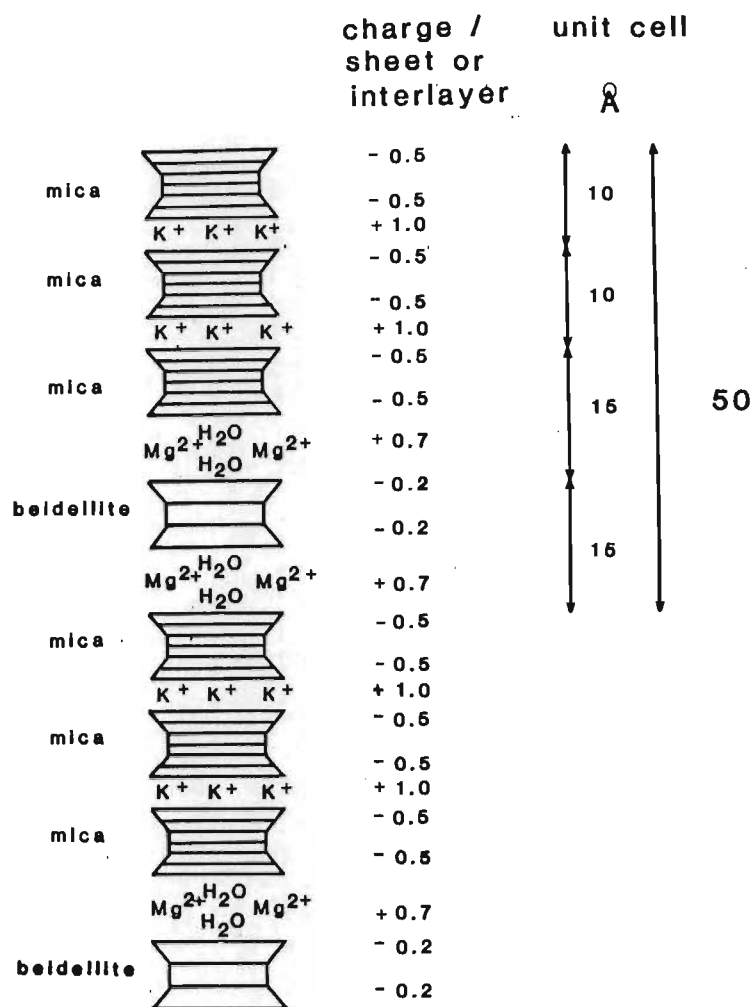


Figure 1.12c Revised concept of an ordered mica ($p = 0,75$)-beidellite ($p = 0,25$) interstratification

Figure 1.12a is effectively 15 Å and not 28 Å. By contrast, a 2:1 mica-beidellite arrangement gives rise to a 1:2 arrangement of mica-vermiculite interlayers (Figure 1.12b) with a stacking sequence of MmMvBv. Here the unit layer is 40 Å thick. Figure 1.12c shows that when three mica layers alternate with one beidellite layer (MMMB), the interlayer sequence is 2 mica 2 vermiculite (mmvv), with a 50 Å unit layer spacing. For such an arrangement, the (002) diffraction spacing would be 25 Å,

identical to the d_{001} value for 1 mica + 1 vermiculite of the classical model for a regular 1:1 interstratification (Figure 1.11). Available diffraction equipment might not reveal the (001) reflection of 50 Å for the Figure 1.12c arrangement because of the high background count at such low values. For these reasons it may well be that past studies which have identified an apparent 1:1 regular interstratification on the basis of a rational series of reflections, beginning with a spacing equal to the unit cell sum of the two components in their pure state, have misinterpreted the X-ray evidence. Instead, the mineral in question may as well have consisted of a 3:1 layer arrangement, with an associated 2:2 sequence of corresponding interlayer types, such that only the second and higher order reflections are revealed on the diffraction pattern.

Some important consequences emerge from this revised model. Currently there is some ambiguity inherent in the fact that vermiculite and illite are defined in terms of the same range of layer charge and yet vermiculite (with a few high charge exceptions) will, after having collapsed to 10 Å following K saturation, re-expand with ethylene glycol solvation to 14 Å (Machajdik and Cicel, 1981) whereas illite, by definition (Bailey et al., 1984), will not. This anomaly is not explained by the classical model. The model, proposed here, on the other hand, views vermiculite as a regular stacking of mica and smectite layers (Figure 1.12a). Increasing asymmetry of charge distribution from one layer to the next has been clearly shown (Lagaly, Schön and Weiss, 1972) to enhance the swelling potential of

smectites. Applied here, this principle permits the prediction of greater swelling capacity in vermiculite compared with illite if the latter does not possess the layer charge heterogeneity suggested by the model for vermiculite. Other ambiguities, such as a paraffin type layer arrangement or a monolayer-bilayer interstratification with alkylammoniumchloride as the charge balancing ion for the same charge density in the interlayer space (Lagaly, 1982) or a smectite-like response to ethylene glycol solvation and vermiculite-like behaviour with alkylammonium-chloride intercalation (Malla and Douglas, 1984) are potentially clarified by the new model.

A corollary also emerges. Just as the regular stacking of two differently charged layers may appear from X-ray diffraction data as a discrete mineral, so may the stacking of identical layers produce the X-ray spacings characteristic of a regular interstratification. This possibility must remain essentially hypothetical since it is untestable, resting as it does upon the requirement that asymmetry of charge distribution exists within each layer and that the resulting polarity of each successive layer along the c axis be reversed, such that successive interlayer spaces have markedly different charge densities. This question is only raised in order to demonstrate the possible alternatives which arise in the interpretation of X-ray diffraction data, and to emphasise that, should this last possibility be demonstrable, the classical model for interstratification would remain theoretically viable.

In conclusion it may be noted that there is some pedogenic evidence in favour of the revised model as it applies to the question of interstratified mica-smectite versus discrete vermiculite. Vermiculite is commonly considered on the basis of relative abundance, to be a highly transient intermediate in the weathering of mica to smectite (Kittrick, 1973).

1.6 Summary and discussion

Layer silicates are highly prone to a number of structural as well as stacking disorders, to charge heterogeneity, and to mixed-layer formation. Each of these factors, singly, may result in line broadening. Discrete minerals, irrespective of structural and/or stacking disorder, must give a rational series of reflections when saturated with divalent ions and ethylene glycol solvated, the only reason for irrationality being small particle size. Interstratifications will always give irregular sequences of peaks, except for regular cases, which are extremely rare, especially in a soil environment.

The ordering of layers in a mixed-layer structure profoundly alters the diffraction pattern, particularly at low angles, from the conditions expected for random stacking and especially for cases where the first order reflections of the components involved are widely separated.

In a two-component interstratification the amount and nature of the components may be worked out from tables and curves, which

show how the combined peaks migrate as the composition changes. For multi-component systems such tables are not available and the nature as well as the amount of the layers may be worked out by reducing the interstratification to a two-component system. Generally, broad shoulders are a strong indication for interstratifications as are peak positions other than regular ones. NB

It must be stressed that the definition of interstratification is based on the stacking of different layers, but the identification by means of XRD follows from the interlayers. The layer itself does not contribute to the XRD characteristics of the various 2:1 layer silicates, as its c-dimension is the same in all cases (6,6 Å). Consequently a regular ABAB structure is classically, but sometimes incorrectly, considered as having an abab interlayer sequence in which $a \neq b$, at least for some treatments. It is shown that the X-ray diffraction data from which the ABAB arrangement is inferred could as well be explained in terms of an alternative AAAB layer sequence, having an aabb interlayer arrangement. The 001 value for the incorrect AaBa assignment is identical to the 002 for the AaAaAbBb unit interlayer interpretation, for which d_{001} is large enough to escape detection. A regular interstratification of mica and smectite layers will be identified as a discrete vermiculite. The differences between similarly charged vermiculite (expanding) and illite (non-expanding) may thus be explained. Regular arrangements currently thought as being 1:1 may well be 3:1 in terms of layers, and 2:2 in terms of interlayers.

CHAPTER 2

MINERALOGICAL STUDY OF DOLERITE-DERIVED SOILS FROM THE IXOPO DISTRICT OF NATAL

2.1 Introduction

Karoo dolerites are ubiquitous in South Africa, cropping out intermittently over an area of some 570 000 km² between latitudes 26°S and 33°S (Orr, 1979). They constitute the parent material for a variety of soils with widely differing field characteristics (Beater, 1947; Beater and Frankel, 1965).

Detailed mineralogical investigation of dolerite-derived weathering products are scarce in South Africa and, with the exception of early works (Marchand, 1924; van der Merwe and Heystek, 1955; van der Merwe, 1962; van der Merwe and Weber, 1965), or deal predominantly with one or other aspect of soil formation on dolerite (de Villiers, 1962; Fitzpatrick and le Roux, 1977). The objectives of this study were (i) to investigate clay mineral formation in a number of soil profiles all derived from dolerite but possessing widely differing morphology; (ii) to establish the extent to which margalititic character, as recognized in the melanic and vertic diagnostic A horizons of the South African Binomial soil classification system (MacVicar, de Villiers, Loxton, Verster, Lambrechts, Merryweather, le Roux, van Rooyen and Harmse, 1977) is associated with clay mineral type; and (iii) to examine the extent to which vertic A horizons are

smectite-dominated and to make a detailed study of the character of the swelling components, previous studies of such soils having dealt with this aspect only superficially.

2.2 Materials and methods

Soil samples were collected from the property known as Melody Ranch in the Ixopo district of Natal, adjoining the road which connects the towns of Ixopo and Highflats. Country rocks comprise shales and fine grained sandstones of the Middle Ecca group which have been extensively intruded by dolerite sills and dykes of Jurassic age.

Relief is fairly marked, having been strongly patterned by the dolerite sills which impart a measure of resistance to denudation on crests and valley side slopes to produce an irregular, boulder-strewn topography in contrast to the smooth, concave-convex relief which develops on the horizontally bedded sediments. The dolerite outcrops are sufficiently extensive to permit the sampling of soils in which contamination of the parent material by colluviation from sedimentary rocks in the vicinity is negligible.

Recorded mean annual precipitation, which falls predominantly (75%) during summer months, is 844 mm, but probably varying orographically by 100 mm or more between the lowest (925 m) and the highest (1 124 m) elevations of the study area (Schönaau and

Boden, 1981). These extremes correspond approximately to bioclimatic groups 6 (moist tall grassveld) and 3 (Midland mistbelt), respectively, as defined by Phillips (1973). The change takes place dramatically over a distance of less than 1 km, with most of the area being intermediate between these classes. Mean annual temperature is between 15°C and 20°C. Soil climate according to the criteria of USDA Soil Taxonomy (Soil Survey Staff, 1975) is thermic, with an ustic soil moisture regime, approaching udic at the highest elevations.

The pedons sampled belong to the Oxisol, Ultisol, Mollisol and Vertisol orders (Soil Survey Staff, 1975) and are accommodated within six soil forms of the SA Binomial system (MacVicar et al., 1977). The major horizons of each profile were collected after making a detailed field description (Table 2.1). The position of the various profiles in relation to topography of the area is shown in Figure 2.1.

Cation exchange capacity and pH. CEC was evaluated using the BaCl₂ method of Gillman (1979). Extractable Ca and Mg were determined by atomic absorption and Na and K by flame emission spectroscopy. Soil pH was measured in a 1:2,5 suspension of soil in 0,01 M CaCl₂.

Particle size analysis was determined without pretreatment (except for Calgon treatment), applying the pipette method described by McKeague (1978), and calculating sand by difference. Dispersion was achieved by ultrasonic agitation (Labsonic 1510, B. Brown, Germany), with Calgon as dispersant.

Table 2.1 Soil profile characteristics for Melody Ranch samples

Profile nos	Soil form (soil series)	Great groups (approximate USDA equivalent)	Soil horizon	Depth (cm)	Munsell colour (moist)	Texture	Structure	Consistence
1	Rensburg (Phoenix)	Typic Pelludert	A ₁	0 - 15	10 YR 1,7/1	c	3 c s bk	mfi, ws, wvp
			A ₂	15 - 32	10 YR 2/1	c	m c a bk	mvfi, wvs, wvp
			G ₁	32 - 45	7,5 Y 4/1	c	c a bk	wvs, wvp
			G ₂	45 - 62	7,5 Y 5/0	c	m	wvs, wvp
			G ₃	62 - 105	5 BG 4/1	c	m	wvs, wvp
			C	110 +	10 YR 5-2			
2	Mayo (Msinsini)	Lithic Argiudoll	A ₁	0 - 35	7,5 YR 2/1	c	3 c s bk	dh, wp
			A ₂	35 - 75	7,5 YR 3/1	c	2-3 v c pr	dh, ws, wp
			B ₁	75 - 95	10 YR 3/2	c	3 m-c s bk	mvfi
			B ₂	95 - 135	10 YR 5/4	c	1 c s bk	mvfi
			C	140 +	10 YR 7/3	c		
3	Arcadia (Rydalvale)	"Lithic" Pelludert	A	0 - 40	7,5 YR 2/1	c	v3 bk	wp
			B	40 - 85	10 YR 4/3	c	4 bk	mvfi
4	Bonheim (Stanger)	Typic Paleudoll	A	0 - 35	5 YR 2/2	c	3 m s bk	mfr - fi
			B	35 - 65	5 YR 3/4	c	2 c s bk	m fr
5	Bonheim (Stanger)	Typic Paleudoll	A	0 - 40	5 YR 2/2	c	3 s bk	mfr
			B	40 - 70	5 YR 3/4	c	1 c s bk	m fr
6	Shortlands (Richmond)	Typic Rhodudult	A ₁	0 - 30	2,5 YR 2/2	c	3 s s bk	mvfi, wss
			A ₂	30 - 60	2,5 YR 2/3	c	2-3 f+m s bk	mvfi, ws, wp
			B	60 - 85	2,5 YR 3/4	c	1-2 f-m s bk	mfi, wp
			C ₁	120	5 YR 5/8	c		
			C ₂	120	7,5 YR 5/6			
7	Hutton (Vimy)	Typic Rhodudult	A	0 - 45	10 R 2,5/2	c	3 s bk	mvfi, wss
			B	45 - 75	2,5 YR 2/3	c	2 f+m s bk	mvfi, ws, wp
8	Hutton (Balmoral)	Typic Umbriorthox	A	0 - 35	5 YR 2/2	c	3 m s bk	mfr - mfi
			B ₁	35 - 80	5 YR 3/4	c	1 c s bk	mfr
			B ₂	80 - 105	5 YR 3/4 - 3/6	c	Apedal	d l - m fi

Horizon nomenclature and abbreviation for colour, texture, structure and consistence according to Soil Survey Staff, 1975

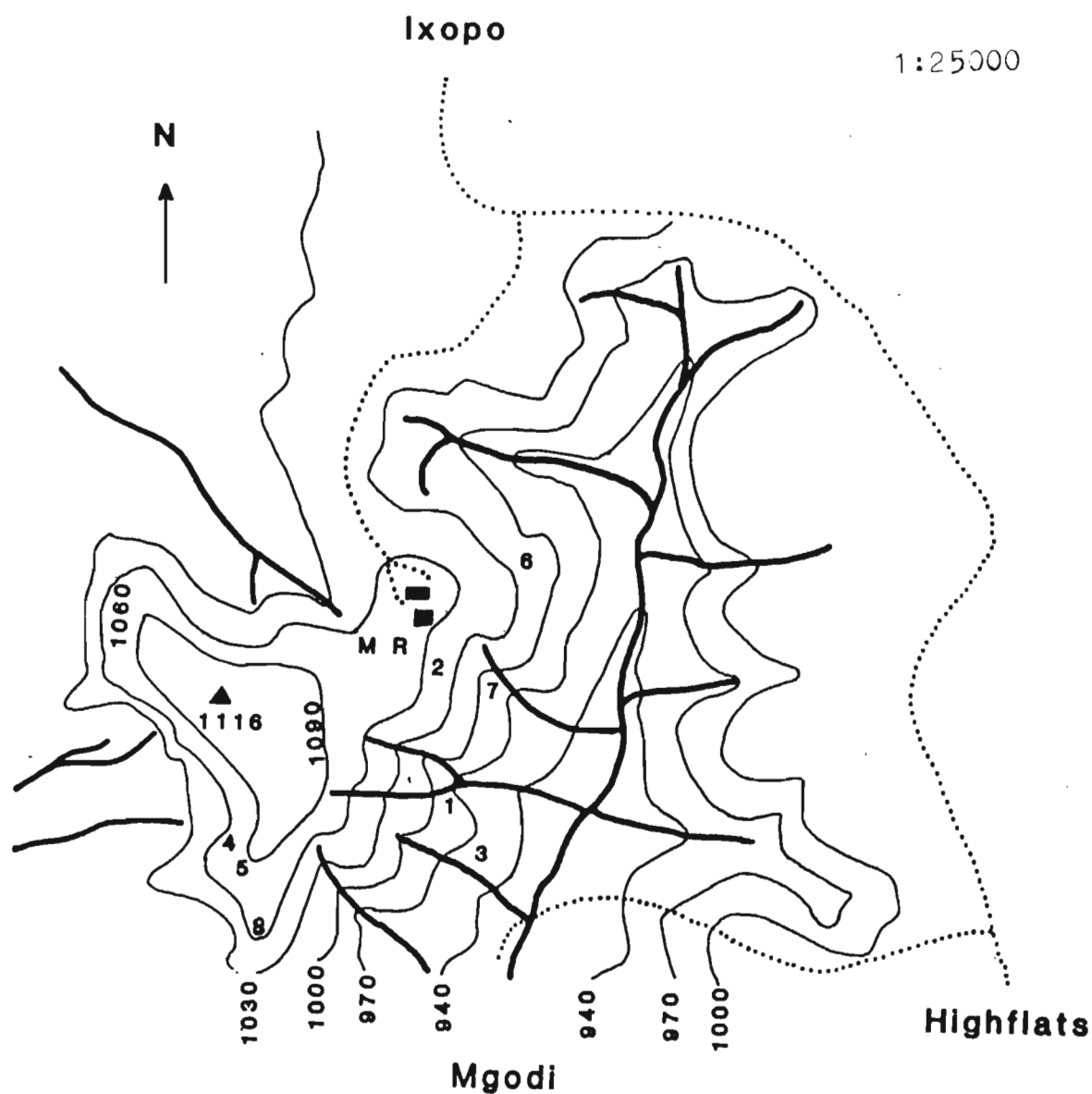


Figure 2.1 Location of sampling sites on Melody Ranch

1 Rensburg	: roads
2 Mayo	_____	: drainage lines
3 Arcadia	_____	: contour intervals (m)
4 + 5 Bonheim	M R	: Melody Ranch homestead
6 Shortlands		
7 + 8 Hutton		

Removal of iron and manganese oxides was effected by the method of Mehra and Jackson (1960) with Na-DCB (sodium dithionite-citrate-bicarbonate). The quantity of Fe and Mn extracted was determined by atomic absorption spectroscopy.

X-ray diffractometry. X-ray data were obtained using a Philips X-ray diffractometer with a graphite monochromator and Fe-filtered Co-K α radiation generated at 40 kV and 40 mA. Oriented specimens were scanned in the step-scan mode at 1 min/1° 2 θ over the 2 θ range 2 - 35°. The semi-quantitative estimation of the whole soil mineral composition was carried out by measuring the height of the strongest peak of each mineral, detectable by means of XRD in the random powder pattern. The values at the various heights were added together and equalled 100%. The amount of the various minerals is presented as peak height percentage.

For the semi-quantitative evaluation of the clay fraction, peak areas (measured as height x half width from the Mg-saturated, air-dried pattern) were used instead of peak heights, the subsequent procedure being the same as for the whole soil minerals. No correction factor was used for any of the minerals.

A range of classical and less widely used methods of mineralogical differentiation were applied. First, material of the whole soil was examined by grinding and mounting into rectangular aluminium frames, the powder being pressed against filter paper covering the surface in order to achieve as random an orientation

as possible.

Secondly, the clay-size fraction was extracted and subjected to a variety of pretreatments as follows. Soil material was dispersed in distilled water by ultrasonication and the $< 2 \mu\text{m}$ fraction separated by centrifugation. In cases where good dispersion could not be achieved after three washings with distilled water, pH adjustment was employed to aid dispersion. Chemical pretreatment for the removal of organic matter, iron minerals and carbonates was avoided, since this may affect the clay characteristics. Clay fractions were rendered homoionic by shaking in a chloride solution of the desired cation for one hour, then leaving to equilibrate overnight. Cations were used in the following concentrations : Mg and K : 1 mol dm^{-3} ; Li: 3 mol dm^{-3} . The flocculated clay was freed of excess salt by repeated centrifugation and dialysis and freeze dried.

Orientation of the clay on glass slides was achieved by the smear method (Gibbs, 1965), so as to provide optimal orientation and the truest reflection possible of the proportions of different clay minerals present.

Expansion tests were performed by solvation with ethylene glycol vapour at 60°C for 24 h and glycerol vapour at $80 - 90^{\circ}\text{C}$ for 24 h (Novich and Martin, 1983), hydrazine, in vacuo for 4 days (Range, Range and Weiss, 1969) and formamide, a few drops being added to the air-dried specimen on the glass slide, which was then X-rayed 10 minutes after formamide addition (Theng and Churchman, 1982;

Churchman and Theng, 1984).

Potassium-saturated samples were heated at 300°C and 500 °C and Li-saturated clays at 290°C, for 4 h.

Two methods were applied for the differentiation of smectite into species : the alkylammoniumchloride method and the Greene-Kelly test (Greene-Kelly, 1953).

Alkylammoniumchloride intercalation. The charge density of the smectite was estimated by comparing the basal spacings of its dodecylammoniumchloride complex with the c_{12} spacings of vermiculite (Lagaly, 1982), beidellite and montmorillonite (Lagaly et al., 1976). The method of intercalation was as follows :

Dodecylamine (to give a final concentration of a 0,1 M solution) was dissolved in a small amount of pure ethanol. A water-ethanol mixture (1 : 1) was slowly added, avoiding intense clouding and the pH adjusted to 6 - 7 with HCl. A 7,5 cm³ aliquot of this dodecylammoniumchloride solution was added to 30 mg of freeze-dried clay. The suspension was heated at 65°C for two days, the solution being replaced after one day. Excess dodecylammoniumchloride was removed by repeated washings (ca. 10) with a water-ethanol mixture (1 : 1) and two final washings with pure ethanol. The paste was then spread on a glass slide, dried at 65°C, stored in a desiccator and analysed by XRD.

Greene-Kelly test. Heating of the Li-saturated sample on the glass slide was avoided because of exchange of Li by Na from the

soda-lime glass (Byström Brusewitz, 1975) and was conducted instead upon freeze-dried clay in a ceramic crucible.

Mica-smectite (glycol) peak migration tables (Table 1.2) and computer-calculated patterns (Figure 1.8) were used for final judgement of the ratio of the smectite species.

Infrared spectroscopy. Infrared absorption spectra were recorded on the Perkin Elmer infrared spectrophotometer 283 using KBr pressed discs containing 1% (4 000 cm^{-1} to 2 000 cm^{-1}) and 0,35% (2 000 cm^{-1} to 200 cm^{-1}) sample material. Weakly adsorbed water was removed by heating the disc overnight at 150°C.

Electron microscopy. Hand-picked white (plagioclase) and black (pyroxene) particles from the Mayo B horizon were cemented on to Al stubs, sputtercoated with gold and examined with a Jeol T 200 scanning electron microscope. A drop of the clay suspension of the same horizon was placed on to a Formvar coated Cu-grid and air-dried before viewing with a Jeol 100 CX transmission electron microscope.

2.3 Results and discussion

2.3.1 XRD investigation

A great variability in the extent of weathering and in the nature of the weathering products characterizes the dolerite derived pedons at Melody Ranch.

The seven soil profiles investigated could be subdivided on the basis of clay mineral composition into :

- (a) smectite dominated soil (Rensburg);
- (b) soils with about equal proportions of smectite and kaolinite (Mayo, Arcadia); and
- (c) kaolinite dominated soils (Bonheim, Shortlands, Hutton).

In the smectite containing profiles (a and b) the whole mineral assemblage included the dolerite derived minerals plagioclase (labradorite), pyroxene (both monoclinic and orthorhombic) and, locally, olivine. The kaolinite dominated soils (c) did not contain any mafic minerals detectable by XRD.

2.3.1.1 Smectite dominated soil

Feldspar and pyroxene dominate the whole-soil mineralogy in the lower half of the profile, decreasing towards the surface mainly in favour of quartz (Figure 2.2).

Smectite and kaolinite are the weathering products of the dolerite.

The clay fraction ($< 2 \mu\text{m}$ diameter) contains vermiculite, beidelite, kaolinite and talc, with the swelling mineral group dominant. Although no significant increase of one mineral group relative to the others could be observed within the profile, there was a decrease in the degree of crystallinity of the 14 Å minerals from the saprolite to the G₂ horizon as shown by peak broadening in Figure 2.3.

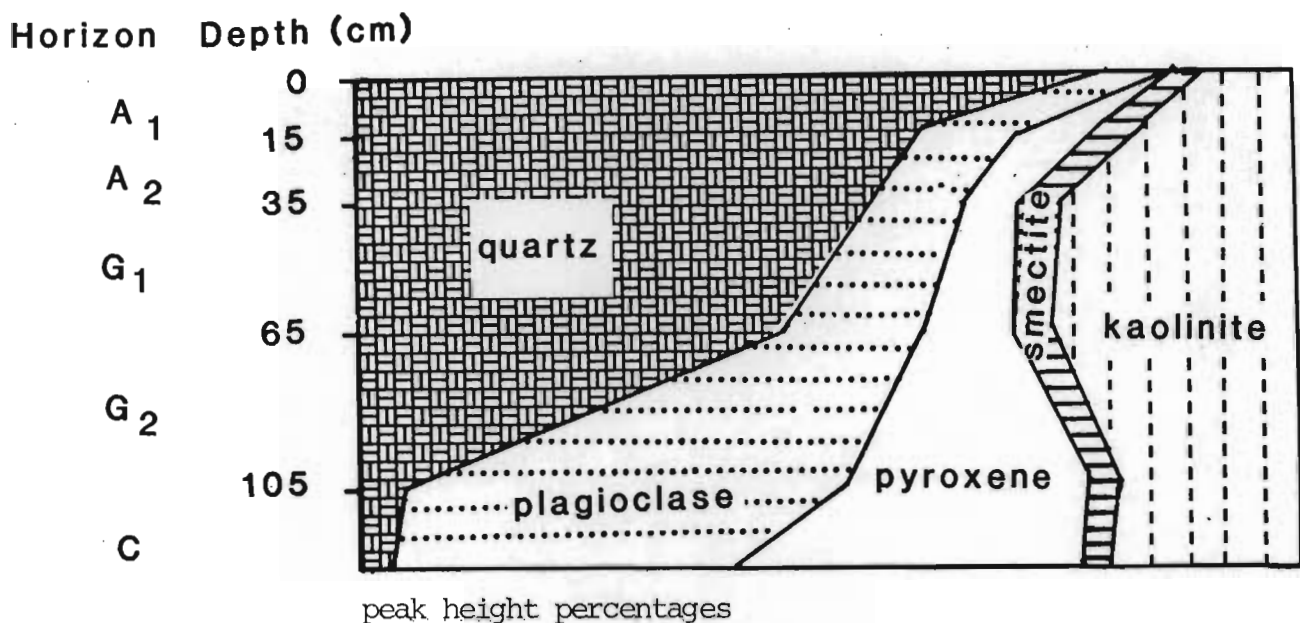


Figure 2.2 Whole-soil mineral distribution in the profile of the Rensburg soil constructed from relative XRD peak heights

Weathering of dolerite appears to result in the formation initially of vermiculite (22 Å reflection in the dodecylammonium-chloride intercalated pattern, 14 Å spacing in the Mg-saturated, glycerol solvated pattern), which is transformed to beidellite (17,7 Å reflection in the dodecylammoniumchloride intercalated state; 17 Å peak in the Mg-saturated, glycerol solvated pattern) with increasing distance from the saprolite (Figures 2.3 and 2.4). The layer charge of this vermiculite must be close to that of the smectite-vermiculite boundary, since the mineral forms an ethylene glycol double layer after Mg-saturation (Figure 2.3) and is characterized by a spacing of 12,4 Å in the K-saturated, air-dried state (Figure 2.5). The beidellitic nature of the smectite in the G₁ and the two A horizons was confirmed by

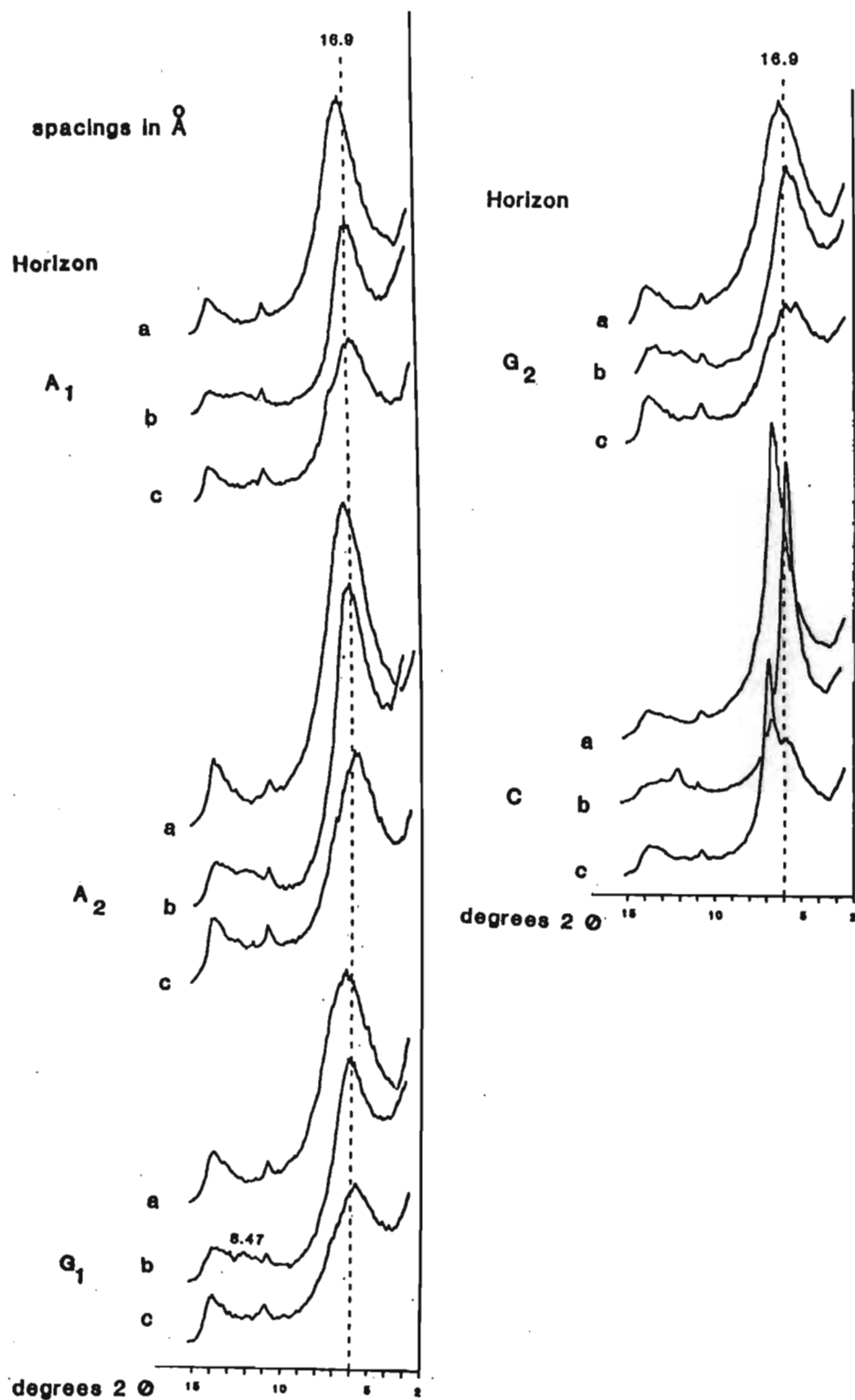


Figure 2.3

XRD traces of the clay fraction (oriented preparation) from horizons of the Rensburg soil profile

(a) Mg-saturated, air-dried

(b) Mg-saturated, ethylene glycol solvated

(c) Mg-saturated, glycerol solvated

(broken line at 16,9 Å represents peak position of discrete smectite treated with Mg + ethylene glycol)

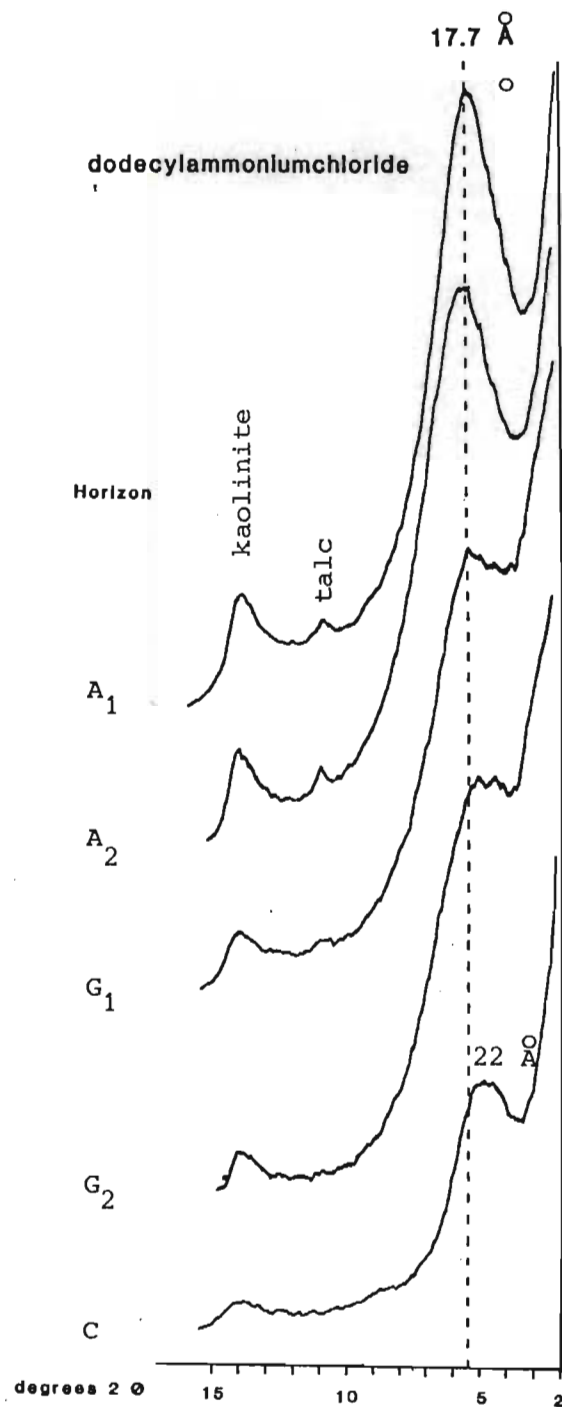


Figure 2.4 XRD traces of the clay fraction (oriented preparation) from horizons of the Rensburg soil profile after dodecylammoniumchloride intercalation (broken line represents peak position of discrete beidellite)

dodecylamine intercalation (17,7 Å; Figure 2.4) and glycerol bi-layer formation after Mg-saturation (Figure 2.3). A broad shoulder in the K-saturated, 500°C-heated sample suggests that the beidellite is partially chloritized (Figure 2.5). The amount of this chloritic component increases towards the surface, reaches its maximum in the A₂ horizon, but is generally low.

A high background between 10 Å and 7 Å indicates interstratified material, the nature of which cannot be identified due to the presence of discrete smectite/vermiculite and kaolinite. The broadness of the "peak", bridging the whole region between kaolinite and the high angle side of the 14 Å mineral indicates an interstratification of components the primary peak maxima of which are widely separated (smectite-kaolinite for example). Absence of halloysite was confirmed by the formamide-test (Figure 2.6).

2.3.1.2 Soils with co-dominant kaolinite and smectite (Mayo and Arcadia profiles)

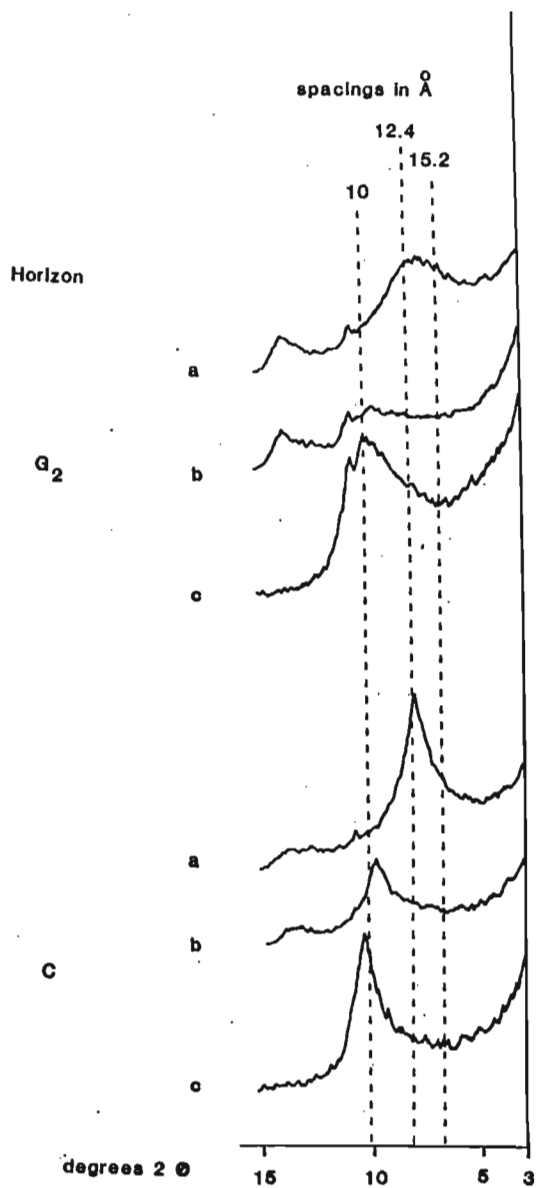
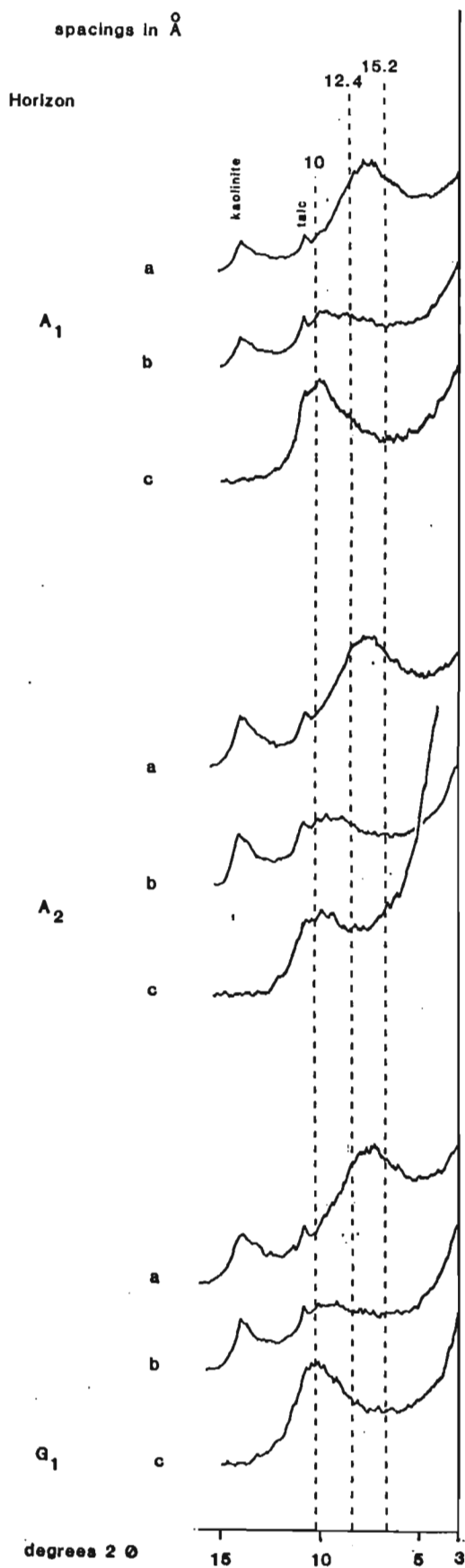
(a) Mayo profile

The whole soil samples consist of labradorite, hypersthene, olivine, quartz, amphibole, kaolinite and smectite (Figure 2.7). The composition of feldspar and pyroxene could be established by XRD investigation of hand-picked white and black grains from the > 500 µm fraction of the saprolite.

Figure 2.5 XRD traces of the clay fraction (oriented preparation) from horizons of the Rensburg soil profile

- (a) K-saturated, air-dried
- (b) K-saturated, 110°C
- (c) K-saturated, 500°C

(Broken lines represent peak positions of collapsed smectite/vermiculite (10 Å), of 14 Å minerals with a water-monolayer (12,4 Å) and a water-bilayer (15,2 Å) in each interlayer space)



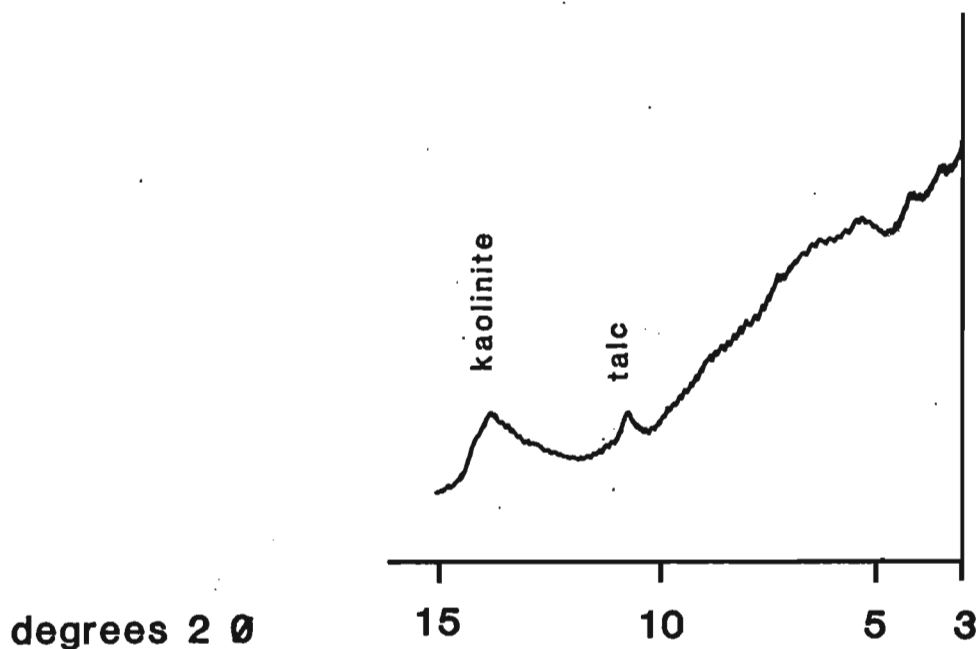


Figure 2.6 XRD trace of the clay fraction (oriented preparation) from the Rensburg G₂ horizon after formamide intercalation

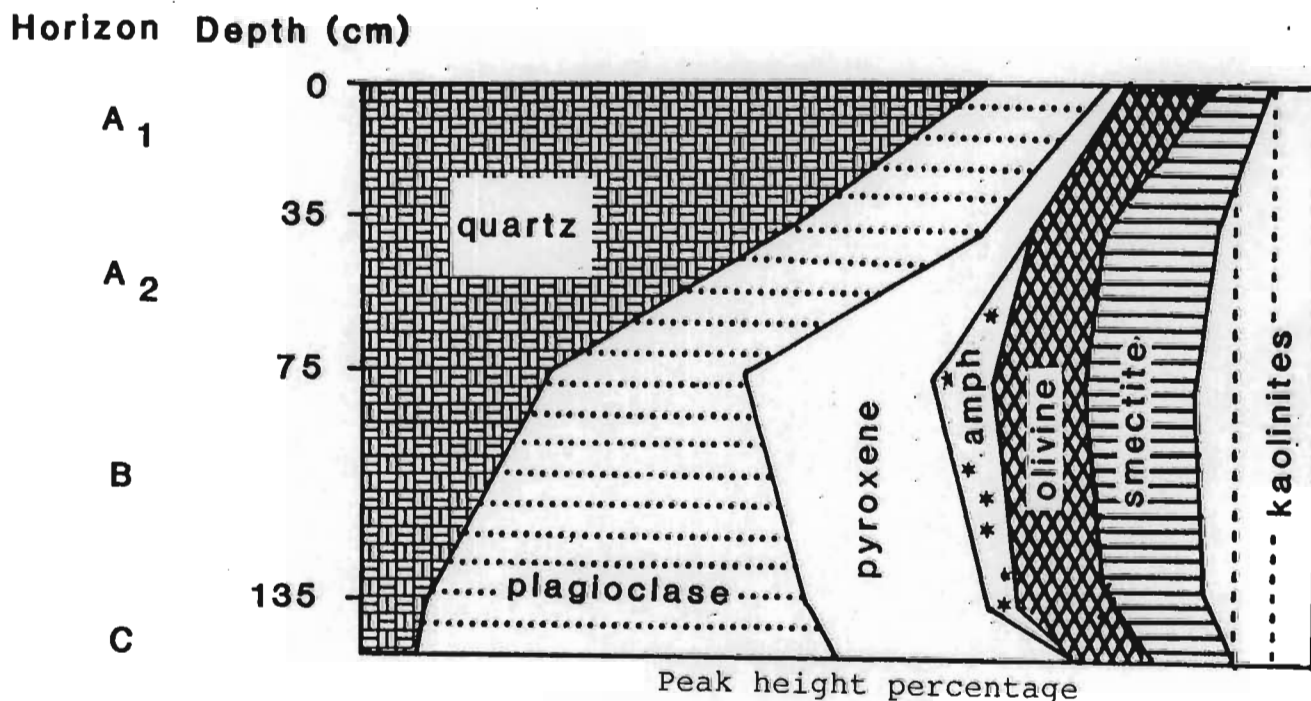


Figure 2.7 Whole-soil mineral distribution in the profile of the Mayo soil (constructed from relative XRD peak heights) (amph = amphibole)

A decrease in the content of primary minerals and an increase of quartz towards the top of the profile is clearly evident (Figure 2.7). Feldspar and olivine seem to be more resistant to weathering than pyroxene, and are still present in the A horizon (Figure 2.7). The presence of olivine in the surface horizon is remarkable, as this mineral is generally assumed to be most susceptible to weathering.

From field observation, a large number of indurated iron concretions are present in the three uppermost horizons. They comprise about 30% of the > 500 um fraction in these horizons. No distinct goethite peak could be observed, however, in the whole-soil patterns. An investigation of these pellets showed that about 80% of them consist of manganite only, the remaining containing goethite and a small quantity of magnetite. Both the manganite and the goethite are very poorly crystalline - the X-ray pattern of the hand-picked concretions showed the strongest reflection only.

Investigation of the hand-picked labradorite and hypersthene grains showed that the clay mineral formation seems to be associated with hypersthene rather than feldspar. No clay peaks were observed in the plagioclase pattern (Figure 2.8) while the hypersthene pattern showed 14 θ and 7 θ reflections and the same peak intensity ratio observed in the pattern of the oriented clay fraction of the Mayo B horizon (Figures 2.9 and 2.10). This observation is in agreement with the findings of some authors (Berner and Holdren, 1977; Wilson, 1975), that plagioclase

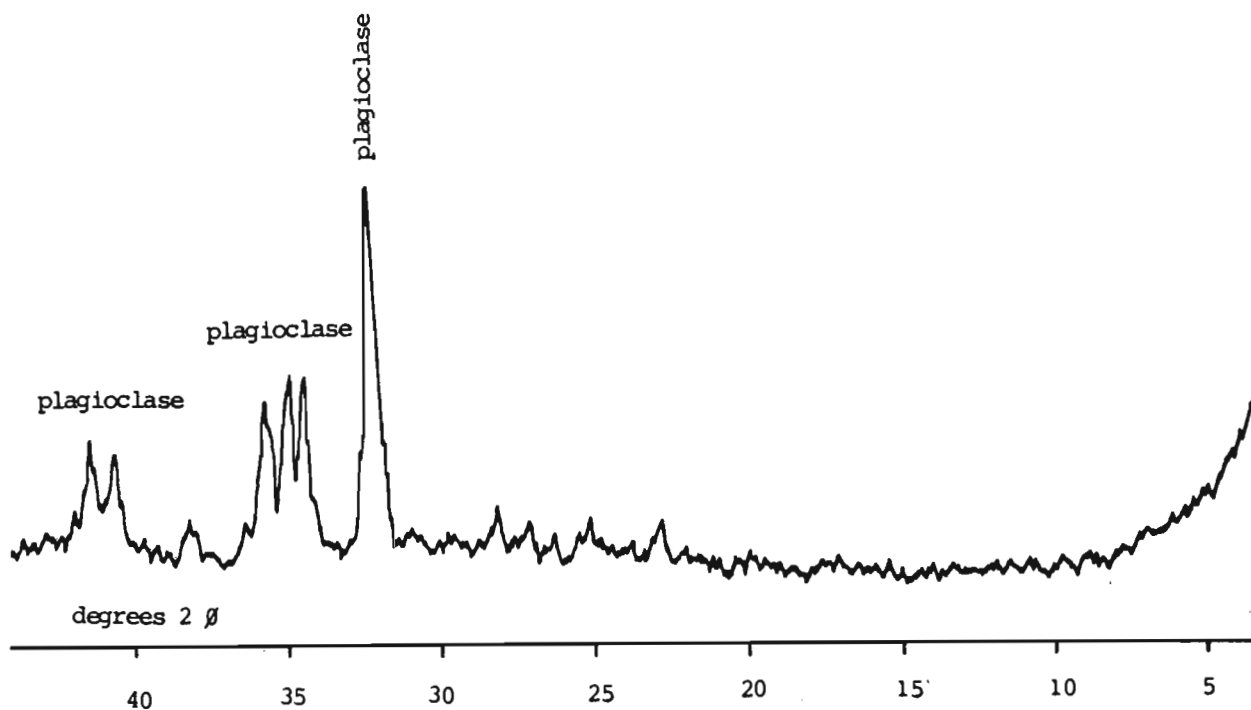


Figure 2.8 XRD powder pattern of hand-picked white grains (plagioclase) from the Mayo B horizon

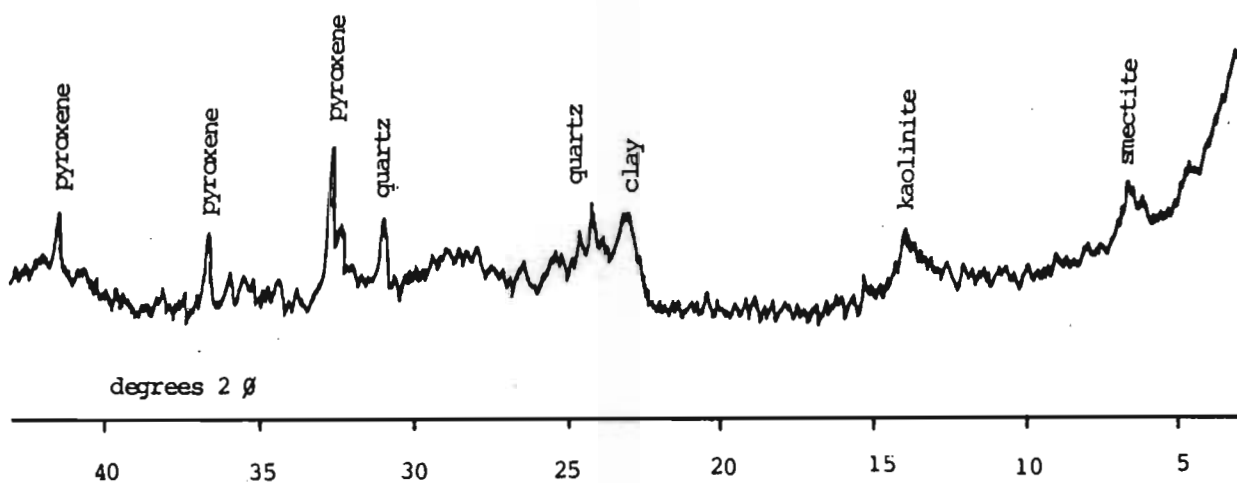


Figure 2.9 XRD powder pattern of hand-picked black grains (pyroxene orh) from the Mayo B horizon

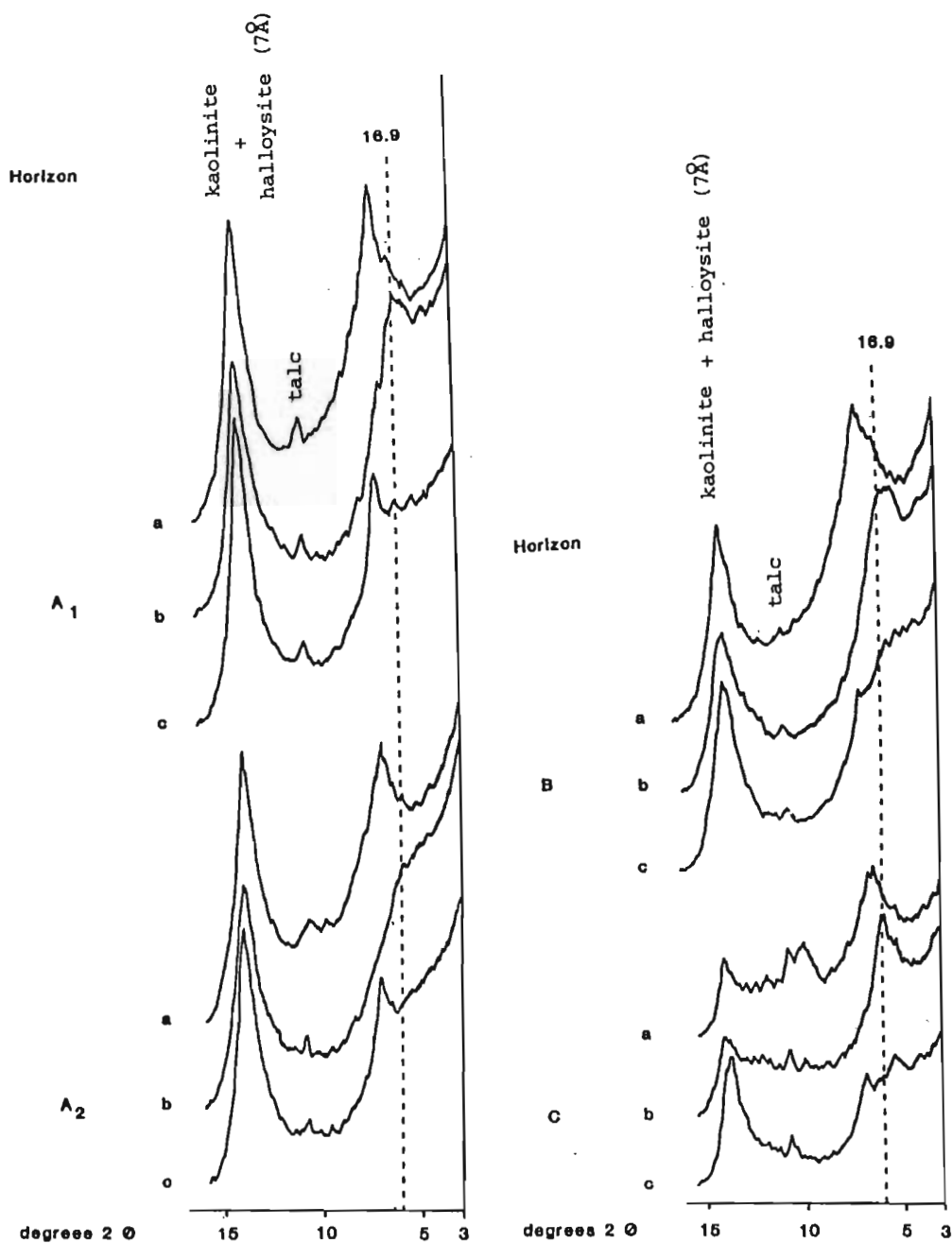


Figure 2.10 XRD traces of the clay fraction (oriented preparation) from horizons of the Mayo soil profile

(a) Mg-saturated, air-dried

(b) Mg-saturated, ethylene glycol solvated

(c) Mg-saturated, glycerol solvated

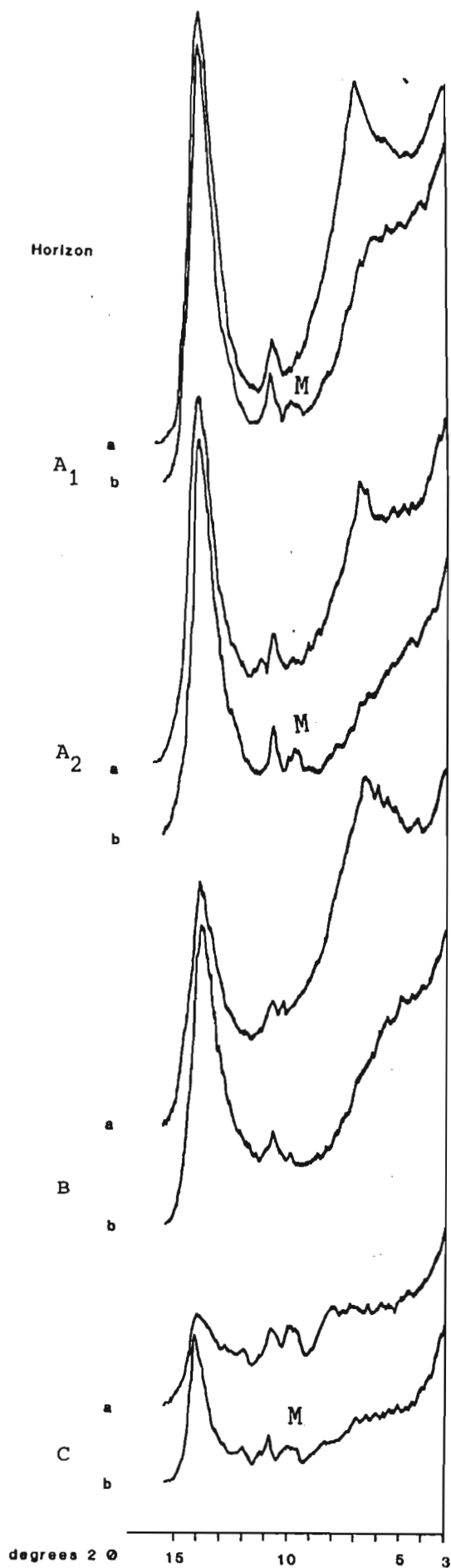
(broken line represents peak position of a discrete smectite with Mg + ethylene glycol)

weathers by releasing ions into solution mainly. By migration of these ions, mainly Al^{3+} , kaolin minerals could be formed by precipitation at the hypersthene surface. The results contradict, however, the observations of a number of authors who regard the formation of smectite or kaolinite/halloysite as the main feature of feldspar transformation (among others Suttner et al., 1976; Eswaran, 1979; Page and Wenk, 1979; Gilkes, Suddhiprakarn and Armitage, 1980).

The formation of kaolinite as a weathering product of primary minerals, containing hardly any aluminium (orthorhombic pyroxenes, olivine) has been reported by many authors (Pion, 1979; Nahon, Colin and Tardy, 1982; Rodriguez, 1982). Scanning electron microscope investigations (Section 2.3.2) of the hand-picked plagioclase and pyroxene grains confirmed the results obtained by XRD methods, concerning the association of clay minerals with pyroxene only.

The clay fraction of the Mayo profile is characterised by considerable diversity in the mineral assemblage: halloysite 10 Å, halloysite 7 Å, kaolinite, vermiculite, montmorillonite and talc could all be determined as discrete minerals; the 14 Å and kaolin groups are present in about equal amounts in all soil horizons (Figures 2.10 and 2.11).

The main differences between soil horizons are in the hydration state of the halloysite, and in the kaolinite/halloysite ratio.



M is discrete montmorillonite

Figure 2.11

XRD traces of the clay fraction (oriented preparation) from horizons of the Mayo soil profile

(a) Li-saturated, air-dried

(b) Li-saturated, 290°C, ethylene glycol solvated

Vermiculite (14 Å in the Mg-saturated, glycerol treated sample; Figure 2.10) is present in each soil horizon, the amount being lowest in the B and C horizons. The layer charge of this vermiculite is probably close to that which characterises the smectite-vermiculite boundary, since the mineral expands with ethylene glycol to 17 Å. (Alternatively, it may be interstratified with smectite.) Discrete montmorillonite (10 Å in the Li-saturated, 280°C, ethylene glycol-solvated pattern) is found in small amounts in the C and the two A horizons (Figure 2.11). The remarkable broadening of the 17 Å peak after application of the Greene-Kelly test suggests that high amounts of montmorillonite are interstratified with beidellite in the smectite crystallite. Comparisons of computer-calculated patterns (Figure 1.8) with the experimental ones suggests that 60 - 70% of the 14 Å component is montmorillonite interstratified with vermiculite and/or beidellite. Charge heterogeneity is also indicated from the K-saturated, air-dried, pattern by peak positions intermediate between 15 Å (water bi-layer) and 12,4 Å (water mono-layer) (Figure 2.12). Discrete beidellite (which would produce a discrete 17 Å peak in the Li-saturated, 280°C, ethylene glycol pattern) does not seem to occur in the Mayo soil.

Halloysite 10 Å (a 10 Å peak in the air-dried pattern irrespective of cation saturation and collapse to 7 Å upon heating to 110°C) seems to be present in the saprolite horizon only (Figure 2.13).

Halloysite 7 Å (a 7 Å peak which expands to 10 Å upon formamide

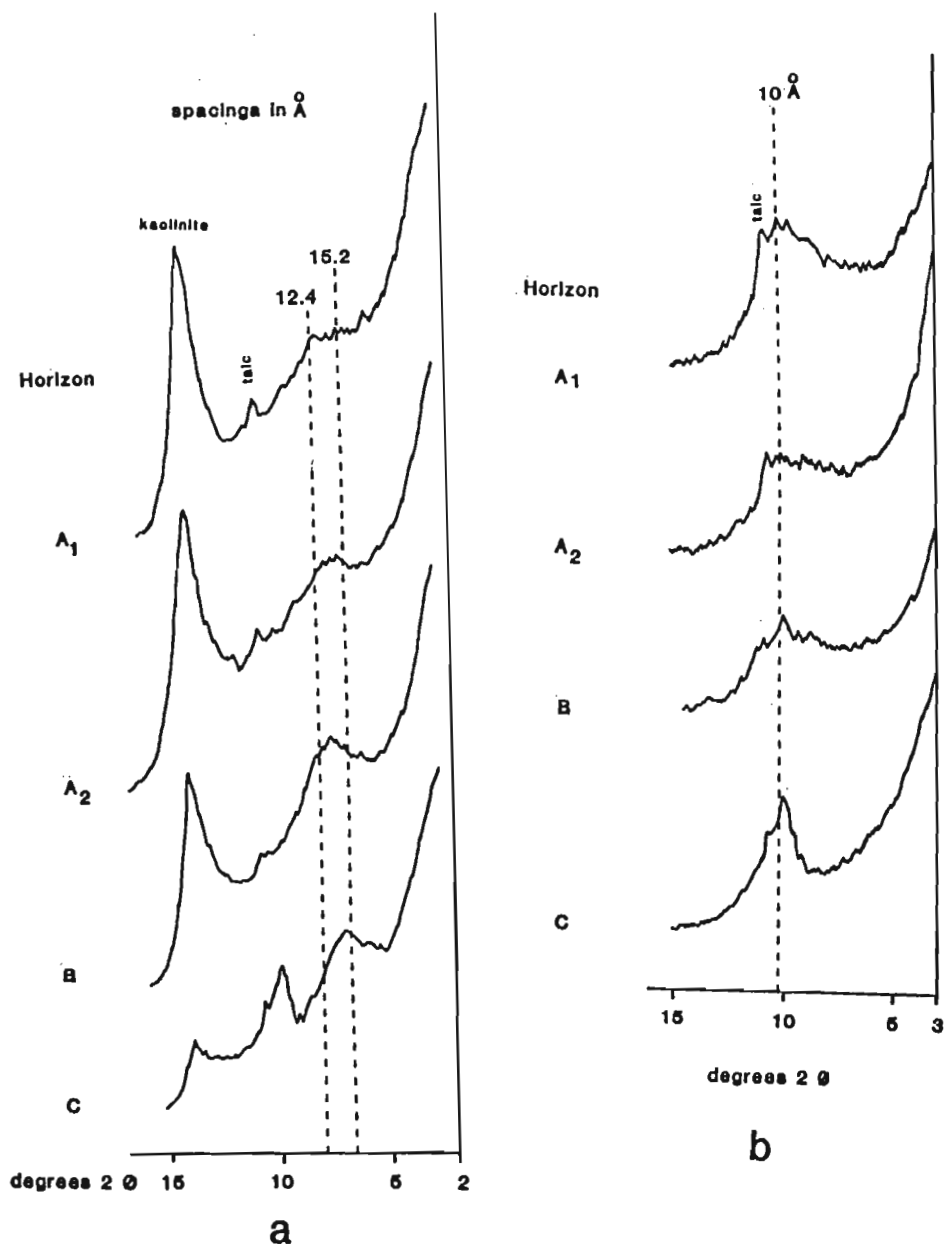


Figure 2.12 XRD traces of the clay fraction (oriented preparation) from horizons of the Mayo soil profile

(a) K-saturated, air-dried (broken lines indicate peak position of smectite with a water mono-layer ($12,4 \text{ \AA}$) and a water bi-layer ($15,2 \text{ \AA}$) in each interlayer space)

(b) K-saturated, 500°C (broken line represents peak position of discrete smectite and vermiculite)

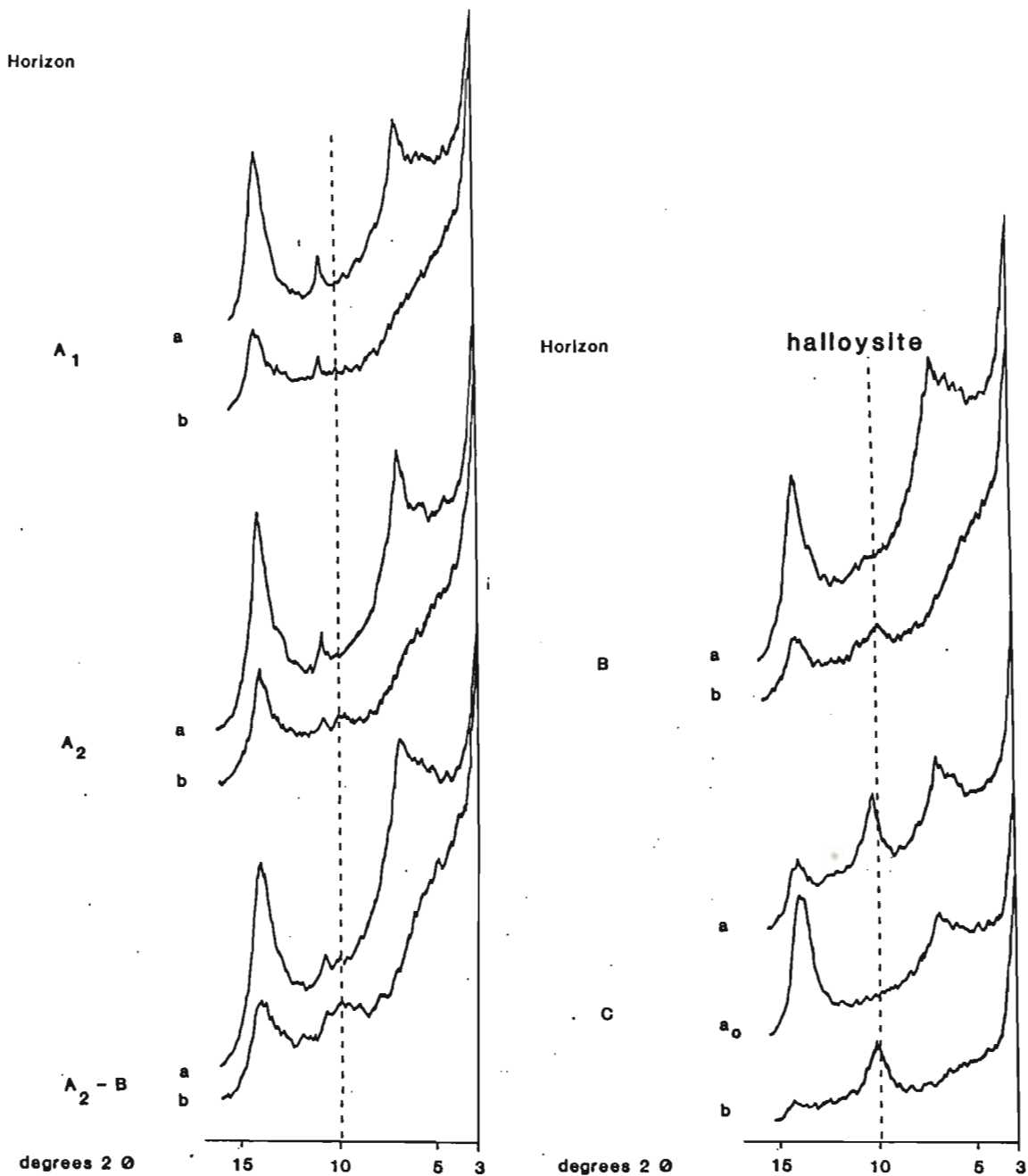


Figure 2.13 XRD traces of the clay fraction (oriented preparation) from horizons of the Mayo soil profile

(a) Mg-saturated, air-dried

(a₀) Mg-saturated, 110°C

(b) Mg-saturated, formamide intercalated

(broken line represents position of the formamide intercalated halloysite (10,4 Å) and of naturally occurring halloysite 10 Å)

intercalation) is present in each horizon with the exception of the surface one.

The content of halloysite decreases towards the top of the profile where it is replaced by kaolinite (Figure 2.13).

These findings support two different observations concerning the genesis of halloysite : (i) the transformation of halloysite (10 Å) to halloysite (7 Å) is a common weathering sequence (Aomine and Wada, 1962; Churchman, Aldridge and Carr, 1972); (ii) halloysite gives way to kaolinite as weathering advances (approach to the soil surface) (Loughnan, 1981).

The smectite in all horizons of the Mayo profile was found to exhibit a gel-like swelling behaviour, i.e. upon standing, the suspension underwent gelation. According to Lagaly, Schön and Weiss (1972), only smectites with a medium to low layer charge and especially a broad variation within these charge limits show this swelling effect. The wide layer charge spectrum of the swelling clay minerals in the Mayo soil profile and their medium to low layer charge is thus in agreement with the findings of Lagaly et al. (1972).

A mineral of the talc group (9,45 - 9,5 Å) is present in very small quantities. More attention is given to this component in Chapter 4.

Profile morphological indications that the upper part of the Mayo soil may have a colluvial origin, could not be

confirmed by similarity of the clay mineral association, unless it is assumed that the colluviated material contains a similar mineral suite.

(b) Arcadia profile

The A and B horizons (whole soil) consist of feldspar, pyroxene, quartz, kaolinite and smectite (Figure 2.14).

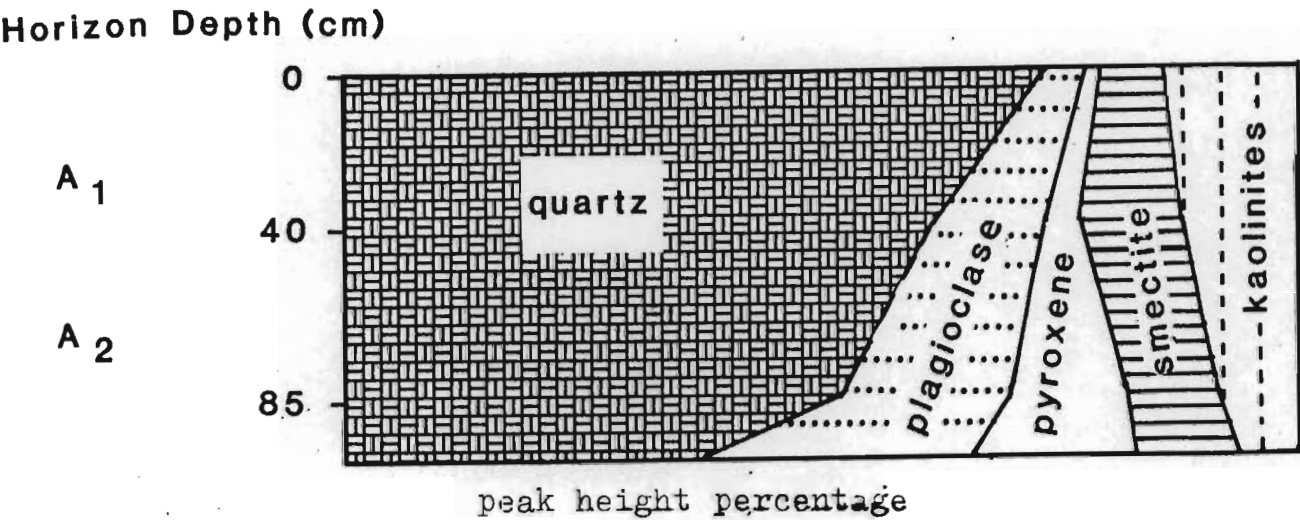


Figure 2.14 Whole soil mineral distribution in the profile of the Arcadia soil (constructed from relative XRD peak heights)

Clay fraction

The clay mineral assemblage of the Arcadia soil closely resembles that of the Mayo with 7 Å and 14 Å phyllosilicates being present in similar proportions. The swelling 14 Å mineral seems to be made up of a component that expands with ethylene glycol but fails to do so with glycerol when Mg-saturated (Figure 2.15). The dominant swelling mineral must therefore be regarded as

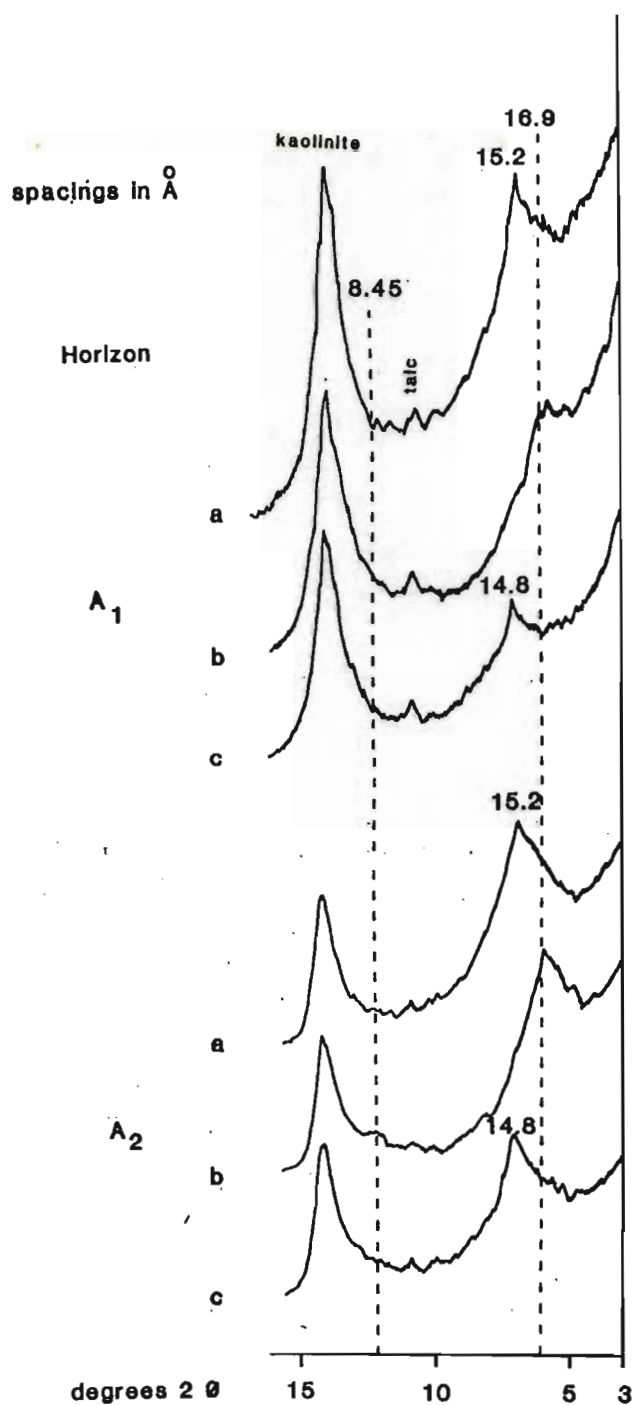


Figure 2.15 XRD traces of the two horizons of the Arcadia soil profile (oriented clay)

(a) Mg-saturated, air-dried

(b) Mg-saturated, ethylene glycol solvated

(c) Mg-saturated, glycerol solvated

(broken lines represent peak positions of discrete smectite with Mg + ethylene glycol)

possessing layer charge characteristics close to the vermiculite-smectite boundary. Small amounts of discrete montmorillonite can be discerned by application of the Greene-Kelly test (Figure 2.16). K-saturation leads to a strong peak broadening, especially in the A₁ horizon with a peak position between that of a water mono-layer and a water bi-layer in the air-dried state, indicating charge heterogeneity (Figure 2.17). Heating the K-saturated sample to 500°C results in a broad peak bridging the > 10 Å region and indicating a high amount of interstratification of chlorite and/or kaolinite in the swelling clay mineral (Figure 2.17).

Halloysite (7 Å) and kaolinite can be discerned on the basis of formamide intercalation (Figure 2.18). No halloysite was detected in the surface horizons. Small amounts of talc are present in both samples.

2.3.1.3 Kaolinite-dominated soil profiles (Bonheim, Shortlands, Hutton)

The primary dolerite minerals have been weathered leaving quartz, kaolinite, "chlorite", talc, gibbsite and goethite (Figures 2.19 and 2.20).

Two dolerite boulders, found at a depth of ca. 120 cm in the Shortlands soil form, 15 - 30 cm below the B₂ horizon, and referred to as C₁ and C₂ in Figure 2.20 and Table 2.1 are composed of goethite, gibbsite and only traces of talc and kaolinite.

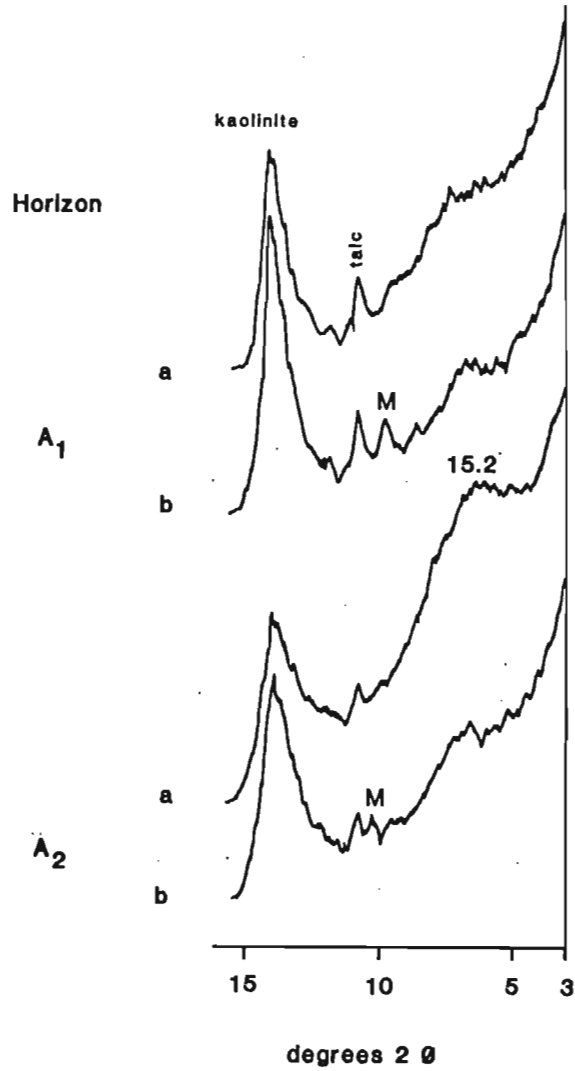


Figure 2.16 XRD traces of the two horizons of the Arcadia soil profile (oriented clay). M is discrete montmorillonite

(a) Li-saturated, air-dried

(b) Li-saturated, 290°C, ethylene glycol solvated

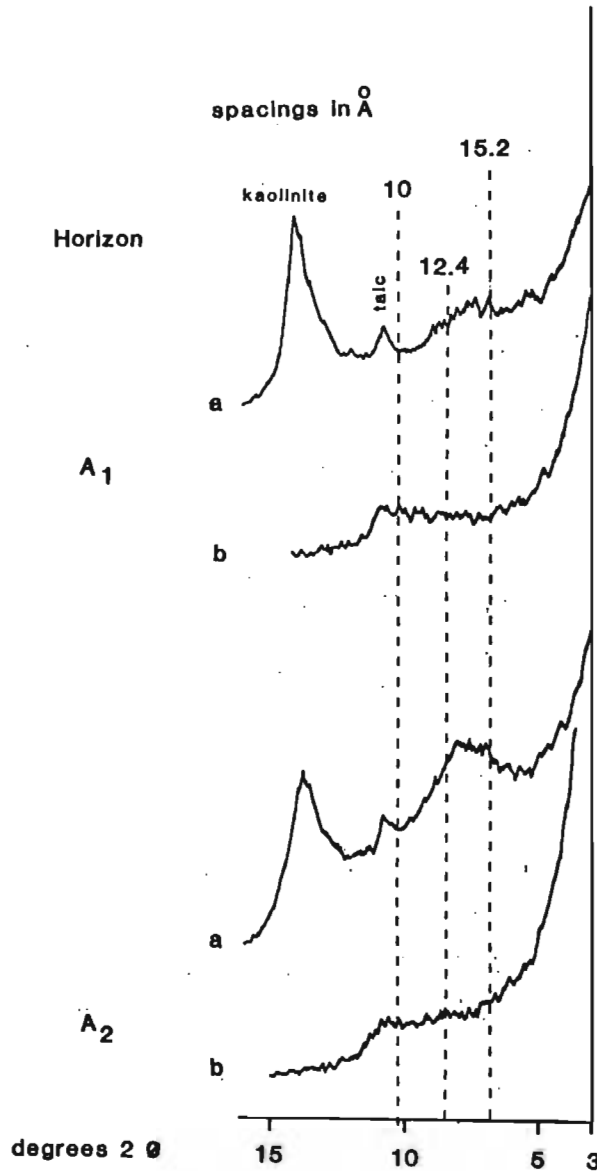


Figure 2.17 XRD traces of the two horizons of the Arcadia soil profile (oriented clay)

(a) K-saturated, air-dried

(b) K-saturated, 500°C

(broken lines represent peak positions of collapsed smectite (10 Å), smectite with a water mono-layer (12,4 Å) and a water bi-layer (15,2 Å))

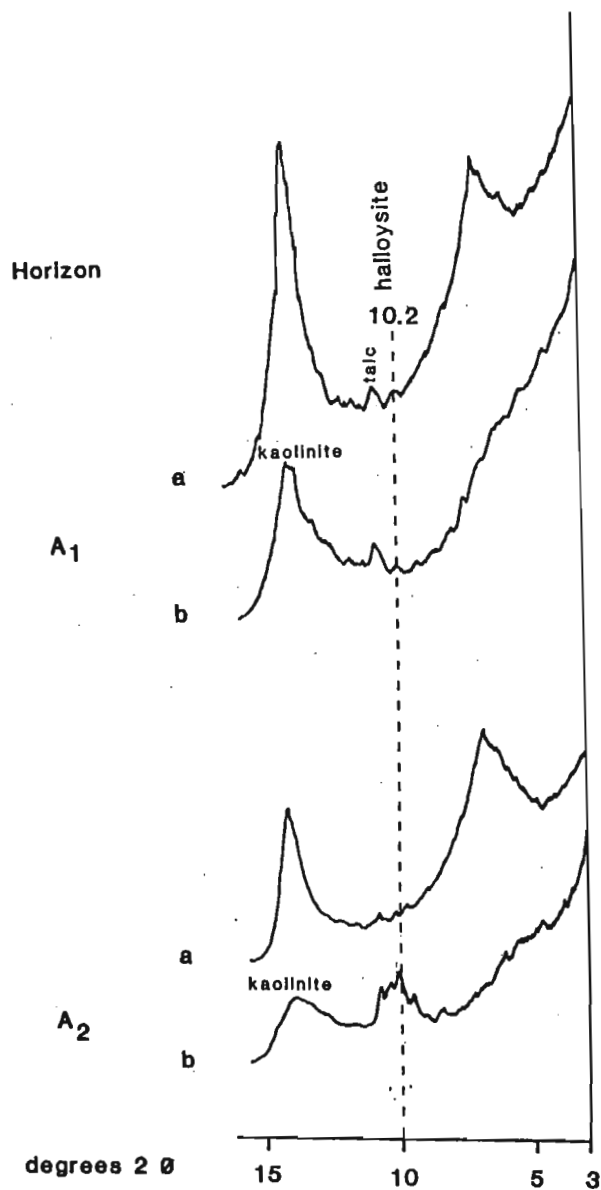


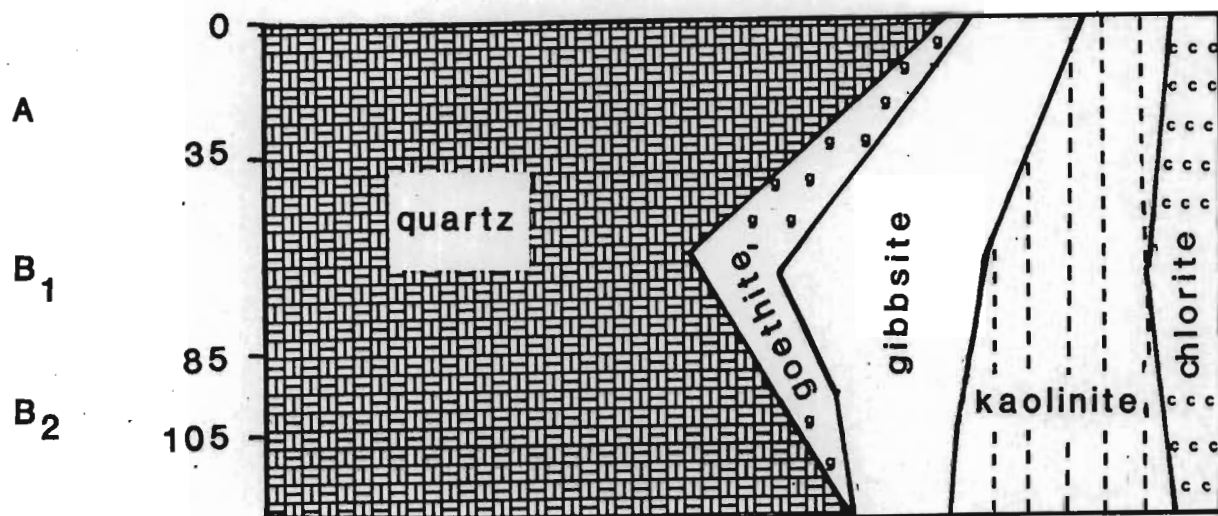
Figure 2.18 XRD traces of the two horizons of the Arcadia soil profile (oriented clay)

(a) Mg-saturated, air-dried

(b) Mg-saturated, formamide intercalated

(broken line represents peak position of formamide intercalated halloysite)

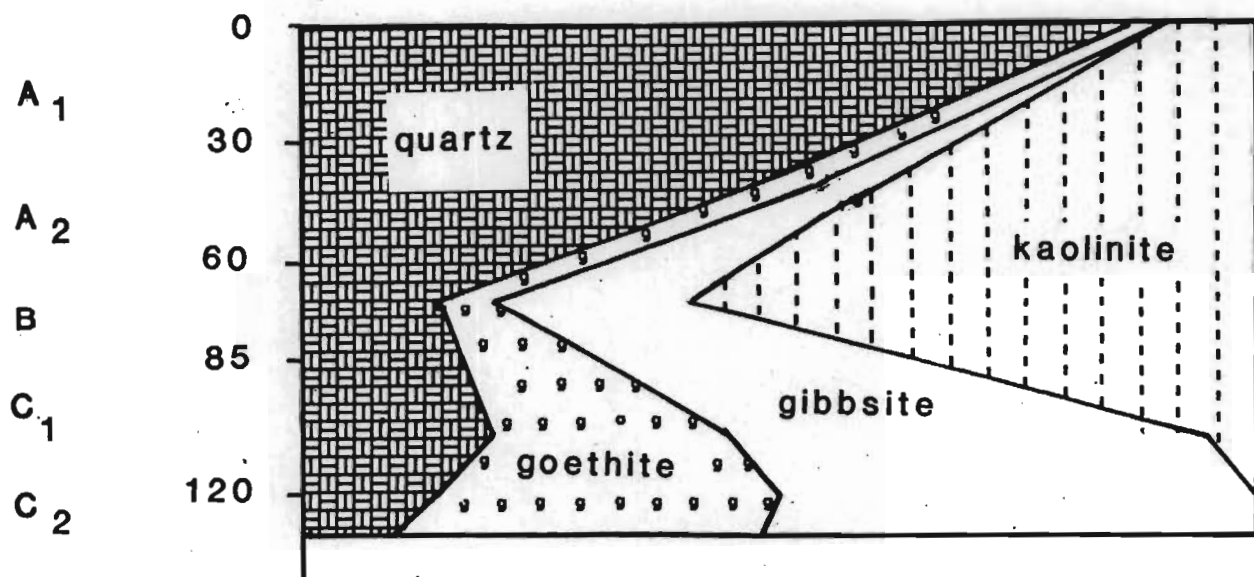
Horizon Depth (cm)



peak height percentage

Figure 2.19 Whole soil mineral distribution in the profile of the Hutton soil (constructed from relative XRD peak heights) (Balmoral Soil Series)

Horizon Depth (cm)



peak height percentage

Figure 2.20 Whole soil mineral distribution in the profile of the Shortlands soil (constructed from relative XRD peak heights)

The clay fractions of the A and B horizons of all three soil series contain a nearly identical clay mineral assemblage : kaolinite, "chlorite" and small amounts of talc. The term "chlorite" is used here to designate the component with a basal spacing of 14,2 Å (Mg-saturated, air-dried), which is not shifted by solvation with ethylene glycol or glycerol (Figure 2.21) or by potassium saturation (Figure 2.22). The reflection disappears upon heating at 300°C (Figure 2.22). No 14 Å related reflection was observed either at 14 Å or at 10 Å, or between these two values, due to either the complete destruction of the clay structure or the formation of interstratifications of two or even three different interlayer types (10 Å, 12,4 Å, 14,2 Å) (see p.36). Although true chlorite structures are reported to be stable to heating up to and even above 500°C, the term "chlorite" has nevertheless been used in preference to smectite or vermiculite due to a lack of collapse after potassium saturation and the non-expansion after ethylene glycol solvation. All five kaolinite-dominated soil profiles contain this type of "chlorite" which is presumed to be of the aluminous variety described by many authors (eg. Rich, 1960; de Villiers and Jackson, 1976), formed through hydroxy interlayers in expansible layer silicates. Small amounts of talc are found in each of the kaolinite dominated horizons.

kaolinite

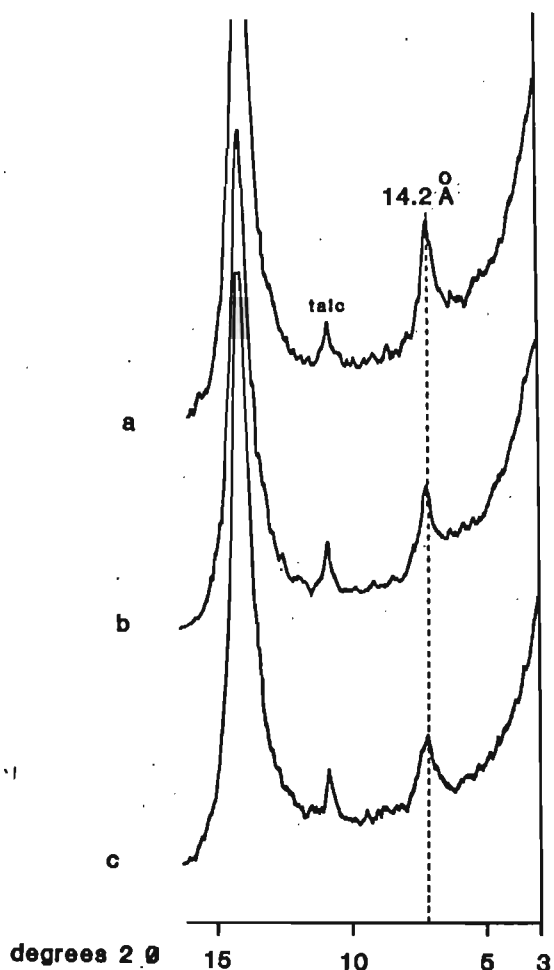


Figure 2.21 XRD traces of the B₁ horizon of the Hutton (Balmoral) profile (oriented clay)

(a) Mg-saturated, air-dried

(b) Mg-saturated, ethylene glycol solvated

(c) Mg-saturated, glycerol solvated

2.3.2 Electron microscopy

Hand-picked white (plagioclase) and black (pyroxene) particles from the Mayo B horizon which were investigated by means of XRD (Section 2.3.1) were also examined under the scanning electron microscope. Despite intensive searching, hardly any clay particles could be found associated with the plagioclase surface (Figure 2.23), confirming the result obtained by means of XRD.

The black pyroxene particles, on the other hand, are covered by platy (smectite, kaolinite) as well as elongated (halloysite) minerals (Figure 2.24).

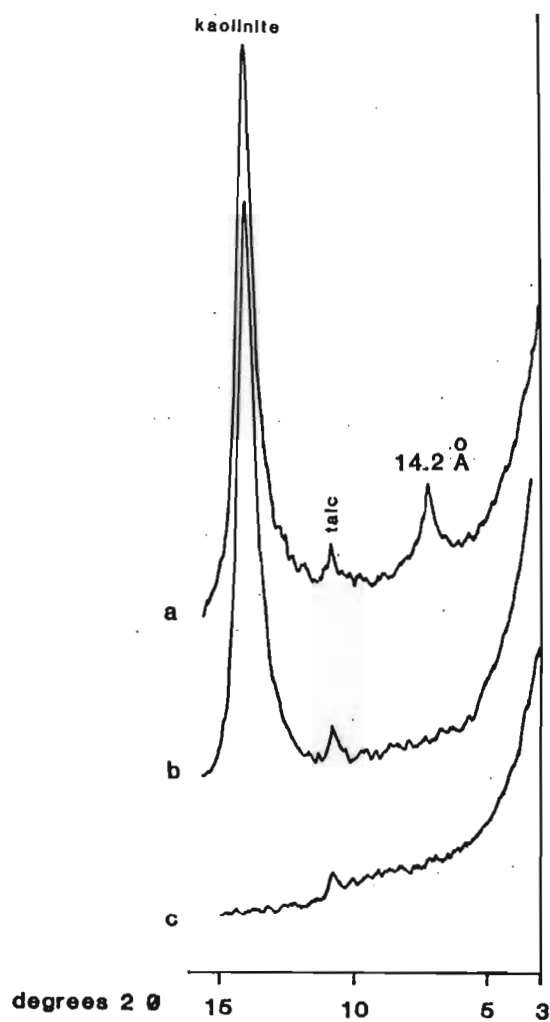


Figure 2.22 XRD traces of the B₁ horizon of the Hutton (Balmoral) profile (oriented clay)

(a) K-saturated, air-dried

(b) K-saturated, 300°C

(c) K-saturated, 500°C

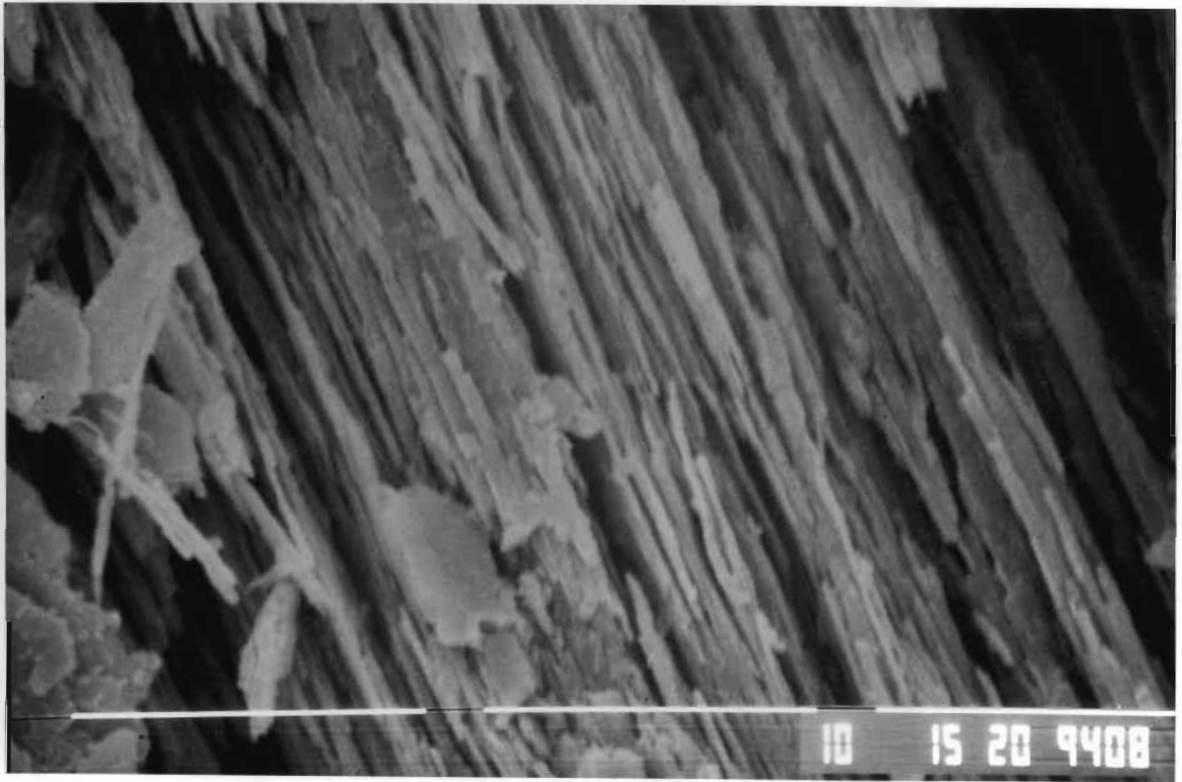


Figure 2.23 Scanning electron micrograph of a hand-picked
 plagioclase particle from the Mayo B horizon
 (magnification 1:3000)

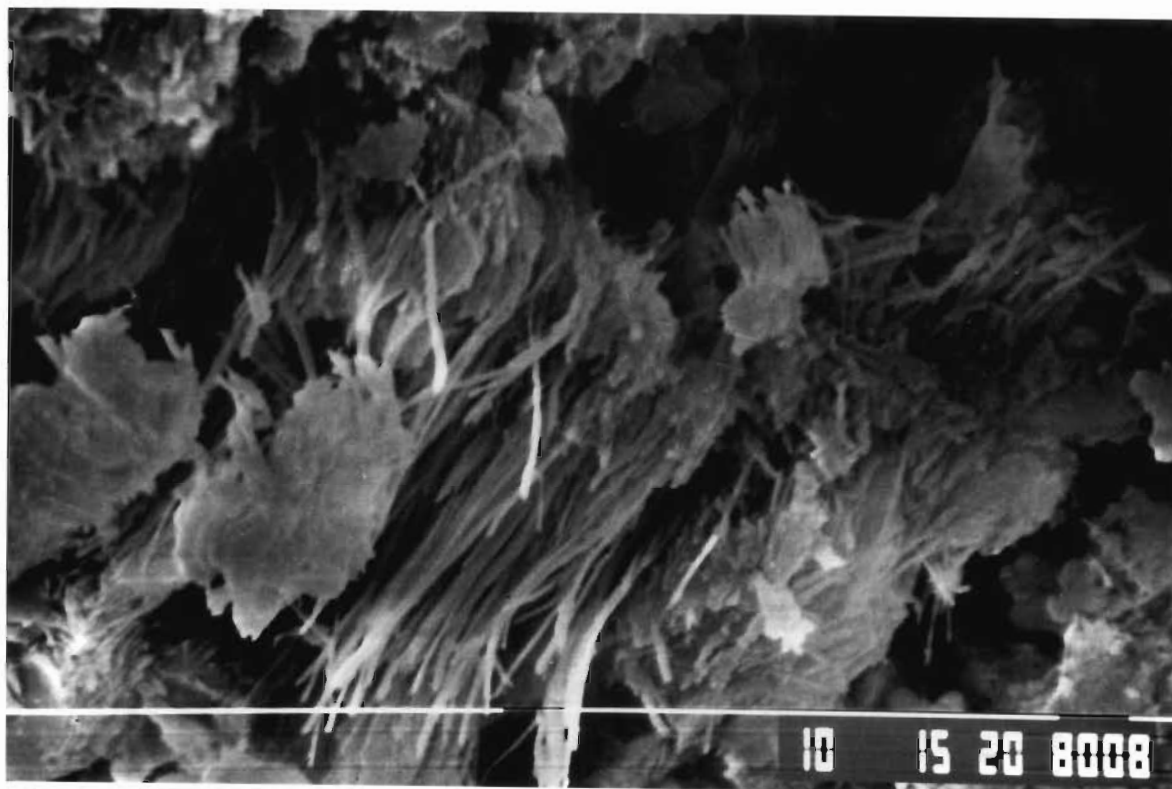


Figure 2.24 Scanning electron micrograph of a hand-picked pyroxene particle from the Mayo B horizon (magnification 1:5500)

2.4 Conclusions

Three distinct clay mineral assemblages have developed by weathering of dolerite on Melody Ranch:

suite (i) vermiculite-beidellite plus small amounts of

kaolinite and traces of talc;

suite (ii) minerals of the 14 Å and 7 Å phyllosilicate group in about equal proportions as well as traces of talc;

suite (iii) kaolinite plus subordinate "chlorite" and traces of talc.

Some important results may be summarized as follows :

- (i) vertic A horizons are not necessarily smectite dominated (Arcadia);
- (ii) smectite may be absent from melanic horizons (Stanger);
- (iii) halloysite (10 Å) gives way to halloysite (7 Å) and finally kaolinite as weathering advances.

A more comprehensive discussion is presented in section 4.5.

CHAPTER 3

MINERALOGICAL ASPECTS OF THE GENESIS OF SWELLING SOILS OF THE HIGHVELD NEAR STANDERTON

3.1 Introduction

Swelling clay soils are widespread in South Africa and have received attention for some time by pedologists interested in their genesis and distribution. There are, however, relatively few studies which have included clay mineralogical analyses, and even these provide fairly superficial reports of the clay mineral groups represented (van der Merwe, 1924; Marchand, 1925; Theron and van Niekerk, 1934; Heystek, 1954; van der Merwe and Heystek, 1955; van der Merwe and Weber, 1965; de Villiers, 1962; Harmse, 1967; Oberholster, 1969a; Taylor, 1972; Fitzpatrick, 1974; Fitzpatrick and le Roux, 1977) compared with the possibilities afforded by more modern methods of investigation. A detailed knowledge of the clay mineralogy of swelling soils is patently valuable in understanding both their genesis and their physical and chemical properties. An opportunity for such detailed study presented itself with the recent completion of a systematic survey of black clays and associated soils on the property of the projected Tutuka power station near Standerton (Fey and Cass, 1983). The soils of this area are representative of much of the Transvaal Highveld; the special interest which they have derives from the fact that two distinctive soil bodies occur, which can approximately be described as (i) black clays, derived from dolerite, and (ii) lighter coloured grey or brown clays, derived from fine-grained

Ecce sediments.

Earlier studies indicated that it is difficult to find objective criteria (apart from colour) by which these soils may be distinguished from one another, since both have a marked swelling tendency (vertic A horizon) and the nature of the underlying geological material would be a presumptuous basis for separation. Loxton (communication with K. Snyman, 1984) proposed a distinction on the basis of crusting versus self-mulching behaviour of the surface horizon, but this criterion has been shown to be flawed by Snyman, Fey and Cass (1985) who in turn proposed other (physical) differentiae. The purpose of the investigation reported here was to conduct a detailed mineralogical (especially clay mineralogical) investigation, anticipating that this might provide a better understanding of the genesis of these two well known soil bodies and the differences between them.

Special emphasis has been placed on the investigation of changes that take place in the clay mineral - and non-clay mineral fractions within each profile. This is of special importance when a possible influence of colluviated material can be inferred, as has been done for some pedons (Fey and Cass, 1983) which have dolerite saprolite but are mapped as shale-derived due to lighter coloured A horizons.

3.2 Materials and methods

An area of approximately 1 000 ha of land adjoining the Tutuka power station near Standerton, Transvaal, was originally surveyed as an ash dump site by the Department of Soil Science and Agro-

meteorology, University of Natal (Fey and Cass, 1983). Along a transect T₁, 31 pits were opened at a distance of 100 m apart for detailed soil description, and 54 samples from 16 soil profiles were taken for mineralogical investigation (Figure 3.1).

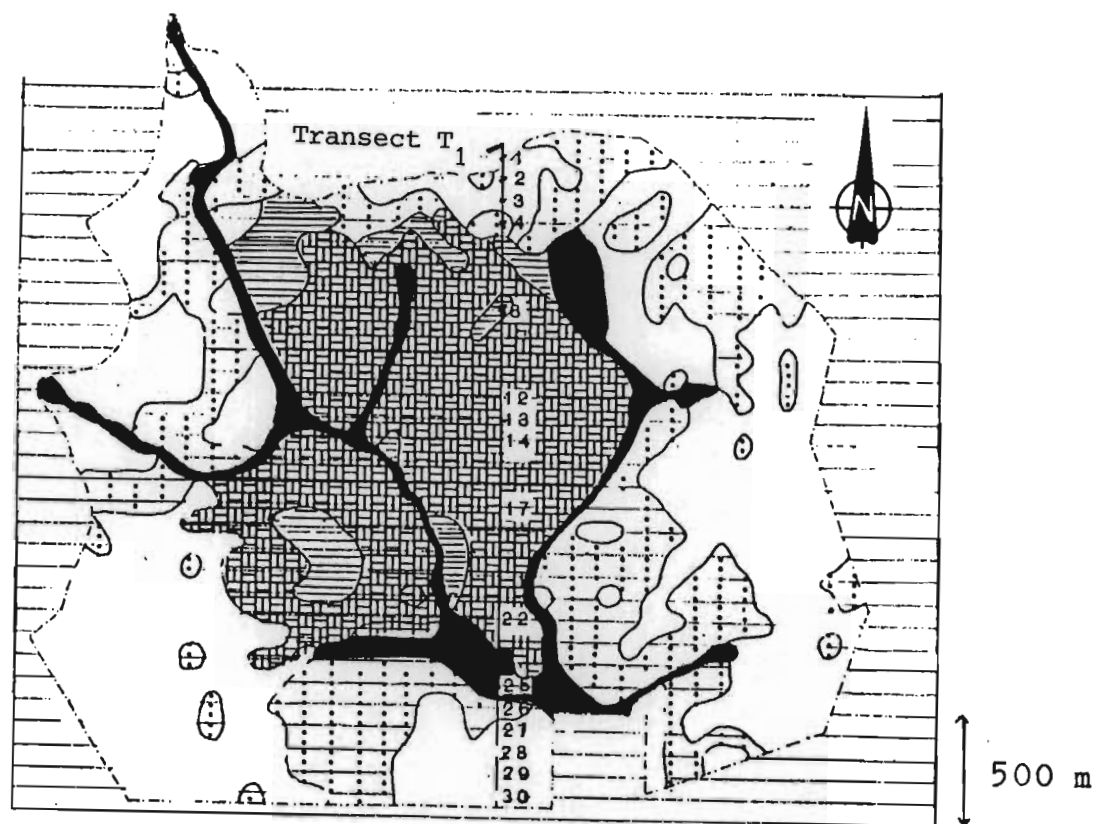




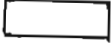



Figure 3.1 Soil series map of Tutuka power station (modified after Fey and Cass, 1983). Numbers indicate pits investigated.

	Gelykvlakte		Survey boundary line
	Arcadia		
	Rensburg (upland, dolerite)		
	Rensburg (upland, mudstone)		
	Rensburg (bottomland)		

The soils were classified as one of two soil forms : Rensburg and Arcadia, according to the Binomial system (MacVicar et al., 1977). Description of these profiles and analytical data may be found in Appendices 2 - 16 and 17, respectively.

The parent materials comprise mudstone and shale of the Eccia formation mainly in the northern part of the transect, and Karoo dolerite sills in the centre of the drainage basin. Figure 3.2 shows the subdivision of transect T₁ into zones based on soil morphology and underlying material.

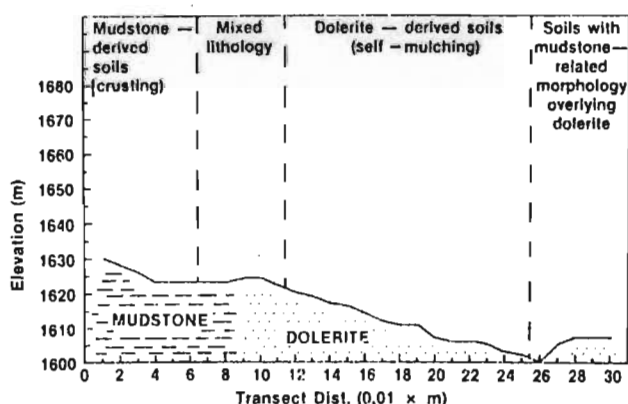


Figure 3.2 Slope profile of transect T₁ from which soils were sampled at 100 m intervals. Vertical scale exaggerated x 20 (after Snyman et al., 1985).

The climatic conditions are subhumid with a mean annual rainfall of about 750 - 800 mm, falling predominantly during the summer months. The locality is situated at an altitude of 1 600 - 1 680 m, and the topography is characterised by very gentle slopes, and most of the area has been cultivated to crops (maize,

sorghum), the remainder being uncultivated grazing land.

In addition to mineralogical analyses by methods described in Chapter 2 (all samples), the following were also carried out on selected samples : transmission electron microscopy of dried clay suspensions with a Jeol 100 CX instrument; total chemical analysis of Li-borate fused discs by X-ray fluorescence spectroscopy using a Phillips PW 1410 instrument with Cr target and LiF crystal; and separation of the heavy mineral fraction (spec. gr. > 4) from a sieved fraction (ca. 100 - 500 μ m) by sedimentation in Clerici solution.

3.3 Results and discussion

3.3.1 X-ray diffractometry

The soil profiles at the Tutuka power station ash dump site can be subdivided mineralogically into three different units, each of which has its own characteristic pattern of non-clay mineral association and of clay mineral formation/alteration from the saprolite to the surface horizon. For reasons which will emerge below, these groups comprise I : pits 12 - 25; II : pits 1 - 8; and III : pits 26 - 30, which refer to dolerite-, shale- and possibly mixed lithological origin, respectively.

3.3.1.1 Whole-soil mineralogy

XRD investigation of the saprolite revealed the following mineral

composition (the minerals are listed in descending order of frequency) :

- (a) dolerite : primary minerals : plagioclase, pyroxene orh, pyroxene mkl, quartz (Figure 3.3);
secondary minerals : smectite, quartz, traces of interstratified clay minerals,
- (b) mudstone/shale : primary minerals : quartz, plagioclase, K-feldspar, mica, chlorite (Figure 3.3);
secondary minerals : interstratified clay minerals; quartz.

The distinction between the two parent materials can easily be made on the basis of the quartz content, which is markedly higher in the sediment-derived saprolites, together with the presence of K-minerals (K-feldspar, mica), which are restricted to shale/mudstone saprolite (Figure 3.3).

The saprolite in pits 1 - 8 is morphologically recognisable as being derived from Eccu sediments, whereas that of pits 12 - 30 is clearly doleritic in origin. The degree of weathering, as estimated from the ratio of the intensities of plagioclase and quartz peaks in the case of dolerite-derived soils and the K-feldspar + mica + chlorite/quartz ratio in the profiles developed on shale, varies significantly.

The weathering of pyroxene seems to take place at a very early stage, since only small amounts of this mineral are observed in the XRD pattern of the dolerite derived saprolite. Literature suggests that smectite can be assumed to be the weathering product.

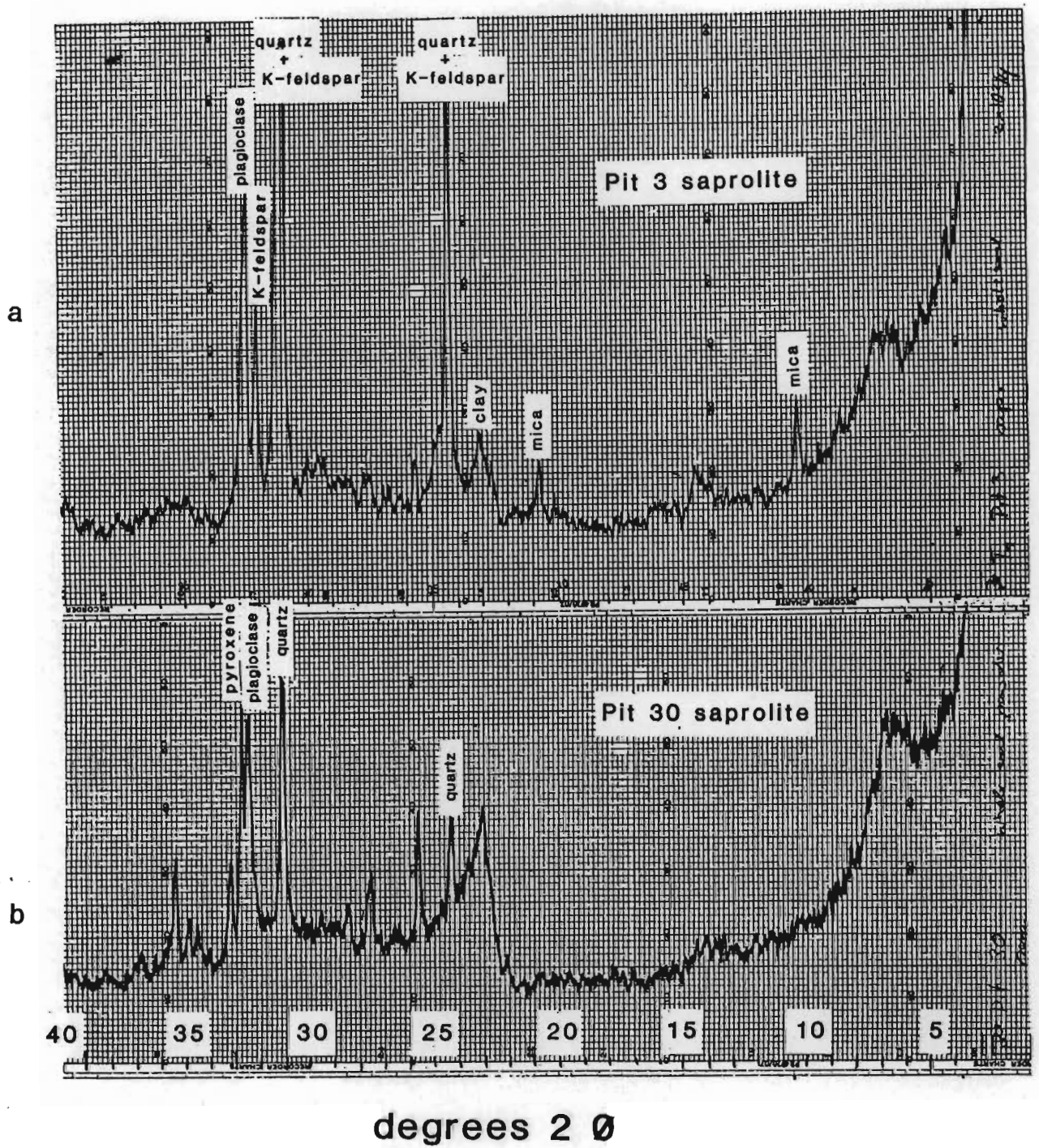


Figure 3.3 X-ray diffraction patterns of two saprolite horizons (a) pit 3 : shale saprolite; (b) pit 30 : dolerite saprolite (random powder mounts, whole-soil)

The unweathered Eccca shale contains mica and chlorite in approximately equal amounts, as demonstrated by investigations of handsorted shale fragments from pit 1 (Figure 3.4). Mica seems to be more resistant to weathering than chlorite, the latter being found in pit 1 only (in the C and G2 horizon), which is the profile with the lowest degree of weathering, whereas mica is present in all horizons of the shale-derived profiles. The possibility also exists that the shale contains two mica varieties, each with a different susceptibility to weathering. The highest degree of saprolite weathering, i.e. the lowest amount of primary minerals, was observed for the C horizon of pits 4 (shale) and 28 (dolerite).

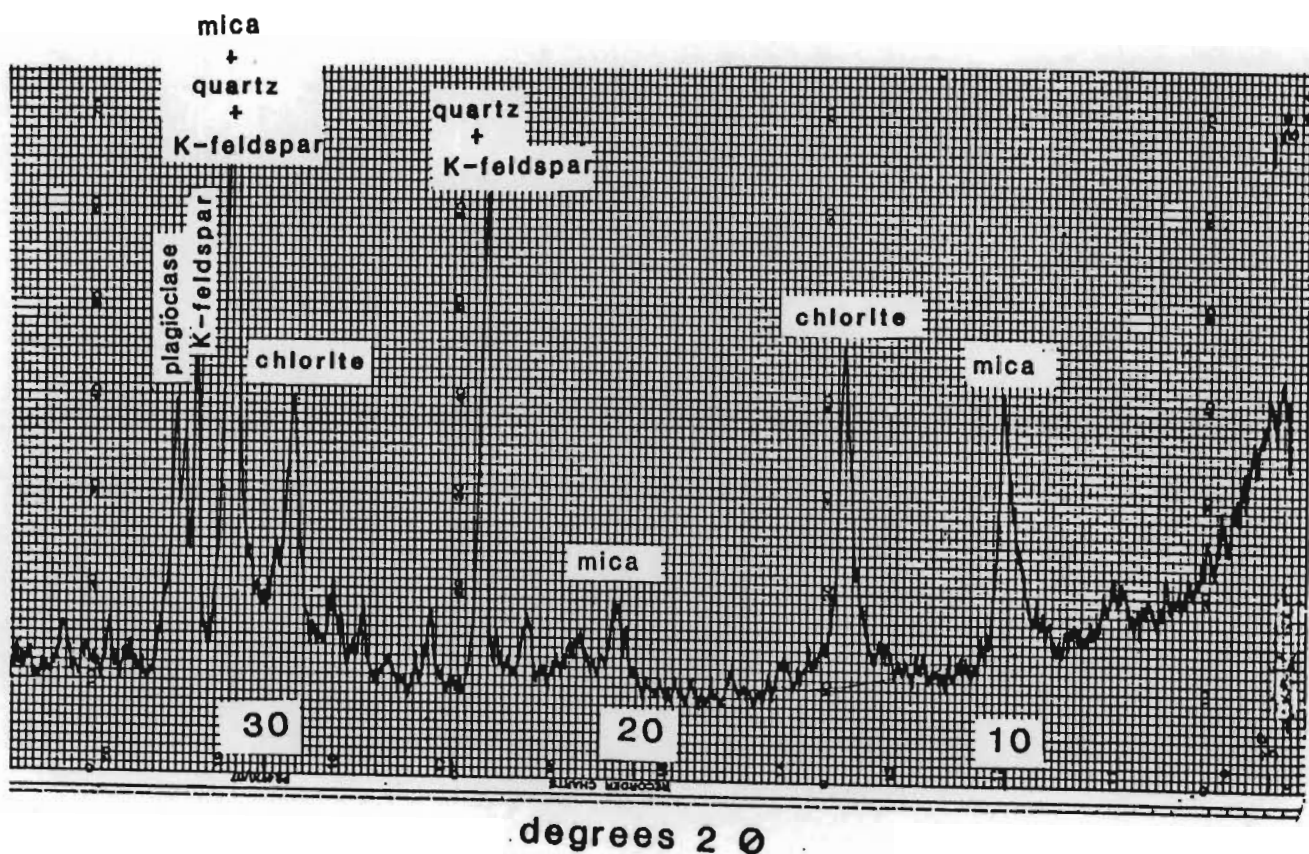


Figure 3.4 XRD pattern of hand-picked shale fragments from the saprolite of pit 1 (random powder mounts)

In all soil profiles, a progressive decrease in the amount of primary minerals is accompanied by an increase in quartz and a decrease in the degree of crystallinity of the clay mineral phase from the saprolite to the uppermost horizon (Figure 3.5).

In general, the non-clay minerals of surface horizons consisted of quartz and small to trace amounts of K-feldspar in the case of pits 1 - 8 (group II), or quartz, plagioclase and small to trace amounts of pyroxene in pits 12 - 25 (group I), and of quartz only in both A and B horizons of pits 26 - 30 (group III).

3.3.1.2 Mineralogy of the clay fraction

The powder diffraction patterns of all clay fractions showed an (060) spacing at approximately 1,5 Å, indicating that the clay fraction is composed of dioctahedral minerals only.

3.3.1.2.1 Group I profiles (pits 12 - 25) derived from dolerite

The < 2 µm fraction of the dolerite derived soils is dominated by well-ordered smectite in all profiles, irrespective of depth. This smectite responds to the various treatments as follows (Figure 3.6) : A peak position of 15,3 Å in the Mg saturated, air-dried state; expansion to 16,9 Å upon glycol- and to 18 Å upon glycerol solvation with Mg and Li as interlayer cations; a peak position of 13,3 - 14,9 Å in the air-dried state with Li as interlayer cation; collapse of the Li saturated sample to 9,8 Å

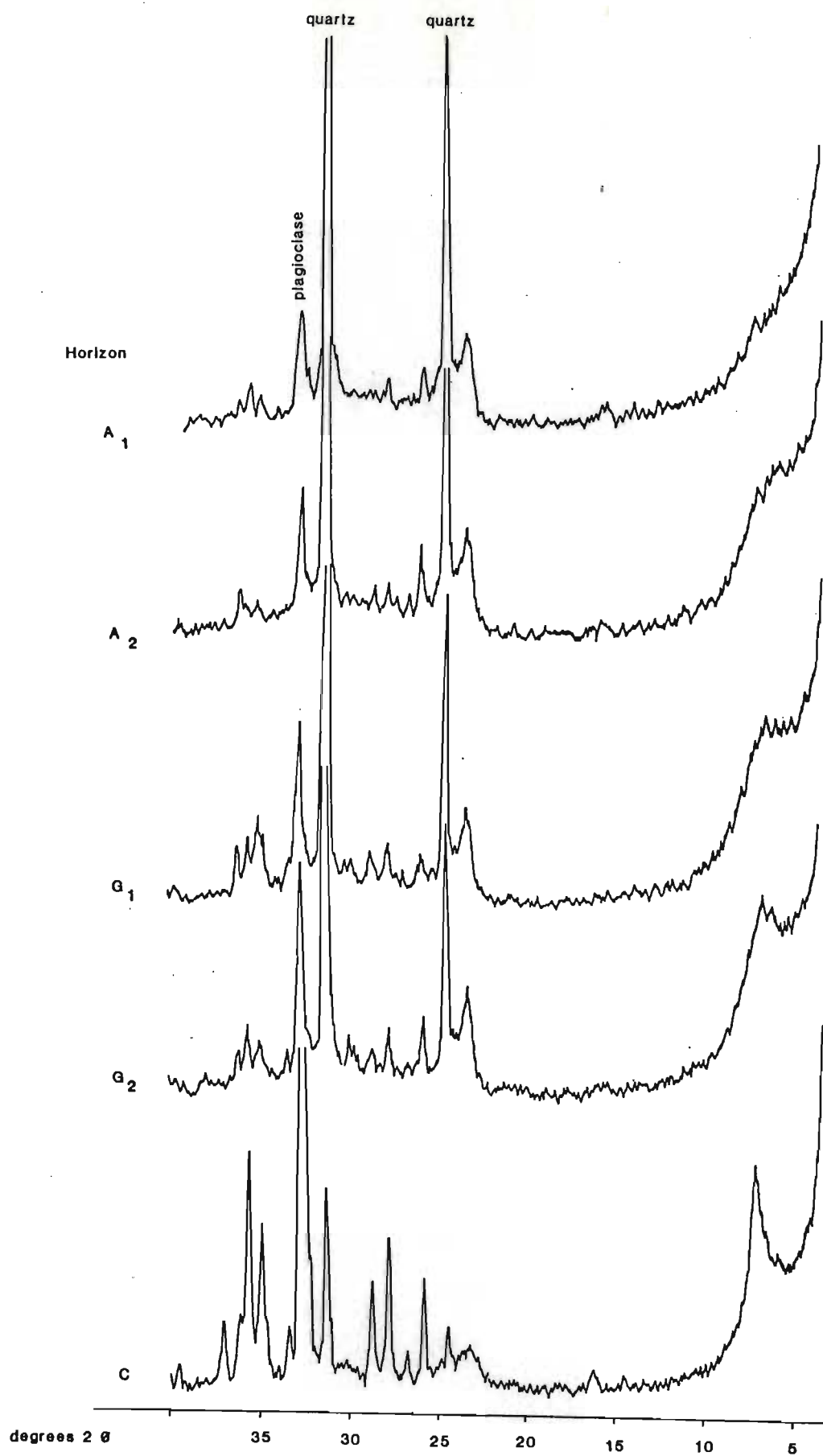


Figure 3.5 X-ray diffraction patterns for whole soil from horizons of pit 25 (random powder mounts)

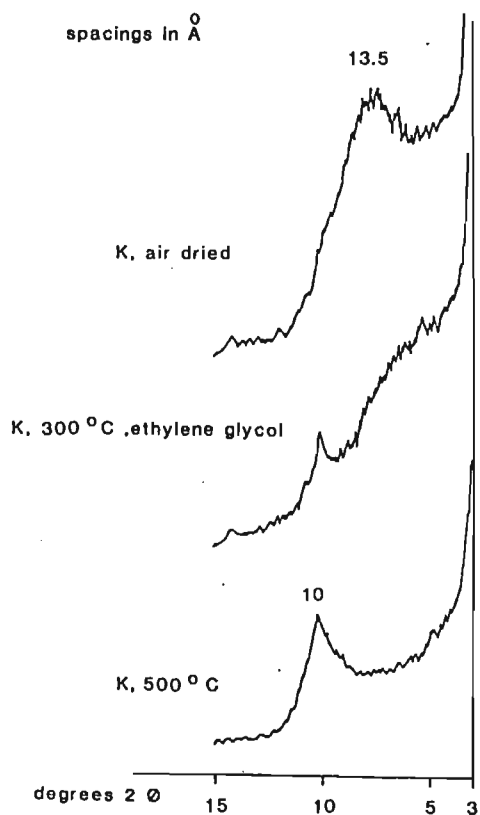
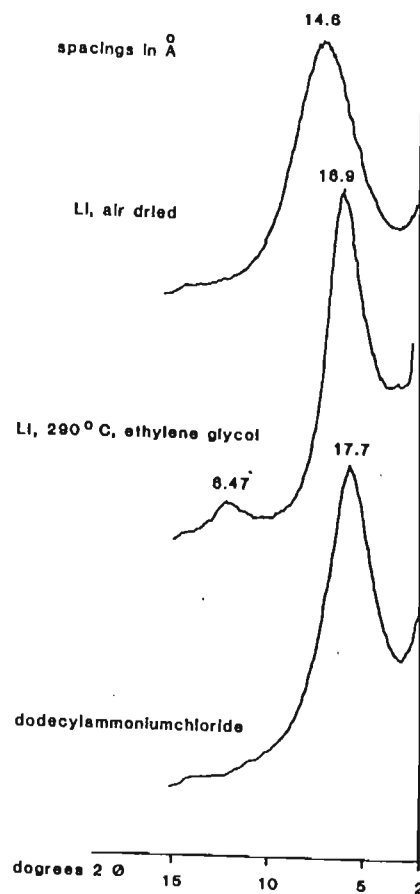
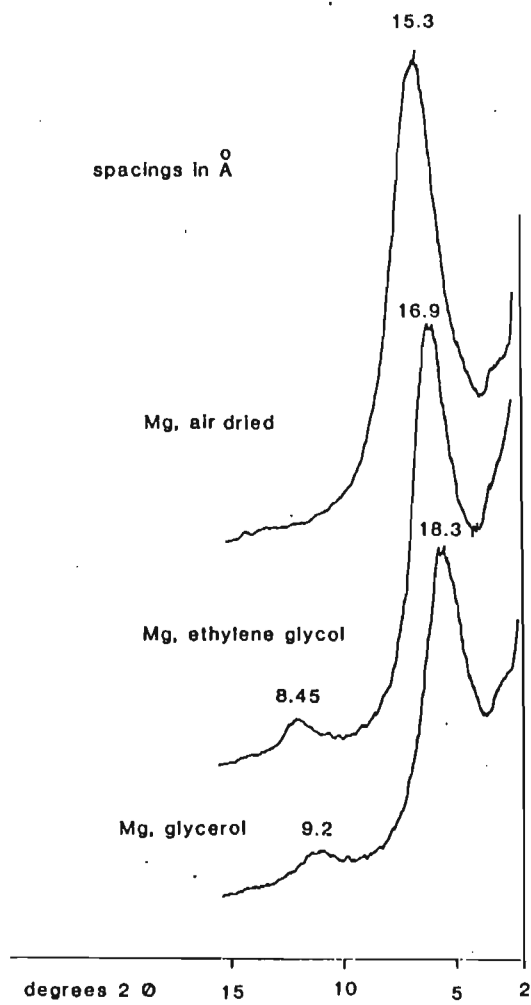


Figure 3.6 XRD traces of the < 2 μ m fraction of the surface horizon of pit 17 (oriented specimen)

upon heating to 290°C and re-expansion to 16,9 Å - 17,6 Å upon glycolation (Greene-Kelly test); a peak position between 12,9 and 14 Å with potassium as interlayer cation; expansion to > 17 Å with glycol, after the K-saturated sample was heated to 110°C, except for a very small amount (< 10%), which remained collapsed (vermiculite) in some samples; collapse to 10 Å after heating the K-saturated sample to 300°C and peak positions at 10, 14 and 17 Å after solvation with ethylene glycol; a 10 Å peak, when the K-saturated sample was heated to 500°C with a low angle shoulder; and formation of a dodecylammoniumchloride double layer (17,7 Å). The absence of any interstratification component in this smectite is demonstrated by the rationality of the peak positions when the Mg saturated sample is solvated with ethylene glycol (Figure 3.6).

The beidellitic nature of the smectite is suggested by the Greene-Kelly test and by the formation of a dodecylammonium-chloride double layer, although random interstratification with montmorillonite is indicated by irrationality of second order reflections when the Greene-Kelly test is applied. Variations in the layer charge distribution between the various smectite layers is confirmed by basal spacings, varying from 12,9 to 14,9 Å after K-saturation and air drying, which lie somewhere between the peak positions characteristic for water monolayer (12,4 Å) and water bilayer (15,2 Å) formation. This peak position indicates that some of the smectite interlayers permit one water layer into their interlayer space, while others permit two water layers. Since the water monolayer-bilayer formation

is charge dependent (Machajdik and Cicel, 1981), any position between 12,4 Å and 15,2 Å is indicative of a smectite (high-charge)-smectite (low-charge) mixed layering.

This charge heterogeneity in the smectite is also confirmed by the broad range of peak positions in the K-saturated, 300°C-heated and glycolated pattern (Figure 3.6): low-charge smectite is reported to form an ethylene glycol double layer, medium-charge smectites form a monolayer, while high-charge smectites and vermiculite remain collapsed (Schultz, 1969).

The amount of low-charge smectite (montmorillonite) can be derived from the Greene-Kelly test: only when montmorillonite and beidellite are present in a sample as discrete minerals (i.e. when each montmorillonite particle consists of more than ca. nine separate units per crystallite which all have low-charge characteristics, and when each beidellite consists of the same amount of high-charged units and when the two minerals are present in a mechanical mixture) will separate 10 Å and 17 Å peaks be observed in the XRD pattern upon application of the Greene-Kelly test (Chapter 1). As soon as the smectite is composed of beidellitic units and montmorillonitic units within the same crystallite, heat treatment to 280°C after Li saturation will result in an interstratification (which is probably random) of irreversibly and reversibly collapsed units - that is, an interstratification of 10 Å and 17 Å units upon glycolation (Chapter 1). This type of interstratification must give the same irrational basal reflections as a mica-smectite mixed-layer mineral and may therefore

be treated as such, using migration curves and tables for their interpretation.

This type of mixed-layering was found to be a general feature of the smectite in this group of samples with the amount of irreversibly collapsed layers (montmorillonite) ranging from < 10 to 60%. The following amount (%) of montmorillonite was estimated from the secondary peak positions in the Li-290°C-ethylene glycol pattern, using the peak migration Table 1.2:

Table 3.1 Percentage of montmorillonite layers in the smectite crystallites

Pit	Horizon				
	A1	A2	G1	G2	C
12	30	30	-	-	20
13	30	30	-	-	30
14	< 10	< 10	-	-	30
17	< 10	< 10	-	-	< 10
25	50	40	50	50	30

Comparison of the shape of the peak with computer calculated patterns (Reynolds and Hower, 1970) (see Figure 1,8) results in similar 10 Å/17 Å ratios (Figure 3.7).

No relationship could be observed between the amount of low-

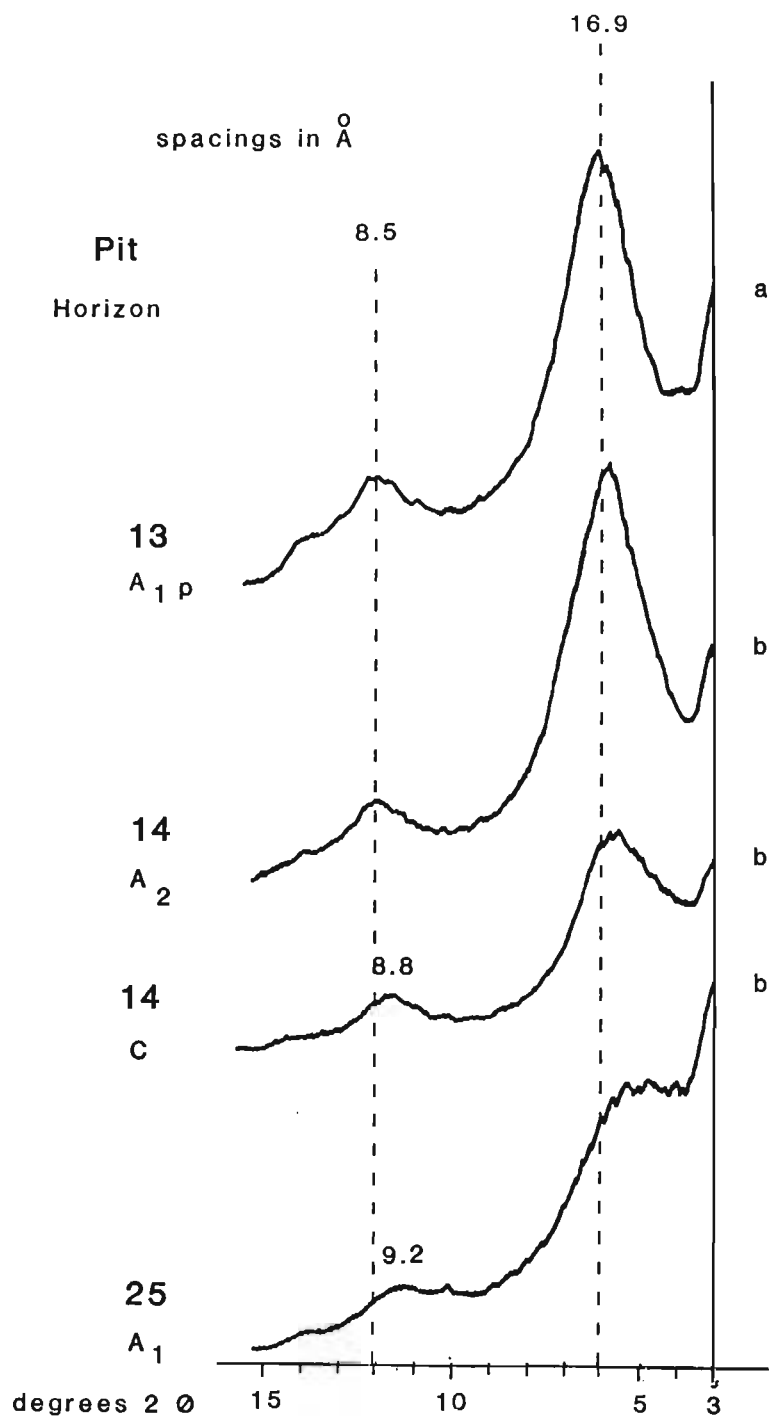


Figure 3.7 XRD traces of selected clay fractions (oriented specimen, Li-saturated, glycolated) without (a) and with (b) heating at 290°C, illustrating variations in shape of the first reflection and position of the second with increasing amount of collapsed (montmorillonite) layers, randomly stacked with expanded (beidellite) layers

charge smectite and position on the transect.

Soil clays for which a high amount of montmorillonite was indicated by the Greene-Kelly test also showed a low peak position after K-saturation in the air dried state, but no such relationship was found for the Li-saturated samples, though in the latter case water monolayer and bilayer complexes are also formed.

The degree of crystallinity of the smectite, as measured by the sharpness of the 001 reflection in the Mg-saturated, air dried state decreased slightly towards the top of some profiles (pit 14, Figure 3.8), while in the case of other profiles (pit 17) a slight increase of the apparent degree of crystallinity was observed. The reason for this broadening cannot be sought in a small particle size nor in the presence of any type of interstratification due to the regularity of the secondary basal reflections, but probably lies in some structural disorder in terms of layer stacking or cation site occupancy (see Chapter 1). A small amount of soil vermiculite (10 Å peak in the K, 110°C, glycol pattern) is present in a number of samples. The formation of vermiculite as a weathering product of orthopyroxene is not unusual and has been reported in a number of cases (Pion, 1979).

Small amounts of interstratified material (10%) are present as well, characterised by a very broad peak, bridging the > 7 Å region after each treatment (except after 500°C) and a shoulder

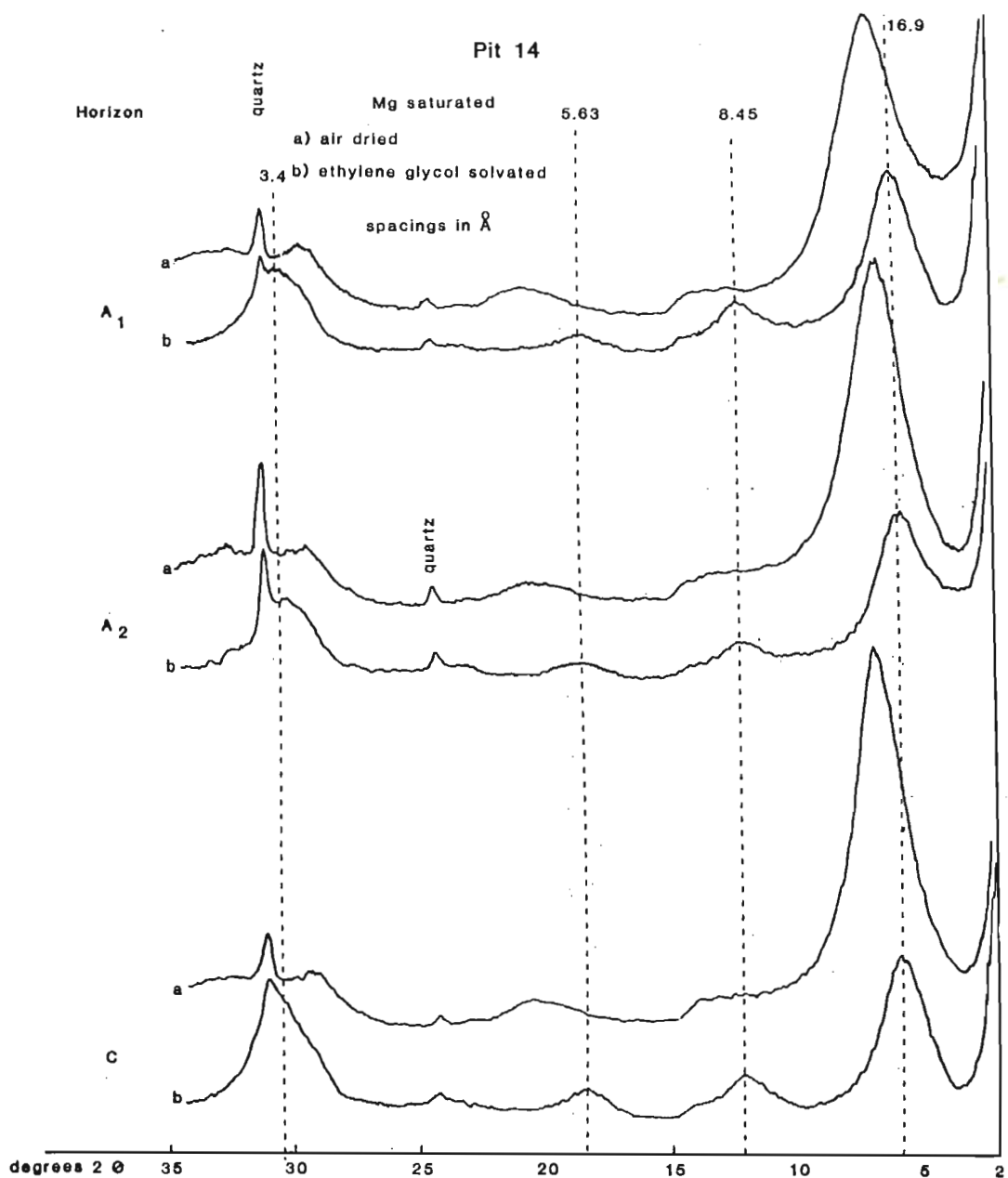


Figure 3.8 XRD traces of the clay fraction of pit 14 (oriented specimen) dashed lines: peak positions of discrete smectite after Mg-saturation and ethylene glycol solvation

at 3,5 Å in the ethylene glycol solvated pattern. Possibilities would include a random stacking of smectite units (3,38 Å) with either kaolinite (3,58 Å) and/or chlorite (3,55 Å) and/or

vermiculite (3,55 Å). No increase or decrease in the amount or the nature of any one of the clay mineral groups could be observed within each profile nor between the various profiles of this group (Figures 3.6 and 3.8).

In summary, the clay fraction of the dolerite derived soil profiles (which are characterized by a low degree of weathering as indicated by the presence of primary minerals, mainly plagioclase, even in the surface horizons) is dominated by a well-ordered smectite, which amounts to about 90% of the clay fraction. The interlayer space of this smectite is characterised by a variation in charge density, as assessed by the response to K-saturation and by the Greene-Kelly test, suggestive of a randomly stacked arrangement of montmorillonite and beidellite layers. The smectite may be slightly Al interlayered, as demonstrated by the response to heating at 500°C (shoulder at low angle side). This interlayering does not, however, affect expansion characteristics with ethylene glycol. On the other hand, the shoulder may alternatively be explained as a minor kaolinite interstratification component, transformed to metakaolinite during heating, but nevertheless separating the smectite units from each other. A slight increase in d values of the (005) smectite after ethylene glycol solvation confirms chlorite and/or kaolinite as interstratification component.

3.3.1.2.2 Group II profiles (pits 1 - 8) derived from shale

Unweathered upper Eccra shale usually contains besides quartz and little plagioclase and K-feldspar the clay minerals mica and chlorite in approximately equal amounts (Drennan, 1964; D. Böhmann, personal communication) (Figure 3.4).

Pedogenic transformations are probably dominated by vermiculitization, smectitization of the chlorite and to beidellitization of mica, with possible interlayer precipitation of hydroxyaluminium species in the course of weathering.

(i) Transformation of chlorite

The weathering products of chlorite have been repeatedly reported in the literature. One weathering sequence which has been proposed is : chlorite - regularly interstratified chlorite/vermiculite - randomly interstratified chlorite/vermiculite - vermiculite - smectite (nontronite, iron-rich beidellite) - kaolinite (Coffman and Fanning, 1974; Herbillon and Makumbi, 1975). The changes required for a transformation of Fe-rich chlorite to smectite and kaolinite would include oxidation and expulsion of structural iron, and the removal of the interlayer sheet - i.e., changes in each of the four sheets (Bailey, 1975; Ross and Kodama, 1976; Goodman and Bain, 1979).

An alternative pathway of weathering is that resulting in the decomposition of the crystal structure itself, yielding amorphous

forms, or the dissolution of the chlorite with or without neoformation of minerals by precipitation (authigenic minerals).

In the shale-derived profiles, there is evidence for chlorite transformation having proceeded to different degrees, which in turn may be assumed to reflect a variable degree of weathering within the soil profile. Generally, chlorite appears to have weathered at a very early stage and is only found as a discrete mineral in the C and G2 horizons of pit 1, which would appear to be the least weathered shale saprolite on the basis of the non-clay mineral association as well.

The weathering of the chlorite appears to proceed via mixed-layer phases, containing chlorite, vermiculite and possibly also smectite, which are random in the case of the saprolite of pit 1, while small amounts of a regular, corrensite-type structure were observed in the saprolite of pit 4. In the saprolites of pits 2, 3 and 8 and in all G horizons, the weathering of chlorite has proceeded to an extent where no chloritic components, either discrete or as part of an interstratification could be observed, as assessed from the absence of a discrete 14,2 Å peak or any broad shoulder in the K, 500°C pattern (Figure 3.9). In the A horizons this shoulder appeared again (Figure 3.9) probably due to hydroxy-interlayering of the smectite component.

The chlorite-vermiculite interstratification of pit 4 is enriched in the coarse clay to silt fraction and could therefore be regarded as having formed via a solid state reaction with

horizon

A₁p

A₂

C

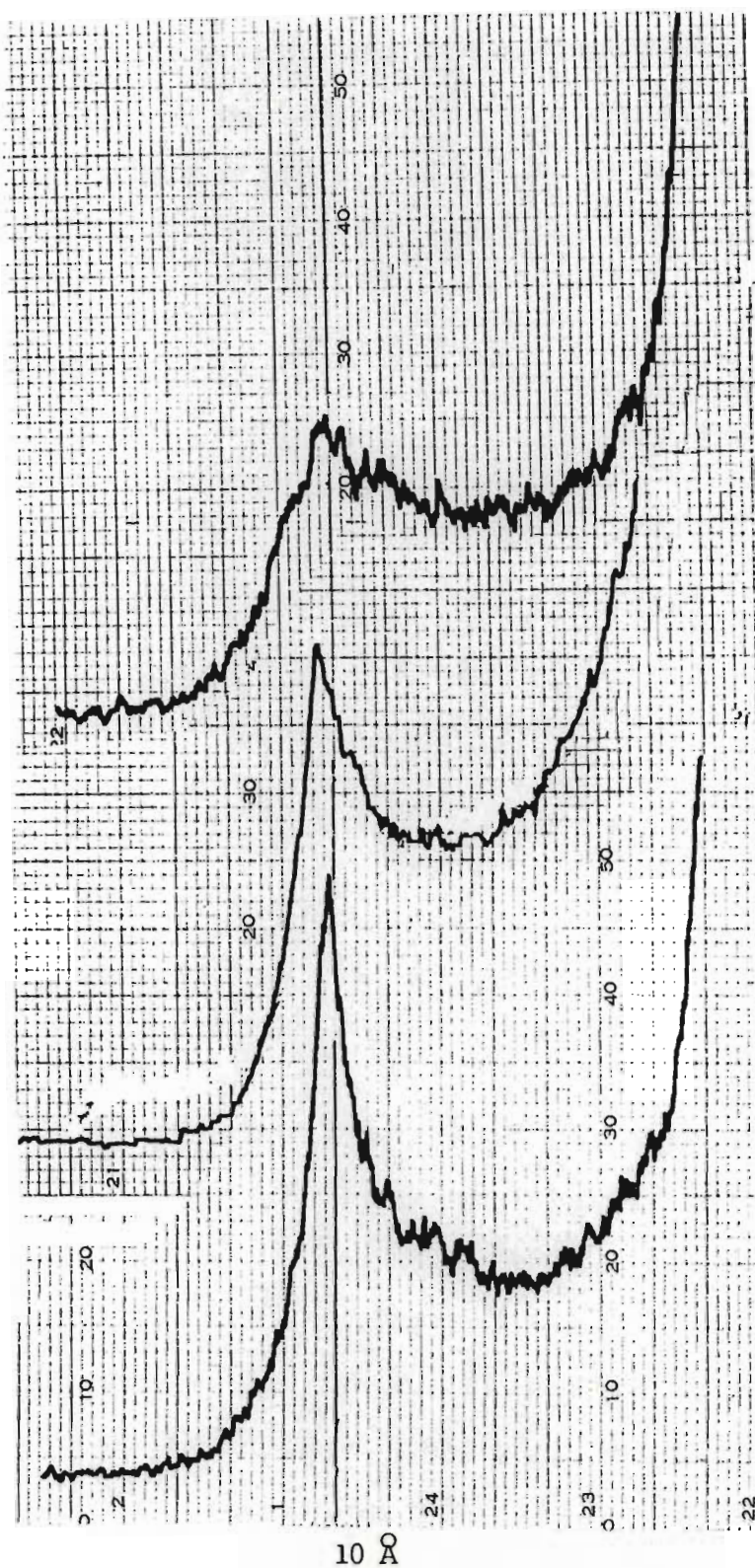


Figure 3.9 XRD pattern of the K-saturated 500°C heated clay fraction from different horizons of pit 2

preservation of the chlorite structure, and not as an authigenic mineral. As this high-charge corrensite occurs together with discrete mica and random mica-smectite and mica-vermiculite interstratifications, the measurement of secondary reflections for regularity is impossible due to superimposition of reflections, and even the (001) reflection is not measurable due to its low intensity. The (002) reflection is characteristic for high-charge corrensite (Figure 3.10, Table 3.2) :

Table 3.2 Peak positions (\AA) of high-charge corrensite (from pit 4, C horizon)

Mg, air dried	14,5 \AA	Li, air dried	13,4 \AA
Mg. ethylene glycol	14,5 \AA	Li, 280°C	12,4 \AA
Mg, glycerol	14,5 \AA	Li, 280°C, glycol	14,4 \AA
K, air dried	12,2 \AA		
K, 110°C, glycol	12,2 \AA		
K, 500°C	12,2 \AA		

The 14,5 \AA reflection in the Mg, glycerol pattern (Figure 3.10) cannot result from discrete chlorite, since this would give a distinct (002) reflection at 7 \AA with an intensity at least twice that of the first order reflection. No peak is observed, however, in the Mg, glycerol pattern at 7 \AA . The peak at 12 \AA in the K, 500°C pattern is the most characteristic one for corrensite when occurring in the presence of other 14 \AA minerals, and rules out vermiculite as a possibility.

The information obtained from the intensity of weathering of the chlorite and the degree of weathering of the Ecca shale saprolite

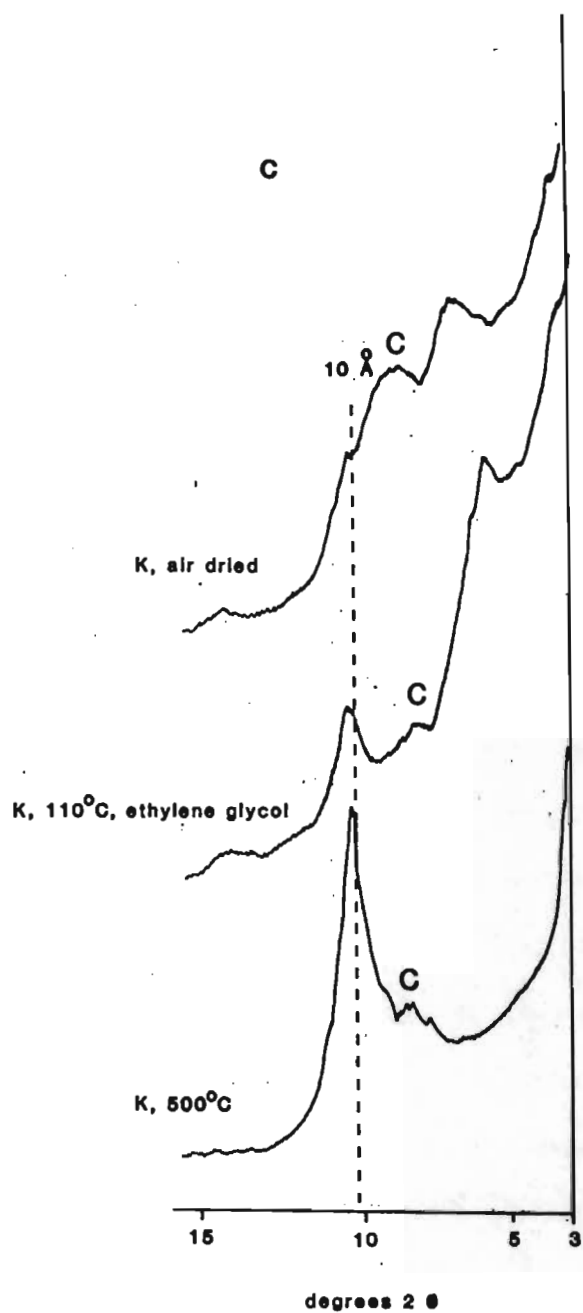
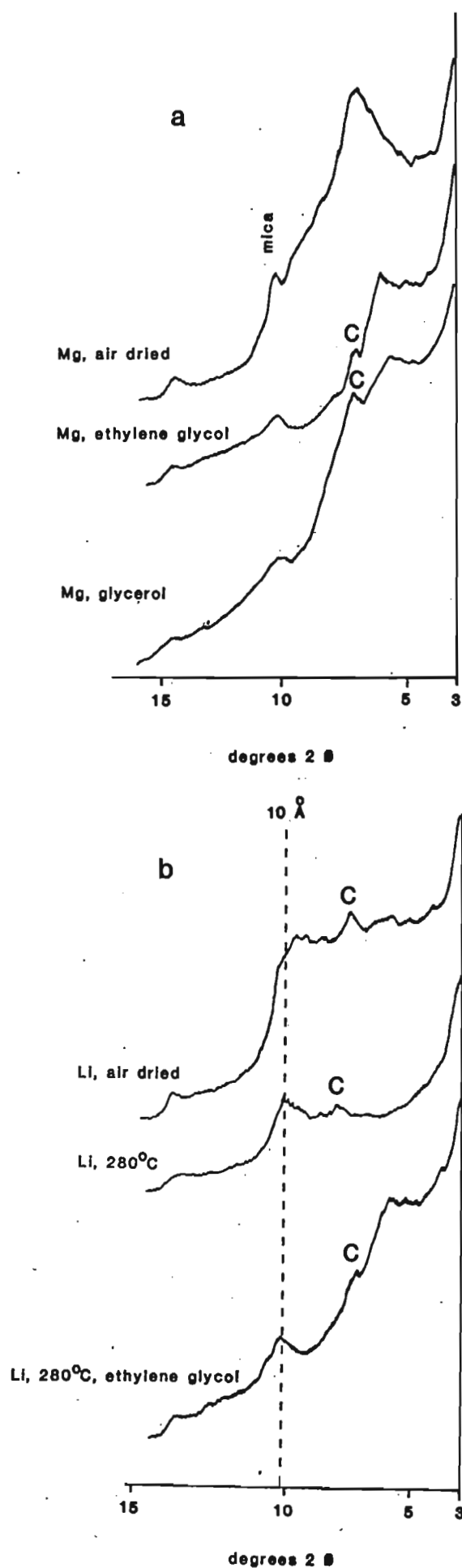


Figure 3.10 XRD traces of the clay fraction of the C horizon of pit 4 (oriented specimen) (a) Mg-saturated; (b) Li-saturated; (c) K-saturated

suggests that pit 1 is the least weathered horizon (discrete chlorite present), followed by pit 4. Pits 2, 3 and 8 are weathered to a much higher degree with no chlorite being detectable even in the saprolite. In no case was it apparent that the weathering of chlorite had proceeded to the formation of a discrete smectite or kaolinite.

(ii) Transformation of mica

The main pathway of mica alteration during weathering and soil formation is generally regarded as a stage-by-stage transformation with preservation of the layer structure through stages of vermiculite and beidellite to kaolinite (Fanning and Keramidas, 1977; Bisdom et al., 1982). Alternatively, a dissolution-precipitation mechanism has been suggested by Nadeau, Wilson, McHardy and Tait (1984). On the basis of layer charge determinations, the transformation of mica into vermiculite and finally into smectite would appear to proceed by two reaction sequences : one reaction path first leads to relatively homogeneous vermiculite, which then alters to heterogeneous smectite. In the other sequence, initially heterogeneous hydromica and vermiculite are formed, which then transform to smectite with similar or different charge heterogeneities (Lagaly, 1982). Vermiculite is regarded in this sequence by some authors as a very short-lived intermediate (Kittrick, 1973). When mica weathers in soils, the exchange of K for hydrated cations in some interlayers is more rapid than in others, resulting in an interstratified structure (Bisdom, Stoops, Delvigne, Curmi and Altemuller, 1982; Lagaly, 1982).

Despite the presence of chlorite and mica in approximately equal amounts in the unweathered shale (Figure 3.4), the clay fraction of the shale-derived soil is dominated by micaceous minerals and their weathering products, mica-smectite interstratifications. Mica weathering, therefore plays the key role in determining the nature of the clay fraction. The essential changes for smectite formation from mica (i.e. depotassication, dealumination plus subsequent silication of the tetrahedral sheet, extensive changes without which the product is unable to possess the lower charge characteristics of smectite) have taken place at least to some extent.

In contrast to the case of chlorite, the weathering products of mica are enriched in the fine clay fraction, which points to authigenic formation at least in part, rather than to a solid-state reaction (Nadeau et al., 1984).

Weathering of mica leads to mica-smectite mixed-layer minerals with small amounts of discrete mica still present in all horizons (Figure 3.11a,b). The amount of discrete mica seems not to vary with stage of soil development. This points to the possible presence of two different types of mica with a different degree of resistance to weathering, for example Fe-rich mica and Al-rich mica. The presence of more than one type of mica in sediments has been confirmed by a number of authors (Glüven, Hower and Davies, 1980; Srodon and Eberl, 1984). The mica component in the mica-smectite interstratifications decreased with increasing distance from the saprolite. The mixed-layer mineral was

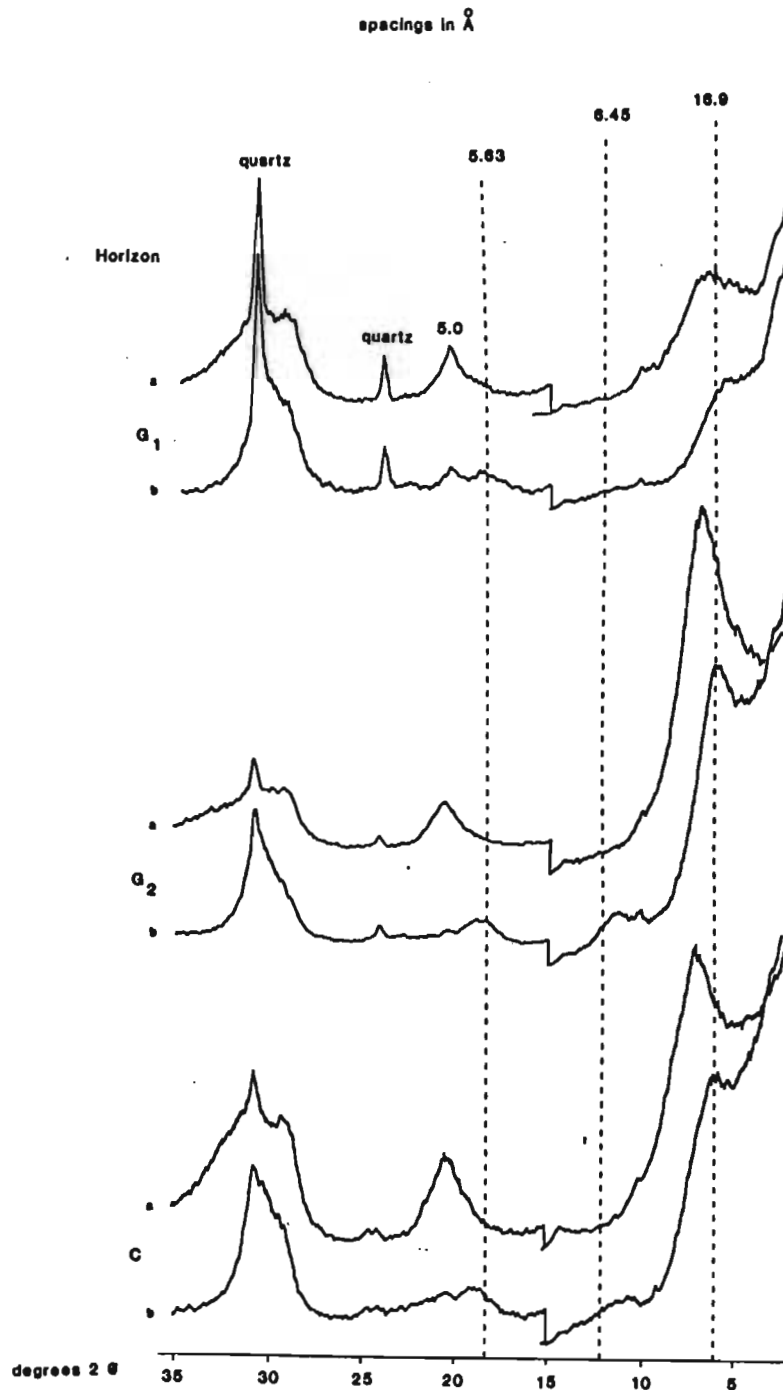


Figure 3.11a XRD traces of the $< 2 \mu\text{m}$ fraction of the C and G horizons of pit 2 (oriented specimen, Mg-saturated): (a) air dried; (b) ethylene glycol solvated; dashed line : peak positions of discrete smectite (Mg, EG), in order to demonstrate shifts due to interstratification. (there is a scale change at $15^\circ 2\theta$.)

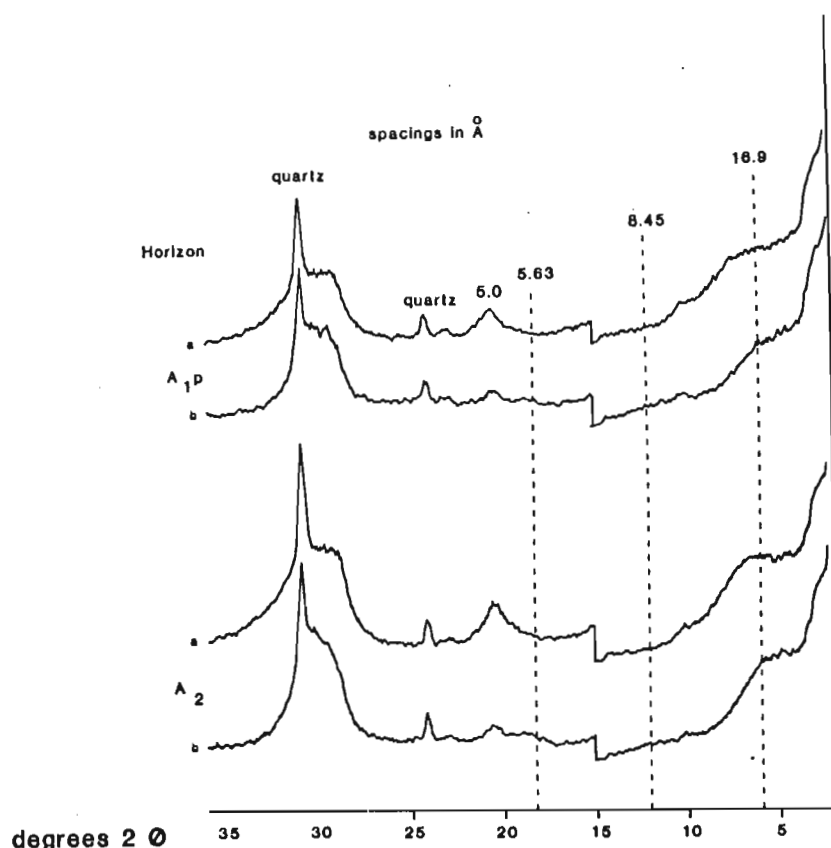


Figure 3.11b XRD traces of the $< 2 \mu\text{m}$ fraction of the two A horizons of pit 2 (oriented specimen, Mg-saturated) as Figure 3.11a

ordered in the case of the deepest horizon of pit 1 only. Peak positions of 27 \AA , $16,3 \text{ \AA}$, $9,1 \text{ \AA}$ and $5,3 \text{ \AA}$ (Mg-saturated, glycolated) indicate the high degree of ordering and a mica content of 56% (Figure 3.12 see also Table 1.1 and Figure 1.7). Since the formation of ordered mixed-layer structures can be considered as a first step in the weathering sequence, this information is consistent with the earlier assessment of least-weathered status made for pit 1 soil. Alternatively, the ordered mica-smectite structure may be the weathering product of K-feldspar. In all horizons of the other pits and in the G2, A2 and A1 horizon of pit 1, the mica-smectite interstratification was irregular, the

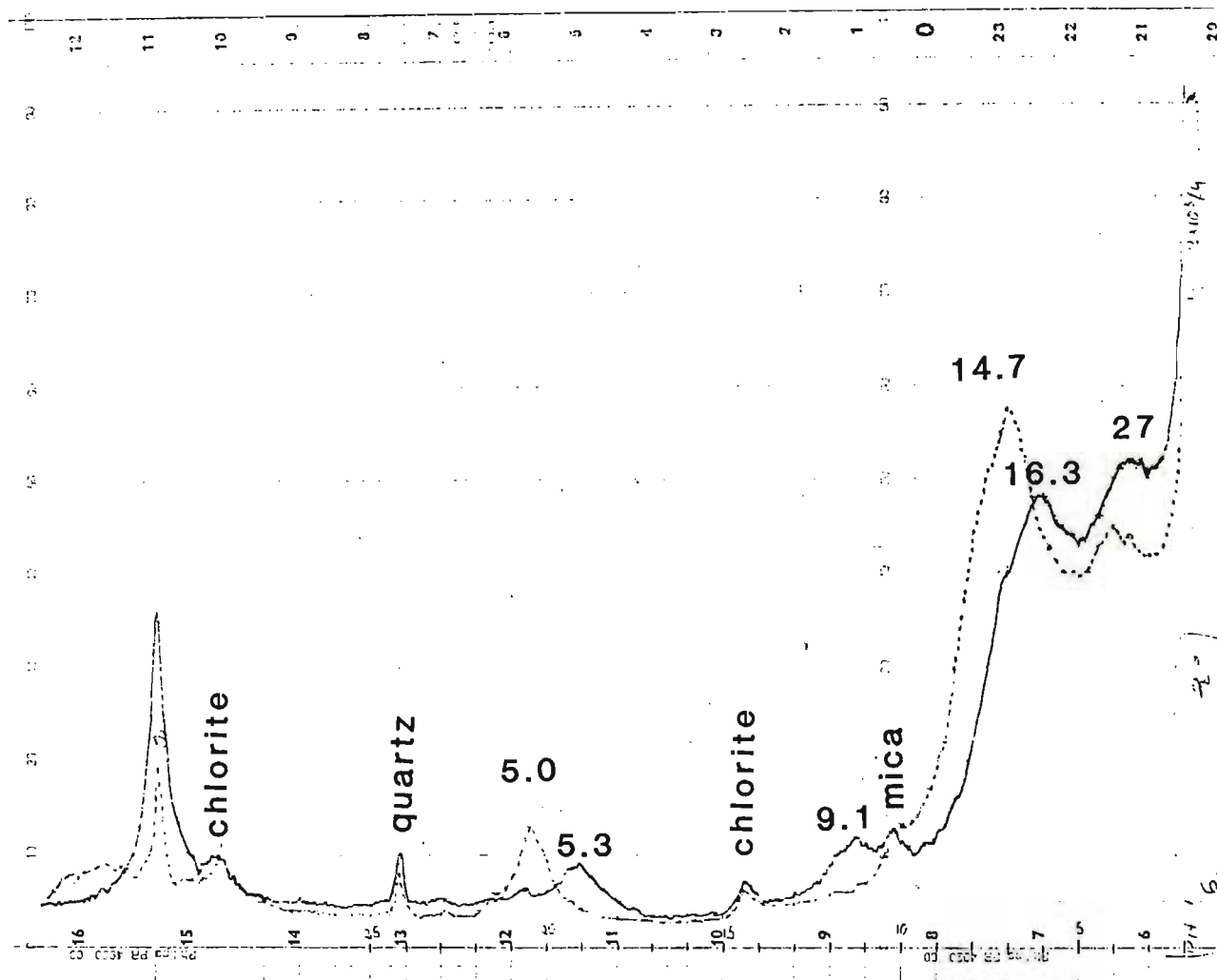


Figure 3.12 XRD pattern of the clay fraction of pit 1, G₂ horizon : dotted line : Mg-saturated, air dried; solid line : Mg-saturated, glycolated

degree of randomization increasing towards the top of each profile. The following peak positions, given in $^{\circ}$ were measured

for the Mg-saturated, ethylene glycol solvated pattern of pit 2 (Figure 3.11), which may be taken as being representative of all shale derived soil profiles except that of pit 1 (the percentage of mica was derived according to Reynolds, 1980) :

Table 3.3 Spacings and composition of the Pit 2 clay

Horizon	Peak position (Å) (Mg + ethylene glycol)			Proportion of mica in the mica-smectite interstratification (%)
A1	?	?	?	
A2	17,5	?	5,54	30
G1	17,8	?	5,45	50
G2	16,9	9,0	5,45	50
C	16,9	9,3	5,35	60

? : not measurable

Randomization led to the elimination of peaks in the > 6 Å region in all surface horizons: peaks become diffuse and increasingly indistinguishable from the background, leaving a series of very feeble peaks in the > 10 Å region. The < 10 Å region is characterized by a lower background. The only peak to be measured had its position at 3,5 Å to 3,3 Å (Mg-saturated, glycolated specimen; Figure 3.11b). This spacing, which is affected by other treatments, is indicative of an interstratification of smectite (3,38 Å) with mica (3,3 Å) and additional chlorite (3,55 Å) and/or vermiculite (3,55 Å) and/or kaolinite (3,57 Å). The subdued shoulder bridging the 10 - 7 Å region in all patterns indicates only small amounts of kaolinite,

if any, in these interstratifications, as does the presence of a peak in the 5 Å region. A broad shoulder on the 10 Å peak after K-saturation and heating to 500°C points to a high degree of chloritization (see Figure 3.9).

The beidellitic nature of the smectite component was confirmed by solvation with dodecylammoniumchloride and by the Greene-Kelly test on those samples which exhibited discrete peaks in the 14 Å region (Figure 3.12).

To summarize: the dominant clay mineral in the shale-derived soil profiles is a smectite-mica interstratification, which is Al interlayered in the top horizons. In deeper horizons, the mica-component is dominant and decreases in favour of a beidellitic component towards the surface. The influence of weathering products of chlorite on the clay fraction is negligible compared to the influence of micaceous weathering products. The degree of weathering must be regarded as moderate only, since in no case was discrete kaolinite formed.

3.3.1.2.3 Group III profiles (pits 27 - 30)

The clay fraction of the doleritic saprolite of this group is dominated by a mineral which is characterized by a 15 Å reflection in the Mg-saturated, air dried state, by expansion to 17 Å with ethylene glycol (Figure 3.13) and to 18 Å with glycerol, and which therefore could be termed smectite if only that part of the

pattern between 25 and 7 Å is considered. There are, however, important characteristics which speak against the smectitic nature of this mineral. These are, firstly, the obvious decrease in intensity of the (003) reflection, compared with discrete smectite from group I samples and, secondly, the increase in the (005) spacing of this mineral to 3,53 Å compared with smectite. Pure smectite must give a 3,38 - 3,4 Å (005) reflection when Mg-saturated and ethylene glycol solvated. Interstratification with mica will result in a decrease in the value of this spacing, while interstratification with either chlorite, vermiculite and/or kaolinite will result in an increase in this value. Thus an interstratification of smectite with one of the three latter components must be present in the C horizon of the samples of pits 26 - 30. The nature of this interstratification component can be readily derived from the strong decrease in the intensity of the reflection at ca. 5 Å and the increased broadening of the first basal reflections. Interstratifications of smectite with vermiculite and/or chlorite must give a well-ordered 14 Å peak in the Mg-saturated, air dried state (a stacking of 14 Å minerals only), and a strong peak at 5 Å, since all three minerals show 5 Å reflections. Only the presence of kaolinite as interstratified component with its basal spacing which is widely different from that of smectite will result in a considerable line broadening of the first basal reflection in the Mg-saturated, air dried state and in a strong decrease of the 003 smectite reflection due to the absence of any kaolinite reflection in this region. Reference to peak migration curves would suggest an interstratification of ca. 50%

kaolinite and 50% smectite. Additional to this, an interstratification with a characteristic "peak" bridging the $> 7 \text{ \AA}$ region is also present.

The amount of smectite-kaolinite interstratification decreases towards the top of the profile on account of the random interstratification, as seen by the increase in the intensity of the broad reflection between 7 and 10 \AA (Figure 3.13).

The irregular interstratification, which amounts to 100% of the clay fraction in the surface horizons, lacks any discrete peak in the $> 4 \text{ \AA}$ region and can be characterized by an intense and very broad peak spanning the $> 7 \text{ \AA}$ region (Figure 3.14).

By comparing the experimental pattern of the interstratification in all the top horizons with computer-calculated and published ones, a composition of 70% kaolinite and 30% partially chloritized smectite (Schultz et al., 1971; Figure 3.15) was found to provide the best estimate of the mineralogical composition of the interstratified material in question. In no case did discrete kaolinite occur in any of these soils (Figures 3.13 and 3.14).

The interstratification could be regarded as a weathering product of smectite and constitutes an intermediate in the weathering of beidellite to kaolinite, reflecting a more advanced stage of weathering than that which characterises group I profiles.

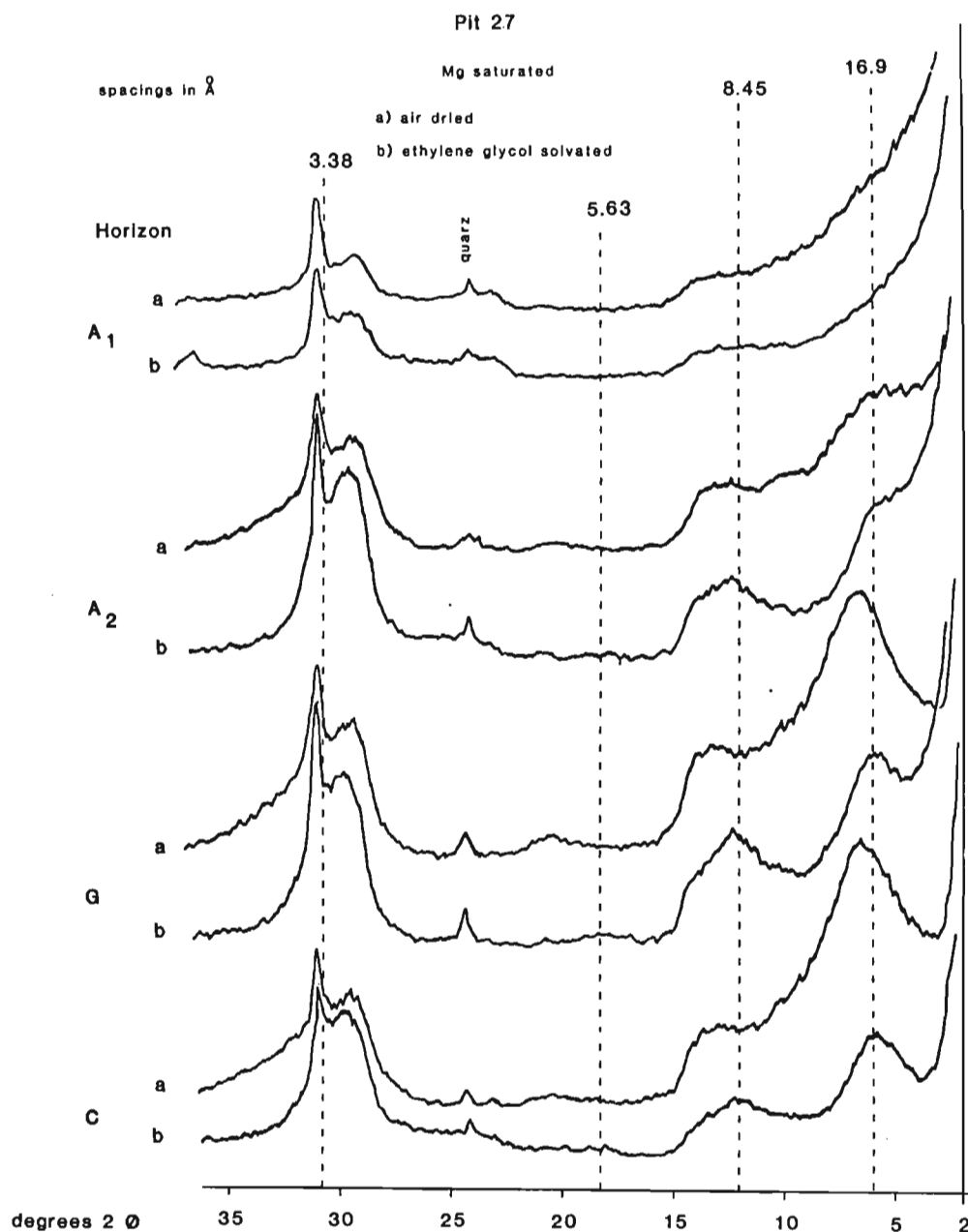


Figure 3.13 XRD traces of the clay fraction of the various horizons of pit 27 (oriented specimen, Mg-saturated) : (a) air dried; (b) ethylene glycol solvated

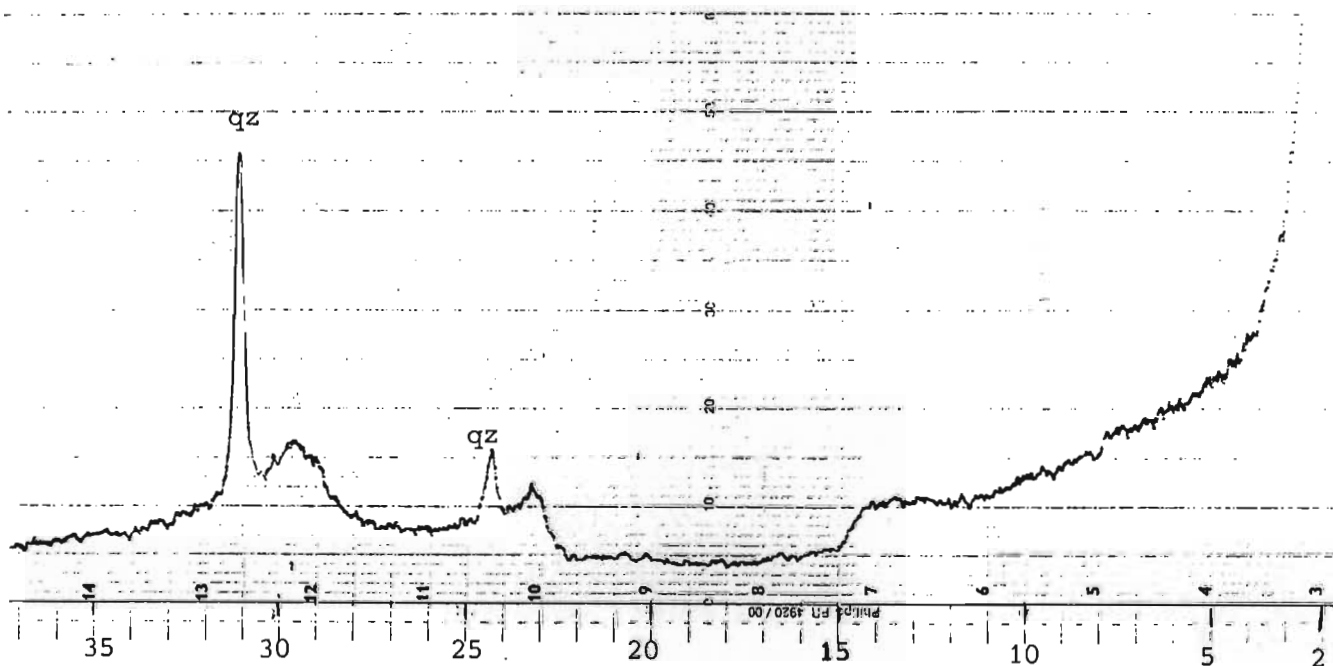


Figure 3.14 XRD pattern of the clay fraction of the A horizon of pit 30 (oriented specimen, Mg-saturated, air dried)

Another, though less likely, explanation for the occurrence of this interstratification is that these soils are contaminated by shale-derived material originating through colluviation from surrounding shale-derived material. The smaller likelihood of this explanation is evident in the nature of the interstratification, particularly with respect to the "peak" intensity in the 7 - 10 Å region, when the K-saturated 300°C, glycolated patterns are compared (Fig 3.16). Although no discrete peak positions in the > 7 Å range can be measured in the surface horizons of either of profile Types II and III, the shape of the peak in each case suggests two different types of interstratification.

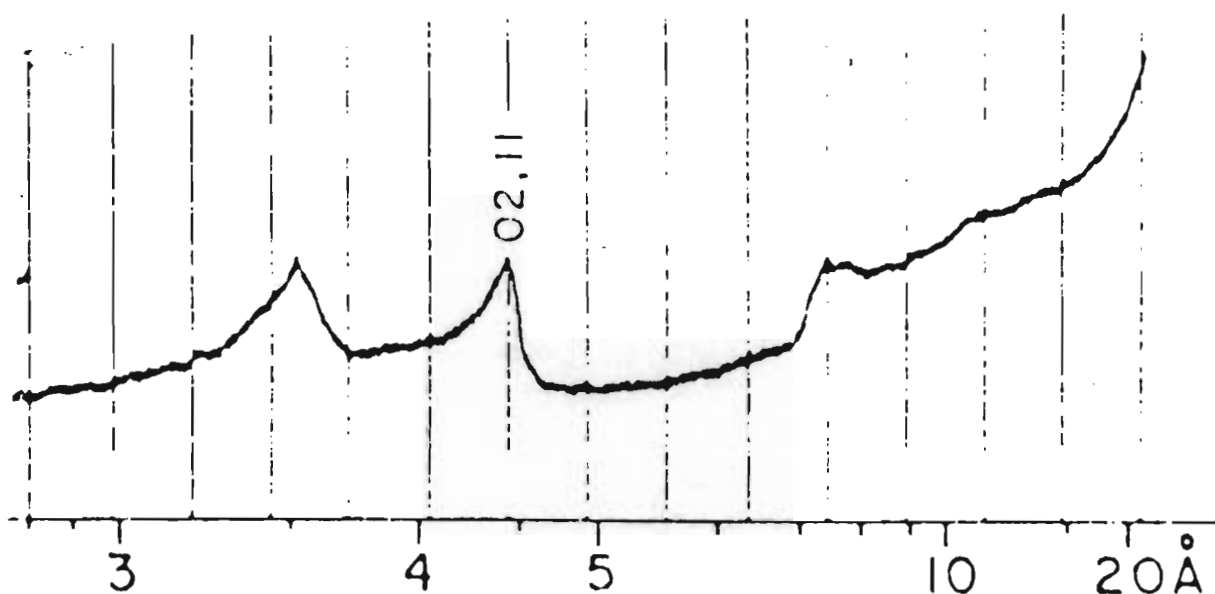


Figure 3.15 XRD traces of a random kaolinite-smectite interstratification with approximately 70% kaolinite (Schultz et al., 1971)

The heavy mineral associations as well as chemical data presented in Sections 3.3.4 and 3.4 also confirm the mineralogical results.

3.3.2 Exchangeable cations and the "degree of crystallinity"

To the extent that the "sharpness of a reflection" may be equated with degree of crystallinity (Weaver, 1960), the swelling 14 Å minerals on the Tutuka transect show considerable variation in crystallinity.

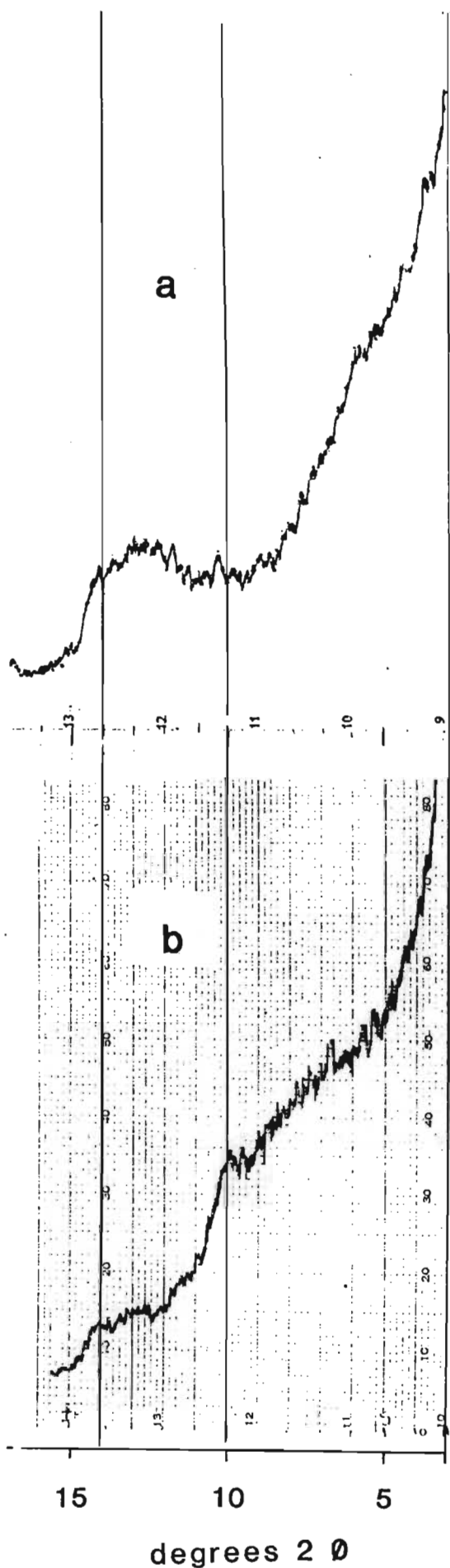


Figure 3.16 XRD pattern of the < 2 μm fraction of two top horizons (oriented specimen, K-saturated, 300°C, glycolated) (a) pit 29 (dolerite saprolite); (b) pit 1 (shale saprolite)

Of interest is the fact that the degree of crystallinity, which may possibly be ascribed to such diverse origins as interstratifications with mica (in the clay of pits 1 - 8), interstratifications with kaolinite (pits 26 - 30) or structural or site-occupancy disorder (pits 12 - 25), is related to the concentration in the soil of total extractable basic cations. In general, the degree of crystallinity is lower in the surface horizon of a profile compared with the saprolite, provided that the amount of primary minerals is very low in the A horizon (pits 1 - 8 and 26 - 30) (Figures 3.11, 3.13). When the amount of primary minerals (especially minerals with divalent cations in their structure such as plagioclase) is high throughout the profile, no apparent dependence of crystallinity upon profile depth can be observed.

The degree of crystallinity of the 14 Å mineral was measured from the pattern of the Mg-saturated, air dried specimen in two ways : (i) from the ratio of the peak minus background heights at 10 Å and 10,5 Å (Weaver, 1960); and (ii) from the angle between the vertical drawn through the peak maximum and the tangent fitting maximally to the low angle shoulder. The relationship between the two indices of degree of crystallinity and total extractable bases (the latter obtained from Appendix 18) are plotted in Figure 3.17 a and b, respectively. In both cases the correlation is strong ($r^2 = 0,87$ and $0,75$, respectively) and the use of either index produces a very similar indication of the nature of

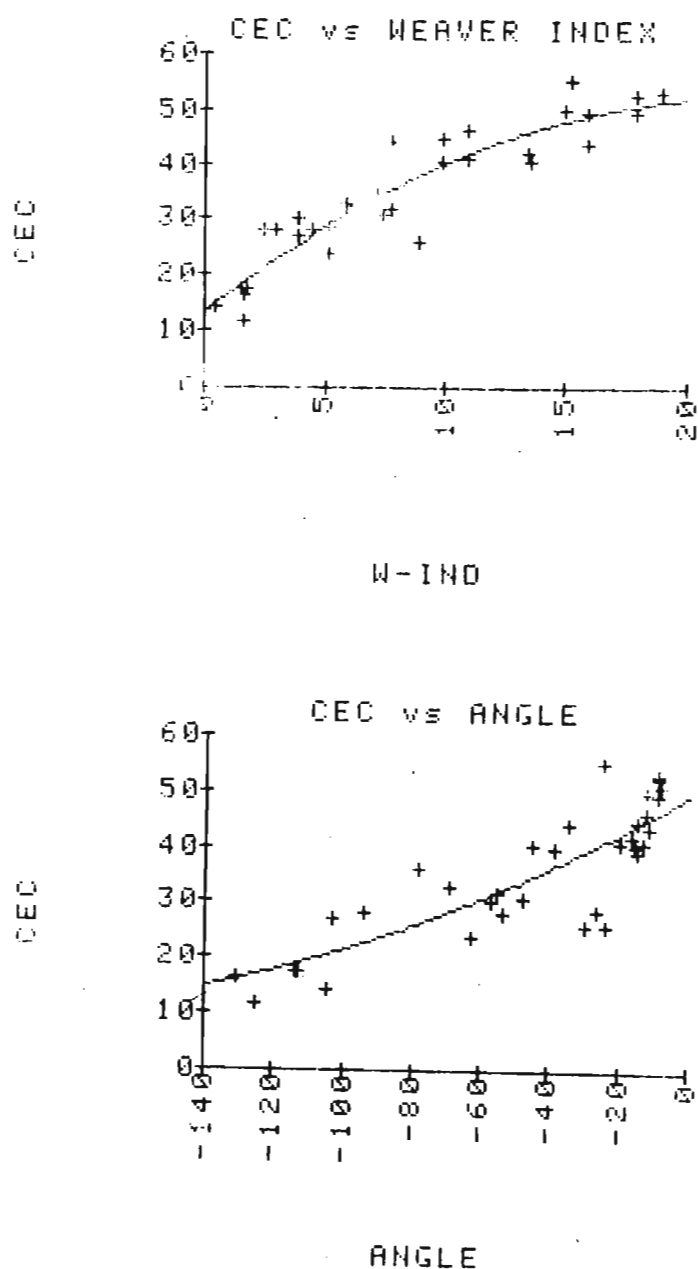


Figure 3.17 Relationship of total extractable bases to indices of crystallinity (a) peak intensity, and (b) angle of deviation of peak shoulder from the vertical, for the 001 reflection of swelling layer silicates in clay fractions from soil profiles on the Tutuka transect. (CEC values are taken from Appendix 18.)

the relationship.

There does not appear to be any obvious way of establishing (a) whether or not the relationship in Figure 3.17 is causal, and (b) if so, which one of the two variables is dependent upon the other. Certainly to the extent that the apparent degree of crystallinity is an indirect measure of the degree of admixture of lower charge mica or kaolinite components with smectite in an interstratified mineral, it might be expected that a lower overall charge, and therefore a lower quantity of exchangeable cations, might follow from an apparent decrease in crystallinity rather than vice versa. Such a suggestion has been put forward before (Millot, 1970; Lucas and Ataman, 1968), although the situation is more likely one of covariance rather than a direct causal relationship.

3.3.3 Electron microscopy

The clay fraction of representative dolerite- and shale-derived materials exhibited one consistent difference under the electron microscope with respect to the shape of the clay particles: dolerite-derived clay appeared as rounded to pseudo-hexagonal particles (Figure 3.18), whereas shale-derived clay plates exhibited a very irregular outline (Figure 3.19) despite the fact that there was no apparent difference in the approximate dimensions of plates in material of either origin. Since the specimens illustrated in Figures 3.18 and 3.19 represent opposite cases of the 001 line broadening ("degree of crystallinity")

discussed in the previous section, it is evident that these apparent differences in crystallinity suggested by X-ray diffractograms are not obviously attributed simply to particle size or mean crystallite dimension. Rather, as suggested earlier, the cause of line broadening is probably the degree of interstratification of the smectite with other (mica or kaolinite) phases and particularly the randomness of stacking. Structural or site-occupancy disorder may also be involved.

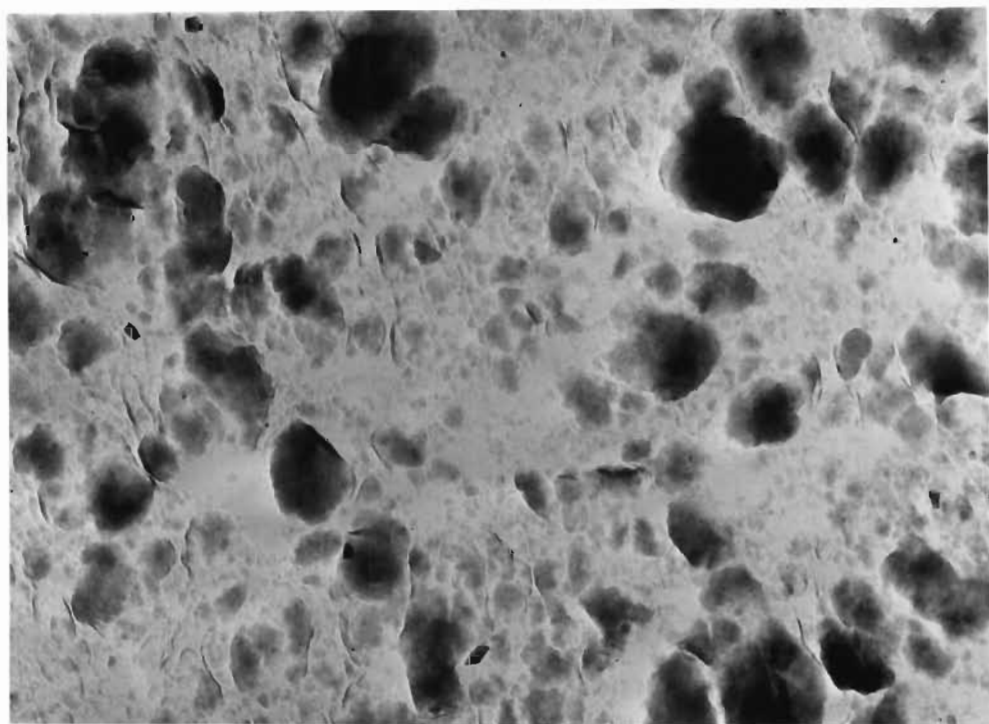


Figure 3.18 Transmission electron micrograph of the clay fraction of pit 17 A₁ (print magnification 1:15 000)

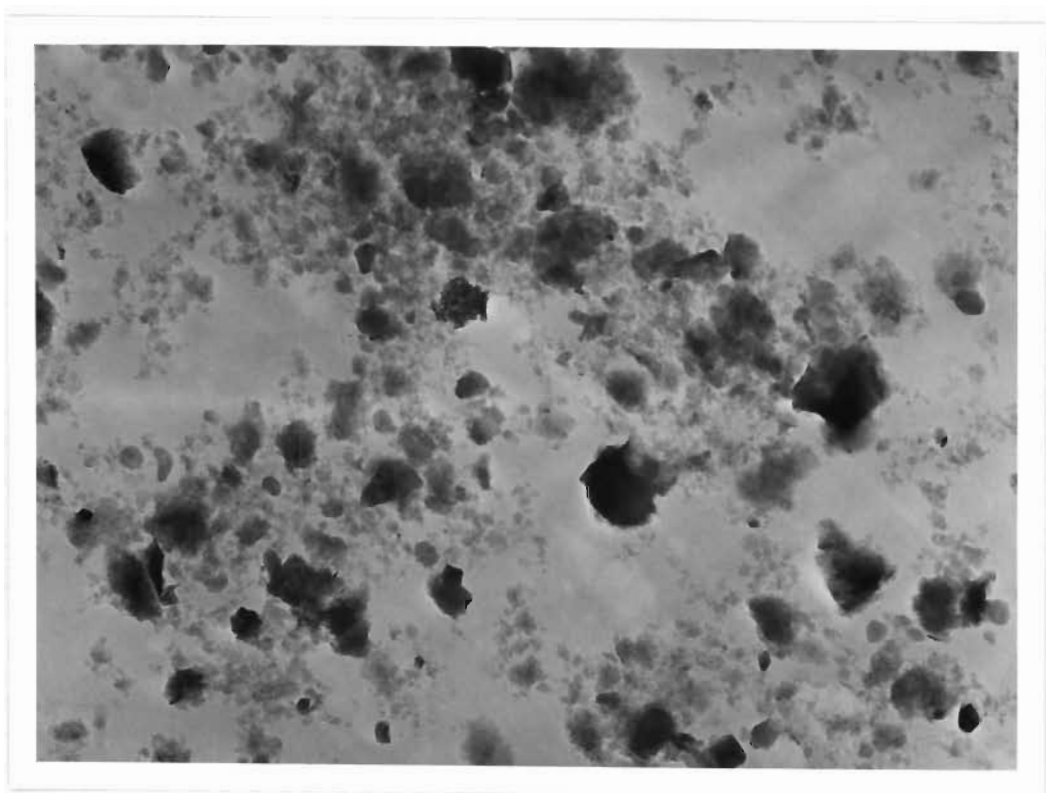


Figure 3.19 Transmission electron micrograph of the clay fraction of pit 2 A₁ (print magnification 1:15 000)

3.3.4 Total chemical analysis

Dolerite, with its predominant pyroxene-plagioclase composition, and shale with a quartz-K-feldspar-plagioclase-mica-chlorite mineral assemblage, may be assumed to weather to clay minerals with differences in chemical composition. These differences can be expected to be more pronounced in the octahedral sheet (Fe, Al, Mg) and the interlayer. With respect to composition a high degree of tetrahedral substitution can be considered as being insufficiently stable to permit mineral persistence under soil-forming conditions. Potassium is likely to be the most diagnostic element for chemically differentiating materials

according to their origin.

Total chemical analysis of deferrated (dithionite-citrate-bicarbonate) Li-saturated clays was performed in an attempt to differentiate between dolerite- and shale-derived soils, particularly with the aim of confirming the origin of the soils of group III (pits 26 - 31), as well as to investigate possible changes with decreasing depth from saprolite to the surface horizon which might be interpreted as a chemical weathering sequence. Chemical analyses of the clay from one representative profile of each of the three soil groups on the transect are shown in Table 3.4. Interestingly there is little to differentiate dolerite- from shale-derived soil clays (pits 17 and 1, respectively) except for the facts that (i) the dolerite-derived profile is characterised by a slightly higher Fe and lower Al concentration, and (ii) the shale-derived profile has clay with a considerably higher K content.

The group III profile (pit 30) has, on the one hand, a greater affinity with the shale-derived soil (pit 1) on the basis of Fe_2O_3 content as well as $\text{SiO}_2/\text{Al}_2\text{O}_3$ ratio while on the other hand there is a stronger relationship between pit 30 and pit 17 (dolerite-derived) with respect to K content, that of pit 1 being at least three to four times higher. The relatively low $\text{SiO}_2/\text{Al}_2\text{O}_3$ ratio of pit 30 clay, especially in the A horizon, is consistent with the XRD evidence for the presence of a kaolinite-smectite interstratification, in turn suggestive of a higher degree of weathering which could militate against the use of K

Table 3.4 Chemical composition of the clay fraction from representative profiles of each of the 3 groups : pit 1 (shale-derived), pit 17 (dolerite-derived) and pit 30 (possible shale colluviation)

	Sample	Weight loss	SiO ₂ /Al ₂ O ₃	SiO ₂	Al ₂ O ₃	Fe ₂ O ₃	MnO	MgO	CaO	Na ₂ O	K ₂ O	TiO ₂	P ₂ O ₅
Pit 1	A ₁ p	19,75	2,31	59,99	26,00	9,15	0,14	1,36	0,85	0,06	1,73	1,20	0,13
	A ₂	20,26	2,12	57,63	27,24	9,86	0,04	1,87	1,06	0,22	1,97	0,91	0,05
	G ₁	20,63	2,33	59,55	25,61	9,89	0,08	1,60	0,33	0,20	1,91	0,95	0,05
	G ₂	18,91	2,35	59,50	25,32	11,71	0,09	1,83	0,19	0,00	1,99	0,94	0,04
	C	11,78	2,63	62,47	23,77	6,88	0,05	2,27	0,37	0,42	3,11	0,79	0,05
Pit 17	A ₁	18,96	2,59	59,49	22,93	14,17	0,24	1,76	0,36	0,00	0,57	0,74	0,10
	A ₂	21,71	2,55	59,04	23,18	14,46	0,09	2,07	0,32	0,14	0,58	0,64	0,07
	C	16,96	3,35	63,09	18,86	11,05	0,11	1,98	1,49	0,41	0,79	1,01	0,05
Pit 30	A ₁ p	19,82	1,97	58,06	29,48	10,39	0,12	0,98	0,29	0,02	0,56	0,74	0,05
	B	20,75	2,12	57,95	27,36	11,22	0,06	0,93	0,30	0,06	0,53	0,92	0,07
	G	18,96	2,21	58,91	26,69	11,82	0,07	1,27	0,22	0,12	0,66	0,86	0,03
	C	19,01	2,18	58,31	26,79	12,35	0,13	1,20	0,23	0,00	0,54	0,69	0,03

content as a basis for establishing the influence of shale or otherwise as parent material (through colluvial aggradation over the doleritic saprolite) in the formation of group III soils. Additional evidence will be examined later in connection with lithology.

3.4 Heavy mineral investigation (with special reference to group III soils and the prevalence of quartz)

Dolerite characteristically contains very little quartz (approximately 5% in the least weathered saprolite horizon of pit 17). An increase in the concentration of quartz from the doleritic saprolite to the surface horizon of a profile could be explained in different ways :

(a) A relative increase in the concentration of primary quartz due to the weathering of pyroxene and feldspar followed by at least partial removal of dissolved weathering products by leaching. In the case of the group III profiles (pits 27 - 30) more than 90% of the original minerals would have to be dissolved to achieve the quartz content of more than 50% which characterizes the surface horizon.

(b) The neoformation of quartz may take place in a pedogenic environment under conditions which are conducive to the formation of iron and manganese hydroxides (Harder and Menschel, 1967; Harder and Fleming, 1970). In the profiles just mentioned, this would have to be a major soil forming process in order to account for the concentration observed.

(c) Colluvial aggradation from surrounding areas in which soils

have formed from more quartzose parent material (eg. shale). Sorting according to particle size during transport may give rise to further enrichment of quartz in sand and silt fractions. Oberholster (1969b) and MacVicar (1978) have regarded quartz in profiles overlying dolerite as being solely of colluvial origin, even when found at depths of 120 cm.

(d) Eluviation of clay (lessivage) from surface horizons (both laterally and vertically) may give rise to enrichment of quartz as a result of its predominantly coarser (silt or sand) particle size.

An approach for testing any possible influence of colluviated material, which is different lithologically from the underlying saprolite, is the investigation of the heavy mineral fraction. In general: heavy minerals are relatively resistant to weathering and to alterations during transport. A different heavy mineral association is therefore a good indication of a lithological discontinuity within a soil profile, and it was considered potentially fruitful to apply this principle to the question concerning the genetic history of the group III soils (pits 27 - 31), which have dolerite saprolite but are mapped as shale-derived (Fey and Cass, 1983) due to their lighter coloured topsoil.

The high quartz content and the lighter coloured surface horizon suggest the domination of shale-derived material, through colluviation, with the quartz being assumed to be detrital and the colour characteristic for shale or at least uncharacteristic

for soils derived from dolerite under the prevailing pedogenic conditions (Oberholster, 1969; MacVicar, 1978; Fey and Cass, 1983). If this assumption is correct, then the shale must influence the heavy mineral fraction in such a way that either the whole fraction is composed of shale-derived heavy minerals or that both dolerite and shale have contributed their characteristic heavy minerals to give a mixed fraction.

The heavy mineral association of the 100 - 500 μ m grain size fraction of the surface horizons of selected shale-derived profiles (pits 1, 2, 3, 4, 6 and 8)) is composed of the following heavy minerals, in order of decreasing abundance : ilmenite, garnet. By contrast, the dolerite-derived surface horizons (pits 14, 15, 17 and 22) contain ilmenite, zircon, magnetite and rutile. The heavy mineral association of the surface horizons of pits 27 - 31 is essentially the same as those derived from dolerite, except for a slightly higher zircon and rutile content. The absence of detectable garnet therefore suggests that the influence of shale-derived material on the formation of these group III soils is not a dominant one. The increase in quartz content from saprolite to surface horizons, which is accompanied by the weathering of smectite to an interstratification with approximately 70% kaolinite and 30% (partially chloritized) smectite, may thus be attributed to a probable combination of the processes listed above, but not necessarily including process (C), that is, the colluvial influence of shale-derived material from surrounding areas.

3.5 Summary and discussion

The aim of the investigation reported in this chapter was to determine the clay and non-clay mineral composition, particularly in relation to parent material and soil morphology, and to thus contribute towards a better understanding of mineral weathering and soil genesis in smectite-forming environments.

The soils of the Tutuka transect can be grouped mineralogically into three classes, each of which has its own characteristic pattern of clay mineral formation/alteration and non-clay mineral association from the saprolite to the surface. The results obtained from the investigation of the clay fractions generally indicate a strong relationship between the clay mineralogy of the saprolite and the nature of the clay fraction in the overlying soil. This is particularly evident where the soils overlies shale saprolite but is also true of soils derived from dolerite. Despite the dominant influence of "inheritance", however, the effect of weathering can readily be discerned.

Dolerite-derived soils

Where the degree of weathering is low, base status is high (see Appendix 18), and primary minerals rich in divalent ions (plagioclase mainly) are still present, the clay minerals that characterize the saprolite persist into the surface horizon as discrete minerals with a high degree of crystallinity. These smectites are characterized by a heterogeneous charge distribu-

tion (ie montmorillonite-Fe beidellite interstratification).

The preservation of high smectite crystallinity in sediments with a high base status has been widely observed and has been attributed to "aggradation" processes taking place in an environment rich in soluble basic cations (Lucas and Ataman, 1968). It may, however, simply reflect the absence of any interstratification combined with a maximal degree of ordering within the clay structure due to the non-fluctuating nature of the chemical environment.

High base status is also consistent with a low degree of desilication and therefore a relative Al content which is too low for kaolinite formation and for Al interlayering of the smectite. With increasing weathering, smectite is apparently unstable and a kaolinite-smectite interstratification is formed (assuming, that is, that the group III soils are predominantly dolerite-derived). These differences in degree of weathering along the same transect may be attributed to one or more factors, the most probable being localized topographic (and therefore drainage) differences.

Shale-derived soils

The primary chlorite was found to have weathered at a very early stage, and the mineralogical differences conforming with the degree of weathering and soil development are thus largely associated with variations in the nature of the interstratification derived from weathered mica, which has been, to varying

degrees, hydrated and transformed into an interstratified structure with beidellite as the main alteration component. The proportion of beidellite and the randomness of the stacking increase with increasing degree of weathering, as does the amount of Al interlayering (chloritization).

Soil colour

The suggestion that lighter soil colours necessarily result from weathering of shale parent material could not be confirmed. This is because the mineralogical investigation of the group III profiles, all of them having dolerite saprolite (but which were classified as shale-derived due to their lighter topsoil colour by Fey and Cass (1983)), was not able to establish any definite influence of shale on these soils.

The present investigation has also suggested that the black humus variety, i.e. the condensed (Flaig, Beutelspacher and Rietz, 1975), poorly crystalline (Wang et al., 1983), "gray" humic acid polymer complex (Kononova, 1975), is associated with a well-ordered smectite (which contains ferric iron in its structure) characteristic of the group I profiles derived from dolerite. Since polymerization is an abiotic process (Flaig et al., 1975; Wang et al., 1983) occurs "interlamellarly" (Singh, 1956), and requires the presence of structural ferric iron as electron acceptor (Theng, 1982), the well-ordered Fe^{3+} - containing smectite of pits 12 - 25 (group I) is ideally suited for this oxidative polymerization of organic matter into black

humic acid complexes. The presence of primary minerals (plagioclase, pyroxene) additional to the smectite ensures a high amount of divalent ions in the soil, necessary for the stability of the black complex. As soon as the interlayer and/or the surface of the smectite is blocked by hydroxides (chloritization of the smectite) as is the case in pits 1 - 8 (group II from shale), and/or the amount of catalytic surface is no longer in large excess with respect to the amount of components to be transformed, no polymerization seems to take place and the humic substances formed/transformed are either of the "brown" (unpolymerized) humic acid type or of the fulvic acid type. Kaolinite dominance in the smectite-kaolinite interstratification of the group III soils could represent a similarly unsuitable condition for the formation of the strongly pigmenting, highly polymerized black humus.

Interestingly, the degree of crystallinity of the smectite, which may be ascribed to such divergent causes as interstratification with chlorite and mica in the case of shale-derived (group II) soils, stacking and/or site occupancy disorder in the cases of dolerite-derived soils of group I, and interstratification with kaolinite in the case of group III soils is clearly related to the quantity of basic cations extractable from the soil and which may be assumed to exist predominantly within the smectite interlayer space.

The topsoil colour seems to be related more directly to the type

of clay mineral and the sand/silt/clay ratio than to the parent material per se. Differences between the soil profiles of group II (shale) and group III (dolerite) are also obvious from investigation of soil physical characteristics (air/water permeability, COLE, modulus of rupture) (Fey, Bühmann, Snyman and Cass, 1984; Snyman et al., 1985).

CHAPTER 4

THE OCCURRENCE OF FE-RICH TALC IN A PEDOGENIC ENVIRONMENT

4.1 Introduction

Formation of talc by hydrothermal alteration of basic rocks or by thermal metamorphism of siliceous dolomites is well documented (Deer, Howie and Zussman, 1962).

Its occurrence as a weathering product was first suggested by Guenot (1970) for a dolomitic parent material from the Congo, while Isphording (1973) reported small quantities of talc in a palygorskite-sepiolite clay deposit from the Yucatan Peninsula, Mexico.

Pion (1979) found talc in Upper Volta as an accessory mineral in kaolinitic or smectitic clays weathered from gabbro.

Eggleton and Boland (1982) have described the topotactic transformation of enstatite to talc via a three stage reaction.

Ideally, talc is a magnesium silicate, $\text{Mg}_3\text{Si}_4\text{O}_{10}(\text{OH})_2$, but the Mg may be partly replaced by elements such as Fe or Ni. An iron-rich talc, close to the ferrous end member position, has been named minnesotaite (Gruner, 1944). The occurrence of minnesotaite has been reported by Blake (1965) in association with stilpnomelane and Mn-Mg-siderite, in an environment subjected to

low grade metamorphism.

A mineral, intermediate in composition between talc and minnesotaite, has been described by Kager and Oen (1983) from a hydrothermal lead-zinc deposit.

Chukhrov, Zvyagin, Drits, Gorshkov, Ermilova, Góilo and Rudnitskaya (1979) were the first to identify the ferric analogue-ferripyrophyllite. The mineral is supposed to be of low temperature hydrothermal origin.

The first report on pedogenic ferruginous talc, containing up to 25 mol % Fe, was published by Paquet, Duplay and Nahon (1982) in samples from the Ivory Coast.

Since reports of talc formed in soil environments are scarce, and only one occurrence is reported from South Africa (Hahne and Fitzpatrick, 1984), preliminary indications of the occurrence of talc in a suite of Natal soils were pursued in more detail.

The objective of this Chapter is therefore to describe the occurrence of pedogenic talc, with a composition intermediate between talc and ferripyrophyllite/minnesotaite, in a suite of soils developed through subtropical weathering of basic igneous rocks.

A method is also presented whereby small amounts of this mineral may be concentrated for more exact study.

4.2 Materials and methods

Environmental conditions, sampling and methods have been described in detail in Chapter 2.

Additional to it, the following procedure for the enrichment and chemical analysis of the Fe-talc has been applied :

Talc enrichment was achieved by heating the clay fraction of kaolinite-containing soil horizons to 510°C for 4 hours, grinding in an agate mortar, and then contacting for about 2 minutes with hot HCl to dissolve iron minerals and amorphous Fe. Washing with distilled water followed. The HCl procedure was repeated until the sample showed a light brown colour. Longer treatment dissolved the talc as well. The residue was then boiled with 0,5 M NaOH for 2,5 minutes for removal of amorphous aluminosilicates (metakaolinite) (Jackson, 1968) and washed with distilled water.

An estimate of Fe:Mg ratio in this enriched talc was obtained with a Kevex energy dispersive X-ray analysis system attached to a JEOL JSM-35 scanning electron microscope.

4.3 Results and discussion

4.3.1 Soil mineral composition

XRD patterns of whole soil samples indicated that orthorhombic

pyroxene and plagioclase were the dominant weatherable minerals present, with some quartz which had become concentrated by weathering. Monoclinic pyroxene was recorded in small quantities only.

Hand-picked black and white grains from saprolite proved to be hypersthene and labradorite, respectively. Interestingly, clay minerals were only associated with the black grains; none could be detected in the white labradorite material. Scanning electron microscopy confirmed this observation, revealing only etched cleavage planes in the case of labradorite whereas hypersthene crystals exhibited surficial clay formation, probably by epitaxial or topotactic crystallization (Figure 2.23).

Qualitative mineralogy of the soil clay fractions is shown in Table 4.1.

In all the smectite-containing samples expansion of the (001) reflection to 17 Å occurred after glycol solvation, and the Greene-Kelly test (Greene-Kelly, 1953) indicated that the species present was beidellite, although in the Msinsini and Phoenix materials the (001) reflection was split into two distinct peaks after some pretreatments (Li-saturated and air dried or glycol solvated; Mg saturated and glycerol solvated) suggesting smectite heterogeneity.

The "chlorite" present in the three more weathered soils (Table 4.1) was unusual in that it was destroyed by heating to 300°C.

Table 4.1 Relative clay mineral composition of the soil clay fractions, based on XRD peak areas

Soil series	Relative abundance			Talc
	Smectite	Kandite	Chlorite	
Balmoral		++++	+	tr.
Richmond		++++	+	tr.
Stanger		++++	+	tr.
Msinsini	+++	++		tr.
Rydalvale	+++	++		tr.
Phoenix	++++	+		tr.

tr. = trace quantities

The 14 Å spacing showed no shift with glycol or glycerol treatments after Na-DCB pretreatment.

Changes with profile depth were generally insignificant except for the fact that, where halloysite material was present, the 10 Å halloysite content decreased towards the surface parallel with the increase in 7 Å halloysite. For more detail see Chapter 2.

The small 9,5 Å peak, the position of which remained unaffected by all specimen treatments, was consistently observed in all the soil clays and has been assigned to talc (Table 4.1, Figures 4.1a, 4.1b, 4.1c). Since the first basal reflection of talc occurs at 9,35 Å, a more detailed investigation of this material was carried out.

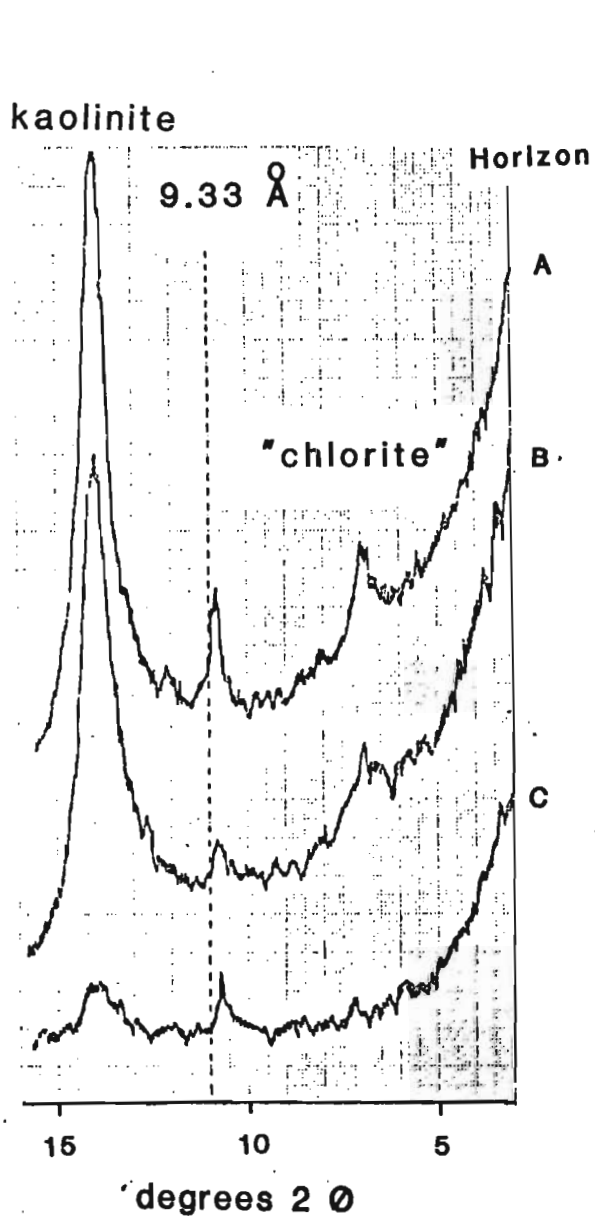


Figure 4.1a Stanger Soil Series : X-ray traces of the $< 2 \text{ \mu m}$ fraction of the untreated sample (oriented specimen)

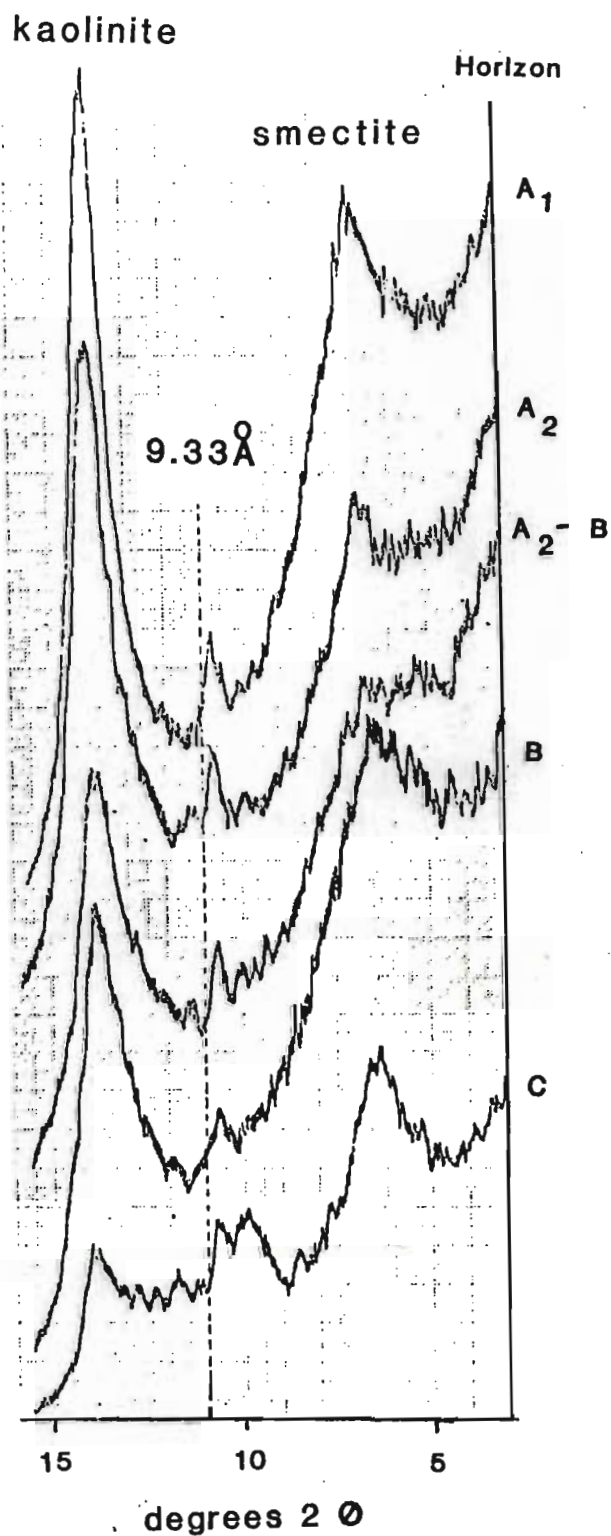


Figure 4.1b Msinsini Soil Series : X-ray traces of the $< 2 \text{ \mu m}$ fraction of the untreated sample (oriented specimen)

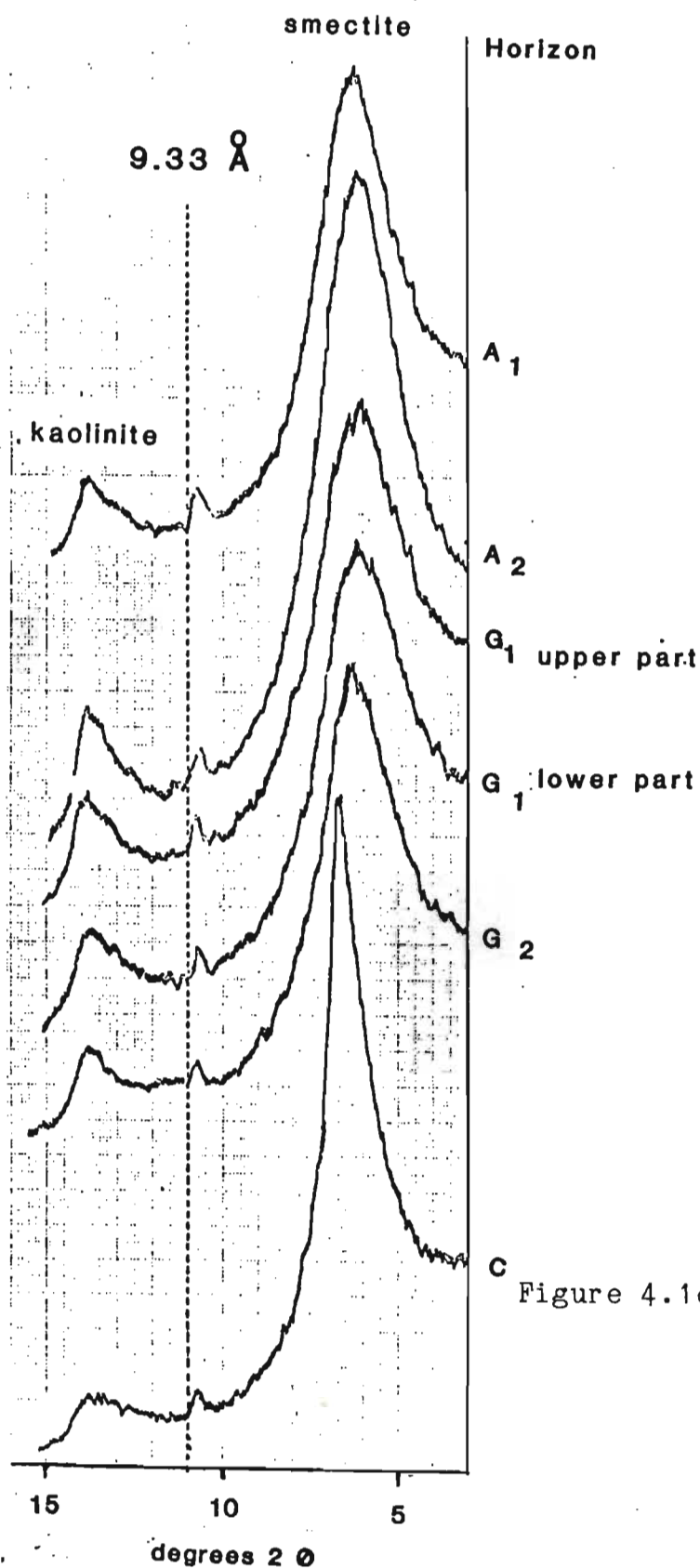


Figure 4.1c

Phoenix Soil Series
: XRD traces of the
< 2 um fraction of
the untreated sample
(oriented specimen)

4.3.2 Investigation of the talc concentrate

4.3.2.1 XRD data

A smectite-free soil (A horizon of the Stanger profile) was selected for talc enrichment to ensure that talc would be the only crystalline phase remaining after heating at 510°C. The result of heating is shown in Figure 4.2. Subsequent chemical dissolution greatly enhanced the intensity of the talc basal reflections (Figure 4.3).

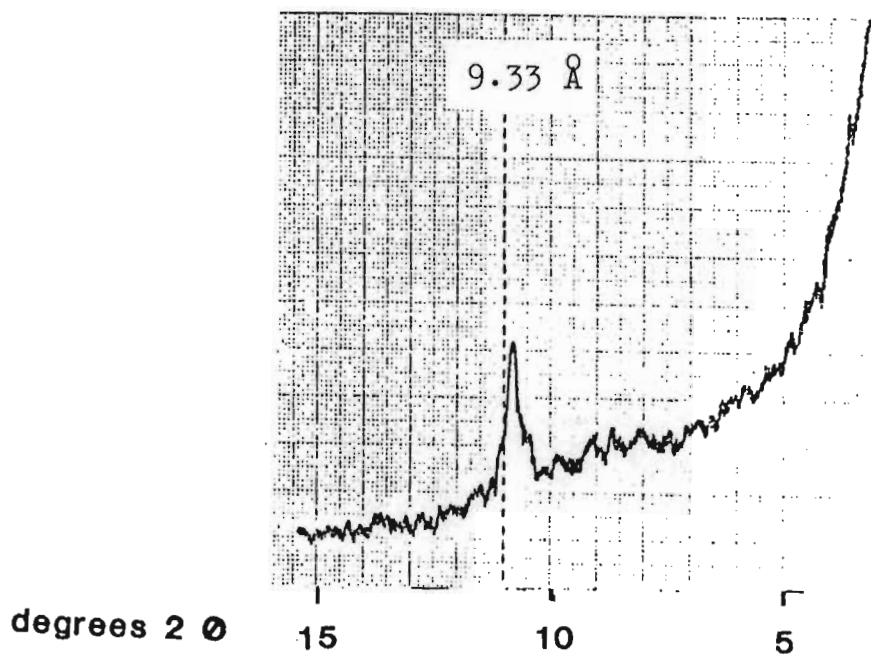


Figure 4.2 Oriented specimen of the Stanger A horizon, heated to 510°C for 4 hours

The enriched talc showed basal reflections shifted from those which are reported for pure talc. The pattern in Figure 4.3 is similar to that of a degraded talc, in which random interstratifications with small amounts of a second mineral such as

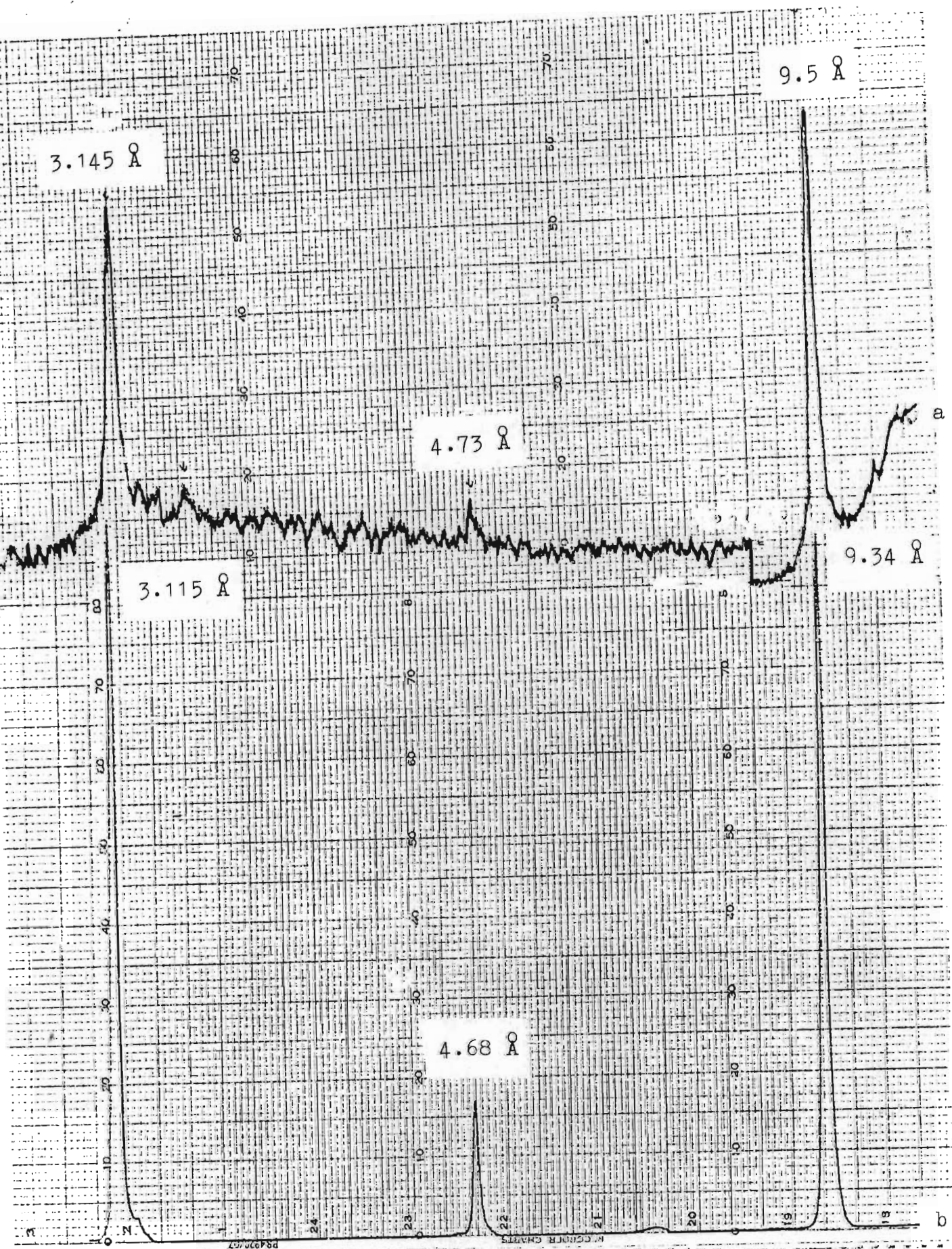


Figure 4.3 XRD pattern of oriented specimen of talc,
 (a) concentrated from the Stanger clay
 (b) commercial talc

saponite has occurred (van der Marel and Beutelspacher, 1976; Brindley, Bish and Wan, 1979). On the other hand the shift could be attributed to the substitution of either Fe^{2+} as in minnesotaite (Blake, 1965) or of Fe^{3+} as in ferripyrophyllite (Chukhrov et al., 1979) for Mg.

The second possibility is more likely, since a talc-saponite or, more generally, any talc-smectite interstratification would respond both to glycol solvation and to heating at 510°C , and no such response was detected.

Chemical data presented by Blake (1965) for minnesotaite and by Chukhrov et al. (1978) for ferripyrophyllite correspond to 90 or more mol % substitution of Fe for Mg. The positions of the basal reflections (Table 4.2) would therefore correspond to about 50 mol % iron substitution.

4.3.2.2 Infrared spectroscopy

The IR spectrum of the talc concentrate differs from that of pure talc (Farmer, 1974) and of a commercial talc with which it is compared in Figures 4.4 and 4.5.

In pure talc, the OH stretching frequency of the Mg_3OH unit remains almost constant at $3\,677\text{ cm}^{-1}$ ($3\,680\text{ cm}^{-1}$ in Figure 4.4), whereas in the soil talc concentrate, additional bands at $3\,650$ and $3\,630\text{ cm}^{-1}$ may be attributed to Mg_2FeOH and Fe_3OH vibrations, while the broader band at about $3\,620\text{ cm}^{-1}$ may be explained by

Table 4.2 Comparison of XRD data for the enriched talc with those of pure talc, minnesotaite and ferripyrophyllite.

Reflec- tion	Minnesota- ite		Talc - this study		Talc		Ferripyro- phyllite	
	λ	I/I _c	λ	I/I _c	λ	I/I _c	λ	I/I _c
002	9,6	100	9,5	100	9,34	vs	9,6	80
004	4,78	20	4,73	5	4,68	w	--	--
006	3,17	50	3,145	40	3,115	s	3,17	7

vs = very strong, w = weak, s = strong

(References : minnesotaite : Blake, 1965; talc : Ross et al., 1968; ferripyrophyllite : Chukhrov, 1979)

some replacement of Mg^{2+} by Al^{3+} , resulting in an Al_2OH vibration at $3\ 630\ cm^{-1}$ (Wilkins and Ito, 1967).

The a_1 ($1\ 040$ and $685\ cm^{-1}$) and e_1 ($1\ 015$ and $450\ cm^{-1}$) Si-O stretching vibrations have different relative intensities in the two talc specimens (Figure 4.5), the a_1 vibration being more intense in the talc concentrate and e_1 more intense in the commercial talc. The absence of any shift in the Si-O stretching band of the soil talc to lower frequencies precludes the possibility of significant tetrahedral Al or Fe substitution.

The band at $535\ cm^{-1}$, attributable to Mg-O vibrations, is common to both spectra (Figure 4.5). Additional bands at 520 and $490\ cm^{-1}$ in the soil talc may possibly be due to Fe-O vibrations.

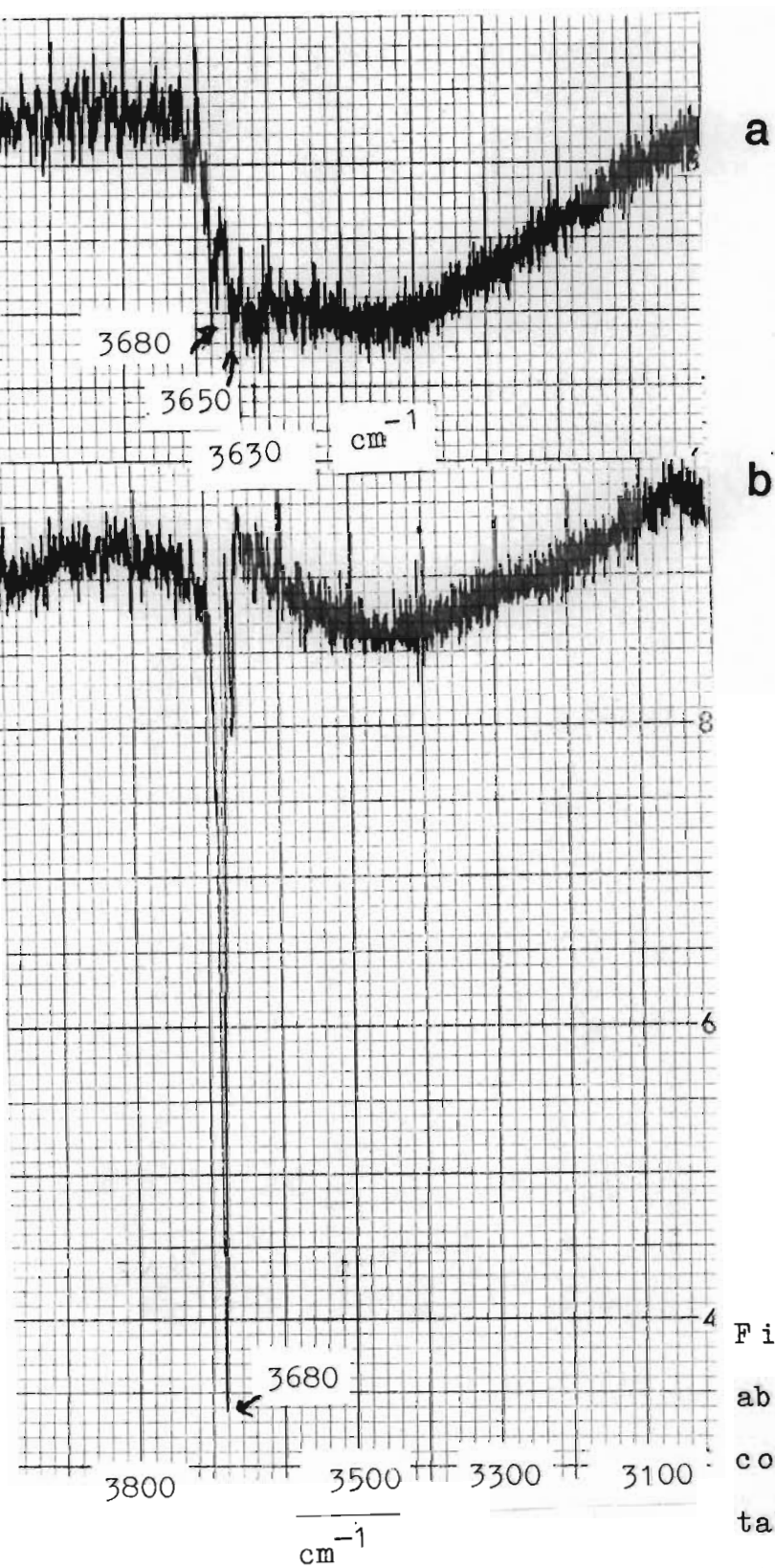


Figure 4.4 Infrared absorption spectra of (a) talc concentrate, (b) commercial talc. Spectra are recorded at concentrations of 1% in pressed KBr discs heated to 150°C.

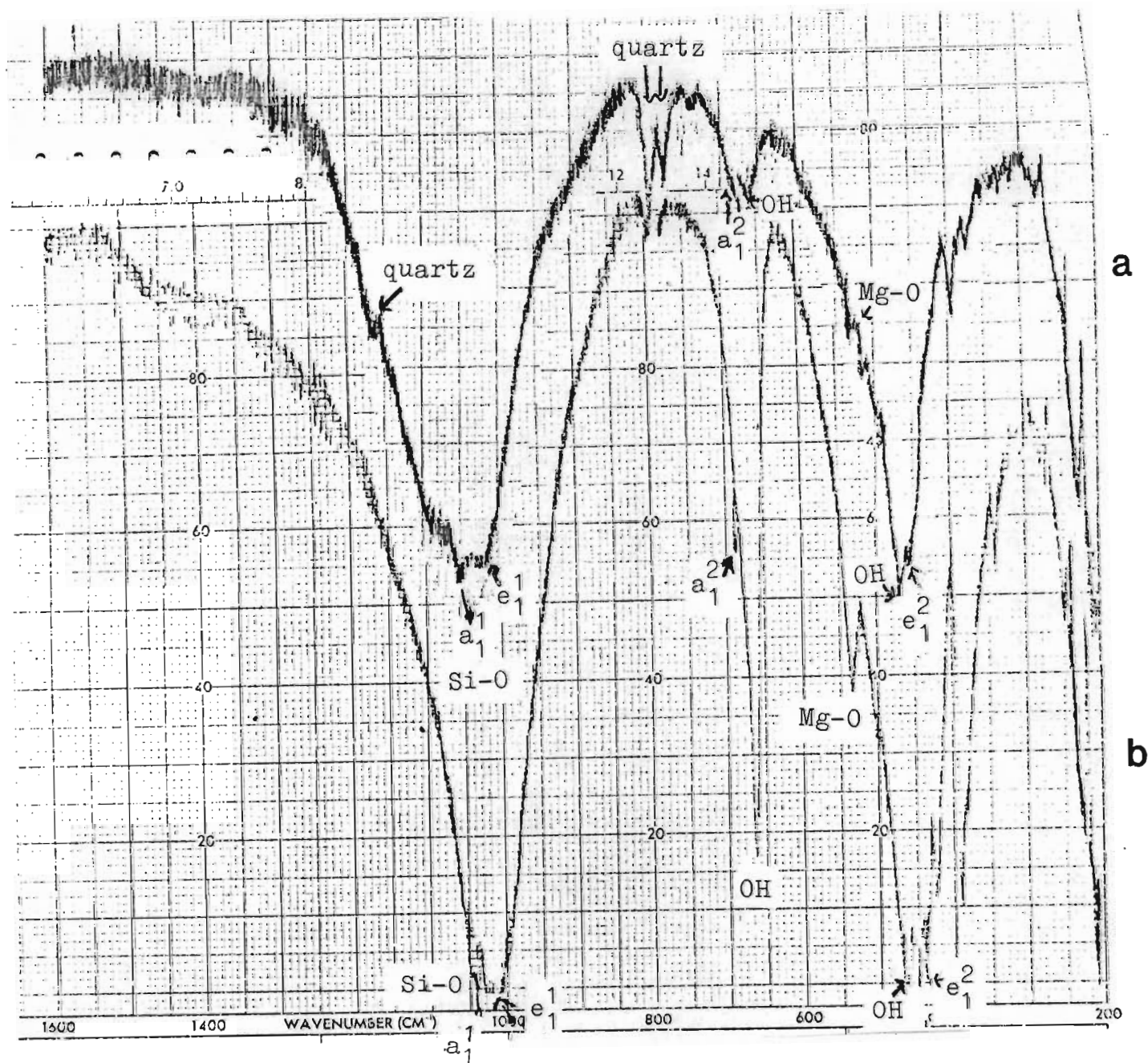


Figure 4.5 Infrared absorption spectra of (a) talc concentrate, (b) commercial talc. Spectra are recorded at concentrations of 0.35% in pressed KBr discs heated to 150°C overnight.

4.3.2.3 Electron microscopy

Investigation of the Fe-talc concentrate by means of electron microscopy revealed the presence of platelets, which closely resemble the pseudo-hexagonal platelets commonly observed in certain phyllosilicate clay specimen (Figure 4.6). They differ from the elongated talc crystals reported by van der Marel and Beutelspacher (1976), characteristic of hydrothermal deposits.



Figure 4.6 Scanning electron micrograph of the talc concentrate (print magnification 1 : 15 000)

4.3.2.4 Chemical composition

The sensitivity of the talc concentrate to destruction by prolonged selective dissolution treatment meant that a complete decontamination of the concentrate with respect to amorphous materials containing Fe, Al and Si would be difficult to achieve. Elemental microanalysis was therefore employed in preference to total chemical analysis of the concentrate.

Positions in the centre of five particles from the field shown in Figure 4.6 were selected for Mg and Fe analyses shown in Table 4.3.

Table 4.3 Five analyses by EDX of separate particles observed by SEM in the soil talc concentrate.

	1	2	3	4	5	Mean	
MgO	13,4	14,7	12,8	17,7	12,9	14,3	content %
FeO	12,8	12,7	12,1	13,4	13,2	12,9	content %
mol %							
Fe/Fe+Mg	35	33	35	30	37	34	

The Fe and Mg contents were estimated from peak areas on the EDX spectrum, and are consistent with those which were predicted by XRD data presented above.

4.4 Conclusions

The absence of a response by the soil talc to glycol solvation or heat treatment as well as the low background on both sides of the peak suggests that, while the XRD pattern closely resembles that of a degraded talc (e.g. randomly interstratified talc-saponite), it is more likely to be due to Fe substitution for Mg in the talc structure. Shifts in the XRD spacings were found to correspond with about 50% replacement of Mg by Fe, and chemical micro-analysis under SEM provided data which were approximately

consistent with this result. Infrared spectroscopy confirmed octahedral substitution.

The mineral therefore seems to be intermediate in composition between the Mg end member talc and the Fe end member minnesotaite or ferripyrophyllite, containing considerably more Fe than the 25 mol % reported by Paquet et al. (1982) for a pedogenic talc (chemical analysis indicated about 34 mol % Fe/Fe + Mg; XRD suggested a somewhat higher value, closer to 50%).

It is remarkable that the Fe-talc is consistently present in trace quantities in all the soils studied, representing extremes from smectite dominated vertisols to a kaolinite + sesquioxide dominated oxisol. Dolerite parent material is the only feature which these soils have in common. Since SEM studies of saprolite indicated that clay formation appeared to be predominantly associated with the hypersthene component, it is possible to postulate the Fe-talc as a first weathering product of the hypersthene (Fe:Mg ~1:1) formed before Al ions from the weathered plagioclase were available for substitutions (tetrahedral or octahedral) resulting in layer charge and therefore in the formation of smectite or chlorite instead of talc. The Fe-talc could retain all or most of the original iron along the lines of enstatite-talc transformation described by Eggleton and Boland (1982). Interestingly, no significant enrichment or depletion of the Fe-talc was observed as a function of depth.

Subsequent examination of a number of dolerite derived soils from

different localities has revealed the occurrence of a small talc peak on XRD patterns to be fairly common and the presence of an Fe rich talc in pedogenic environments may often have been overlooked in the past because of its very low concentrations. The method for enrichment of soil talc employed in this study is difficult to apply reproducibly because of the necessity for a very brief contact time with selective dissolution reagents in order to avoid destruction of the talc itself. It should, however, be useful in confirming the presence and nature of trace amounts of pedogenic talc during routine soil clay mineralogical investigation, particularly if the clay fraction is dominated by 1:1 layer silicates which are amenable to selective destruction by heating.

4.5 General discussion of phyllosilicate clay formation at Melody Ranch and Tutuka

The mechanism of weathering of primary minerals and the genesis of specific clay minerals is known to depend on a number of factors, including the dominant soil-forming factors (Jenny, 1941; Chesworth, 1973) as well as the micro-structure of the parent rock and micro-environment prevailing at the various stages of mineral formation.

Weathering of dolerite

Dolerite with its plagioclase-pyroxene composition is an interesting parent material in the study of clay genesis, as no

phyllosilicate precursor exists in this basic igneous rock. The clay mineral suite of soil pedons developed from dolerite must have formed by precipitation out of solution or by topotactic transformation within the starting mineral.

In reviewing the literature on the weathering of plagioclase and pyroxene, a great number of weathering products are reported (Table 4.4).

Weathering of pyroxene may lead to the following alteration products (Figure 4.7).

Pion (1979) found that weathering of pyroxene is closely connected to the internal drainage conditions within the parent rock and the nature of the layer silicate that forms depends on the particular micro-environment. Interesting in this respect is the possible co-existence of talc with components of the "alteration smectitique" as well as the "alteration kaolinitique".

Summarising the results obtained from literature study on the weathering of pyroxene and plagioclase it is evident that both minerals may weather to vermiculite, smectite and kaolinite. Talc, chlorite and amphibole are related to pyroxene only, while halloysite is reported from weathered plagioclase.

Table 4.4 Alteration products derived from weathering of
plagioclase as reported by the various authors

Alteration product	Author
Beidellite (vermiculite?)	Proust and Velde, 1978
Beidellite	Frank-Kamenetzky <u>et al.</u> , 1980
Montmorillonite (<u>sensu lato</u>)	Helgeson <u>et al.</u> , 1969; Suttner <u>et al.</u> , 1976; Eswaran, 1979; Page and Wenk, 1979
Kaolinite	Basham, 1974; Suttner <u>et al.</u> , 1976; Eswaran, 1979; Gilkes <u>et</u> <u>al.</u> , 1980
Halloysite	Petrovic, 1976; Eswaran, 1979; Keller, 1978; Rodriguez, 1982
Halloysite (7 Å)	Eswaran, 1979; Gilkes <u>et al.</u> , 1980
Halloysite (10 Å)	Gilkes <u>et al.</u> , 1980
Gibbsite	Gilkes <u>et al.</u> , 1980; Eswaran <u>et</u> <u>al.</u> , 1977
Boehmite	Petrovic, 1976
Amorphous material	Correns and Engelbrecht, 1938; Basham, 1974; Petrovic, 1976
Ions (Na ⁺ , Ca ²⁺ , Al ³⁺ , H ₄ SiO ₄)	Basham, 1974

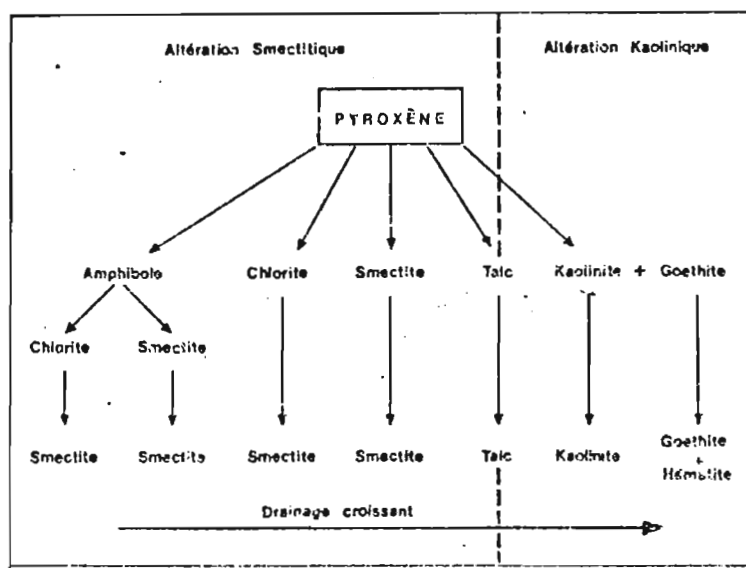


Figure 4.7 Alteration products derived from weathering of pyroxenes (Pion, 1979)

Weathering of shale

The mineral composition of Ecca shale could be established from hand-picked shale fragments as : quartz, plagioclase, K-feldspar, mica, chlorite.

Quartz is resistant to weathering.

Plagioclase may be expected to weather to products similar to those described before.

K-feldspar is reported to form kaolinite or halloysite as alteration products (Keller, 1976; 1978). Eggleton and Buseck(1980) in their comprehensive work on weathering of K-feldspar, demonstrated that phases with 10 Å spacing are formed first which crystallize to sheets of illite-smectite mixed-layer minerals.

Meunier and Velde (1976) made the observation that the feldspars in granite may weather to smectite. The new phases develop along junctions of grain boundaries but, where the feldspar was in contact with quartz, no new phases were evident. This observation may be of significant importance for it suggests that in the presence of larger amounts of quartz the weathering mechanism is restricted to transformation of existing phyllosilicates rather than to neoformation.

The weathering products of mica and chlorite have been described in detail in section 3.3.1.

Weathering of dolerite

The doleritic parent material at Melody Ranch and Tutuka, with its labradorite-hypersthene-dominated mineral composition, weathers to soil profiles with distinct clay mineral assemblages. Suite 1 is dominated by beidellite (Rensburg profile at Melody Ranch; group 1 profiles at Tutuka). Small to trace amounts of kaolinite are found in all horizons and traces of talc in the Melody Ranch samples. The profiles are characterised by a very uniform mineral composition and no changes in the nature of the clay species and the relative proportions of the clay mineral groups could be observed from the saprolite to the surface horizon. The C horizon in the Melody Ranch profile is an exception as it contains vermiculite together with beidellite. This vermiculite seems to be an unstable component and is apparently readily transformed to beidellite, suggesting the operation of a charge-lowering mechanism. The presence of plagioclase and pyroxene in the surface horizons of these profiles indicates a low degree of weathering. The uniform clay

mineral composition points to an homogeneous environment. In contrast to the observation of Ildefonse et al. (1979), smectite and vermiculite dominate in the saprolite.

The Eccca shale at Tutuka (suite 2 profiles) weathers to mica-beidellite interstratifications which may be random or ordered and in which the proportion of mica decreases from approximately 50% in the C horizon to ca. 20% in the surface horizon. The mica-smectite interstratifications must be regarded as a weathering product of the micaceous shale component, but weathering of K-feldspar to this type of mixed-layer mineral is possible as well (Eggleton and Buseck, 1980).

Chlorite weathers at a very early stage via ordered chlorite-vermiculite or chlorite-smectite interstratifications. Chlorite-derived weathering products are absent in the G and A horizons.

Suite 3 is characterised by minerals of the 14 Å and 7 Å phyllosilicate group in about equal proportions as well as traces of talc (Arcadia and Mayo soil profiles at Melody Ranch). A wide spectrum of clay minerals is represented in each soil horizon. Interestingly, all minerals reported in the literature as weathering products of either plagioclase or pyroxene are present in the Mayo profile : amphibole, vermiculite, beidellite, montmorillonite, kaolinite, halloysite (10 Å), halloysite (7 Å), talc and sesquioxides, except for chlorite which is known to be very short-lived (Pion, 1979). The weathering of the dolerite

to clay minerals which represent different degrees of weathering (kaolinite, smectite) is probably only possible in an environment characterised by a broad variation in micro-environmental conditions.

The replacement of halloysite (10 Å) by kaolinite and halloysite (7 Å), as reported by Gilkes et al. (1980) and finally by kaolinite only has been observed as well as the co-existence of vermiculite, beidellite, and montmorillonite. The presence of vermiculite in the surface horizon indicates the absence of a charge-lowering mechanism in these type 2 profiles.

Interestingly, the weathering products seem to be closely linked with the pyroxene component only. From XRD studies it is evident that clay minerals are absent in the hand-picked plagioclase grains while 14 Å as well as 7 Å minerals are observed in association with the pyroxene grains in proportions similar to those found in the clay fraction. Electron microscope studies confirm the presence of platy and tubular structures in connection with the pyroxene and the apparent absence of any clay component in the plagioclase grains. As hypersthene is characterized by a very low Al content, the formation of halloysite on the pyroxene grain is possible only if Al is derived from plagioclase. The formation of Al-rich phyllosilicates on mafic minerals, which contain Al as trace component only is not uncommon (Nahon et al., 1982).

Suite 4 mineral assemblage is dominated by kaolinite (Bonheim,

Shortlands, Hutton profiles at Melody Ranch) which is indicative of a high degree of weathering. Small amounts of "chlorite", which may well be an Al-interlayered vermiculite or smectite (in view of the destruction of the structure upon heating to 300°C) and traces of talc are present as well. Surprisingly, halloysite is absent from these soils.

Suite 5 is characterised by a monomineralic clay composition (group 3 profiles at Tutuka). Weathering product of the dolerite is a smectite-kaolinite interstratification, in which the kaolinite component gradually increases from approximately 50% to 70% from the saprolite towards the surface horizon. In the saprolite, some discrete smectite may be present as well or the interstratification may show a high degree of segregation.

Differences in environmental or micro-environmental conditions may account for the formation of beidellite in the suite 1 profiles and a smectite-kaolinite interstratification in the suite 4 profiles at Tutuka, which are derived from the same doleritic parent material and situated close to each other.

Some important results may be summarised as follows.

1. In the Melody Ranch profiles there is no obvious relationship between topography as dominant soil-forming factor and clay mineral assemblages. Kaolinite-dominated soil profiles are situated at higher as well as lower altitude than smectite-containing ones (Figure 2.1, profiles 2, 4 and 7).
2. At Tutuka, where parent material was the dominant soil-

forming factor, the differences in the clay mineral assemblages between dolerite and shale-derived profiles are obvious, but micro-environmental conditions exert a strong influence on the nature of the clay fraction as well.

3. In all soil profiles weathering of the parent material involves the immediate synthesis of the clay mineral assemblage characteristic of the type.
4. Minerals of the swelling clay mineral group are found as discrete minerals only in horizons where plagioclase is present as well.
5. Weathering of pyroxene seems to be the dominating factor in clay genesis at Melody Ranch.
6. Vertisols always contain smectite, either as a discrete mineral (Rensburg and Arcadia profiles at Melody Ranch, group 2 profiles at Tutuka) or as interstratification component (groups 2 and 3 at Tutuka). Proportions of ca. 30% smectite, either as discrete mineral or an interstratification component with mica/chlorite or kaolinite seem to be sufficient to create vertic characteristics.
7. Soils with melanic A horizons may (Mayo profile at Melody Ranch) or may not (Stanger profile at Melody Ranch) contain smectite.
8. Vermiculite may be stable in a soil profile (Mayo profile at Melody Ranch) or may be transformed to beidellite (Rensburg profile at Melody Ranch), i.e. a charge-lowering mechanism may or may not operate.
9. Pedogenic talc was detected in trace amounts in the Melody Ranch profiles both in smectite and in kaolinite-dominated

profiles, i.e. associated with clay minerals representing different degrees of weathering.

10. No significant variations were observed in the proportions of the various phyllosilicate groups between the saprolite and the surface horizon for all the profiles investigated. The influence of colluviated material on the profiles should therefore be negligible.

Results 6 and 7 may be of value in any further studies which aim at examining a possible mineralogical basis for soil classification or in refining concepts of genesis associated with these diagnostic horizons of the SA classification system.

CHAPTER 5

THE MINERALOGY OF POTASSIUM FIXATION IN SOILS

5.1 Introduction

The supply of potassium from fertilizer application to crops can be strongly affected by the mineral content of a soil, especially by its clay mineral content. One would therefore like to predict the selective sorption and fixation properties of a clay for potassium simply by characterizing the clay. This goal requires a fundamental understanding of both the exchange process and the influence of clay crystal chemistry on this process.

The potassium fixation can be viewed as a three-stage process : (1) a cation is selectively adsorbed into the interlayer space of a clay mineral, the selective adsorption being related to the K concentration in the soil solution, pH, temperature, ion hydration, grain size, the levels of Ca^{2+} and Mg^{2+} in soil solution, the characteristics of the absorbing surface, the presence of hydroxy-aluminium interlayers and the presence of Al ions on the exchange sites (among others, Bolt, Sumner and Kamphorst, 1963; Kozak and Huang, 1971; Wood, 1980; Goulding and Talibudeen, 1984a,b).

(2) the cation is dehydrated by the negatively charged interlayer surface. The combination of a high negative lattice charge and low dehydration energy for K^+ results in the dehydration of K within these interlayer spaces and the collapse of the structure

to a 10 Å spacing;

(3) the cation migrates into hexagonal holes.

Cations will be held in the holes by an energy greater than that necessary for step 2 because fixation in the holes allows the cation to approach more closely to the seat of the negative charge (Eberl, 1980). Steps 1 and 2 cannot be dealt with separately, because as soon as dehydration takes place, the selective adsorption of the structure for potassium increases strongly (Sawhney, 1972).

The potassium fixation step 2 is charge dependent. The magnitude of the negative charge and its distribution in the mineral structure is obviously the most important parameter controlling the fixation process. Individual authors, however, disagree considerably with each other when investigating the question in detail. Weaver (1958), MacKenzie (1963) Weir (1965) and others have stated that the chief factor controlling fixation of potassium is the tetrahedral charge, while others (Schultz, 1969; Sawhney, 1970, 1972; Horvath and Novak, 1975; Eberl, 1980) claim that the total charge is the most important factor. Jenkins and Hartman (1982) postulate from electrostatic calculations that layer charge created in the octahedral sites is much more effective in the expulsion of interlayer water and Egashira et al. (1982) regard both a high total charge in combination with a high degree of tetrahedral substitution as the factor promoting potassium fixation.

If the layer charge is the most important factor for the contractibility of the smectite interlayer upon potassium saturation, certain characteristic values or limits of values are to be expected. From the electrostatic calculations of Jenkins and Hartman (1982) it is evident that a layer charge $> 0,5/\text{unit cell}$ is necessary before interaction of water molecules with the silicate layer can take place. At lower values the predominant term is the K^+ -water interaction.

The unit cell layer charge postulated by various authors for reversible and irreversible fixation of potassium is :

Eberl (1980)	0,77/0 ₁₀	(OH) ₂	(reversible?)
Machajdik and Cicel (1981)	1,00	"	(irreversible)
"	0,60	"	(reversible)
Weaver and Pollard (1973)	0,81	"	(reversible?)
Besson <u>et al.</u> (1975)	0,6	"	(reversible)

As vermiculite has a layer charge of this magnitude, the phenomenon of potassium fixation is normally linked to the occurrence of soil vermiculite, but beidellite and even montmorillonite with considerably lower charge have been reported to fix K^+ (Weir, 1965; van Olphen, 1966; Davis, 1972; Bajwa, 1981). However, not only the absolute value of negative charge is responsible for the decrease in replaceability and the fixation of potassium.

Treatment with H_2O_2 , which caused a slight decrease in the net negative charge of vermiculites and vermiculitized biotites

(Barshad and Kishk, 1968, 1970; Farmer, Russel, McHardy, Newman, Ahlrichs and Rimsaite, 1971; Ross and Rich, 1974), resulted in an increase in selective sorption and fixation of K^+ . As oxidation by H_2O_2 is associated with a loss of protons by conversion of OH^- ions to O^{2-} in the octahedral layer (Farmer et al., 1971), the screening effect of hydroxyl H^+ on the interlayer potassium is reduced, resulting in a stronger bonding. Similarly, the replacement of OH^- by F^- ions results in an increased fixation of K^+ . But it is not only the oxidation of structural iron by H_2O_2 treatment which may result in a loss of protons: removal of protons from octahedral OH -groups by other means (e.g. heat treatment) results in an uptake of K^+ far above the initial cation exchange capacity and strong fixation of potassium (Heller-Kallai, 1975).

The protonation-deprotonation effect upon oxidation and reduction of vermiculites has been investigated by Veith and Jackson (1974).

The influence of organic matter on potassium fixation, as proposed by Ross (1971), must be treated with caution: measurements of potassium sorption were conducted on clay samples before and after removal of organic matter by H_2O_2 , thus changes in K replaceability need not necessarily reflect the influence of organic matter (Douglas and Fiessinger, 1971). Another factor possibly affecting the ease of exchange of interlayer potassium is the orientation of the structural OH groups (Giese, 1979). A

wide variation in OH orientation is observed in 2 : 1 phyllosilicates, both dioctahedral and trioctahedral. The angle between the OH and the basal plane varies between 1,3 and 183,30, measured with respect to the M1 site (Giese, 1979). In trioctahedral structures the three filled M sites create a stable OH orientation approximately normal to the 001 plane. The dioctahedral structures present an unique situation in which the OH can easily move closer or further away from the vacant M1 site as the distribution of charges varies among the interlayer positive charge and the tetrahedral and octahedral negative charges. An increased inclination of the OH-dipole vector away from the normal results in a more electronegative environment and consequently in a stronger fixation of interlayer potassium in dioctahedral structures compared with trioctahedral ones.

Parent material may also exert a strong influence on the fixation of potassium in smectites (Grim and Bradley, 1955; Bolt et al., 1963; Horvath and Novak, 1975). Investigating potassium fixation in natural and synthetic montmorillonites, Horvath and Novak (1975) noticed that the fixation of K⁺ in synthetic smectites was negligible despite a high layer charge both in the tetrahedral and octahedral layer, while smectites derived from mica fixed considerable amounts of potassium. As the charge density in synthetic minerals is more or less uniform all over the structure, they assumed that smectites formed from phyllosilicates with a high charge density will possess some relics of this property. They agree with Bolt et al. (1963) that there exist specific centres in a smectite structure that are decisive for

potassium fixation and direct the mineral to achieve its original mica composition.

Potassium may also be fixed at a layer charge lower than 0,77 charges/unit cell if the clay is dried. Numerous reports have verified that changes in exchangeable potassium levels can occur in soils that are dried or heated (Coffman and Fanning, 1974; Gaultier and Mamy, 1979; Plancon, Besson, Gaultier, Mamy and Tchoubar, 1979). It was found that K^+ fixation after one oven drying was up to four times that of wet fixation (Coffman and Fanning, 1974). When montmorillonite is submitted to alternating wetting and drying cycles, potassium becomes progressively non-exchangeable. This decrease in exchangeability is explained by structural reorganisation from an initially random layer orientation, in which the perfect superimposition of the centres of the hexagonal holes of adjacent sheets of two neighbouring layers is restricted to one layer in five and the tetrahedral rotation angle is 50° , to a stacking in which all ditrigonal cavities of adjacent layers are facing each other (Plancon et al., 1979). An increase in K fixation after several wetting and drying cycles has also been confirmed by Gaultier and Mamy (1979) for a bi-ionic Ca-K-montmorillonite.

But there may be a reaction involved other than only the reorientation of the structure. Smectite and possibly also vermiculite surfaces are widely known to act as Brønsted acid and/or as a Lewis acid or Lewis base. Brønsted acidity (that is proton donating ability) increases dramatically as soon as the water

content is less than 5% by mass. "Dry" Ca-montmorillonite, for example, can protonate ammonia to an extent approaching the CEC of clay. Brønsted sites arise essentially from dissociation of interlayer water according to the reaction $[M(H_2O)_x]^{n+} \rightarrow [M(OH)(H_2O)_{x-1}]^{(n-1)+} + H^+$ (Theng, 1982), converting the exchangeable cations to their hydroxides, thus rendering part of the cations non-exchangeable and increasing the apparent layer charge. Protons from structural groups can and do exchange with those from surface adsorbed water, especially hydroxyl groups linked to ferric octahedral iron (Heller-Kallai, 1982). The ability of a smectite to act as a Brønsted acid depends on the amount of tetrahedral substitutions and the valency and size of the interlayer cation, being more pronounced the higher the tetrahedral charge and the smaller and more highly charged the interlayer cation.

But the clay mineral structure itself and thus its ability to selectively adsorb and fix potassium is also sensitive to variations in environmental conditions. The effect of pH on the clay-salt interactions has been very intensively investigated (Maes and Cremers, 1979; McBride, 1980). A small reduction in pH may convert a binary system, with two cations competing for the exchange sites into a ternary one, with protons from interlayer and/or octahedral positions participating in the reactions (Karickhoff and Bailey, 1976; Heller-Kallai, 1982). A further decrease in pH may result in partial dissolution and sorption of Al in the interlayers.

In view of the complexity of the system no scheme has so far been developed that will account for more than one or two aspects of potassium fixation in clay structures.

But there are also some non-clay minerals which are known for their ability to fix potassium. Allophane, zeolite and feldspar are examples of such minerals. Van Reeuwijk and de Villiers (1968) showed synthetic aluminosilicate gels retaining varying amounts of K against replacement by common alkali and alkaline earth cations. However Sticher (1972) pointed out that the properties of the aluminosilicates used may have been characteristic of freshly prepared gels and not representative of natural allophanes, as the K content of natural allophanes lies around 0,1% in various representative samples.

The Na/K ratio of zeolite in sedimentary rocks is considerably lower than that in the surrounding lake- and soil-water. This may be an indication that they have a strong affinity for K and a capacity to fix it. Schuffelen and van der Marel (1955) included an artificial zeolite in the series of soils and minerals which they tested for potassium fixation and found that it fixed more K than most other materials examined and that K could also be fixed by feldspar.

A second mechanism for potassium fixation in soils is considered to happen via formation of insoluble K compounds, especially aluminosilicates-phosphates. Kim, Gurney and Hatfield (1983a, 1983b) reported K fixation via formation of K-Al and K-Fe

taranakites.

Farmers in the sugar belt region of Natal, Malawi and Swaziland are occasionally faced with a very poor response of sugarcane to potassium fertilizer application (Wood, personal communication). An unexplained anomaly exists regarding some soils in Swaziland. Ammonium-acetate extracts indicate that the amount of exchangeable potassium is usually very high but sugarcane leaf samples from the same sites often contain less than the threshold percentage (1,05%) of K. Some of these soils also show no shortage of non-exchangeable potassium (Thompson, 1981).

The aim of the present study is to seek an explanation of the strong potassium fixation of selected soils (kindly provided by Dr R A Wood) through an investigation of the nature of the soil minerals, especially the soil clays.

This task is especially interesting, as there is only little information available on the mineralogy of K-fixing soils in South Africa (Bredel and Coleman, 1968; le Roux and Rich, 1969; le Roux and Sumner, 1969; le Roux et al., 1970).

Two soil samples from Germany (kindly provided by Dr G C H Venter) known to exhibit a strong K-fixing capacity, are included in the investigations.

5.2 The problem of the relationships between layer charge density and XRD spacings for smectite-vermiculite

As previously indicated, the identification of various clay

minerals is normally based on the position and possible shift of a series of basal reflections, applying auxiliary pre-treatments. Generally, a discrete clay mineral must give a rational series of basal reflections with $d_{005} \times 5 = d_{004} \times 4 = d_{003} \times 3 = d_{002} \times 2 = d_{001}$ (Å) with a low background to both sides of the peak maximum.

It is relevant to repeat here that the differentiation between vermiculite and smectite must be made on the basis of the layer charge, tentatively set as being greater or less than $0,6/O_{10}(OH)_2$ unit cell, and not on the basis of peak positions. In general the differentiation between vermiculite and smectite from XRD patterns is based on the 14 Å diffraction peak of vermiculite and the 18 Å diffraction line of smectite, when glycerol liquid is added to a Mg-saturated clay (Brindley, 1966; Harward et al., 1969). However, neither the glycol- nor the glycerol-determined smectite-vermiculite boundary coincides with the definition proposed by the AIPEA Nomenclature Committee (Bailey, 1980). For example, Egashira et al. (1982) described a "high charged" smectite with a "vermiculitic" layer charge, of $0,8/O_{10}(OH)_2$ unit cell, which expanded to 18 Å upon glycerol solvation. The ethylene glycol test tends to over-estimate smectite and the glycerol test to under-estimate it, as compared with the AIPEA definition (Srodon and Eberl, 1980).

The contraction of the basal spacing induced by potassium saturation seems to be the only reliable reaction, characteristic for vermiculite (Harward et al., 1969; Douglas, 1977; MacEwan and Wilson, 1980). For soil vermiculite an additional heat

treatment at 110°C is suggested (Alexiades and Jackson, 1965).

But according to Machajdik and Cicel (1981), 10 Å as well as 12,5 Å peak positions are possible for vermiculite after K-saturation and air drying.

Similarly unsolved is the question concerning a possible re-expansion of the K-saturated 10 Å lattice upon glycol solvation. Collapse without further expansion (Egashira et al., 1982) or formation of a glycol monolayer (Machajdik and Cicel, 1981) are possible responses.

By K saturating montmorillonites, which give a rational series of basal reflections in the air-dried as well as in the glycol and glycerol solvated state, mixed-layer structures are formed (Muravyev and Sakharov, 1970; Cicel and Machajdik, 1981). The existence of the following layers was confirmed after K-saturation in the air-dried state : (a) a collapsed layer (10 Å); (b) a structure with one layer of water molecules (12,4 Å); (c) a structure with two layers of water molecules (15,2 Å). Three different layers have also been confirmed after ethylene glycol solvation : (d) a non-expanded layer (10 Å); (e) a structure with one interlayer of ethylene glycol molecules (14,2 Å); (f) a structure with two layers of ethylene glycol molecules (16,9 Å).

Any peak position other than those mentioned above results from interstratifications of two or even three different layer types

(Cicel and Machajdik, 1981). In their study of montmorillonites from various parts of the world, Cicel and Machajdik (1981) could show that all air-dried K-montmorillonites were composed of at least two, but mostly three different layer types, type (f) being the most common in the investigated samples (Table 5.1).

Table 5.1 Probability coefficients for the 10 Å, 14,2 Å and 16,9 Å layers of potassium-saturated, ethylene glycol solvated montmorillonites from various parts of the world and the corresponding peak positions after air-drying and ethylene glycol solvation as well as the total layer charge, calculated for $O_{10}(OH)_2$ (modified after Cicel and Machajdik, 1981)

Location	Charge	Probability coefficient			Peak position Å	
		p10 Å	p14 Å	p16,9 Å	Air-dried	Ethylene glycol
Askangel, USSR	0,53	-	0,36	0,64	12,5	16,2
Borsa, CSSR	0,37	0,20	-	0,80	12,08	17,48
Branany, CSSR	0,48	0,30	0,10	0,60	11,51	16,63
Chambers, USA	0,59	-	0,75	0,25	12,31	14,84
Belle Fourche, USA	0,43	0,14	-	0,86	11,51	16,75
Jelsovy Potok, CSSR	0,48	0,26	0,12	0,62	11,66	16,69
Manito, USA	0,64	0,21	0,69	0,10	13,10	13,87
Michajlov, Bulgaria	0,58	0,35	-	0,65	11,98	16,96
Polkville, USA	0,57	0,39	0,18	0,43	11,60	16,02
Pyzevskij, USSR	0,49	0,05	0,17	0,78	12,35	16,32
Sampor, CSSR	0,56	0,15	0,70	0,15	12,37	14,18
Zajsanskij, USSR	0,32	-	0,60	0,40	12,18	15,19

Generally the air-dried samples contained more 10 Å layers than those solvated with ethylene glycol. This is evidently caused by the fact that the dipole moment of ethylene glycol ($\mu_{EG} = 2,28 \text{ D}$) is greater than that of water ($\mu_{H_2O} = 1,87 \text{ D}$) (Weast and Astle, 1978).

Machajdik and Cicel (1981) found excellent agreement between the local charge densities of the unit structures (d) - (f) with layer charge and expansibility of mica, vermiculite and smectite (Table 5.2).

Table 5.2 Local charge density calculations (Machajdik and Cicel, 1981)

Interlayer	Local charge densities on the layer (esu/uc)		
	QA	QC	QE
K ⁺ , ethylene glycol	1,99	1,20	0,56
NH ₄ ⁺ , ethylene glycol	2,70	1,60	0,72
	Mica	Vermiculite	Smectite
Total layer charge (esu/uc)	2	1-1,6	0,5-1,2
	no expansion	complex with 1 layer of ethylene glycol	complex with 2 layers of ethy- lene glycol

QA = 10 Å
 QC = 14,2 Å
 QE = 16,9 Å

Charge calculated for O₂₀(OH)₄

Thus the peak position of a potassium saturated smectite provides valuable information on the proportions of local charge densities, both in the air-dried and especially in the glycolated state.

The difficulties in the interpretation of XRD patterns when the clay fraction is composed of a two- or even three-component interstratification has been outlined in Chapter 1.

Interpretation of the amount of two minerals in a two-component interstratification is possible with the aid of tables and curves which show how the (001)/(002), the (002)/(003) and the (003)/(004) peaks migrate as the relative proportions of the different layers change (Reynolds and Hower, 1970; Reynolds, 1980) (Table 1.1, Figure 1.8). But the use of these tables and curves is limited by the unfortunate fact that the peak positions also depend on the stacking arrangement and migrate with the tendency of segregation as well as the crystallite size (Figure 5.1).

5.3 Materials and methods

Surface horizons of 11 soil profiles from sugar-producing areas of northern Natal, Malawi and Swaziland were investigated mainly by means of X-ray diffraction. The soils are identified as Arcadia, Vimy, Phoenix and Milkwood soil series (from Natal), Kwezi (K-set) and Rondspring (R-set) from Swaziland and Canterbury, Somerling and Sucoma (from Malawi). Boden 3 and

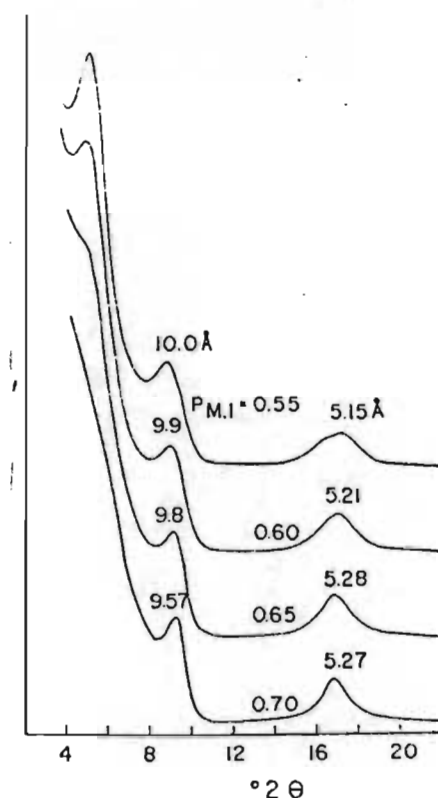


Figure 5.1 Effects of segregation of illite and of montmorillonite on calculated diffractometer ($\text{Cu K}\alpha$) patterns of interstratified illite-montmorillonite with 70% illite; the bottom pattern is for random interstratification (no tendency for segregation defined by $P_{M.I} = 0,7$). Curves with smaller $P_{M.I}$ represent increasing segregation. Values in Å corresponding to positions of maxima are also given. (From Reynolds, 1980.)

Boden 5 are a Parabraunerde and an Aueboden from Germany, respectively. Selected properties of these K-fixing surface soils are presented in Table 5.3. The methods used have been described previously (Chapter 2).

Table 5.3 Selected properties of K-fixing surface soils

Soil	pH CaCl_2	Clay (%)	NH ₄ -exchangeable cations (cmol(+) kg ⁻¹)					Sum of cations per unit clay (cmol(+) kg ⁻¹)
			Ca	Mg	K	Ka	Na	
Arcadia	7,15	58	36,8	20,0	0,4	0,3	0,2	98,9
Kwezi	8,00	58	53,5	9,0	0,7	0,4	0,2	109,3
Mayo	5,50	25	12,9	4,1	0,3	0,2	0,1	69,6
Canterbury	6,60	56	14,2	9,8	0,6	0,5	0,8	41,8
Rondspring	7,60	25	18,0	4,3	2,0	1,4	0,1	97,6
Milkwood	5,65	42	8,6	6,5	0,9	0,9	0,2	38,6
Phoenix	5,95	39	11,5	9,5	0,6	0,5	0,2	55,9
Somerling	6,25	45	53,5	7,2	0,7	0,5	0,3	137,1
Vimy	6,90	41	19,8	12,4	0,6	0,4	0,5	81,2
Sucoma 8478	6,25	36	10,1	7,0	nd	0,5	0,4	50,0
Sucoma 8492	6,00	43	29,5	7,1	nd	0,5	0,4	64,0
Boden 3	6,6	37	14,0	1,8	0,3	0,3	0,2	44,0
Boden 5	6,6	38	15,0	2,2	0,3	0,3	0,3	48,0

a Potassium extracted by Ba

5.4 Results and discussion

5.4.1 XRD investigation

Whole soil

XRD investigations of the random whole soil powder samples showed quartz to be the dominant non-clay mineral. A characteristic of

all the samples is a remarkably high content of primary feldspars. This is indicative of a low degree of weathering. Depending on the feldspar varieties present, the soils could be ascribed to one of two parent material groups as follows : (i) plagioclase dominant in the non-clay fraction besides quartz, suggesting dolerite as parent material : Arcadia, Kwezi, Canterbury, Milkwood, Somerling and Vimy (Figure 5.2). A less likely possibility is Dwyka as parent material due to the relatively high feldspar and low quartz content; (ii) both potash feldspar and plagioclase, indicative of granite, gneiss or sedimentary parent materials (Ecca shale) : Mayo, Rondspring, Phoenix, Sucoma 8492, Sucoma 8478 (Figure 5.3) as well as Boden 3 and Boden 5 (Figure 5.4). Additional to the abovementioned minerals, the following non-phyllosilicates could be positively identified : pyroxene (Arcadia), Gibbsite (Milkwood), Calcite (Mayo) traces, Magnetite and Maghemite (Canterbury), and Goethite (Somerling, Kwezi, Vimy, Canterbury).

X-ray diffraction analysis of clay fractions

XRD analysis has revealed the presence of a variety of clay minerals, both discrete (kaolinite, mica, vermiculite) or as part of more or less random interstratifications. A common feature is the strong 060 reflection at 1,495 - 1,507 Å which indicates that the major clay minerals are dioctahedral.

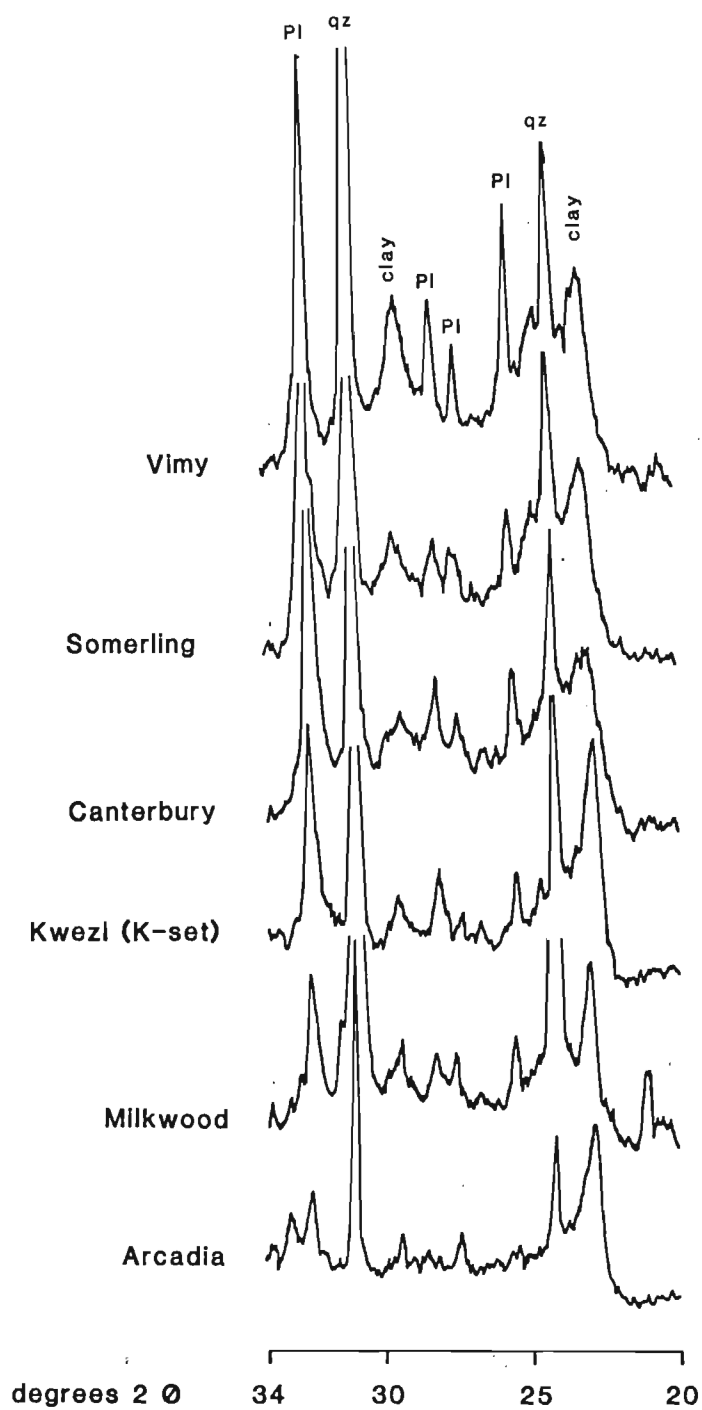


Figure 5.2 Whole soil XRD patterns of samples, containing plagioclase as the only feldspar variety besides quartz

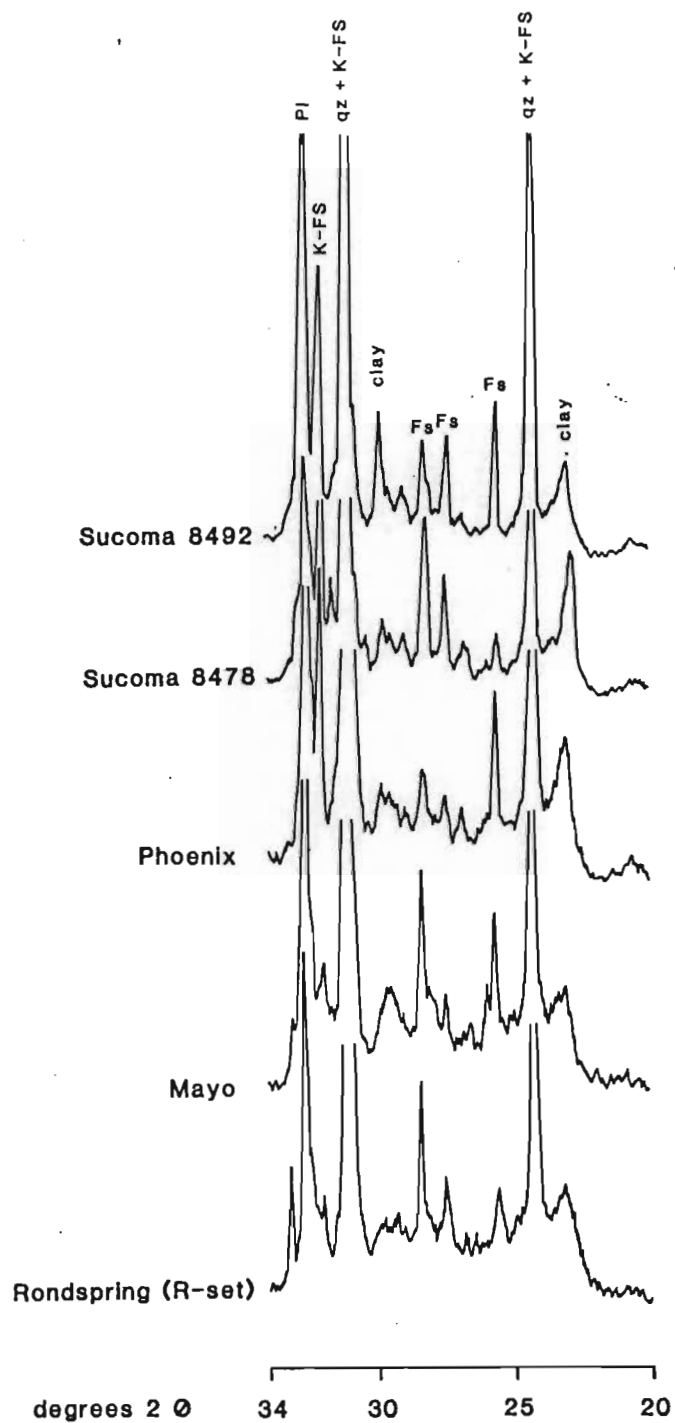


Figure 5.3 Whole soil XRD patterns of samples, containing K-feldspar + plagioclase besides quartz

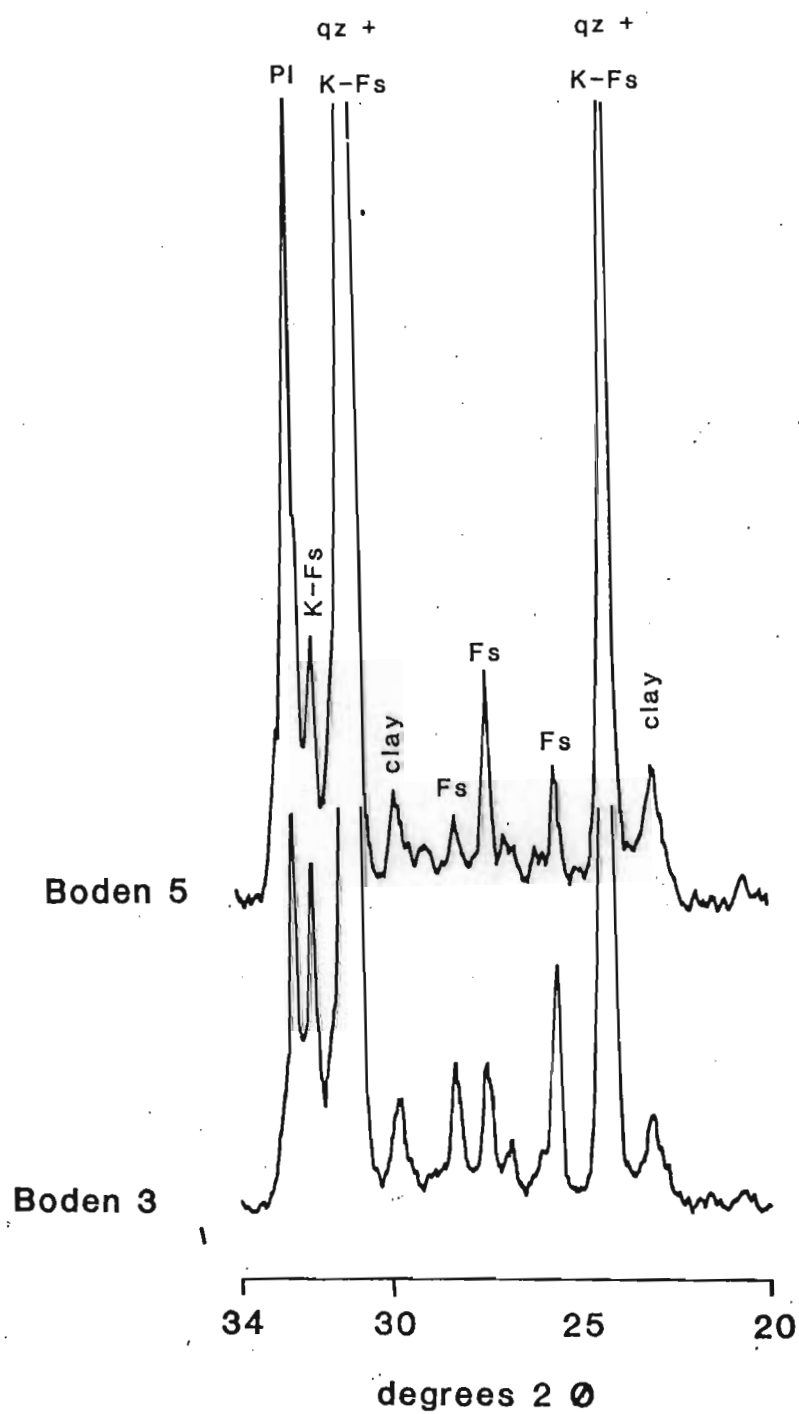


Figure 5.4 Whole soil XRD patterns of K-fixing samples from Germany

- (i) Polymineralic, with high-charge vermiculite (Vimy, Phoenix, Boden 3, Boden 5)

The XRD pattern of the Vimy sample is characterized by two peaks of about equal peak area in the Mg-saturated air-dried state (Figure 5.5) : a 7,3 Å (kaolinite) peak and a reflection at 15 Å with a broad shoulder to lower 2θ values. This 15 Å peak is the combined reflection of the following clay minerals : vermiculite with an "illitic" layer charge (collapses to 10 Å without further expansion after K saturation; 14 Å after Mg saturation, glycerol solvation); chlorite traces (14 Å regardless of saturating cation, solvation or heat treatment); corrensite (12,4 Å after K saturation, 500°C); smectite, as part of an interstratification (14 - 18 Å in the Mg, ethylene glycol and glycerol pattern; > 14 Å in the K, 110°C, ethylene glycol pattern).

The presence of large amounts of discrete kaolinite renders an exact determination of this interstratification impossible due to the interference of the 002 reflection of kaolinite with the peak in the 3,33 Å - 3,5 Å region, which is best suited for characterizing this type of multicomponent-interstratification.

The Phoenix sample contains the following clay mineral assemblage (Figure 5.6) :

high charge vermiculite (14 Å in the Mg-saturated, glycerol solvated state, irreversible collapse to 10 Å upon potassium saturation evident as an increase in the intensity of the

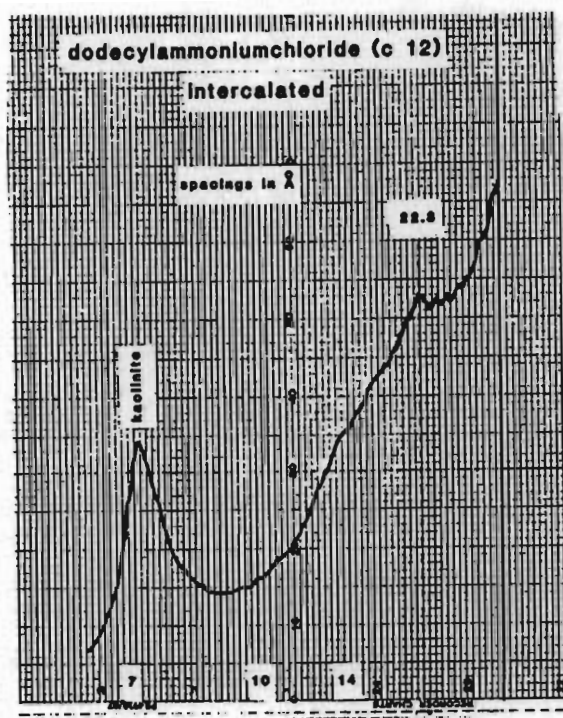
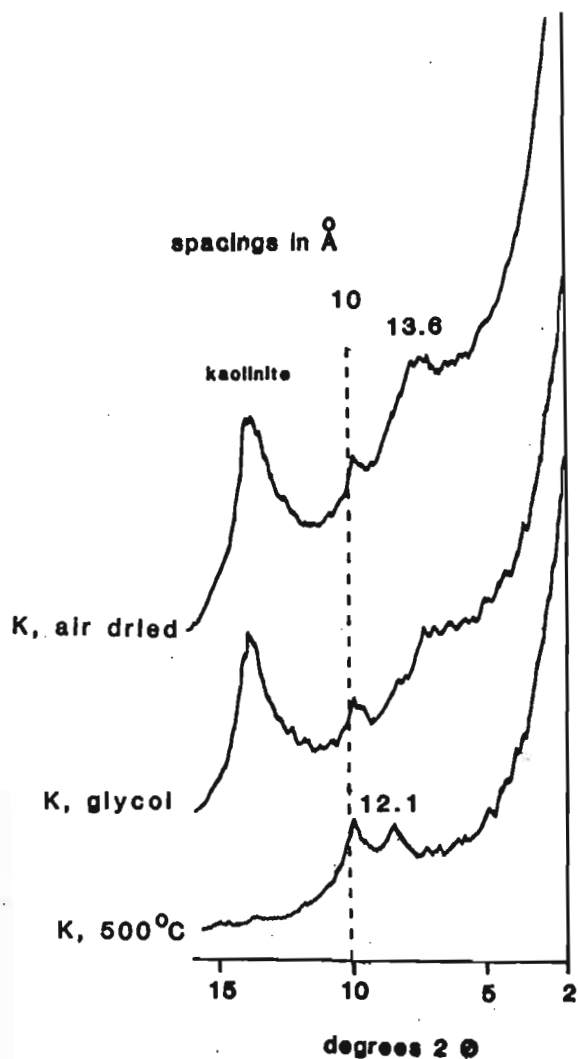
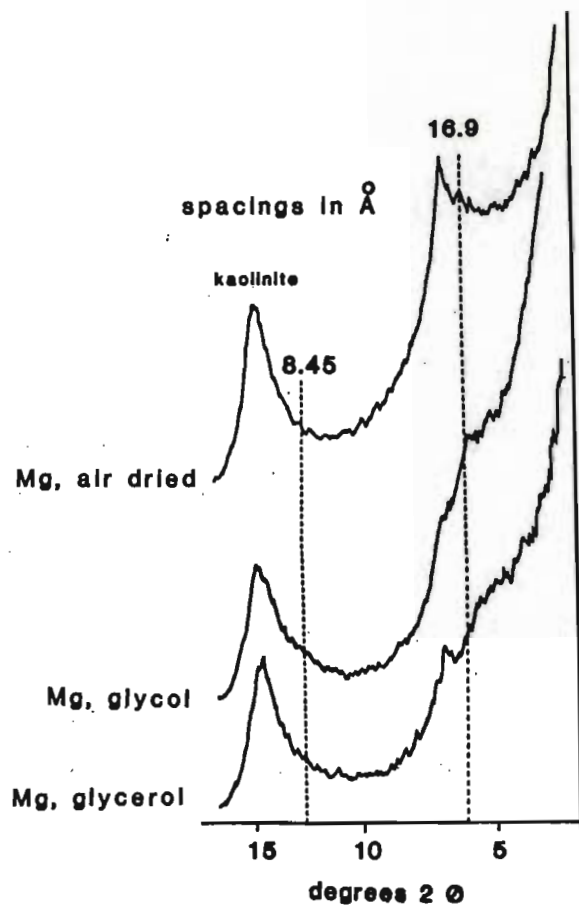


Figure 5.5 XRD traces of the < 2 um fraction of the Vimy sample (oriented specimen)

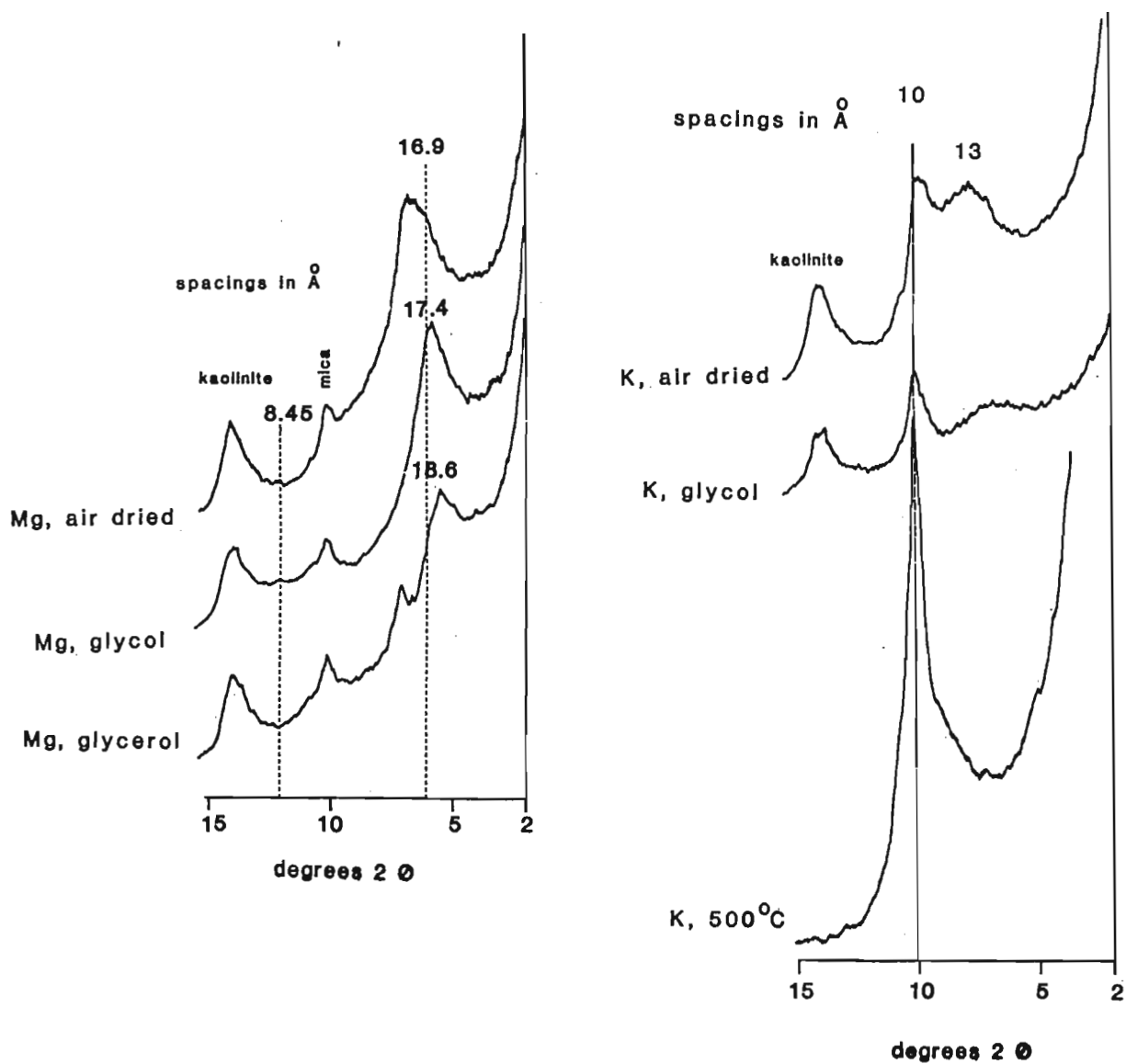


Figure 5.6 XRD traces of the < 2 um fraction of the Phoenix sample (oriented specimen)

10Å peak);

kaolinite;

mica;

smectite as part of an inter-stratification with mica, and possibly also vermiculite or possibly also as discrete mineral.

The layer charge determination using the alkylammoniumchloride procedure (Figure 5.7) confirms the presence of vermiculite and a mineral with a beidellitic layer charge (similar to that which will be described for group 2 soils).

Comparing XRD patterns, the interstratification in the Phoenix sample is characterized by similar (001) peak positions as those found in the group 2 interstratifications (to be shown later), while its pattern (Mg-saturated, glycolated) resembles the pattern with 50% mica and 50% montmorillonite, published by Reynolds and Hower (1970). No chloritic component is present in the Phoenix interstratification.

The XRD patterns of the Boden 3 and Boden 5 samples from Germany are dominated by a 14 Å interstratification, which fails to expand upon glycerol solvation, when Mg saturated (Figures 5.8 and 5.10) and only partially expands with ethylene glycol. K-saturation leads to an irreversible collapse of part of the 14 Å structure, as indicated by the increased intensity of the 10 Å peak (Figure 5.9). This part of the 14 Å mineral may therefore be called high charged vermiculite and provides logical answer to

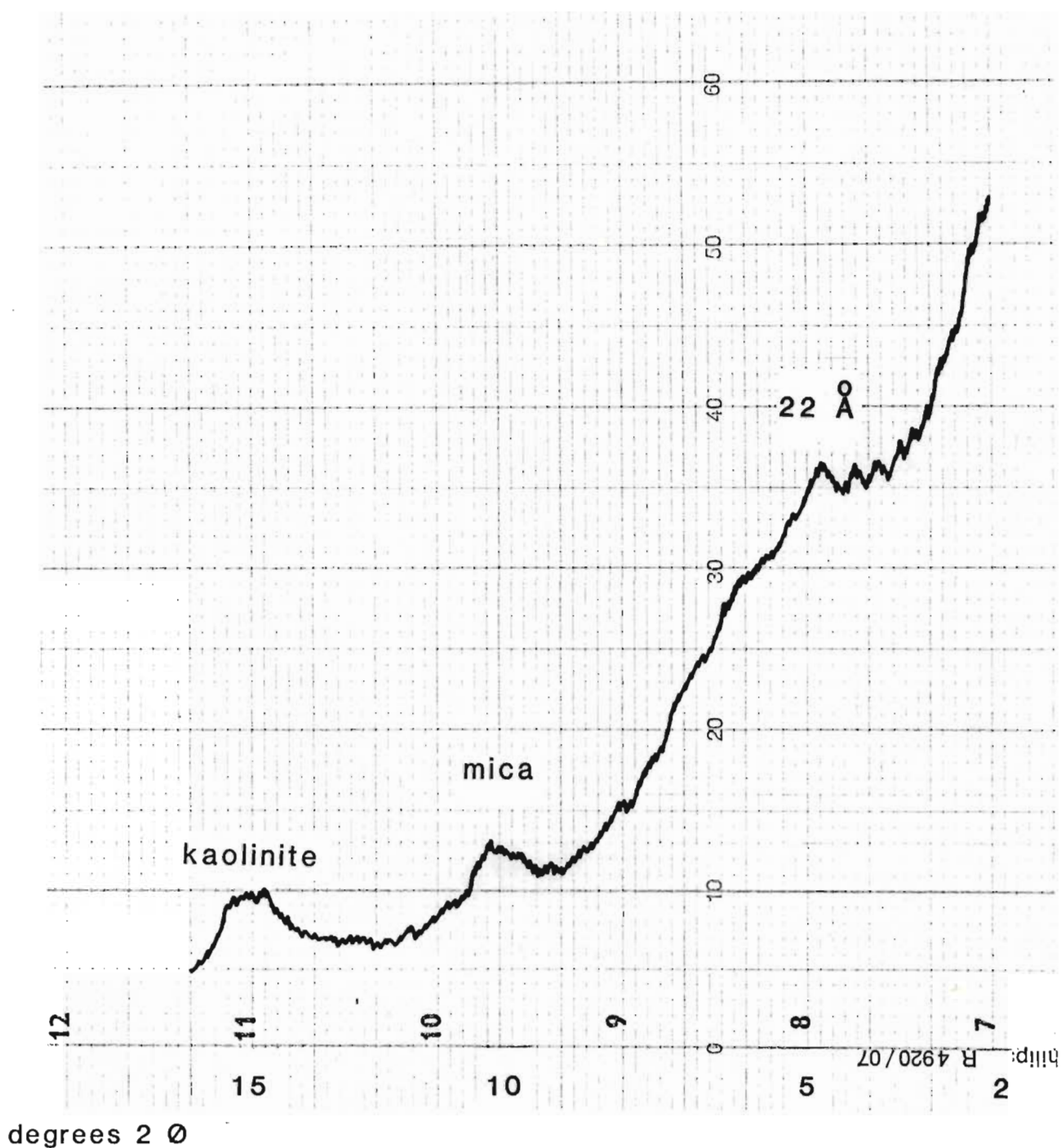


Figure 5.7 X-ray diffraction pattern of the Phoenix sample (< 2 um fraction, oriented specimen) with dodecylammoniumchloride as interlayer cation complex

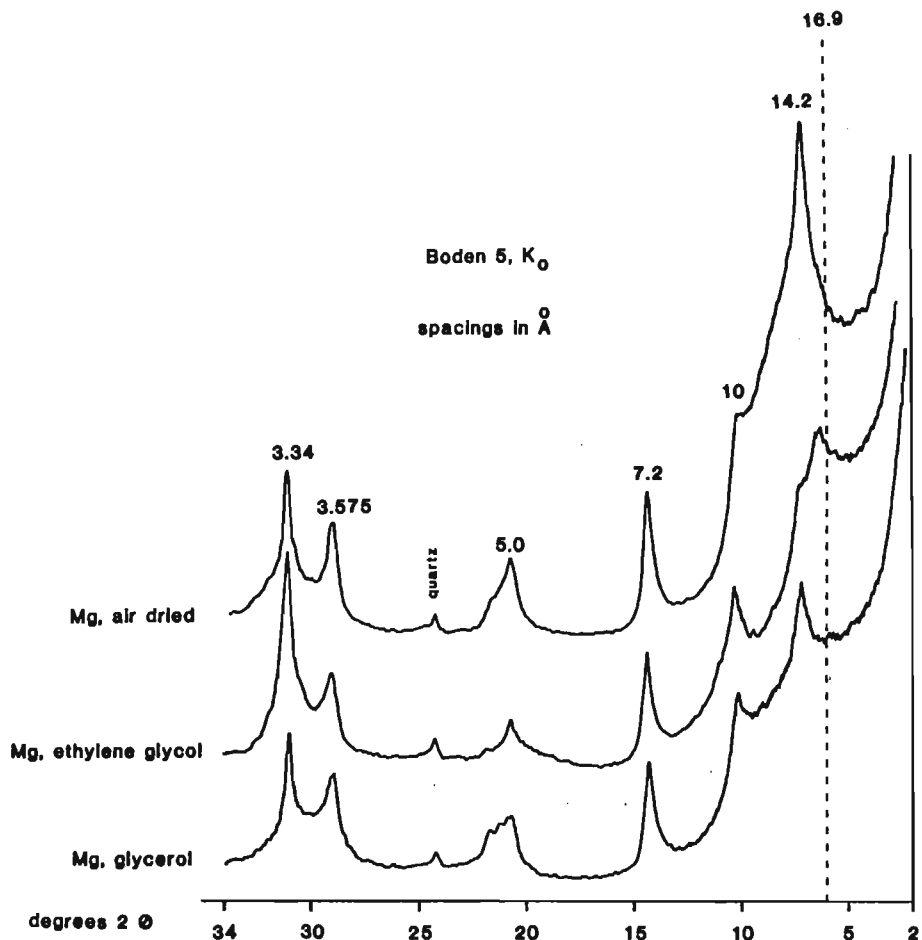


Figure 5.8 XRD traces of the < 2 μm fraction of Boden 5 (oriented specimen)

the K-fixing capacity reported for the two German soils (Nemeth and Forster, 1976). A second part of the 14 Å structure forms a water as well as ethylene glycol monolayer with K as interlayer cation (Figure 5.9). This part is characterized by a broad shoulder at higher Å values for both treatments, but cannot be termed discrete smectite due to the peak broadening, pointing to an interstratification with smectite as major component. This interstratification will probably also account for the high background in the Mg-saturated samples.

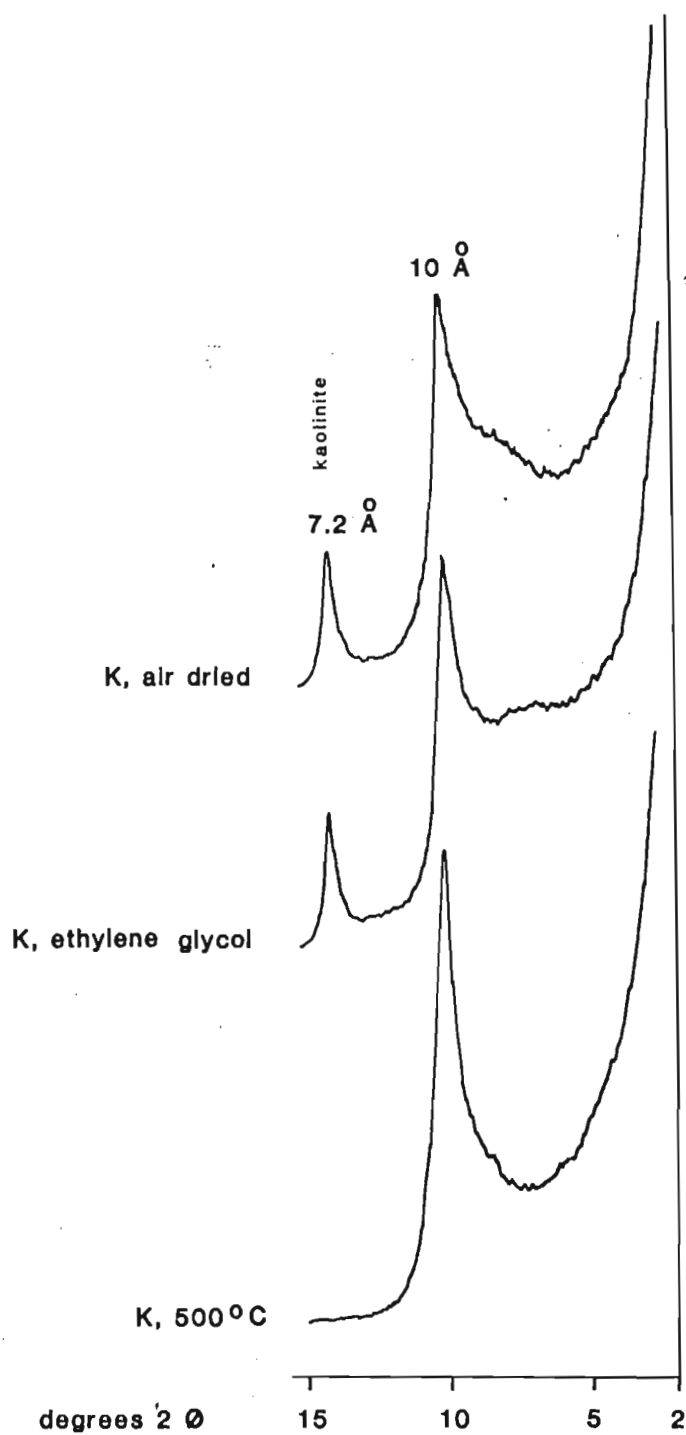


Figure 5.9 XRD traces of the $< 2\text{ }\mu\text{m}$ fraction of Boden 5 K_0 (oriented specimen). Boden 3 K_0 is nearly identical

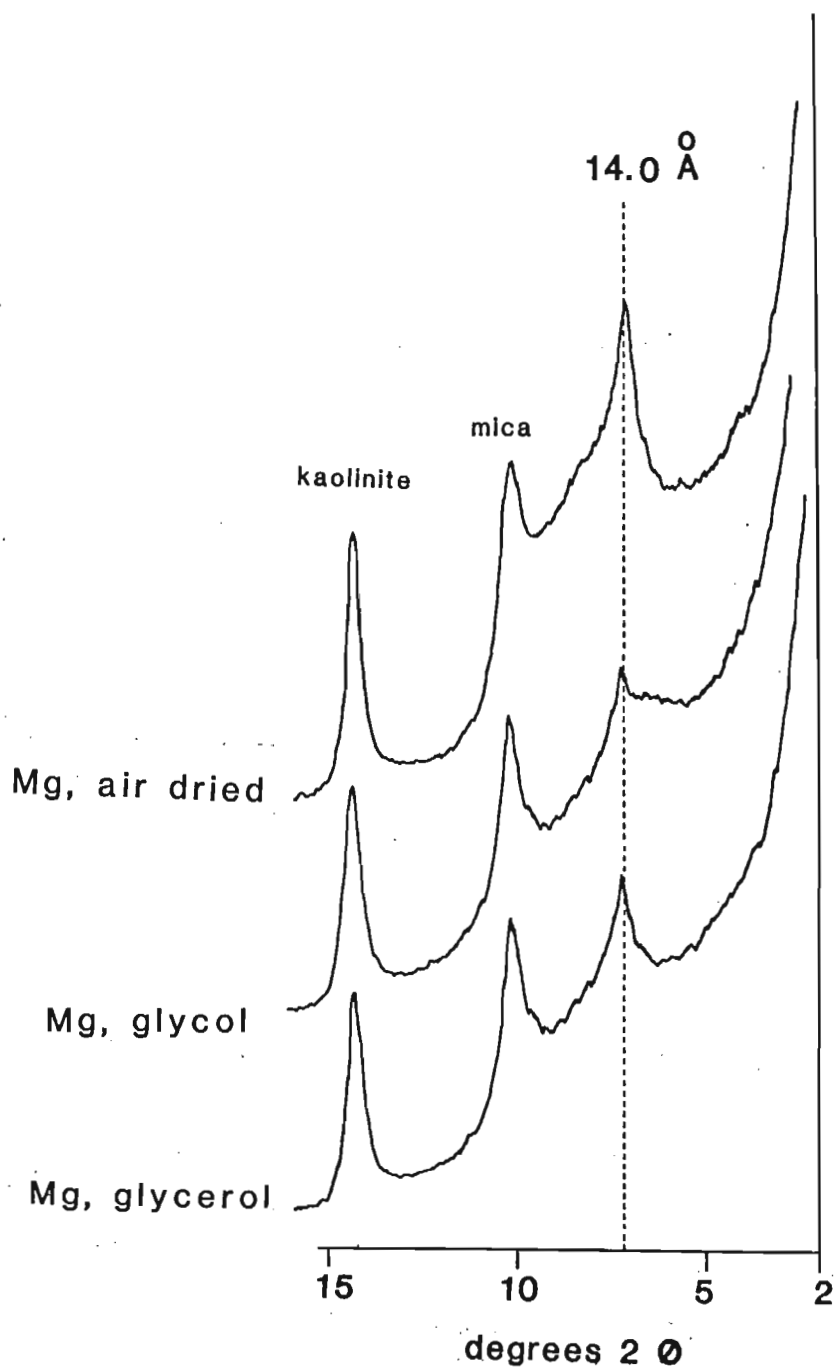


Figure 5.10 XRD traces of the < 2 μm fraction of Boden 3
(oriented specimen)

Kaolinite and small amounts of mica are present in both samples. Chlorite is absent.

Boden 5 K₂ represents Boden 5 K₀, when the equivalent of 150 kg K₂O/ha has been added. Only a slight increase in the intensity of the 10 Å peak (collapsed vermiculite) is visible, indicating that only a small part of the K-fixing interlayers has been filled (Figure 5.11). A much higher amount of K₂O/ha will therefore be necessary to satisfy K-requirements of these soils.

To summarize this, group (i) contains, in addition to appreciable kaolinite, a clay component in which potassium saturation induces lattice contraction (upon air-drying) to 10 Å which resists re-expansion following glycol solvation. As the layer charge necessary for this type of contraction is an "illitic" one (Machajdik and Cicel, 1981) this component is regarded as mainly responsible for the potassium fixing capacity evident in Vimy, Phoenix, Boden 3 and Boden 5. A 14Å peak in the Mg-saturated, glycerol-solvated XRD pattern allows the mineral to be termed high-charge vermiculite. The group also contains significant amounts of an interstratification comprising smectite, mica and possibly also chlorite and/or vermiculite. As will be seen later (during the discussion of group 2 soils) such interstratifications may also contribute to K-fixation by these soils.

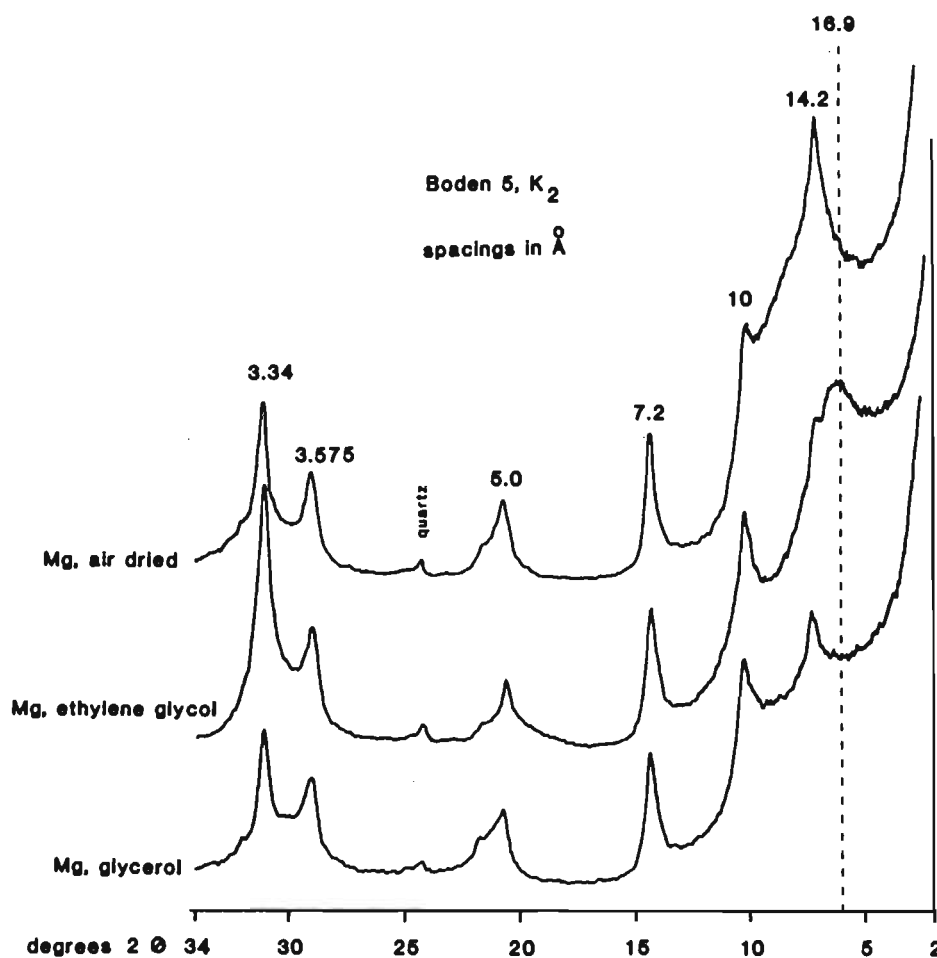


Figure 5.11 XRD traces of the < 2 μm fraction of Boden 5 after the equivalent of 150 kg K₂O/ha has been added

- (ii) Monomineralic mica-beidellite interstratification
(Kwezi, Arcadia)

The Kwezi and Arcadia soil samples can be characterized by an almost monomineralic clay fraction, with only traces of kaolinite and talc respectively (Figures 5.12 and 5.13).

For both samples the d values of the basal reflections after Mg saturation are too high in the air-dried as well as in the glycol and glycerol solvated state to account for a pure smectite (Figures 5.12 and 5.13). Thus an interstratified structure must be assumed. The presence of smectite as a major component in this interstratification is confirmed by its expansion after glycol and glycerol solvation (Figures 5.12 and 5.13). The 002 basal reflection of the Mg-saturated, glycol solvated sample at $> 8,45 \text{ \AA}$ ($16,9 + 2$) indicates mica as the second inter-stratification component. Interpretation of the amount of the two minerals is possible with the aid of tables which show the migration of the $(001)_{10 \text{ \AA}} / (002)_{16,9 \text{ \AA}}$ diffraction peak in its relation to the relative proportions of the two components (Table 1.2) Peak positions at $8,80 \text{ \AA}$ and $8,75 \text{ \AA}$ indicate 35% and 25% mica respectively. The proportion of mica would be even higher if a three component interstratification with a non-expanding 14 \AA mineral (chlorite and/or vermiculite) is assumed. The presence of minor amounts of chlorite is confirmed by a shoulder towards the lower 2θ region in the K, 500°C pattern (Figures 5.12 and 5.13). The presence of this shoulder also indicates that chlorite is part of an interstratification and not a discrete mineral, as the latter would give rise to a 14 \AA reflection. Unfortunately, the $(001)_{10 \text{ \AA}} / (002)_{16,9 \text{ \AA}}$ peak position varies with varying degree of segregation (Figure 5.1) as well as the crystallite thickness (MacEwan, 1956). Therefore the method of Cradwick and Wilson (1978) has also been applied, where the

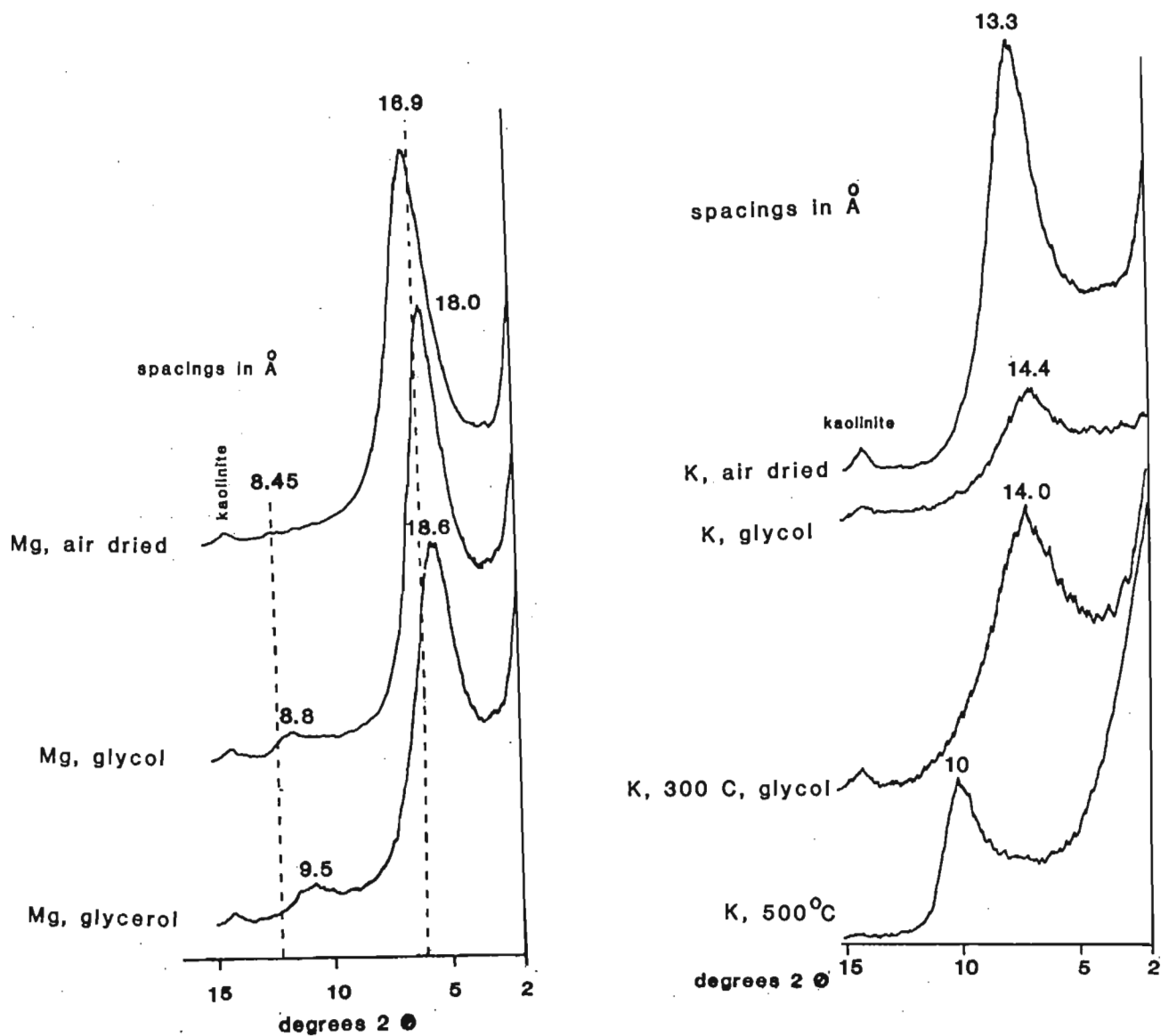


Figure 5.12 XRD traces of the Kwezi soil sample (oriented clay) (broken lines represent peak positions of discrete smectite, treated with Mg + ethylene glycol)

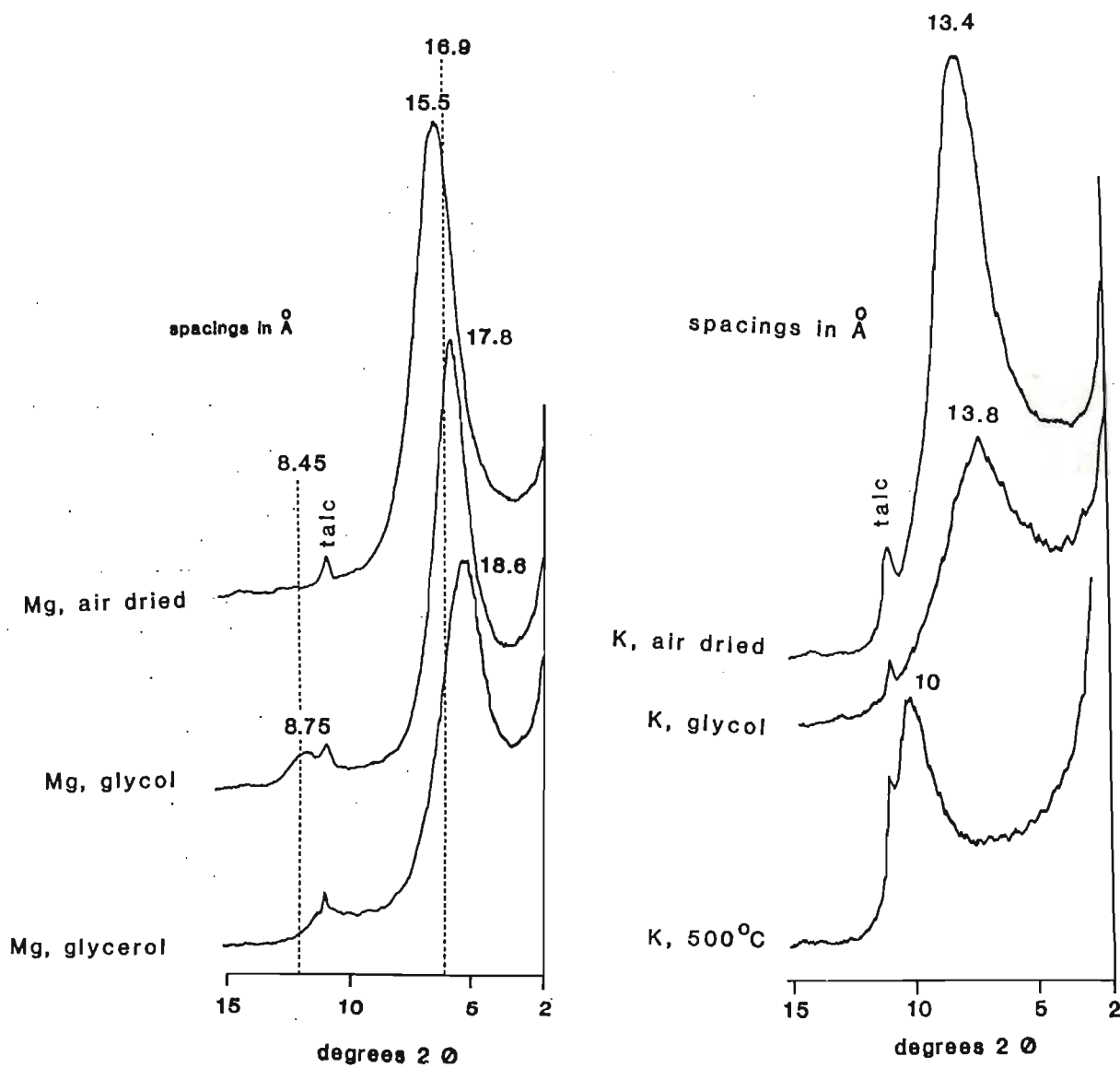


Figure 5.13 XRD traces of the Arcadia soil sample (oriented clay) (broken lines represent peak positions of discrete smectite, treated with Mg + ethylene glycol)

proportions of the components of the interstratification are estimated by comparing published calculated patterns with the experimentally recorded diffraction curves.

Basal spacings of 3,39 Å, 5,64 Å and 8,75 Å for the Arcadia soil sample (Mg-saturated, glycolated) (Figure 5.14) would correspond to an interstratification with about 30% mica and 70% smectite, with a stacking arrangement intermediate between (i) and (ii) (Figure 5.14 compared with Figure 5.15) or 30% mica and 70% of an "expanding" vermiculite. Similar mica contents can be assumed from the peak positions after potassium saturation. A 13,4 Å spacing after air-drying and expansion to 13,8 Å on glycolation in the Arcadia soil sample is due to a smectitic material very similar to the Manito sample investigated by Machajdik and Cicel (1981) (Table 5.1), with about 20% mica, 70% vermiculite and 10% smectite (on condition that vermiculite may form a water-monolayer (12,4 Å) upon K-saturation and air-drying) and expand to 16,9 Å upon glycolation.

For the Kwezi sample, slightly higher mica values can be estimated from the Mg-saturated, glycolated basal spacings (8,8 Å), while lower mica contents result from the interpretation of the potassium saturated patterns.

Interestingly, both clay minerals admit one layer of glycol into their interlayer space after potassium saturation and heat treatment at 300°C. This spacing of 14 Å is regarded as being

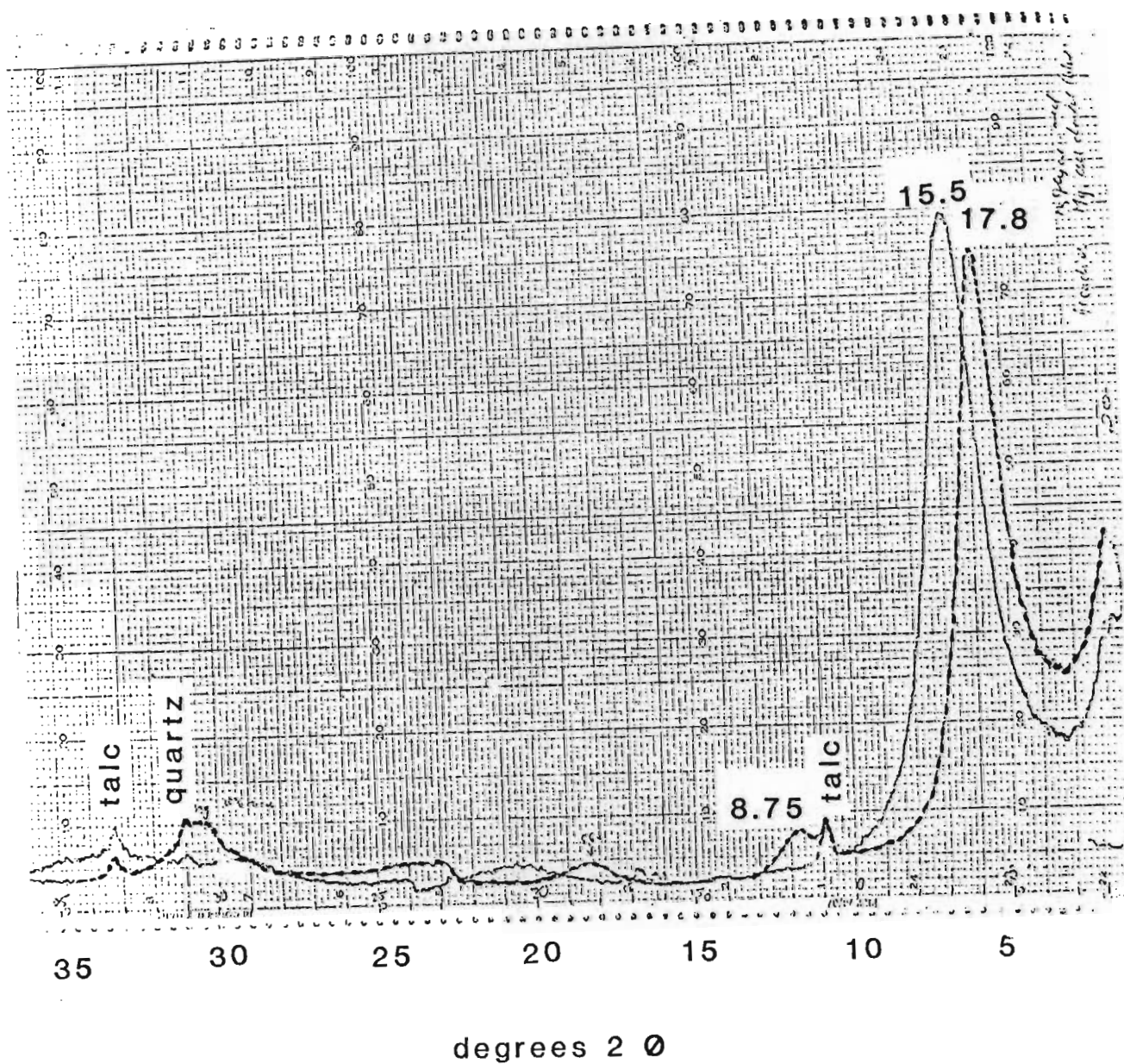


Figure 5.14 XRD pattern of the Arcadia soil sample (<2 μ m fraction, oriented specimen)
 ----- Mg-saturated, ethylene glycol solvated
 ————— Mg-saturated, air dried

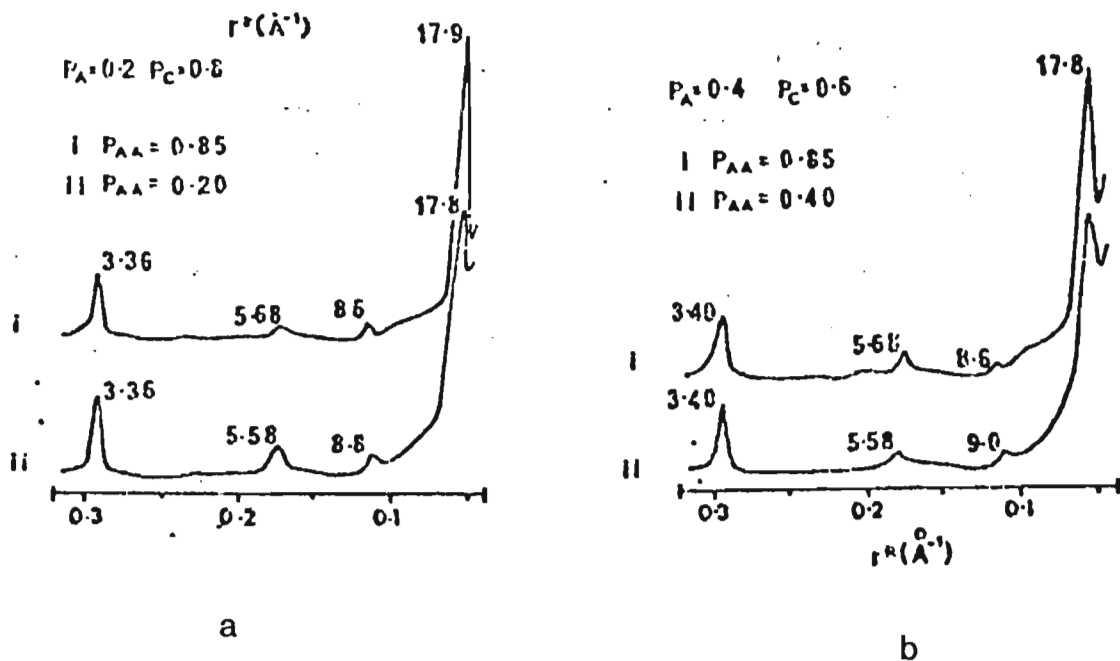


Figure 5.15 Calculated X-ray diffraction curves for interstratifications of mica and smectite for different stacking arrangements (from Cradwick and Wilson, 1978)

- (a) mica (10 \AA) 20% smectite ($16,9 \text{ \AA}$) 80%
 (b) mica (10 \AA) 40% smectite ($16,9 \text{ \AA}$) 60%

characteristic for a medium to high charged smectite (beidellite) with a layer charge per $\text{O}_{10}(\text{OH})_2$ unit cell of 0,40 - 0,43 (Schultz, 1969; Weaver and Pollard, 1973).

The formation of a glycerol monolayer complex with glycerol vapour and a bi-layer complex upon solvation with glycerol liquid also indicated a beidellitic interstratification component in Arcadia (Harward and Brindley, 1965).

The Greene-Kelly test also confirmed the beidellitic nature of the smectite component in the group 2 soil samples (Figure 5.12).

Additional information on the layer charge can be obtained by application of the alkylammonium method (Lagaly et al., 1976). Using dodecylamine (C_{12}), the basal spacing of a montmorillonite varies between the values of a monolayer (13,6 Å) and a bi-layer (17,7 Å), beidellite forms a bi-layer complex while vermiculite expands beyond 20 Å due to a paraffin-like structural arrangement of the dodecylammonium molecules.

Both clay samples form a bi-layer with dodecylammoniumchloride, thus the smectite component can be characterized as beidellite with a layer charge $> 0,33/\text{uc}$ (Figure 5.16). Unfortunately interstratifications can only be picked up by the alkylammonium method when they are regular and the components present in amounts $> 40\%$ (Lagaly, 1979), which is not the case for the group 2 samples.

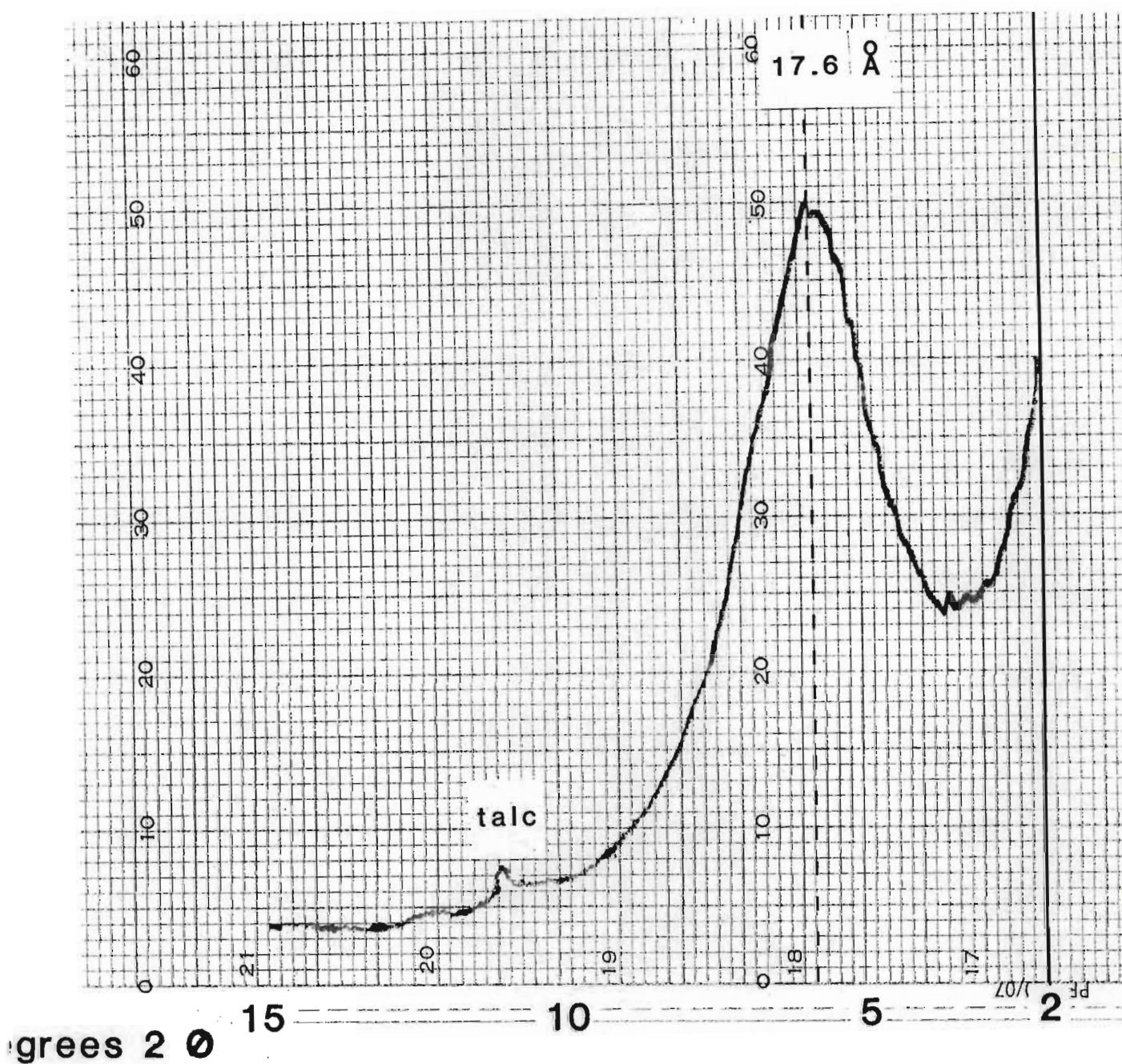


Figure 5.16 XRD pattern of the > 2 μm fraction of the Arcadia sample (oriented specimen) after solvation with dodecylammoniumchloride

Summarized, it can be concluded that the clay mineral that constitutes more than 95% of the clay fraction of the soil samples Kwezi and Arcadia is a well crystallised, random beidellite-mica interstratification with about 20 - 30% mica

layers.

- (iii) Polymineralic, with mica-smectite interstratifications

The seven remaining samples (Milkwood, MIS Sucoma 8492, MIS Sucoma 8478, Rondspring, Somerling, Phoenix, Mayo) contain major amounts of mica (trace amounts in Mayo) as well as kaolinite. The secondary basal reflections of these minerals seriously interfere with the characteristic secondary peaks of an interstratification which is the third component of these soils (Figures 5.17 and 5.18). This mixed-layer mineral consists of smectite (expansion of the lattice on ethylene glycol and glycerol solvation; collapse to 10 Å upon heating the K-saturated sample to 500°C) and mica (broad low angle shoulder in the Mg-saturated, air-dried as well as ethylene glycol and glycerol solvated patterns (Figures 5.17 and 5.18)) as well as chlorite in some of the samples (Somerling, Rondspring and Mayo) indicated by a shoulder towards lower 2θ values in the K-saturated 500°C pattern and differences in the peak shape of the Mg-saturated, air-dried compared with the glycolated and glycerol solvated ones. This interstratification is random in all cases. In samples, where chlorite is absent as interstratification component (Milkwood, Sucoma, Phoenix), the mixed-layer mineral seems to be composed of mica and smectite only indicated by the similarity of the peak shape of the first basal reflection after Mg-saturation in the air-dried stage compared with the ethylene glycol solvated and glycerol solvated one. This similarity in peak shape also excludes vermiculite as interstratification

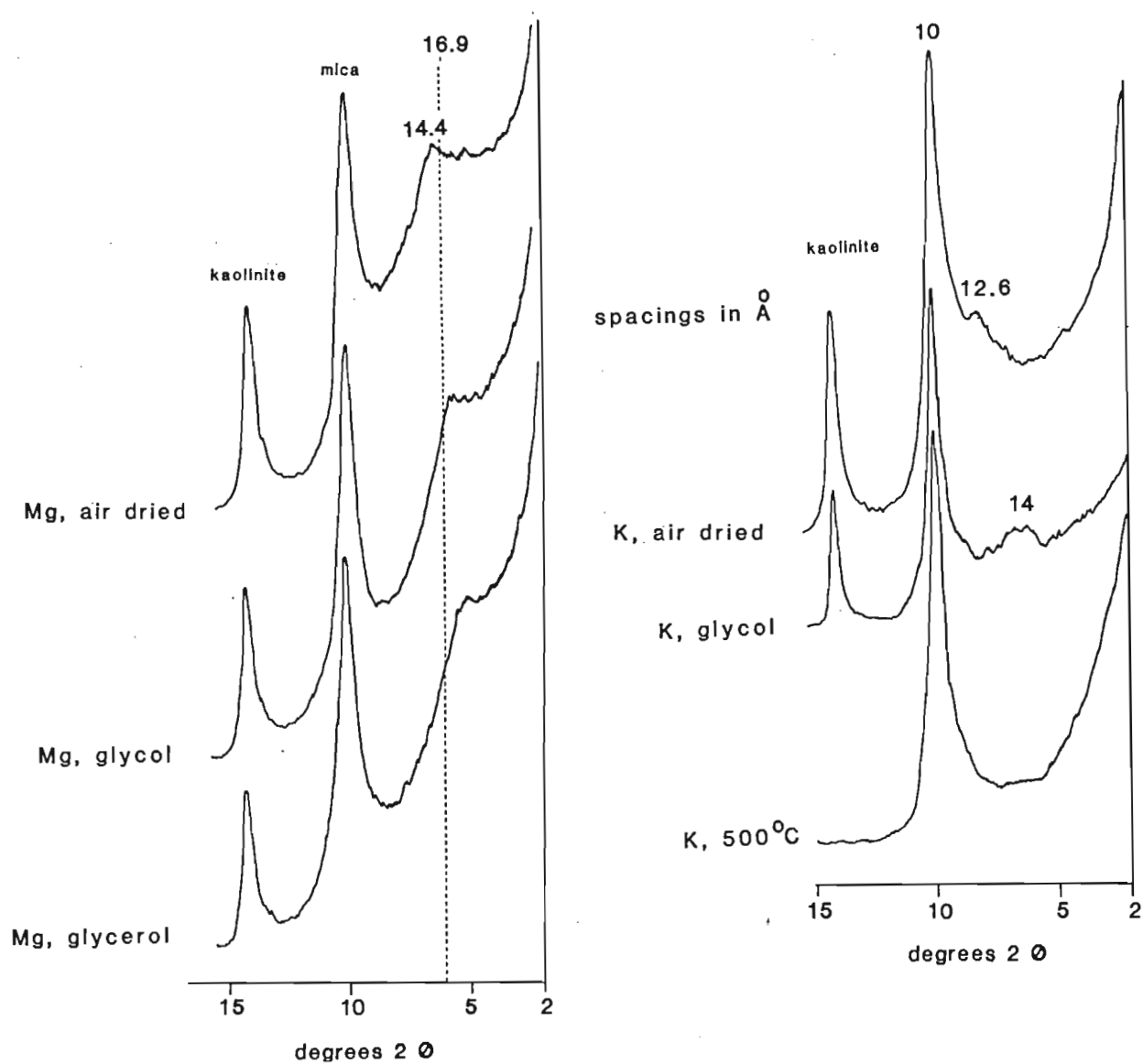


Figure 5.17 XRD traces of the > 2 μm fraction of sample MIS 8492 Sucoma (oriented specimen). Sample MIS 8478 is almost identical.

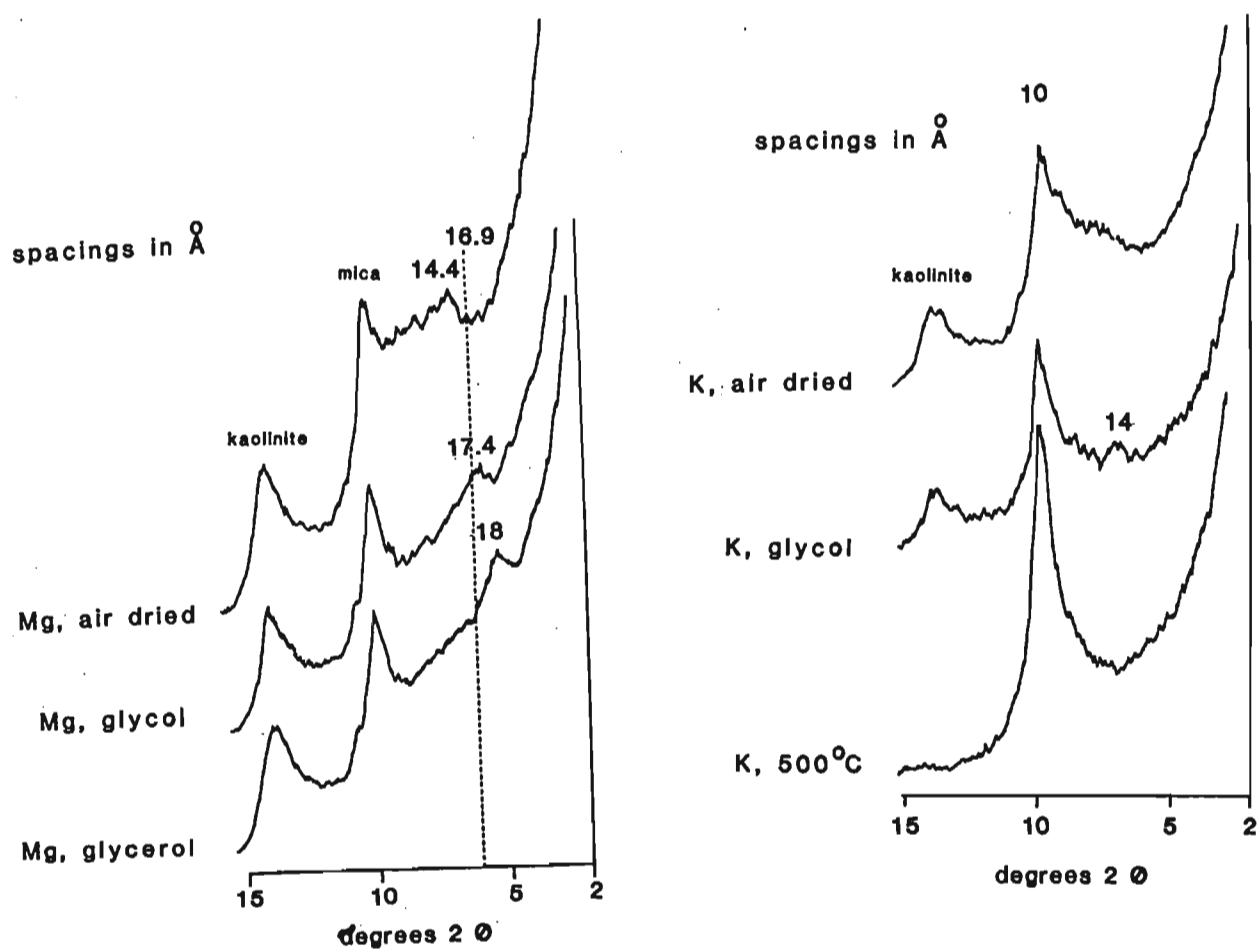


Figure 5.18 XRD traces of the < 2 μm fraction of the Milkwood soil sample (oriented specimen)

component (Figures 5.17 and 5.18).

Comparison of the experimental with computer-generated patterns (Figure 1.8) suggests a composition of ca. 60% mica and 40% smectite for Milkwood, MIS Sucoma 8478, 8492 and Vimy.

5.4.2 Chemical analysis of some K-fixing soils

The chemical composition of some K-fixing clays is presented in Table 5.4.

Total chemical analysis of deferrated (dithionite-citrate-bicarbonate) Li-saturated clays was performed in an attempt to compare results obtained from XRD investigation with the amount of certain cations, especially potassium. All samples investigated contain potassium in concentrations that would correspond to 15 - 68% mica by assuming that micaceous layers contain 10% potassium. Neither the Arcadia and Kwezi soil samples, nor Vimy or Canterbury contain any discrete mica, detectable by means of XRD. As all these soils are characterized by a mica-smectite interstratification, the K-values may probably be explained as reflecting the micaceous or illitic interstratification component in these interstratifications.

Table 5.4 Chemical composition of some of the K-fixing samples (< 2 um fraction ,
deferrated, Li-saturated)

Sample	SiO ₂	Al ₂ O ₃	Fe ₂ O ₃	FeO	MnO	MgO	CaO	K ₂ O	Na ₂ O	TiO ₂	P ₂ O ₅
Arcadia	57,63	25,99	9,71	0,78	0,02	2,01	0,82	1,97	0,06	0,92	0,09
K-set Kwezi	59,86	23,34	11,89	0,69	0,24	1,76	0,31	2,03	0,03	0,76	0,12
Vimy	56,57	29,38	8,77	0,97	0,13	0,98	0,23	1,56	0,01	0,84	0,10
Milkwood	61,55	19,96	8,43	1,14	0,03	3,73	0,35	3,11	0,43	0,69	0,22
Canterbury	58,91	24,19	9,27	1,18	0,07	1,27	0,22	3,46	0,12	0,86	0,03
MIS 8478	51,80	23,47	9,46	1,41	0,16	2,94	1,53	6,83	0,08	1,12	0,69

5.5 Discussion and conclusions

All the soils included in this study are known from field experiments to fix potassium (Wood, personal communication; Nemeth and Forster, 1976). This being so, it is clear from the results reported in this paper that high charge vermiculite is not the only clay mineral capable of fixing potassium, since vermiculite was absent from the soils in groups (ii) and (iii). Group (ii) clays consist solely of a mica-smectite interstratification which is common also to the clays of group (iii) soils and is thereby implicated as the component responsible for K-fixation in the majority of the soils examined.

The interstratification exhibits the following structural variations :

- the minerals cover a range from 20% to 60% (or possibly more) mica layers;

- the stacking order is random in all cases, the degree of random orientation varying greatly;

- the dioctahedral nature of the 2 : 1 layer silicate clays is significant: dioctahedral minerals fix potassium more strongly than do trioctahedral, for structural reasons (Giese, 1979).

As interstratifications with mica and smectite are typical weathering products of micaceous parent materials, the observation of Grim and Bradley (1955), Bolt et al. (1963) and Horvath and Novak (1975) is confirmed, that the parent material

may exert a strong influence on the fixation of potassium in smectitic soils but in a different way than assumed by the authors. It is possibly not "the smectite" that fixes the potassium, but a mica/smectite interstratification which was not recognized as such by the abovementioned authors (who unfortunately did not publish their XRD patterns). Due to the difficulties in recognizing this type of interstratification, especially in the presence of discrete mica or smectite (as outlined in Chapter 1), it is possible that other authors, too may have misinterpreted their X-ray patterns. The "high-charge" smectite, described by Egashira et al. (1982), for example, gives an XRD pattern which closely resembles that of a mica/smectite interstratification with about equal amounts of the two components (Figure 5.19).

The "smectite" reported by Niederbudde and Fischer (1980) which is preferred over vermiculite as a sink for potassium, is more likely a random interstratification of approximately 70% mica and 30% smectite with a tendency towards illite segregation (Figure 5.20). A peak position of 18,6 Å in the glycerol solvated state is definitely too high for pure smectite and the "illite" peak position at 10,2 Å is too high as well. The mixed-layer nature of this "smectite" can also be confirmed by Niederbudde and Fischer's (1980) finding that the potassium content of the newly formed illite calculated from the increase in illite in the clay fraction and the increase in K content was as low as 2,25% - 1,41%. By assuming that the micaceous layers contain 10% K (illite may contain even less), an increase in K content of 2%

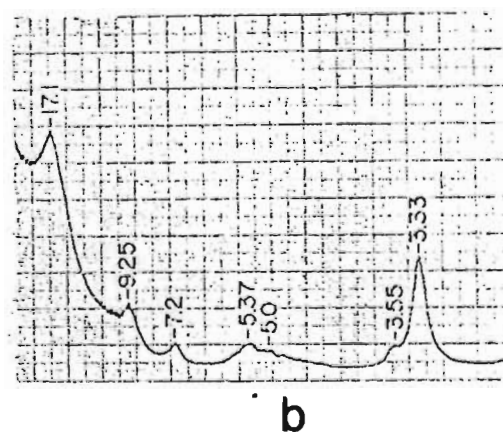
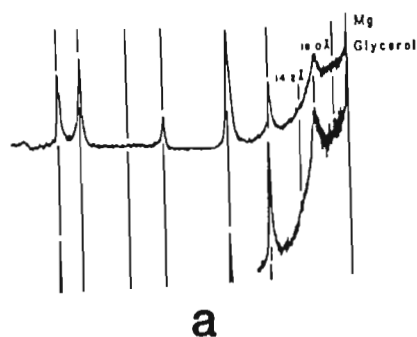


Figure 5.19 X-ray diffraction pattern of (a) the "high-charged" smectite of Egashira et al. (1982) Mg-saturated, glycerol solvated, compared with (b) the calculated pattern of a randomly interstratified mica/smectite (glycolated) with 50% mica layers (Reynolds and Hower, 1970)

would explain a 100% increase in illite when an interstratification with 80% mica and 20% smectite is the starting material. The question arises what interstratification exactly means. Is an interstratification of mica and smectite composed of alternating layers of the two components, as assumed for the calculated XRD pattern, or does interstratification mean that the layer charge is not located symmetrically on both sides of the interlayer space, as suggested by Machajdik and Cicel (1981)? If the potassium fixation occurs in the interlayer region, belonging to mica and smectite together, then the fixation is

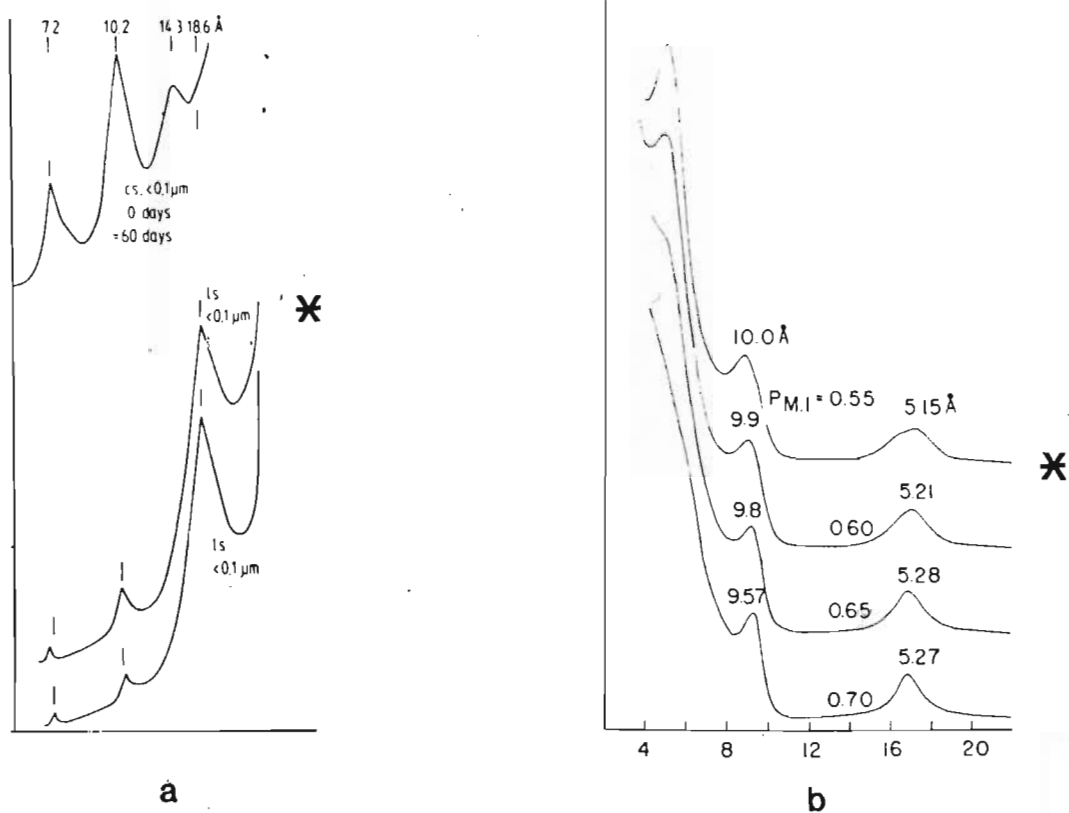


Figure 5.20 (a) X-ray traces of a K-fixing soil (glycerol solvated) (Niederbudde and Fischer, 1980)
 (b) calculated diffractometer patterns of interstratified illite-(glycol) montmorillonite with 70% illite and with increasing tendency for illite segregation from bottom to top (Reynolds, 1980)
 Compare starred curves.

expected to be the higher, the more more ordered the structure and the more closely the two components approach the 50% content.

Data indicate that mica-smectite structures tend to have a total

layer charge greater than that satisfied by fixed cations (Hower and Mowatt, 1966; Schultz, 1969; Roberson and Lahan, 1979). It is possible that this excess charge increases the energy with which potassium is held in the interlayer space.

Some important results may be summarized as follows :

1. K-fixation may be attributable to the presence of either (or both) dioctahedral high-charge vermiculite as a discrete mineral (readily detectable by XRD), or interstratifications containing mica and dioctahedral smectite (which are more difficult to identify).
2. Accordingly, it would appear that soils containing high-charge vermiculite will fix potassium (to an extent depending on the amount of this mineral present) but that not all K-fixing soils necessarily contain vermiculite.
3. The interstratifications encountered in this study were all random, but regular interstratifications (which are much more rare) will presumably behave in similar fashion.
4. Random mica-smectite interstratifications probably form relatively easily in soils of early to intermediate weathering stages derived from parent materials rich in mica and feldspars. From this study, it would seem that eutrophic or at least mesotrophic base status is a covariant requirement, which is logical in so far as acidic conditions or advanced weathering stage will produce interlayering with, and charge balancing by, polymeric hydroxy-aluminium species, thus lowering surface charge and pre-empting K-fixation.

CHAPTER 6

MINERALOGICAL FACTORS ASSOCIATED WITH STRONG SWELLING IN SOILS AND CLAYS

6.1 Introduction

Swelling, and conversely shrinkage, are very important properties of soils and sediments due to their influence on water balance and related consequences both for agronomic management, soil conservation and engineering.

The distinctive morphological and physical properties of "active" soils are caused by the presence of substantial amounts of "expanding" lattice minerals in conjunction with a high total clay content. Smectite and to a much lesser extent vermiculite are generally reported to cause the problems of "expansive" soils.

The genesis of swelling soils is therefore assumed to take place in conditions that favour the synthesis of smectite: a profile environment rich in Mg and Ca, and a high silica potential. Factors that favour such environments are basic parent material, impeded drainage and semi-arid climate.

In South Africa, the problem of expansive soils was brought to the attention of engineers as early as 1950. The first

symposium on expansive soils was published in 1957 (de Bruijn, Collins and Williams).

Fluvio-lacustrine deposits, weathered norite and weathered Eccle shale constitute the parent material for these active soils (Simons and Williams, 1963; de Bruijn, 1963; Williams and Jennings, 1977; Williams and Donaldson, 1980), but information on the clay mineral content is extremely scanty.

The objective of the present investigation was to contribute to the knowledge of highly swelling soils through investigation of the clay fraction.

This task was especially interesting as material was made available from some of the most problematic regions of South Africa.

Water adsorption by smectites and vermiculites has been described in terms of an initial crystalline phase (intercrystalline swelling) and a later osmotic phase (osmotic, unlimited, high or indefinite swelling) (Figure 6.1). The former results from the adsorption of up to three first "layers" of water in the inter-layer space, driven by surface and cation hydration energies. Further adsorption of water, whereupon the layers separate completely from one another and lose their parallel orientation, has been termed osmotic, or double layer swelling, since it has been considered to be due to chemical potential gradients between free and adsorbed water (Norrish, 1972).

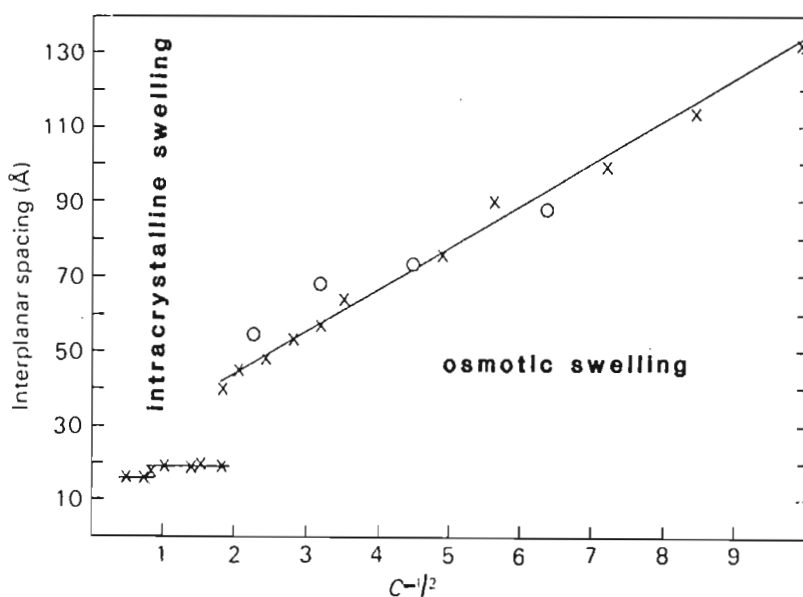


Figure 6.1 Change of approximate mean spacing between layers of montmorillonite with reciprocal of square root of concentration (c) for Na-saturated clay (after Norrish, 1954) x in NaCl solution, o in Na₂SO₄ solution

A quantitative treatment of osmotic swelling is based on the Gouy-Chapman double layer theory. While this theory has limitations due to simplifying assumptions, predicted osmotic pressures have corresponded fairly well with swelling pressures, developed by Na-montmorillonite (Walker, 1975). Measured swelling pressures of Ca-montmorillonite, however, fall well below values predicted in a similar manner.

The Gouy-Chapman theory assumes surface charge to be smeared out and the counterions to be point charges, leading to unrealistically large ion concentrations at high potentials. To correct this deficiency, Stern (1924) postulated the existence of an adsorbed layer of finite-sized counterions adjacent to the surface. The potential in the Stern layer falls off linearly from its surface value (ψ_0) to the so-called Stern potential (ψ_δ). Beyond the Stern layer (of thickness $\delta \sim 5 \text{ \AA}$ for clay systems) the Gouy-Chapman or diffuse double layer extends into the bulk solution (Figure 6.2). A further refinement was proposed by Grahame (1947) who recognized an inner and outer Helmholtz layer or plane. The latter is thought to occur just outside the Stern layer, marking the boundary between the fixed and mobile part of the diffuse double layer ("plane of shear"). At this plane the potential is zeta (ζ) (Figure 6.2).

A theoretical analysis of the interaction between colloidal particles has been developed by Derjaguin and Landau (1941) and, independently, by Verwey and Overbeek (1948). The fundamental feature of what is now known as the DLVO theory is that this interaction and, hence, colloidal stability, is determined by a combination or superposition of the interparticle double layer repulsion energy (V_r) and the van der Waals attractive energy (V_a) (Figure 6.3). Of prime importance is the occurrence of an energy maximum (V_m) at intermediate distances. This maximum may be considered as an energy barrier which the particles must overcome. The height of V_m therefore determines the relative stability of the system. But when the applicability of the DLVO

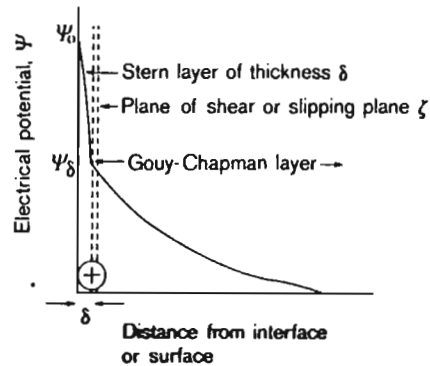


Figure 6.2 Variations of the electrical potential with distance from the surface according to Stern (1924) and Grahame (1947). The broken line nearest to the surface marks the extension of the Stern layer of thickness δ , coinciding approximately with the inner Helmholtz plane (IHP) of potential ψ . The other broken line indicates the outer Helmholtz plane (OHP), identified with the "plane of shear" or "slipping plane" of potential ζ (Theng, 1979).

theory to clay systems is tested, modifications have to be introduced into both the repulsion and the attraction terms before experimental data can be satisfactorily interpreted.

Factors which affect inter-particle repulsion are the degree of face-to-face associations (Banin and Lahav, 1968), which can be modified by ultrasonication or air-drying, and charge heterogeneity within the crystallite, i.e. an unequal surface potential of two interacting silicate layers (Lagaly et al., 1972). The

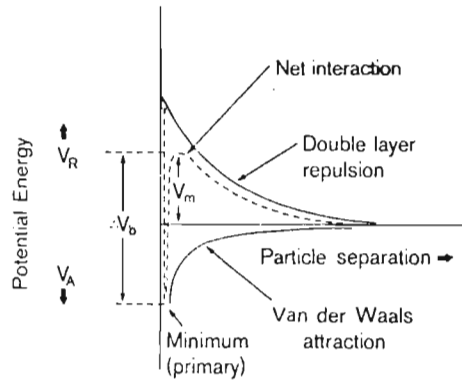


Figure 6.3 Diagram showing the energy of double layer repulsion (V_R) and of Van der Waals' attraction (V_A), together with the net or total interaction energy (V_T) for parallel flat plates, as a function of particle (plate) separation. The interaction curve shows a deep (primary) minimum at close separations. V_m is the energy barrier to particle coagulation and ΔV_b is the barrier to redispersion (Theng, 1979).

attractive forces between clay particles are still more difficult to establish since their nature is incompletely understood (Norrish, 1972). Van der Waals' forces can account for only a very small part of the interparticle attraction in the case of infinite swelling. Apparently, forces arising from edge-to-face and edge-to-edge bonding are far more significant. Van Olphen (1963) has raised the possibility that the edge surfaces carry a

positive diffuse double layer in neutral and acidic suspensions although the overall electrophoretic mobility of the particles is negative.

The swelling behaviour of condensed clay in water and electrolyte solutions, such as do occur in soils, is vastly more complex. For such systems the DLVO theory cannot be used to predict adsorbed water (Quirk, 1968), because wetting results in strain relaxation and the formation of a gel structure within which much of the water is enmeshed (Theng, 1979). On the other hand, some sediments and soils fail to show extensive swelling - even in the presence of large amounts of swelling clay minerals and the apparent absence of any cementing agents in the interlayers.

Though literature on the subject is comprehensive, it is restricted to model cases: i.e. discrete minerals, mono-ionic solution composition, etc.

Studies of water-clay interactions have been made with smectite, mostly montmorillonite, few with vermiculite or illite. No information is available on the swelling capacity of interstratifications with water, except for hydroxy-interlayered smectites. With Na as charge balancing cation, some beidellites expand beyond 20 Å, whereas others yield spacings of about 15 Å, as do saponite and vermiculite (Suquet et al., 1975). However, all these minerals show indefinite swelling when saturated with Li, except for vermiculite with a very high charge (Table 6.1), which illustrates the importance of ion size in this respect. Osmotic swelling may also occur with K-saturated montmorillonite,

Table 6.1 001 spacing (Å) of water solvation complexes of smectites and vermiculites (after Suquet et al., 1975)

Clay mineral	Exchangeable cation					
	Li	Na	K	Ca	Mg	Ba
Montmorillonite	Ind	Ind	(1) {Ind } (15,5)	19,1	19,4	18,7
Beidellite (2)	Ind	15,2	12,7	(18,7s (15,4vw	18,6	
(3)	Ind	Ind	12,55	18,6	18,58	18,38
Saponite	Ind	15,2	12,6	(18,6vw (15,4s	(18,9s (15,7s	(18,5s (15,9vw
Vermiculite	{Ind (15	14,9	(1) {12,6 (10,4	14,9	14,7	15,7

(1) According to the origin and history of the sample.

(2) Beidellite from Rupsroth, Germany; unpublished data of R Glaeser.

(3) Beidellite from Black Jack Mine (Idaho); Weir, 1960.

Ind = indefinite swelling, s = strong, vw = very weak

although K-beidellite and K-saponite usually, but not always, form single to double layer hydrates.

With divalent or trivalent cations, unlimited swelling is not observed. Two or three water layers are permitted into the interlayer space (Table 6.1). It is interesting to note that an expanded Na-clay, if treated with a K solution of low concentration, does not contract, whereas if treated with Ca

solution, it does. The "expanded" Ca system is thus absolutely unstable (MacEwan and Wilson, 1980). This contradicts results obtained from Na-activation experiments, where a Ca smectite as starting material is ideal and a certain Ca/Na ratio is suggested for maximal swelling (Marais, personal communication). It also contradicts observations (Emerson and Bakker, 1973) from highly swelling soils and sediments where divalent ions commonly outnumber monovalent cations in the soil solution.

The extent to which marked swelling occurs in clays is dependent on a number of solution and mineral structure characteristics (Table 6.2). Smectites with the highest swelling behaviour show charge densities in the range 0,28 - 0,33/ $O_{10}(OH)_2$ unit cell with a broad spectrum within this short range, independent of chemical composition (Lagaly et al., 1972).

6.2 Materials and methods

Soil samples, comprising some of the most expansive soils known in South Africa in terms of engineering problems, have been investigated. All localities with the exception of the Vredefort sample are building sites. The environmental conditions for the various localities are listed below.

Vereeniging is situated at about 1 420 m above sea level. The climate is classified as humid mesothermal (Cwb) with an average summer rainfall of 685 mm per annum and an annual evapotranspiration of 1 650 mm (Donaldson, 1965). The soil is classified as

Table 6.2 Clay mineral and solution characteristics that influence the osmotic/intracrystalline swelling ratio of smectites

Intracryst.			Osmotic			
Fe ²⁺	Fe ³⁺	Mg	Al	Ions in octahedral sheet		
9,05	----->8,9			b-axis spacing		
1,51	1,49			060 reflection		
Fe ²⁺	----->Fe ³⁺			valency of iron		
0,7	----->0			tetrahedral substitution/O ₁₀ (OH) ₂		
0,7	----->0,2			charge density		
verm.	sap.	beid.	montm.	clay group/species		
0	----->100			dielectric constant of solution		
> 10 ⁻¹ ^{decreasing} ----->				electrolyte concentration		
-----> ^{increasing}				temperature		
> 2 ----->				particle size		
< 0,2 um						
tri + di	----->mono			valency of counterions		
Cs	-->Rb	-->NH ₄	-->K	-->Na	-->Li	species of monovalent ion
0	----->			>0,05	charge heterogeneity	
face-to-face		edge-to-edge		bonding		

highly expansive (Williams and Jennings, 1977). The soil profile is alluvial (ca. 7 m) on weathered Dwyka (Williams and Jennings, 1977).

The Girl Guide hall site at Rosebank, Cape Town, is situated at

12 m above sea level and the climate is classified as mediterranean with an average winter rainfall of 627 mm per annum and an average annual evaporation of 1122 mm (Donaldson, 1965). The soil is classified as moderately expansive.

The general climatic conditions of the Doreen Court site at Roodepan near Kimberley can be described as warm semi-arid with an annual summer rainfall of about 380 mm and has evaporation of 780 mm (Williams, 1980). The soil is classified as moderately expansive.

Onderstepoort is situated at an altitude of 1 210 m. The mean annual precipitation, which falls predominantly during the summer months, is 710 mm, mean annual potential evapotranspiration is reported at 830 mm (Donaldson, 1965). The climate is classified as humid mesothermal (Cwb) (de Bruijn, 1973). The soil is classified as having a very high potential expansiveness (Williams and Jennings 1977).

A sample has been included which was collected from the Vredefort area. The soil exhibits a strong swelling tendency (slickensides, cracks, etc.), but fails to respond to soda-activation (Marais, personal communication).

One soil sample from a Vertisol at Kriel (pit 23) has also been investigated.

The mineralogy of highly swelling soils from two other

localities : Tutuka power station and Melody Ranch, has been reported in previous chapters.

Table 6.3 Sample localities, parent materials and sample donators

Locality	Parent material	Donater
Onderstepoort	Norite	A A B Williams
Vereeniging	Alluvial, on Dwyka shale	A A B Williams
Kimberley	Dwyka shale varves	A A B Williams
Cape Town	?	A A B Williams
Kriel	?	J M de Villiers
Vredefort	Dolerite (?)	B Marais

Additional methods to those reported in previous chapters comprise the application of the Free Swell Test, which is performed by pouring dry soil, passing a No. 40 sieve into a frame, filled with water and resting on a filter paper, which is in contact with the water, and noting the swelled volume (= final volume) (Duncan, 1969). The material is then dried at 40°C (= initial volume) and the plasticity index (PI) measured as $\left[\frac{\text{final volume} - \text{initial volume}}{\text{initial volume}} \right] \times 100 = \text{PI} \%$. The relationship between the PI values and the swelling capacity is given as follows :

PI = < 25% low swelling capacity

PI = 25 - 35% medium swelling capacity

PI = 35 - 50% high swelling capacity

PI = > 50% very high swelling capacity

The swelling capacity of the clay fraction has been determined by the measurement of the magnitude of expansion of the Na-saturated, freeze-dried clay fraction as the volume increase of 100 mg clay dispersed in 25 ml of a 1,0 M and 0,1 M NaCl solution as well as a 0,5 M CaCl_2 solution, following Egashira and Ohtsubo (1983). The end volumes of the samples investigated were compared with those of montmorillonite ($> 4 \text{ cm}^3$) and kaolinite ($2,5 \text{ cm}^3$).

6.3 Results and discussion

6.3.1 XRD results

XRD analysis has revealed the presence of a variety of clay minerals, both discrete (kaolinite, mica, smectite) or as part of an ordered or random interstratification. A common feature is the strong 060 reflection at $1,495 - 1,51 \text{ \AA}$ which indicates that the major clay minerals are dioctahedral.

On the basis of the clay mineral suites, the soils can be subdivided into two groups denoted by the swelling constituent as follows :

- (a) smectite-dominated, with kaolinite (traces to medium high amounts). The highly swelling soils of Onderstepoort and Vereeniging and the Vredefort sample belong to this group as do the Rensburg soil at Melody Ranch and the group 1 soils at the Tutuka power station.

(b) mica-smectite interstratifications with discrete kaolinite and mica. Discrete smectite was not detectable in these soils. The soils from Kriel, Kimberley and Cape Town show this type of swelling component, as do the group 2 pedons at Tutuka power station. While in the samples from Kimberley the amounts of mica and kaolinite ranged below 10%, kaolinite amounted to about 50% in the samples from Cape Town, with mica being as abundant ($\pm 25\%$) as the mica-smectite interstratification.

6.3.1.1 Smectite dominated soil profiles

(a) Onderstepoort

(i) Whole soil

The whole-soil mineralogy is dominated by the mineral composition of the noritic parent material : Ca-rich plagioclase and pyroxene (orh and mkl). Concretions of calcite and amygdale fillings consisting of prehnite, Mn-rich ilmenite and richterite have been identified. The amount of these primary minerals decreased towards the surface on account of quartz, but plagioclase is still present in considerable amounts in the A horizon.

(ii) Clay mineralogy

The clay fraction in each horizon is dominated by discrete smectite, which is characterized by the following peak positions : a 15,2 Å peak position in the Mg-saturated, air-dried state, indicating a water double layer. Expansion to 16,9 Å upon

solvation with ethylene glycol with higher order reflections being exact sub-multiples of the expanded first order reflection indicates the absence of any interstratified components in this smectite. Glycerol solvation led to a lattice expansion to 18 Å, which excludes the presence of vermiculite in this structure (Figure 6.4).

A 17,7 Å spacing after dodecylammoniumchloride intercalation allows the smectite to be identified as beidellite (Lagaly et al., 1976) (Figure 6.5).

The spacing of the Li-saturated, air-dried smectite increases from 14,3 Å in the C horizon to 15,1 Å in the A₁ horizon (Figure 6.6). While a value of 15,1 Å is characteristic of a water bi-layer, any spacing below indicates interstratifications of water monolayer-water bi-layer units and thus charge heterogeneity of the smectite. Heating the Li-saturated sample resulted in expulsion of interlayer water (9,8 - 9,9 Å). Subsequent solvation with ethylene glycol re-expanded part of the interlayer regions : a peak at > 16,9 Å characterizes this re-expansion, while the position of the second order peak at 8,8 (C horizon) to 8,65 Å (A horizon) are indicative of 20 - 30% montmorillonite layers, randomly interstratified with beidellite layers (Figure 6.6). Comparison of the peak shape with computer calculated patterns (Reynolds and Hower, 1970) results in a similar ratio of 10 Å (montmorillonite) : 16,9 Å (beidellite) components.

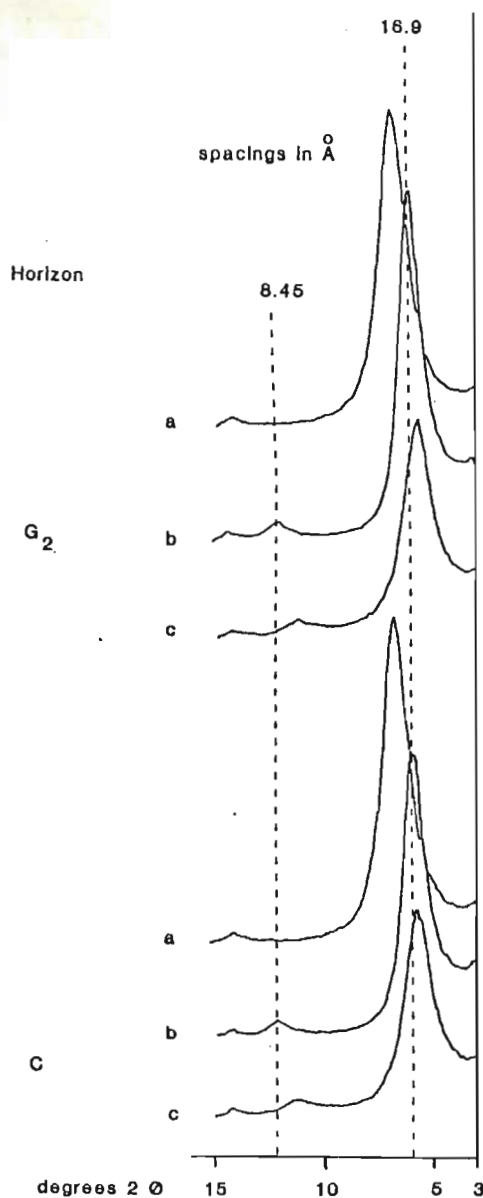
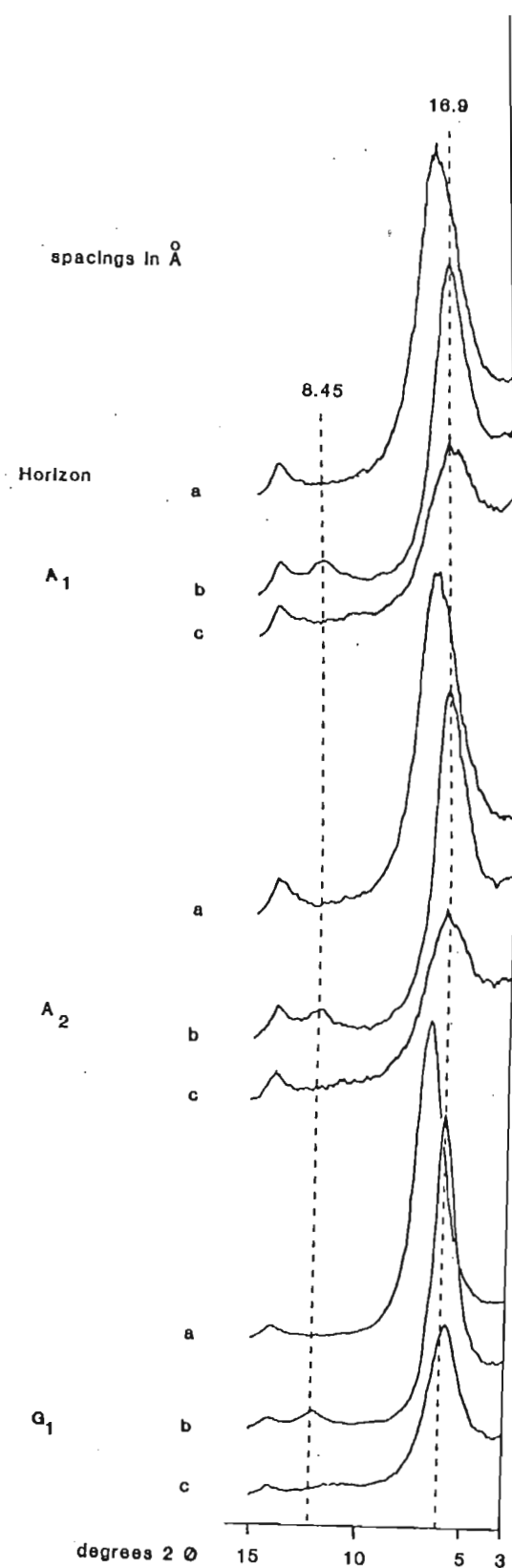


Figure 6.4 XRD traces of the various horizons of the Onderstepoort soil profile (oriented clay)

(a) Mg-saturated, air-dried

(b) Mg-saturated, ethylene glycol solvated

(c) Mg-saturated, glycerol solvated

(broken line represents peak position of discrete smectite treated with Mg + ethylene glycol (b))

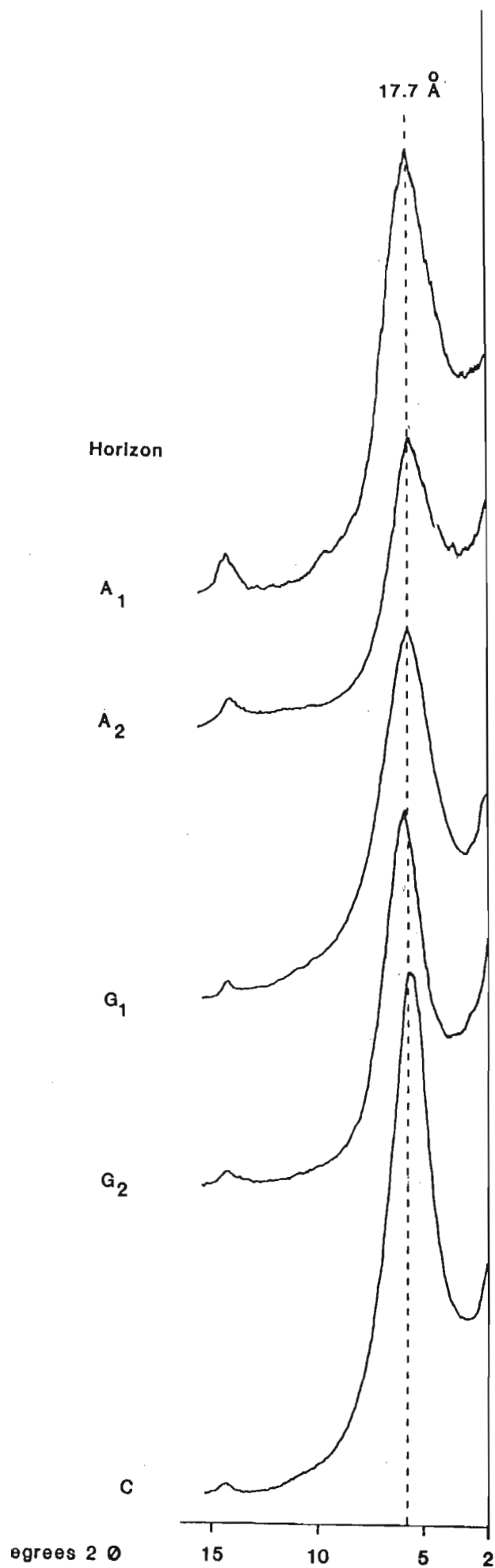


Figure 6.5 XRD traces of the various horizons of the Onderstepoort soil profile after dodecylammoniumchloride intercalation (oriented clay) (broken line represents peak position of discrete beidellite)

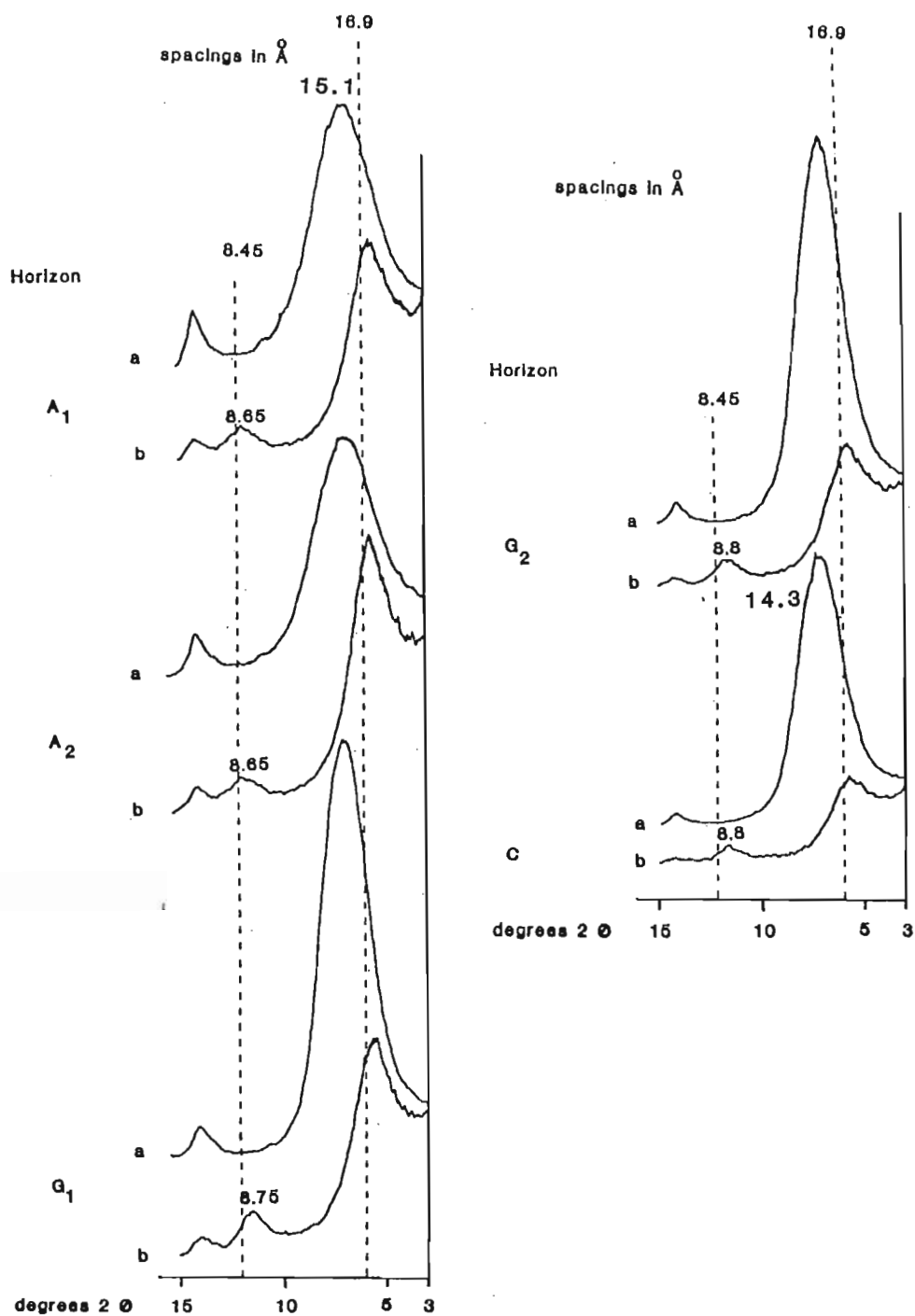


Figure 6.6 XRD traces of the various horizons of the Onderstepoort soil profile (oriented clay)

(a) Li-saturated, air-dried

(b) Li-saturated, 280°C, ethylene glycol solvated

(broken lines represent peak positions of discrete beidellite treated with Li + 280°C + ethylene glycol)

Variations in the charge density between various interlayers is also indicated from the peak positions of the K-saturated, air-dried smectite : values between 12,6 Å and 13,5 Å indicate smectite water-monolayer-smectite water-bilayer interstratifications (Figure 6.7). A peak position of ca. 15 Å in the K-saturated 300°C, ethylene glycol solvated pattern also indicates the predominantly beidellitic nature of the smectite (Schultz, 1969). The irreversible collapse of the clay structure to 10 Å upon heating to 500°C confirms the identification of the dominant mineral as smectite while a shoulder at the low angle side points to small amounts of a smectite-chlorite or/and kaolinite interstratification additional to the discrete beidellite (Figure 6.7).

(b) Vereeniging

Samples have been provided from two localities in Vereeniging (Civic Centre and Brand Muller Drive). While only one sample was available from the alluvial soil at the Brand Muller Drive locality, three samples, also of alluvial origin (Williams and Jennings, 1977; Laboratory report, Soil Mechanics Division, 1971), were investigated from the Civic Centre locality. The depth is given as ca. 0,75 m (VCC1), 1,50 m (VCC2) and 3,75 m (VCC3). As the four samples from Vereeniging have a nearly identical mineral composition, only the results for sample VCC2 are presented.

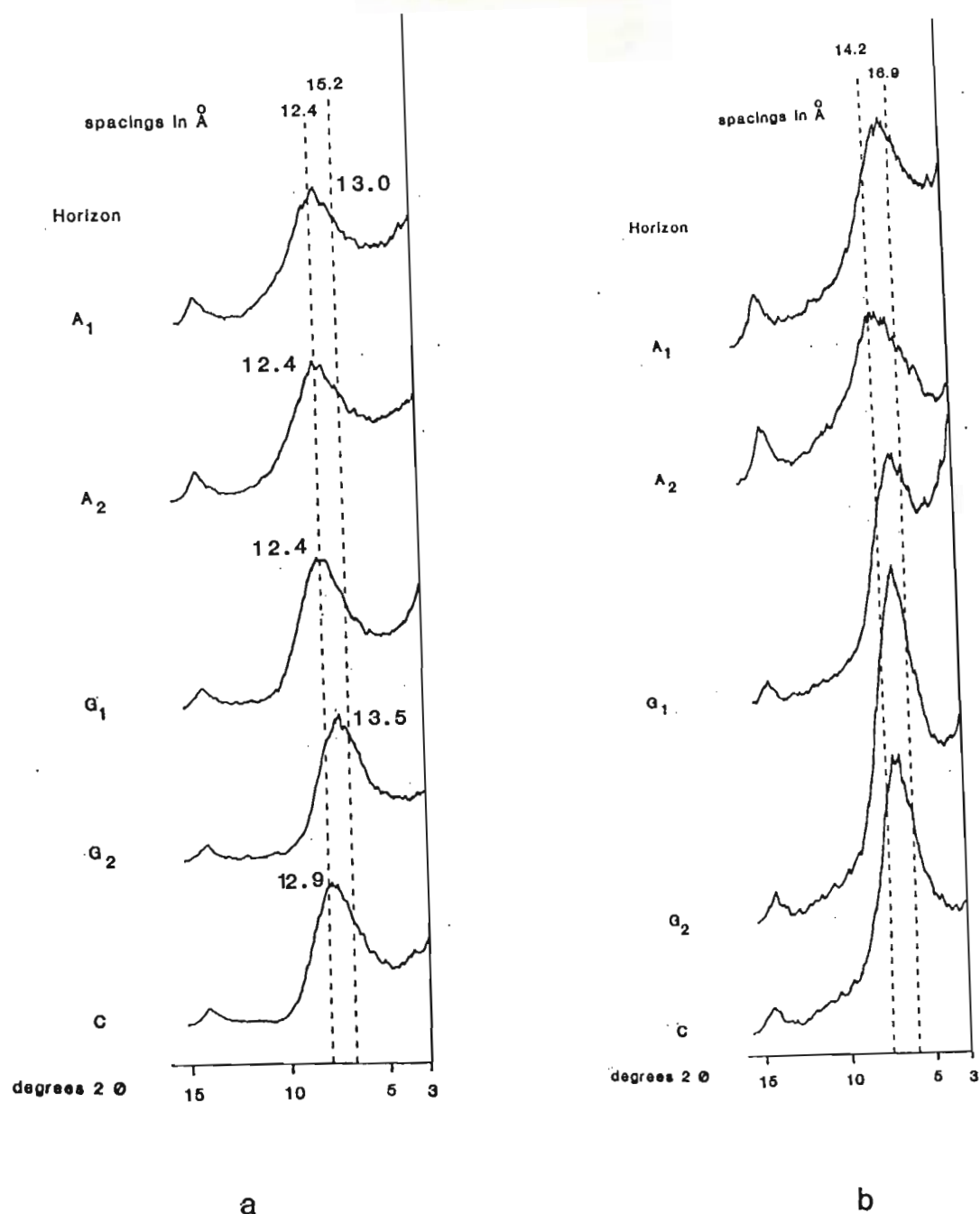


Figure 6.7 XRD traces of the various horizons of the Onderstepoort soil profile (oriented clay)

(a) K-saturated, air-dried (broken lines represent peak positions of discrete smectite, where the interlayer permits one water layer (12,4 Å) or two water layers (15,2 Å))

(b) K-saturated, 300°C, ethylene glycol solvated (broken lines represent peak positions, characteristic of ethylene glycol monolayers (14,2 Å) and bi-layers (16,9 Å))

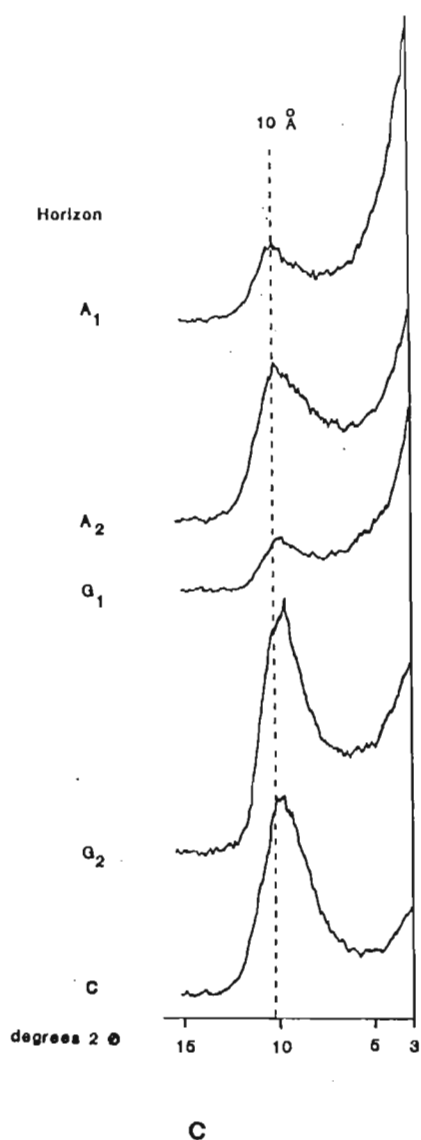


Figure 6.7 (c) XRD traces of the various horizons of the Onderstepoort soil profile (oriented clay), K-saturated and heated to 500°C (broken line represents peak position of smectite treated with K + 500°C)

(i) Whole soil

Quartz dominates the non-clay fraction with small amounts of plagioclase being detectable by means of XRD in all four samples.

(ii) Clay fraction

The $< 2 \mu\text{m}$ fraction is composed of smectite, kaolinite and mica. The smectite is characterized by a $15,2 \text{ \AA}$ peak in the Mg-saturated, air-dried pattern (water bi-layer) (Figure 6.8) and expansion to $16,9 \text{ \AA}$ upon ethylene glycol solvation. The rationality of the higher order reflections ($8,45 \text{ \AA} \times 2 = 16,9 \text{ \AA}$)

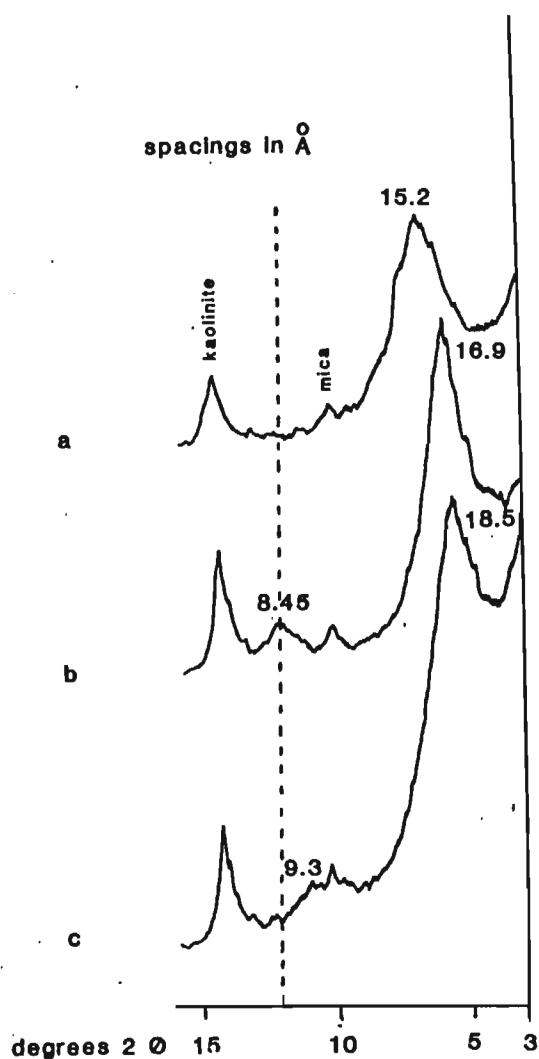


Figure 6.8 XRD traces of the Vereeniging (V_{CC2}) soil sample (oriented clay)

(a) Mg-saturated, air-dried

(b) Mg-saturated, ethylene glycol solvated

(c) Mg-saturated, glycerol solvated

(broken line represents peak position of discrete smectite treated with Mg + ethylene glycol)

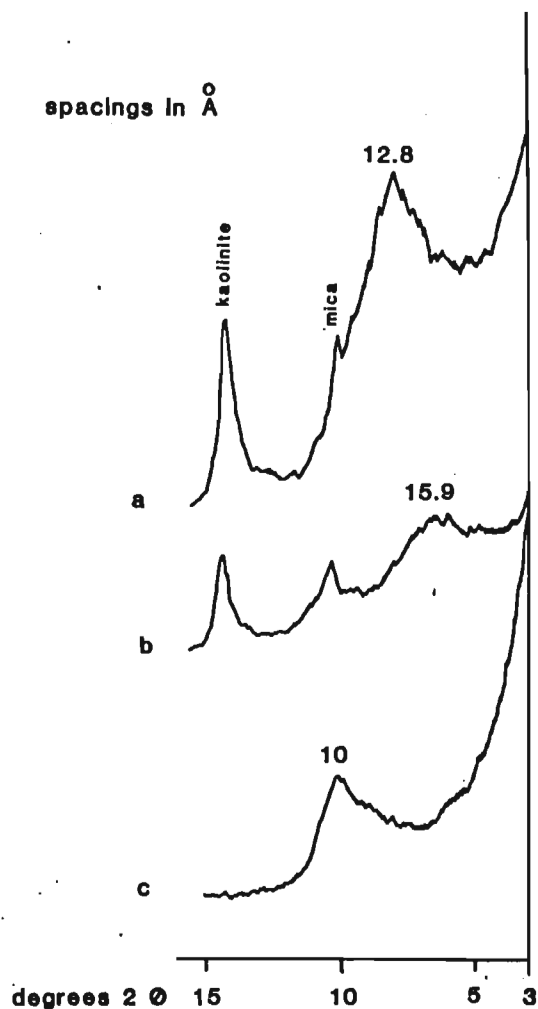


Figure 6.9 XRD traces of the Vereeniging (V_{CC2}) soil sample (oriented clay)

(a) K-saturated, air-dried

(b) K-saturated, 300°C, ethylene glycol solvated

(c) K-saturated, 500°C

indicates the absence of non-smectite interstratification components in this smectite (Figure 6.8). However expansion to as much as 18,5 Å upon glycerol solvation and the development of a shoulder at the low angle side of the peak points to some interstratification components which should be close to the smectite-vermiculite boundary, as they fully expand with ethylene glycol, but permit only a glycerol monolayer into their interlayer space (high charge beidellite, low charge vermiculite?) (Figure 6.8).

A peak position of 12,8 Å in the K-saturated, air-dried state indicates charge heterogeneity of the smectite (water monolayer-water double layer formation) (Figure 6.9), as does the expansion of the smectite structure to 15,9 Å after K-saturation, heating to 300°C and ethylene glycol solvation (ethylene glycol monolayer-bilayer formation) (Figure 6.9). The collapse of the structure to 10 Å after 500°C heating confirms the identification of the 2 : 1 layer silicate as smectite (Figure 6.9).

Charge heterogeneity within the smectite crystallites is also indicated from the Li-saturated, air-dried pattern by a peak position of 14,6 Å (water monolayer-bilayer complexes) (Figure 6.10). Interlayer water is expelled from the Li-saturated smectite upon heating to 280°C (Figure 6.10). Part of the interlayers re-expand when ethylene glycol solvated, but a peak position of 9,3 Å points to as much as 60% montmorillonite layers in the smectite crystallite (Figure 6.10), while the peak shape points to ca. 50%. Intercalation with dodecylammoniumchloride

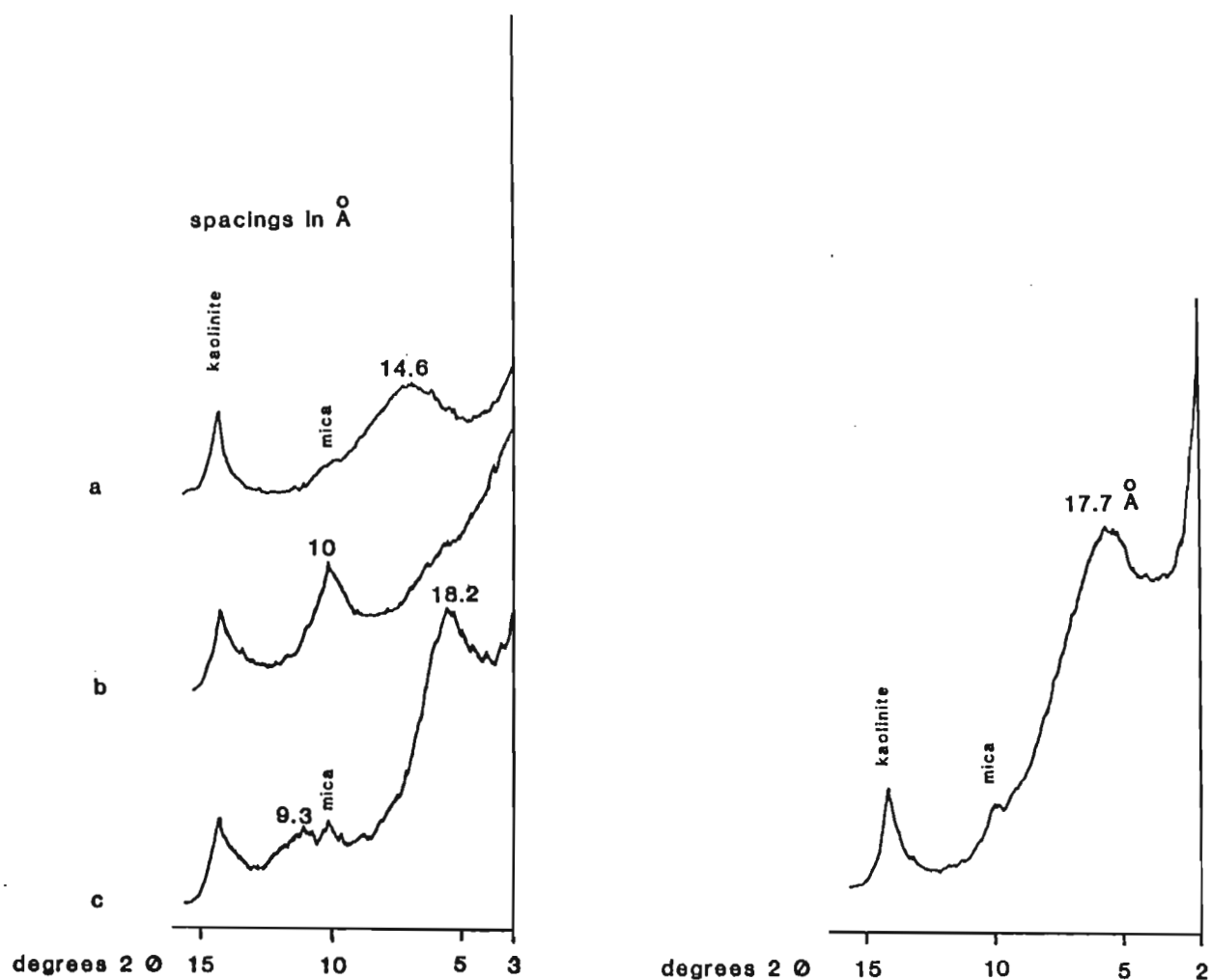


Figure 6.10 XRD traces of the Vereeniging VCC2 soil sample (oriented clay)

(a) Li-saturated, air-dried

(b) Li-saturated, 290°C

(c) Li-saturated, 280°C, ethylene glycol solvated

Figure 6.11 XRD traces of the Vereeniging VCC2 soil sample (oriented clay)

Dodecylammonium-chloride intercalated

results in a peak position of 17,7 Å, characteristic of beidellite, but the broad low angle shoulder points to a higher amount of non-beidellitic components (Figure 6.11).

The smectite component in the Vereeniging soil must therefore be regarded as discrete smectite with about equal amounts of beidellitic and montmorillonitic components, with part of the beidellite close to the smectite-vermiculite boundary.

The identification of the 7,3 Å mineral as kaolinite is confirmed by the collapse of the structure when heated to 500°C (Figure 6.9).

(c) Vredefort sample

The Vredefort sample is characterized as highly swelling (slickensides, cracks, etc). The sample is composed of the following minerals :

(i) Whole soil

Quartz and small amounts of plagioclase constitute the non-clay fraction.

(ii) Clay fraction

The < 2 µm fraction is dominated by smectite with a high degree of crystallinity. Kaolinite is present in trace quantities.

The Mg-saturated smectite can be characterized by a water double-layer in the air-dried state (Figure 6.12), an ethylene glycol double layer with rational second order reflections, indicating double layer formation in each of the interlayer regions of the

various smectite crystallites and thus proving the absence of any non-smectite interstratification components. However a 18,5 Å peak after glycerol solvation, which is slightly too high, indicates some interstratification components in the smectite, which fully expand with ethylene glycol, but form a glycerol monolayer (low charge vermiculite, high charge beidellite) (Figure 6.12).

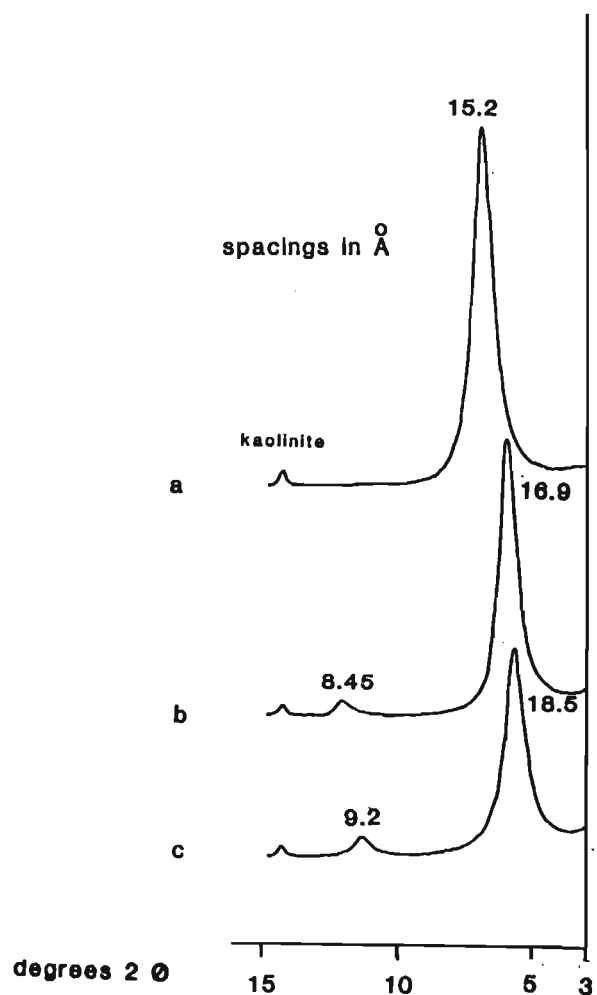


Figure 6.12

XRD traces of the Vredefort sample (oriented clay)

(a) Mg-saturated, air-dried

(b) Mg-saturated, ethylene glycol solvated

(c) Mg-saturated, glycerol solvated

A 12,4 Å peak in the K-saturated, air-dried pattern indicates the presence of water monolayers in each of the interlayer spaces of the smectite crystallites (Figure 6.13) and points to discrete beidellite as the smectite species (Machajdik and Cicel, 1981).

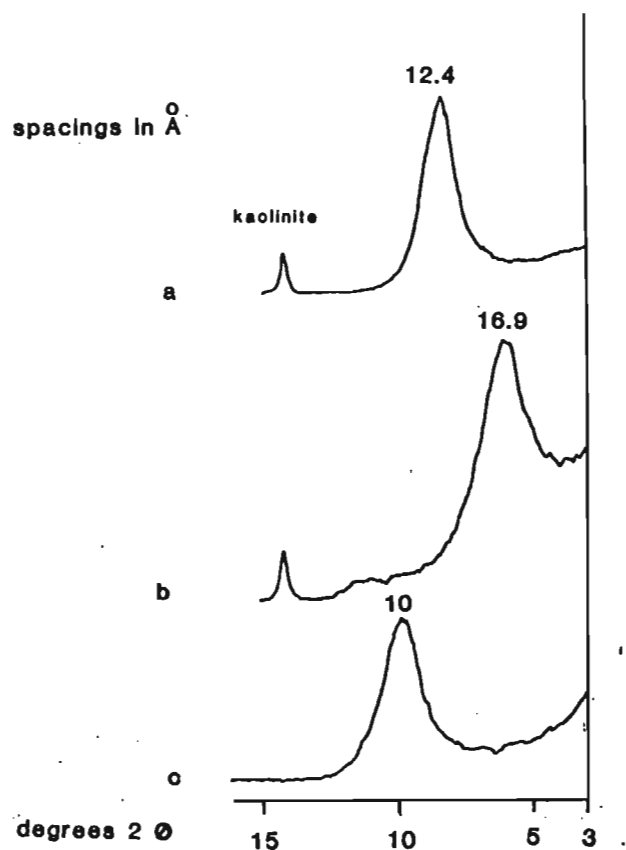


Figure 6.13

XRD traces of the Vredefort sample (oriented clay)
 (a) K-saturated, air-dried
 (b) K-saturated, 300°C, ethylene glycol solvated
 (c) K-saturated, 500°C

In contrast to this, the expansion of the K-saturated, 300°C sample to 16,9 Å is reported to be characteristic of montmorillonite (Schultz, 1969) (Figure 6.13). Heating the K-saturated sample to 500°C confirms the smectitic nature of the swelling 2 : 1 layer silicate and the absence of chloritic interstratification components due to the regular shape of the peak (Figure 6.13).

Li-saturation results in a broad peak with a maximum at 14,2 Å, indicating a charge heterogeneity of the smectite (Figure 6.14). The smectite structure collapses to 10 Å when heated to 280°C (Figure 6.14), with part of the interlayers re-expanding upon ethylene glycol solvation. A second order peak position of 9,1 Å points to approximately 50% montmorillonite layers (or better interlayers), as does the shape of the first peak at 18,4 Å (Figure 6.14).

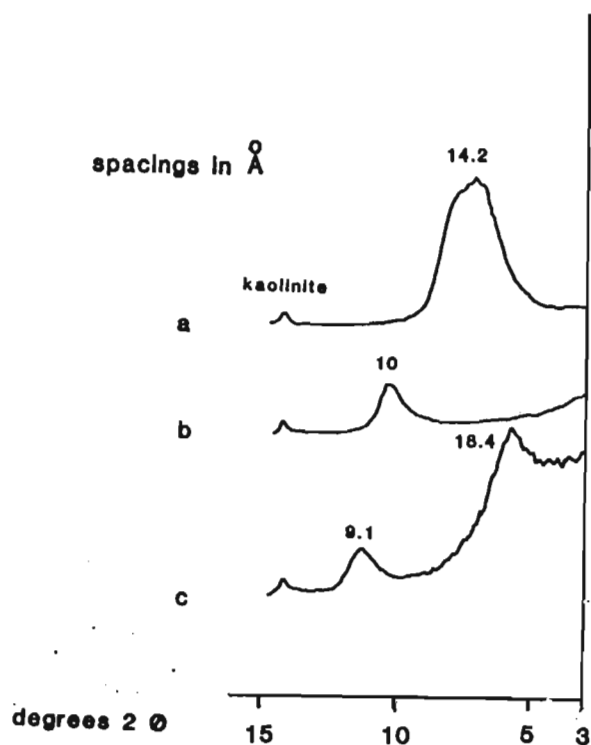


Figure 6.14

XRD traces of the Vredefort sample (oriented clay)

(a) Li-saturated, air-dried

(b) Li-saturated, 290°C

(c) Li-saturated, 290°C, ethylene glycol solvated

Intercalation with dodecylammoniumchloride results in a c₁₂ double layer formation, indicative of discrete beidellite (Lagaly et al., 1976) (Figure 6.15). The kaolinitic nature of the 7,3 Å mineral is confirmed by the absence of a 7 Å peak from the K-

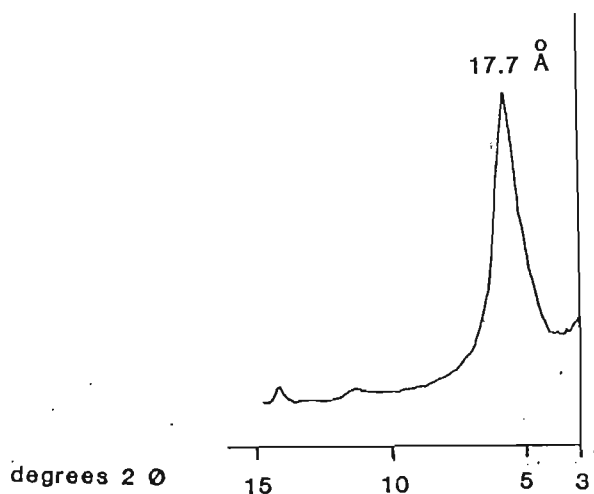


Figure 6.15 XRD trace of the Vredefort sample, intercalated with dodecylammoniumchloride (oriented clay)

saturated, 500°C pattern.

To summarize the results, the Vredefort sample is dominated by a discrete smectite with a high degree of crystallinity. Some treatments point to the identification of this smectite as discrete beidellite (water monolayer formation with K as interlayer cation, dodecylammoniumchloride bi-layer formation), while other treatments indicate montmorillonite-beidellite interstratifications (Greene-Kelly test, re-expansion to 16,9 Å with ethylene glycol after K-saturation and heating to 300°C).

6.3.1.2 Soils with a mica-smectite interstratification as the swelling component

(a) Kimberley

Samples have been provided from a depth of 3,50 - 3,75 m and 10,50 m. As the material at 3,50 - 3,75 cm depth consists of

varves, i.e. finely banded red and grey layers, the two different layers have been investigated separately and are reported as varves grey and varves red, respectively.

(i) Whole soil

The non-clay fraction consists of quartz, K-feldspar and plagioclase, quartz being by far the dominant mineral. The red varves also contain hematite.

(ii) Clay fraction

The $< 2 \text{ }\mu\text{m}$ fraction is dominated by a mica-smectite interstratification. Traces of kaolinite and mica are detected in the grey part of the varves and small amounts of kaolinite with traces of mica are found at the depth of 10,5 m.

The mica-smectite interstratification exhibits both random and ordered peak characteristics :

A 25 Å peak in the Mg-saturated, air-dried state of the red varves must be interpreted as a superlattice reflection ($10 \text{ Å} + 15 \text{ Å}$), as must a secondary peak position at 14 Å, which is too low for discrete Mg-saturated smectite (Figure 6.16), thus indicating an ordered structure. Expansion of the first order peak to 30,2 Å indicates the presence of a swelling component in this ordered interstratification. The absence of any detectable peak at 8,45 (002 smectite) and 5,63 Å (003 smectite) confirms the absence of any discrete smectite (Figure 6.16) despite a 16,9 Å peak in the Mg-saturated, ethylene glycol solvated pattern. A second order reflection at 9,34 Å and a third order reflection at 5,39 Å indicate mica-smectite interstratification with

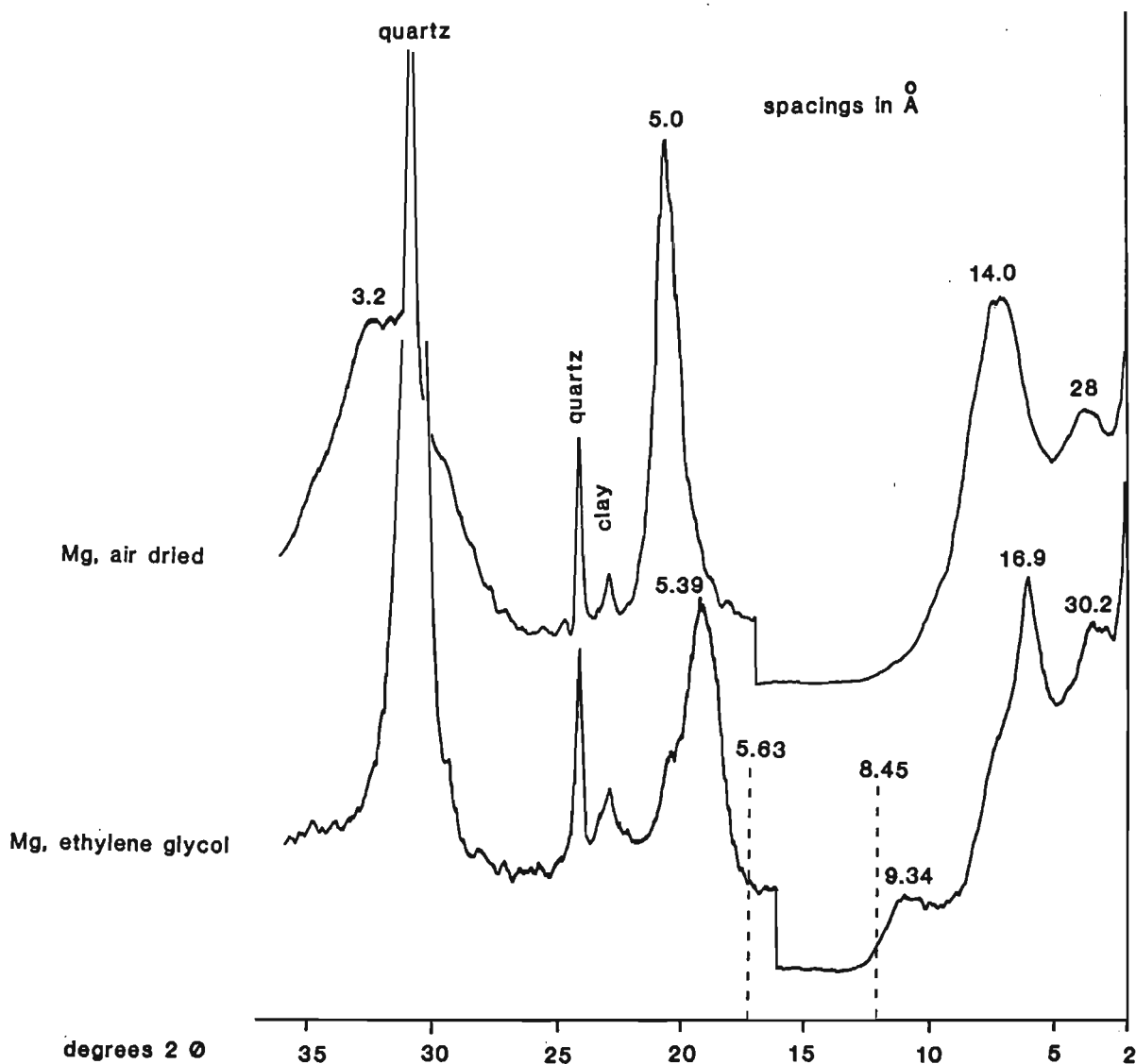


Figure 6.16 XRD traces of the red varve material from Kimberley (oriented clay)
(broken lines represent peak positions of discrete smectite, treated with Mg + ethylene glycol)
There is a scale change at $16^\circ 2\theta$.

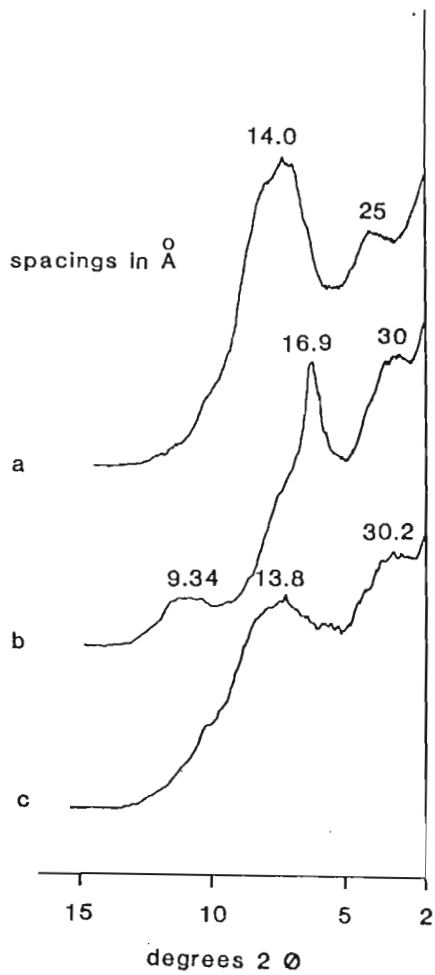
approximately 60% mica (Figure 6.16), both ordered and random.

Glycerol solvation expanded the first order peak to 30.2 \AA , but

the second order peak became broadened with a peak maximum of 13,8 Å (Figure 6.17). From this it must be concluded that a high proportion of interlayers permit only one glycerol layer and part of the swelling component must therefore be characterized as high charge beidellite or vermiculite (Figure 6.17). The grey varve material exhibits very similar expansion characteristics with respect to Mg-saturation and solvation with ethylene glycol and glycerol (Figure 6.17 ii). The mica-smectite interstratification from the depth at 10,5 m is less ordered, as indicated by the absence of a superlattice peak in the Mg-saturated, air-dried pattern and the very broad peak, bridging the > 10 Å region upon glycerol solvation (Figure 6.17 iii).

K-saturation resulted in a peak position of 11,2 Å in the air-dried state in all three samples. This position is characteristic of a 10 Å (mica, vermiculite) - 12,4 Å (beidellite) interstratification. A similar peak position characterizes the Kimberley sample, when the K-saturated interstratification is heated to 300°C and subsequently ethylene glycol solvated, with the exception that the 10 Å component increases in amount. Heating the K-saturated sample to 500°C resulted in collapse of the structure to 10 Å and the transformation of the kaolinite into metakaolinite. The absence of chlorite, either discrete or in an interstratification is also confirmed by the K, 500°C pattern (Figure 6.18 i, ii and iii).

Li-saturation results in a lower degree of ordering (probably through transformation of the ordered two-component interstrati-



iii

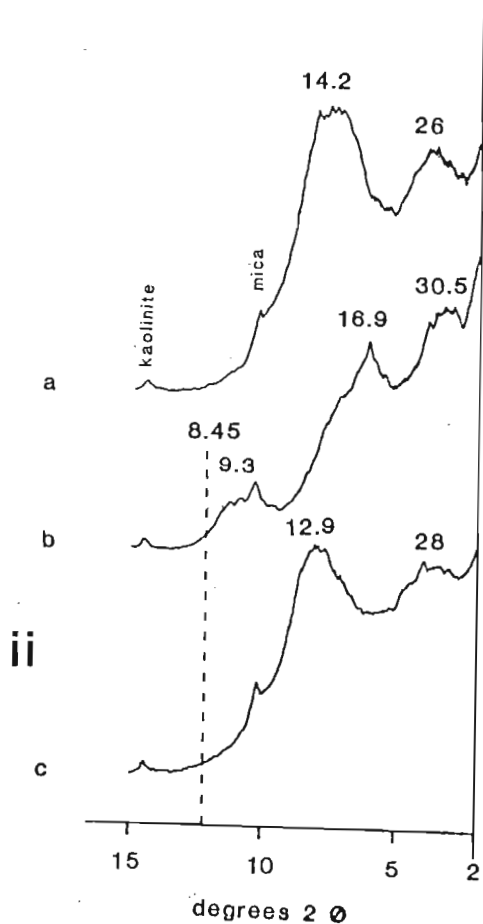
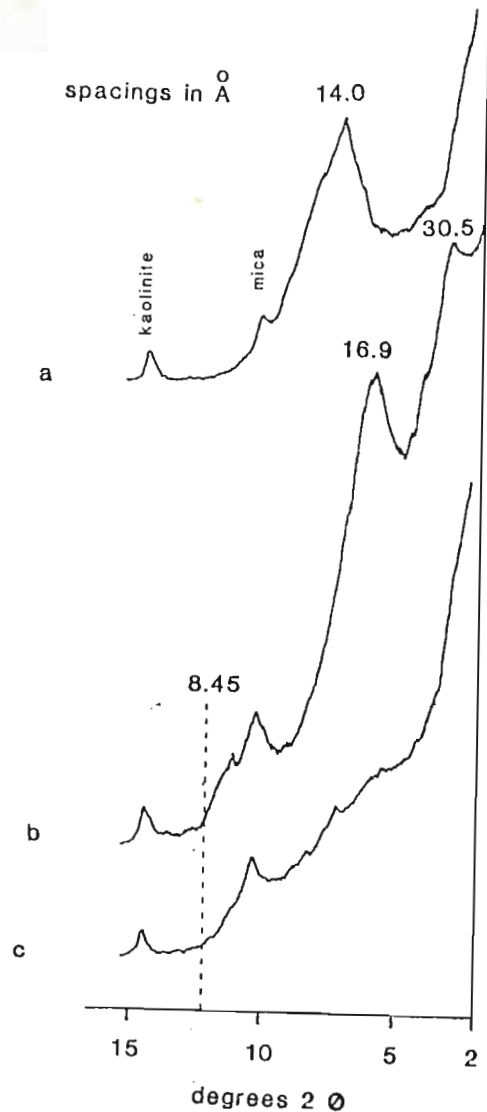


Figure 6.17

XRD traces of the Kimberley soil

(i) varves, red (3,50 - 3,75 m)

(ii) varves, grey (3,50 - 3,75 m)

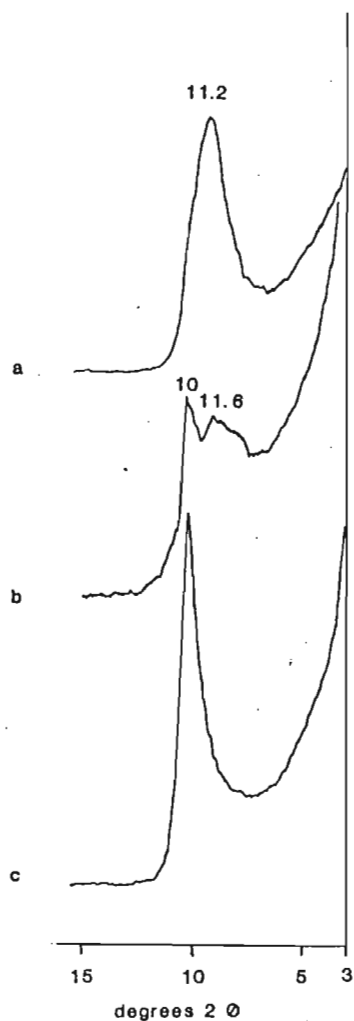
(iii) 10,50 - 10,75 m

(a) Mg-saturated, air-dried

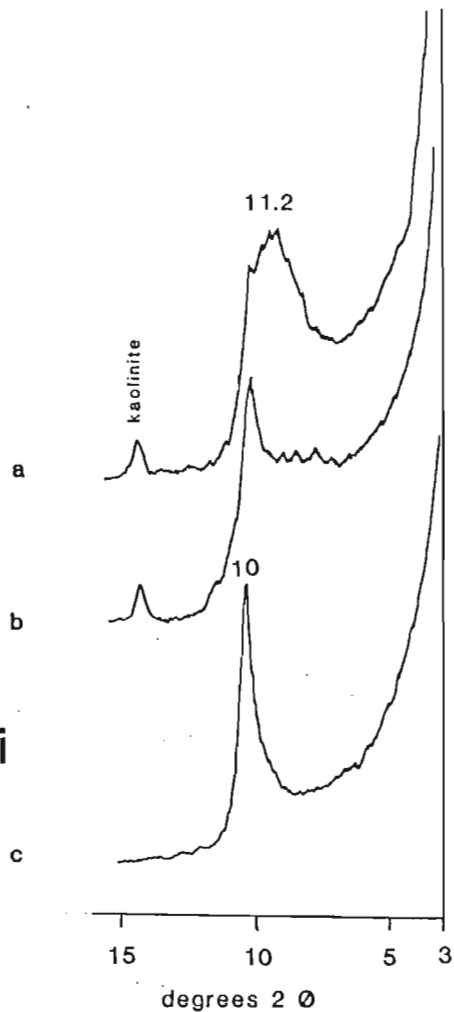
(b) Mg-saturated, ethylene glycol solvated

(c) Mg-saturated, glycerol solvated

i



iii



ii

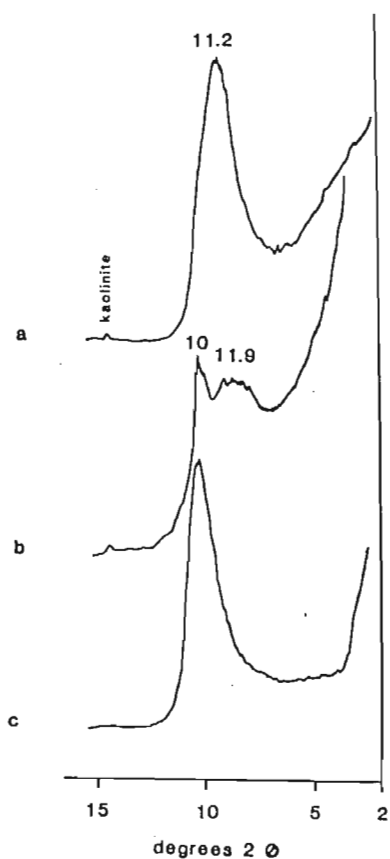


Figure 6.18

XRD traces of the
Kimberley soil
(i) varves, red
(3,50 - 3,75 m)
(ii) varves, grey
(3,50 - 3,75 m)
(iii) 10,50 - 10,75 m

(a) K-saturated,
air-dried
(b) K-saturated,
300°C, ethylene gly-
col solvated
(c) K-saturated,
500°C

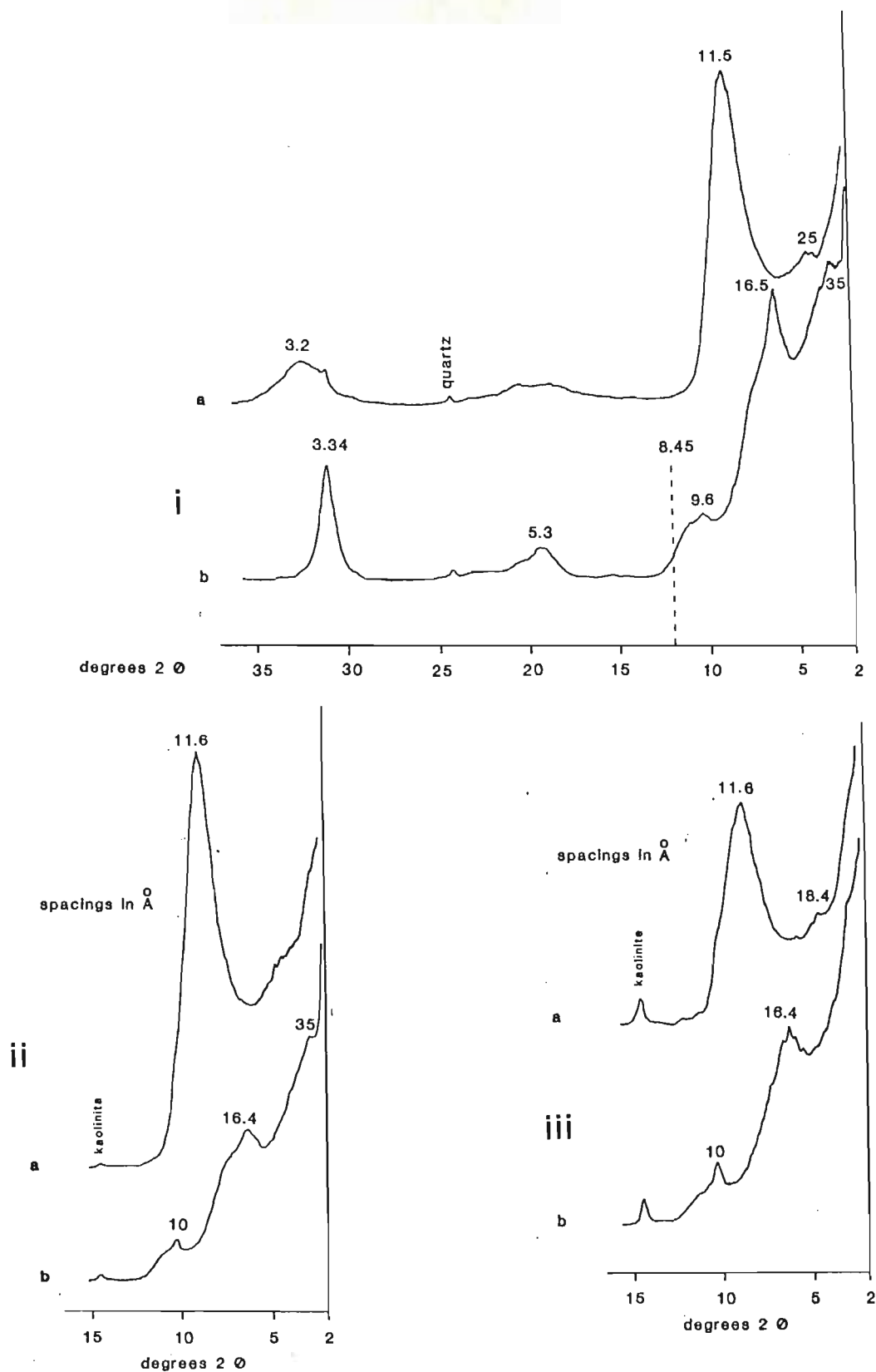


Figure 6.19 XRD traces of the Kimberley soil (oriented clay)

- (i) varves, red (3,50 - 3,75 m)
- (ii) varves, grey (3,50 - 3,75 m)
- (iii) 10,50 - 10,75 m
- (a) Li-saturated, air-dried
- (b) Li-saturated, 280°C, ethylene glycol solvated

fication into a three-component 10 Å - 12,4 Å - 15,2 Å interstratification) as indicated by the decrease of the first peak. A peak position in the Li-saturated, air-dried state of 11,5 - 11,6 Å is too low for discrete smectite or vermiculite and can only be explained as a 10 Å - 12,4 Å interstratification. The application of the Greene-Kelly test led to an increase of the characteristic 001 mica - 002 smectite peak position from 9,34 Å (65% 10 Å layer) to 9,6 Å (85% 10 Å layer), the difference (20%) accounting for montmorillonite (Figure 6.19).

Intercalation with dodecylammoniumchloride also confirms the presence of an ordered mica-beidellite interstratification by a peak position of 28 Å (10 Å + 17,7 Å), plus a randomly interstratified beidellite-mica interstratification with some non-beidellitic components (vermiculite?), leading to an increase in the peak position from 17,7 Å to 18,4 Å (Figure 6.20).

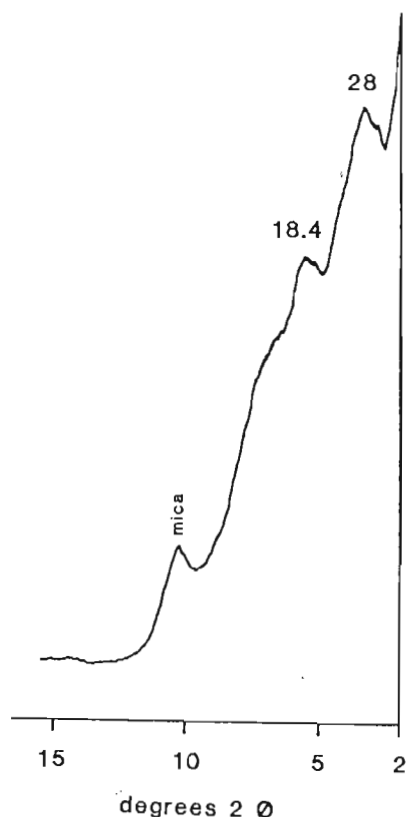


Figure 6.20

XRD trace of the Kimberley red varves, dodecylammoniumchloride intercalated (oriented clay) spacings in Å

(b) Kriel Vertisol

The soil sample from Kriel must be regarded as containing one of the most highly swelling clay components investigated, as it is characterized by a strong hydrogel-forming capacity (thixotropic clay) despite a clay content below 40%.

(i) Whole soil

The non-clay mineral fraction is dominated by quartz with smaller amounts of K-feldspar and plagioclase also present.

(ii) Clay fraction

The < 2 μm fraction contains a mica-smectite interstratification as swelling component, ca. 30% discrete mica and traces of kaolinite.

The interstratification is characterized by a peak position of 16,9 \AA in the Mg-saturated, air-dried state and a peak shape closely resembling that of a random mica-smectite interstratification with approximately 50% mica (Figure 6.21). The shape of the peak remains approximately the same when the Mg-saturated clay is ethylene glycol solvated, indicating the presence of two components only. The absence of a peak at 8,45 \AA indicates the absence of any discrete smectite in this soil sample (Figure 6.21).

Expansion to above 18 \AA upon glycerol solvation permits the identification of the swelling component as smectite (Figure 6.21). K-saturation leads to the elimination of a discrete

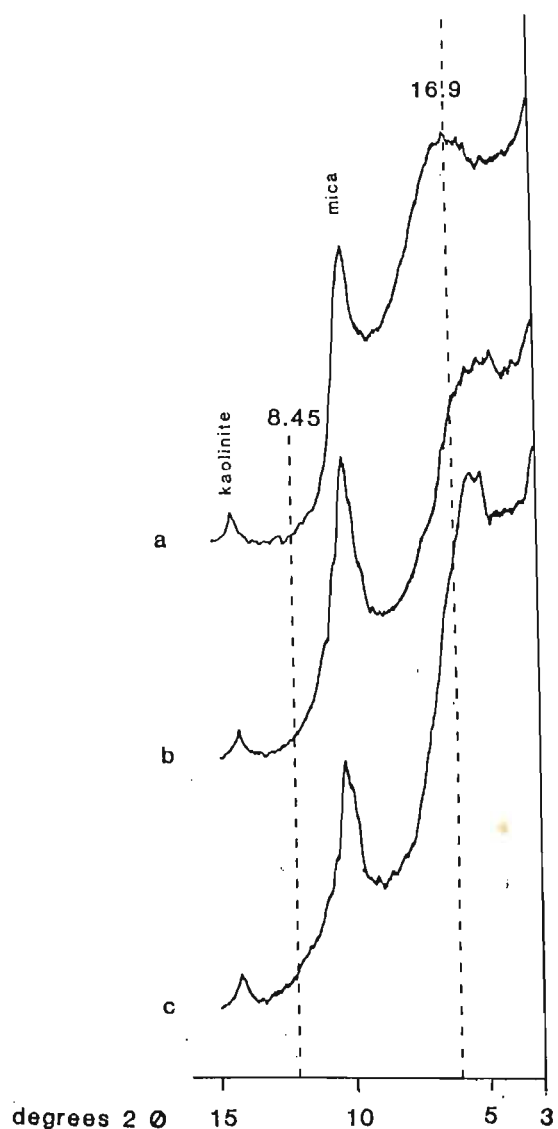


Figure 6.21

XRD traces of the soil sample from Kriel (oriented specimen)

(a) Mg-saturated, air-dried

(b) Mg-saturated, ethylene glycol solvated

(c) Mg-saturated, glycerol solvated

(broken lines represent peak positions of discrete smectite, treated with Mg + ethylene glycol)

peak in the air-dried state probably due to the transformation of the two-component interstratification into a three-component 10 Å - 12,4 Å - 15,2 Å interstratification (Figure 6.22). Heating to 500°C results in a 10 Å peak with a small shoulder at the low angle side, indicative of small amounts of a chloritic and/or kaolinitic interstratification component (Figure 6.22).

A 14,5 Å peak in the Li-saturated, air-dried pattern indicates a

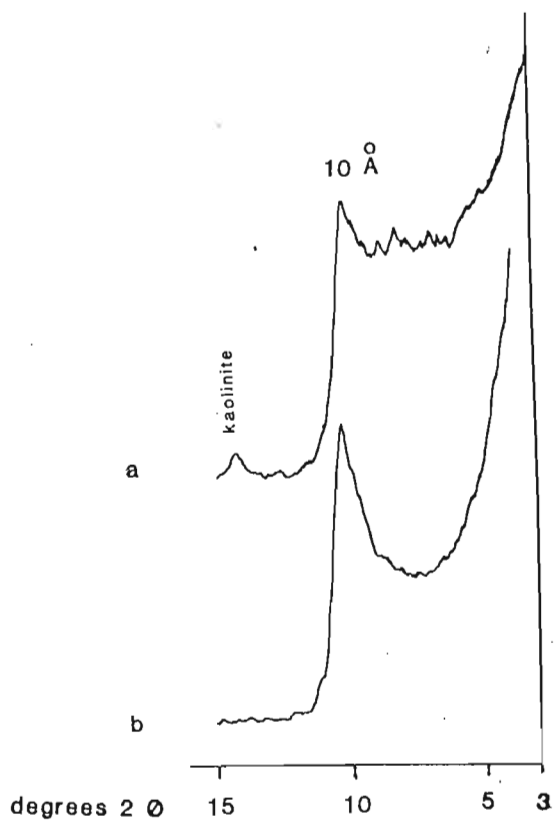


Figure 6.22

XRD traces of the soil sample from Kriel (oriented clay)

(a) K-saturated, air-dried

(b) K-saturated, 500°C

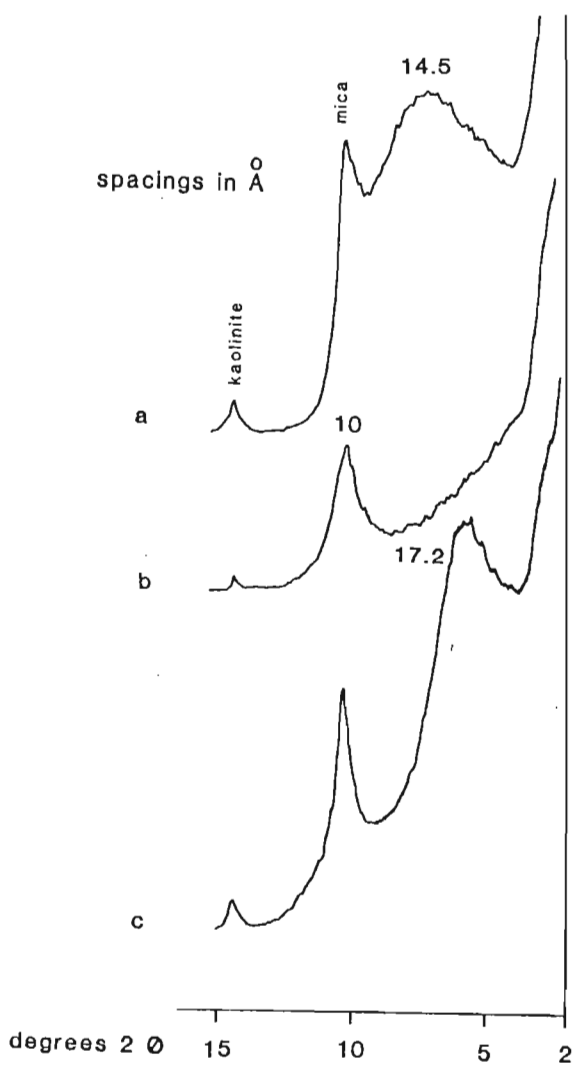


Figure 6.23

XRD traces of the soil sample from Kriel (oriented clay)

(a) Li-saturated, air-dried

(b) Li-saturated, 280°C

(c) Li-saturated, 280°C, ethylene glycol solvated

high amount of water-double layer units (Figure 6.23). From the shape of the peak after heating the Li-saturated sample to 280°C and consequent ethylene glycol solvation (Greene-Kelly test), an increase in the amount of the 10 Å layers cannot be worked out due to the similarity of the shape of the peak compared with that of the Mg-saturated, ethylene glycol solvated sample.

Dodecylammoniumchloride intercalation also leads to a decrease in the degree of crystallinity of the interstratification, probably due to the transformation of the two-component interstratification into a three-component interstratification (10 Å - 13,6 Å - 17,7 Å) or (10 Å - 17,7 Å - 22 Å) (Figure 6.24), the expansion to > 18 Å indicating beidellite as major smectite component.

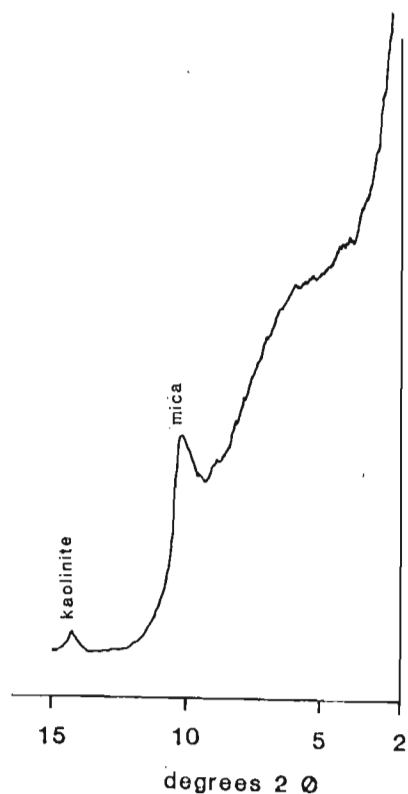


Figure 6.24
XRD traces of the
soil sample from
Kriel (oriented
clay) after dodecyl-
ammoniumchloride
intercalation

It can be concluded that the swelling component in the sample

from Kriel is identical to a random mica-smectite interstratification with about equal amounts of each component. The smectite species involved is more probably a beidellite than a montmorillonite.

(c) Cape Town

The soil from the Girl Guide hall at Cape Town differs from the rest of the highly swelling soils that have been described above by the presence of the swelling component in the $> 2 \mu\text{m}$ fraction only. The clay fraction is characterized by the absence of any appreciable amount of swelling material.

(i) Whole soil

The whole-soil XRD pattern is dominated by quartz. Small amounts of well crystallized hematite and goethite are also detectable. Kaolinite, mica and an ordered mica-vermiculite or mica-beidellite interstratification are the main clay components in the whole-soil fraction (Figure 6.25). The ordered mica-vermiculite(?) - beidellite(?) interstratification is characterized by a superlattice reflection at about 24 \AA in the Mg-saturated, air-dried state with a secondary reflection of $11,3 \text{ \AA}$, i.e. a peak position between that of discrete vermiculite/beidellite (ca. 15 \AA) and discrete mica (10 \AA) (Figure 6.25). Both positions are typical of ordered structures. Solvation of the Mg-saturated interstratification with glycerol leads to no increase in the basal spacings, indicating vermiculite as interstratification component (Figure 6.25). Solvation with ethylene glycol on the other hand, results in an expansion of the

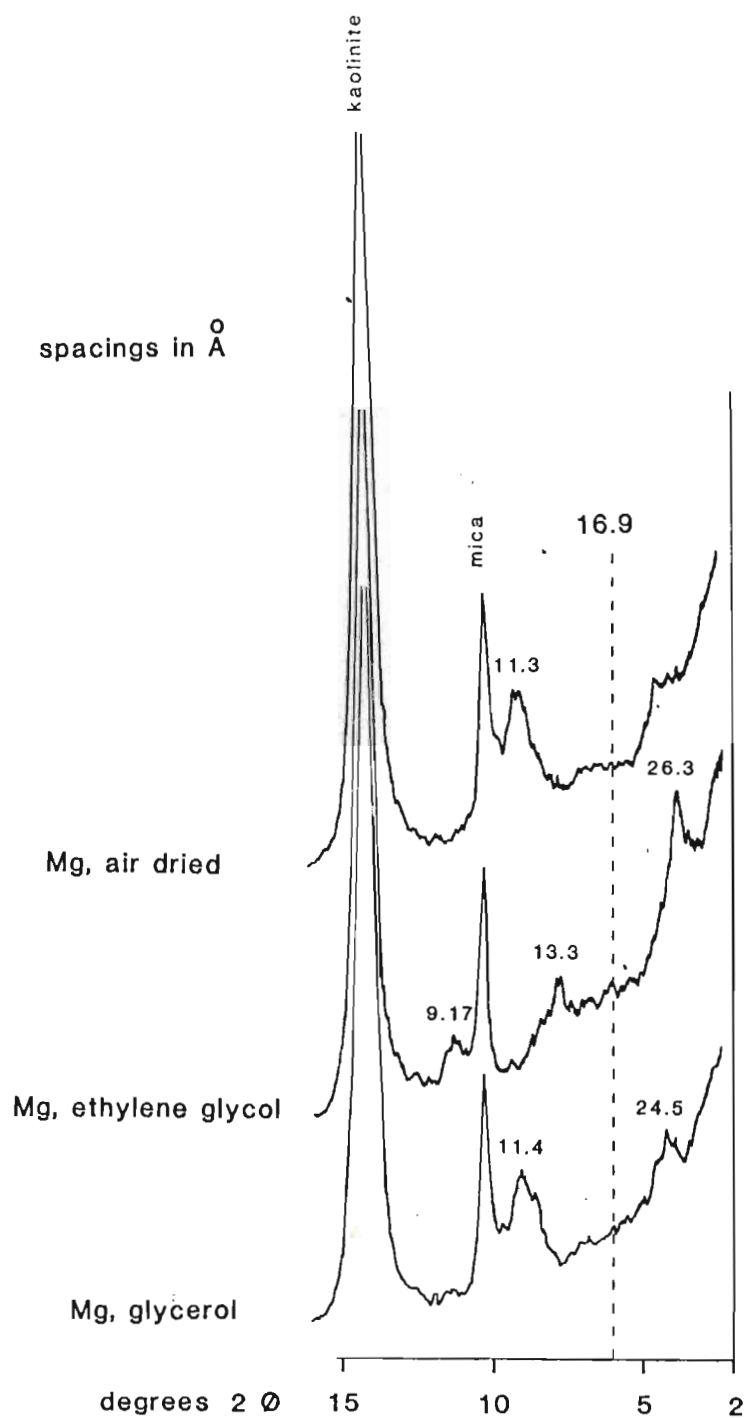


Figure 6.25 XRD traces of the soil sample from Cape Town (whole soil smear) (broken line represents peak positions of discrete smectite, treated with Mg + ethylene glycol)

structure to 26,3, 13,3 and 9,17 Å and points to beidellite as the second component. The near rational higher order reflections and the peak position at 9,17 Å indicate approximately equal amounts of mica and smectite or vermiculite (Figure 6.25).

(ii) Clay fraction

Kaolinite and mica are by far the dominant components of the < 2 µm fraction of the Cape Town soil (Figure 6.26).

A very small and broad 16,9 Å reflection is observed in the Mg-saturated, ethylene glycol solvated pattern. The absence of any smectite peak in the Mg-saturated, air-dried and glycerol solvated pattern (Figure 6.26) points to the presence of random interstratification with about 30% smectite in this clay sample. Random mica (70%) - smectite (30%) interstratifications are characterized by a peak position of 10 Å in the air-dried state and a segregation into smectite (16,9 Å) and mica peaks upon solvation with ethylene glycol. K-saturation of the whole soil sample led to collapse of the structure to nearly 10 Å, pointing to vermiculite as an interstratification component.

To summarize the results, the swelling component in the Cape Town soil sample is either a mica-vermiculite or mica-beidellite interstratification. It is enriched in the non-clay fraction and may therefore be regarded as an early weathering product of mica.

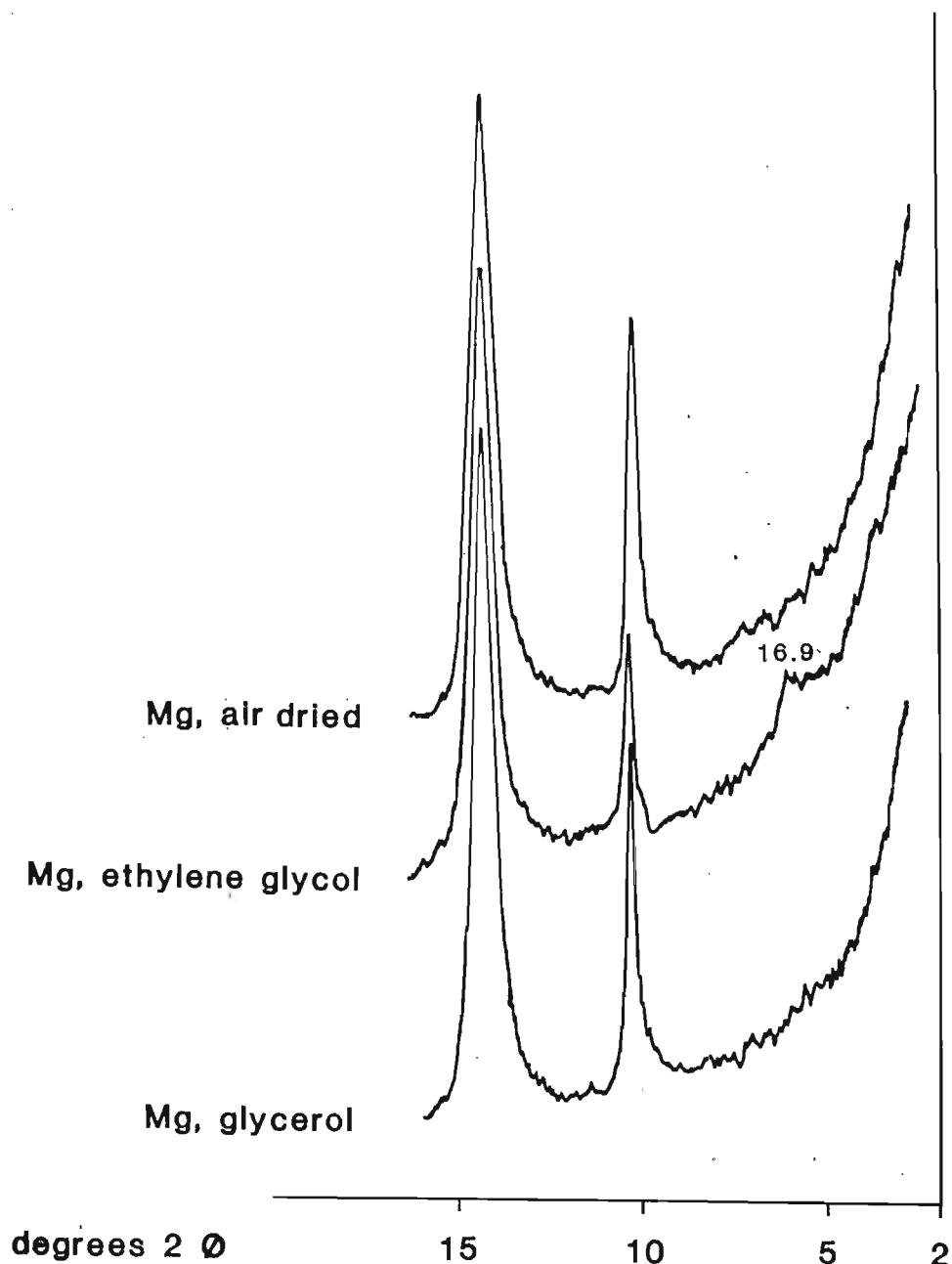


Figure 6.26 XRD traces of the soil sample from Cape Town
(oriented clay)

6.3.2 Major elements chemical analyses

Major elements chemical analyses, performed on the $< 2 \mu\text{m}$ fraction after iron removal (Na-CBD) and Li-saturation confirms results obtained from investigation of the clay mineralogy (Table 6.4).

(a) Smectite dominated soils

The absence of a micaceous interstratification component or of discrete mica is indicated by the low K_2O values in the case of the Onderstepoort and Vredefort samples. Small amounts of discrete mica, detected in the Vereeniging samples, are confirmed by low K_2O values in these soils.

(b) Mica-smectite interstratification as swelling component

The mica-smectite interstratification in the samples from Kimberley, which contain ca. 55 - 60% mica, as measured from second order peak positions, gives K_2O values of 3,5 to 4%. These values are too low for a micaceous layer charge of 1 (10% K) in the 10 Å layers and point to an illitic species, interstratified with the swelling component.

The presence of discrete mica as well as mica-smectite-vermiculite interstratification finds its expression in K_2O values of 5,11% for the Kriel soil sample and 3,83% for the Cape Town material. The presence of discrete mica renders the confirmation of the clay composition difficult.

The iron content of ca. 10% Fe_2O_3 in the soils, where discrete smectite dominates the clay fraction, is generally much higher than the Fe values of 2,15 - 2,75% Fe_2O_3 , reported for commercial bentonite deposits from Japan, Germany and America (Vogt and Köster, 1978), while the Mg values are similar to those reported for commercial bentonites.

Table 6.4 Total chemical analyses of the < 2 μ m fraction (deferrated, Li-saturated) of soils which exhibit a strong swelling capacity

	SiO ₂	Al ₂ O ₃	Fe ₂ O ₃	FeO	MnO	MgO	CaO	Na ₂ O	K ₂ O	TiO ₂	P ₂ O ₅	Loss ignition (H ₂ O-)
Onderstepoort A ₁	63,10	20,21	9,01	1,09	0,02	2,21	0,98	0,10	0,10	1,50	0,04	20,10
A ₂	63,09	18,86	8,99	1,11	0,01	1,98	1,49	0,00	0,09	1,41	0,05	19,96
G ₁	61,09	23,85	9,23	1,13	0,06	2,67	0,21	0,02	0,20	1,01	0,09	20,83
G ₂	62,03	21,87	9,06	1,12	0,03	3,23	0,28	0,00	0,11	0,49	0,01	21,19
C	59,04	23,68	11,71	1,45	0,09	2,07	0,22	0,14	0,08	0,64	0,67	21,71
Vereeniging CC ₂	61,09	23,85	9,17	1,13	0,06	1,67	0,24	0,12	1,20	0,98	0,04	17,75
BMD (Na-sat!)	57,98	25,13	9,14	1,13	0,03	1,71	0,39	2,37	0,81	0,95	0,03	18,25
Vredefort	60,95	26,53	4,98	1,07	0,14	3,68	0,47	0,13	0,21	0,82	0,01	20,93
Kimberley Var _{red}	63,24	25,66	2,83	0,35	0,01	2,23	0,19	0,12	3,49	0,84	0,08	12,80
Var _{grey}	63,18	26,06	1,86	0,23	0,01	2,45	0,51	0,48	4,08	0,78	0,04	12,25
10,50 - 10,75 m	63,25	25,98	2,05	0,51	0,02	2,39	0,40	0,21	3,98	0,97	0,04	12,60
Kriel	61,65	17,96	8,43	1,04	0,03	3,73	0,35	0,43	5,11	0,79	0,12	16,39
Cape Town	55,87	31,98	5,41	0,98	0,02	1,62	0,12	0,21	3,11	0,40	0,01	10,31

Small amounts of Ca may indicate some CaCO_3 in the sample while Ca, Na and/or K values may also be derived from traces of feldspar, the amount being too low to be detected by means of XRD.

6.3.3 Measure of expansiveness

(a) The plasticity index values

The whole soil sample was used for the determination of the volume change. The following values were obtained :

Table 6.5 PI values

	PI%	
Onderstepoort A ₁	37) high swelling
A ₂	45	
G ₁	57	very high swelling
G ₂	42) high swelling
C	49	
Vereeniging CC ₂	38	high swelling
BMD	!!77,1	very high swelling
Vredefort	48	high swelling
Kimberley Varred	35) high swelling
Vargrey	44,1	
10,50 - 10,75	48,5	high swelling
Kriel	!!83	very high swelling
Cape Town	17,5	low swelling

The PI values, being a measure of expansiveness, confirm the classification of the soils as highly expansive, except for the Cape Town soil, which is reported to be moderately expansive, but

is characterized by PI values < 25 , i.e. as low swelling. The Kimberley samples, on the other hand, having also been reported as moderately swelling, are highly swelling in terms of the PI values.

(b) Magnitude of expansion of the clay fraction

The final volume values of 100 mg freeze-dried, Na-saturated clay, dispersed in 25 ml of a NaCl (1,0 M and 0,04 M) and a CaCl_2 (0,05 M) salt solution are given in Table 6.6. The final volume in the Na solution has been reached after approximately three weeks.

Table 6.6 Magnitude of expansion

	1,0 M NaCl (cm ³)	0,04 M NaCl (cm ³)	0,5 M CaCl_2 (cm ³)
Onderstepoort A ₁	9,0	9,0	1,95
A ₂	10,2	9,8	2,0
G ₁	9,40	9,35	2,35
G ₂	9,25	9,30	2,35
C	9,80	10,15	2,85
Vereeniging CC ₂	8,45	9,05	3,05
BMD	8,55	8,65	2,70
Vredefort	8,00	8,50	3,05
Kimberley Var _{red}	5,55	6,20	1,95
Var _{grey}	5,65	5,60	2,00
10,50 - 10,75 m	5,20	4,85	3,05
Kriel	7,10	8,00	2,75
Cape Town	5,25	4,85	1,70

As the final volume for the Na-saturated clay in a NaCl solution is approximately 4 cm³, compared with no more than 2,5 cm³ in a CaCl₂ solution, all soil samples investigated belong to the highly swelling type (Egashira and Ohtsubo, 1983).

6.3.4 Infrared spectroscopy

Infrared investigations prove the absence of any nontronite by the absence of a main vibration band in the 487 - 495 cm⁻¹ wave number range. A weak AlFeOH adsorption near 885 cm⁻¹ confirms structural iron in octahedral positions (Figure 6.24), except for the Kimberley sample, where the amount of structural iron is very low. Except for the AlFeOH band, the IR spectra resemble those of kaolinite more closely than those of montmorillonite or interstratifications, despite the low kaolinite content compared with smectite or interstratifications.

6.4 Conclusions

Highly swelling soils from six different localities have been investigated. The soil material from three localities (Onderstepoort, Vereeniging and Vredefort, but also the group 1 soils from Tutuka and the Rensburg soil from Ixopo) contain smectite as the dominant clay mineral, which provides a logical answer to the high expansion capacity of these soils as indicated experimentally by their engineering behaviour and empirically by plasticity index (Table 6.5) and volume expansion (Table 6.6) values. The smectite species involved is most probably

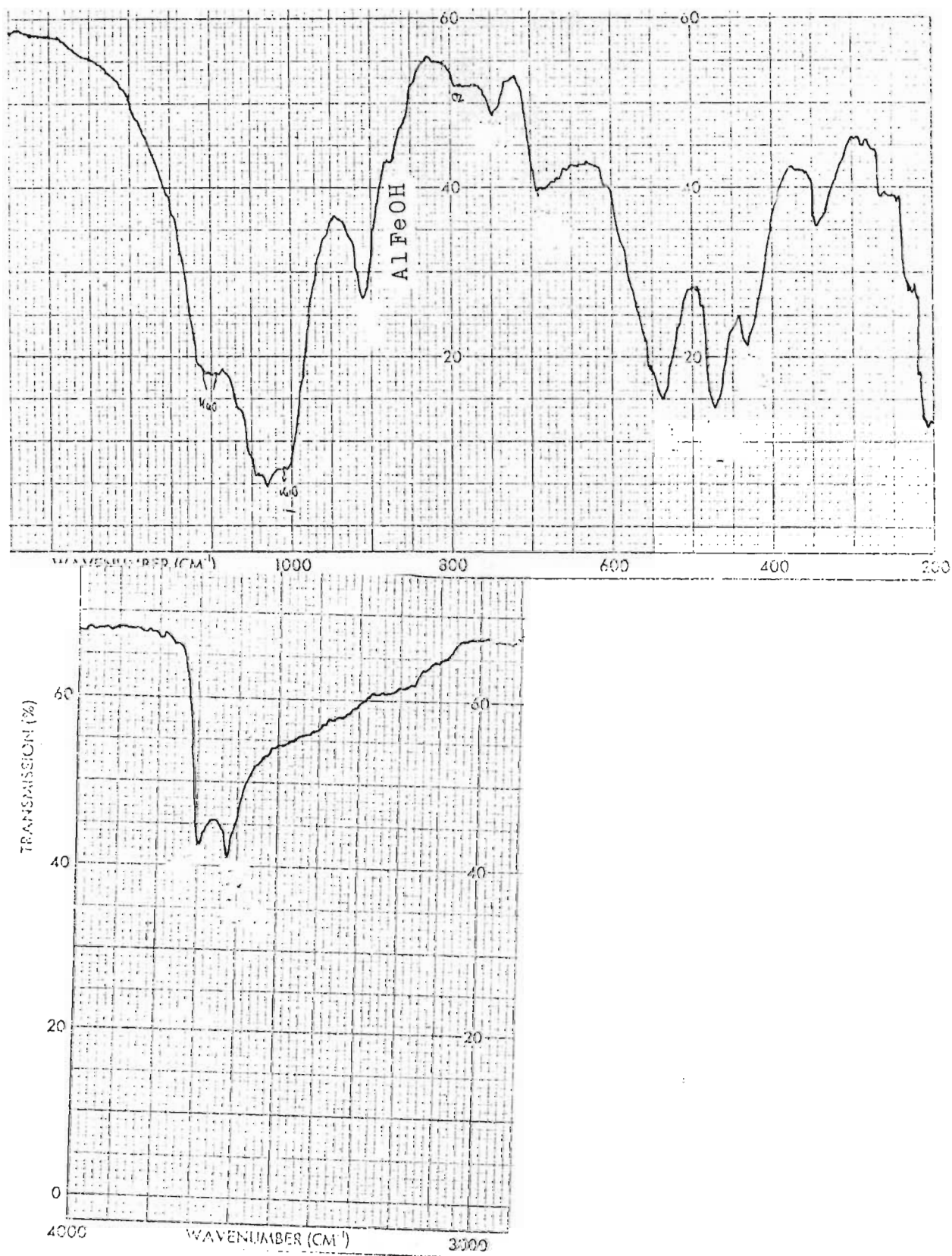


Figure 6.24 IR spectrum of the Vereeniging CC₂ soil

beidellite, but different methods do not yield identical results. The minerals of the smectite group can be characterized by a heterogeneous charge distribution, a prerequisite for high swelling capacity, as it renders the clay independent of the salt concentration of the soil solution (Lagaly et al., 1972) by overcoming the energy barrier to particle coagulation. Soils from the remaining three localities do not contain any discrete smectite detectable by XRD. The clay fraction of these soils is composed of a mica-beidellite or mica-vermiculite interstratification in two cases (Kimberley, Cape Town) and a mica-low charge smectite interstratification in the case of the Kriel soil. The interstratification was random in the Kriel soil, ordered in the Cape Town material and both random and ordered in the Kimberley varves. The group 2 soil from Tutuka may also be placed into this group.

The highly swelling soils are characteristic in two respects:

- (a) in the grain size distribution pattern. The percentage of fine clay is remarkably high in the smectite-dominated soil, reaching values up to 95% of the clay fraction (Appendix 19). According to Theng (1979) and Vogt and Köster (1978), a high proportion of fine clay is necessary for a soil to exhibit hydrogel-forming, and thus a very high swelling, capacity.
- (b) in the Fe : Mn ratio of the Na-DCB extract. The Fe : Mn ratio varies between 10 : 1 for the soil group (a) and ranges below 450 : 1 in the soil group (b). A ratio of several 1 000 : 1 is commonly found in Natal soils (Fitzpatrick, 1978). It is

well possible that this high Mn content not only reflects environmental conditions prevailing during the formation of these soils but that the Mn oxy-hydroxides exert an influence on the formation of a highly swelling clay (Fe-rich!) by aiding electron transfer reactions during oxidation and/or reduction processes, common in G horizons. In any case, the most highly swelling soils are characterized by a low Fe : Mn value in the Na-DCB extract (Appendix 19).

When comparing the clay mineral characteristics necessary for a high swelling capacity (Table 6.2) with the results obtained from the investigation of the clay fraction of the soils described in Chapter 6, the clay minerals tend to exhibit osmotic swelling due to the following structural features :

- Al as dominant ion in octahedral position;
- dioctahedral structure;
- Fe³⁺ in excess of Fe²⁺;
- small particle size;
- charge heterogeneity (either from one smectite layer to the next or as mica-swelling clay interstratification).

A position between intracrystalline and osmotic swelling is indicated by :

- tetrahedral substitutions (beidellite as dominant smectite species;
- interstratification of mica with a swelling component close to the vermiculite-smectite boundary);
- clay group/species (beidellite rather than montmorillonite, vermiculite/beidellite as interstratification component).

REFERENCES

- Alexiades, C.A. and Jackson, M.L., 1965. Quantitative determination of vermiculite in soils. *Soil Sci. Soc. Am. Proc.* 29, 522-527.
- Alietti, A. and Mejsner, J., 1980. Structure of a talc-saponite mixed layer mineral. *Clays Clay Min.* 28, 388-390.
- Aomine, A. and Wada, K., 1962. Differential weathering of volcanic ash and pumice, resulting in formation of hydrated halloysite. *Am. Min.* 47, 1024-1048.
- Bagin, V.I., Gendler, T.S., Dainyak, L.G. and Kuznin, R.N., 1980. Mössbauer, thermomagnetic and X-ray study of cation ordering in high-temperature decomposition in biotite. *Clays Clay Min.* 28, 188-196.
- Bailey, S.W., 1975. Chlorites. In Gieseking, J.E. (ed.) *Soil components, Vol. 2, Inorganic Components.* Springer, New York, pp.191-263.
- Bailey, S.W., 1980. Summary of recommendations of AIPEA nomenclature committee. *Clays Clay Min.* 28, 73-78.
- Bailey, S.W., 1982. Nomenclature for regular interstratifications. *Clay Min.* 17, 243-248.
- Bailey, S.W., Brindley, G.W., Fanning, D.S., Kodama, H. and Martin, R.T., 1984. Comment: Report on the clay mineral society nomenclature committee for 1982 and 1983. *Clays Clay Min.* 32, 239-240.
- Bajwa, M.I., 1981. Soil beidellite and its relation to problems of potassium fertility and poor response to potassium fertilizers. *Plant and Soil* 62, 299-303.
- Banin, A. and Lahav, N., 1968. Particle size and optical properties of montmorillonite in suspension. *Israel J. Chem.* 6, 235-250.

- Barshad, I. and Kishk, F.M., 1968. Oxidation of ferrous iron in vermiculite and biotite alters fixation and replaceability of potassium. *Science* 162, 1401-1402.
- Barshad, I. and Kishk, F.M., 1970. Factors affecting potassium fixation and cation exchange capacities of soil vermiculite clays. *Clays Clay Min.* 18, 127-137.
- Basham, I.R., 1974. Mineralogical changes associated with deep weathering of gabbro in Aberdeenshire. *Clay Min.* 10, 189-202.
- Beater, B.E., 1947. Chemical composition of some Natal coastal dolerites and their alteration products. *Soil Sci.* 64, 85-96.
- Beater, B.E. and Frankel, E., 1965. Alterations in chemical composition during the progressive weathering of Dwyka tillite and dolerite in Natal. *Proc. S. Afr. Sugar Technol. Ass.* 39, 250-253.
- Berner, R.A. and Holdren, J.G.R., 1977. Mechanism of feldspar weathering : some observational evidence. *Geology* 5, 369-372.
- Berry, L.G. (ed.), 1974. Selected powder diffraction data for minerals I. edition. Joint committee on powder diffraction standards. Pennsylvania, USA.
- Besson, G., Estrade, H., Gattineau, L., Tchoubar, C. and Mering, J., 1975. A kinetic survey of the cation exchange and the oxidation of a vermiculite. *Clays Clay Min.* 18, 318-322.
- Besson, G., Glaeser, R. and Tchoubar, C., 1983. Le césium, révélateur de structure de smectites. *Clay Min.* 18, 11-19.
- Betts, A.V., 1966. Mineralogy of a soil profile formed on dolerite II Bethal black clay, Transvaal. *S. Afr. J. Agric. Sci.* 9, 49-66.
- Bisdom, E.B.A., Stoops, E., Delvigne, J., Curmi, P. and Altemüller H-J., 1982. Micromorphology of weathering biotite and its secondary products. *Pedologie* 23, 225-252.

- Blake, R.L., 1965. Iron phyllosilicates of the Cuyuna district in Minnesota. *Am. Min.* 50, 148-169.
- Bolt, G.H., Sumner, M.E. and Kamphorst, A., 1963. A study of the equilibria between three categories of potassium in an illitic soil. *Soil Sci. Soc. Am. Proc.* 27, 294-299.
- Borchard, G.A., 1977. Montmorillonite and other smectite minerals. In Dixon, J.B. and Weed S.B. (eds.) *Minerals in soil environments*. Soil Sci. Soc. Am., Madison, Wisconsin, USA. pp.293-330.
- Brindley, G.W., 1966. Ethylene glycol and glycerol complexes of smectites and vermiculites. *Clay Min.* 6, 237-259.
- Brindley, G.W., Bish, L.D. and Wan, H.M., 1979. Compositions, structures and properties of nickel-containing minerals in the kerolite-pimelite series. *Am. Min.* 64, 615-625.
- Brindley, G.W. and Brown, G., (eds.), 1980. X-ray identification and crystal structures. *Min. Soc., London*.
- Byström Brusewitz, A.M., 1975. Studies of the Li test to distinguish between beidellite and montmorillonite. *Proc. Int. Clay Conf.*, Bailey, G.W. (ed.). Applied Publishing Ltd., Wilmette, Illinois. pp.419-428.
- Bühmann, C., Fey, M.V. and de Villiers, J.M., 1985. Aspects of the X-ray identification of swelling clay minerals in soils and sediments. *S. Afr. J. Sci.* 81, 505-509.
- Cass, A., 1980. The influence of pore structural stability and internal drainage rate on selection of soil for irrigation Ph.D. thesis, University of Natal, Pietermaritzburg.
- Chesworth, W., 1973. The parent rock effect in the genesis of soil. *Geoderma* 10, 215-225.

- Chukhrov, F.V., Zvyagin, B.B., Drits, V.A., Gorshkov, A.I., Ermilova, L.P., Goilo, E.A. and Rudnitskaya, E.S., 1979. The ferric analogue of pyrophyllite and related phases. Proc. VI Int. Clay Conf., Oxford. Mortland, M.M. and Farmer, V.C. (eds.). Elsevier, Oxford, pp.55-64.
- Churchman, G.J., Aldridge, L.P. and Carr, R.M., 1972. The relationship between hydrated and dehydrated states of an halloysite. Clays Clay Min. 20 : 241-246.
- Churchman, G.J. and Theng, K.G., 1984. Interactions of halloysite with amides : mineralogical factors affecting complex formation. Clay Min. 19, 161-176.
- Cicel, B., 1974. Validity of structural formulae of montmorillonite by calculating methods. Cited by Horvath and Novak, 1975.
- Cicel, B. and Machajdik, D., 1981. Potassium and ammonium treated montmorillonites I Interstratified structures with ethylene glycol and water. Clays Clay Min. 29, 40-46.
- Coffman, C.B. and Fanning, D.S., 1974. Vermiculite determination on whole soil by cation exchange capacity methods. Clays Clay Min. 22, 271-283.
- Correns, C.W. and von Engelhardt, W., 1938. Neue Untersuchungen über die Verwitterung des Kalifeldspats. Chem. Erde 12, 1-22.
- Cradwick, P.D., 1975. On the calculation of one-dimensional scattering from interstratified material. Clay Min. 10, 347-356.
- Cradwick, P.D. and Wilson, M.J., 1972. Calculated X-ray diffraction profiles for interstratified kaolinite-montmorillonite. Clay Min. 9, 395-402.
- Cradwick, P.D. and Wilson, M.J., 1978. Calculated X-ray diffraction curves for the interpretation of a three component interstratified system. Clay Min. 13, 53-64.

- Curtis, C.D. and Spears, D.A., 1971. Diagenetic development of kaolinite. *Clays Clay Min.* 19, 209-217.
- Davis, C.E., 1972. Behaviour of potassium in some West Indian soil clays. *Clay Min.* 9, 287-295.
- de Bruijn, C.M.A., 1963. Swelling characteristics of a decomposed norite soil profile at Onderstepoort (Transvaal). *Proc. 3rd Reg. Conf. Afr. Soil Mech. Found. Eng. Salisbury*, 27-30.
- de Bruijn, C.M.A., 1973. Moisture distribution in southern African soils. *Proc. 8th Int. Conf. Soil Mech. Found. Eng., Moscow*, 37-44.
- de Bruijn, C.M.A., Collins, L.E. and Williams, A.A.B., 1957. The specific surface, water affinity and potential expansiveness of clays. *Clay Min. Bull.* 3, 17, 120-128.
- Deer, W.A., Howie, R.A. and Zussman, J., 1962. Rock forming minerals III sheet silicates. Longmans, London.
- Derjaguin, B.V. and Landau, L.D., 1941. Theory of the stability of strongly charged lyophobic soils and of the adhesion of strongly charged particles in solutions of electrolytes. From Lagaly, Schön and Weiss, 1972.
- de Villiers, J.M., 1962. A study of soil formation in Natal. Ph.D. thesis, Univ. of Natal, Pietermaritzburg.
- de Villiers, J.M. and Jackson, M.L., 1976. Cation exchange capacity variations with pH in soil clays. *Clay Min.* 19, 161-176.
- Donaldson, G.W., 1965. A study of level observations on buildings as indication of moisture movements in the underlying soil. In *Moisture equilibria and moisture changes in soils beneath covered areas*. Butterworth, Australia, pp.156-164.

- Douglas, L.A., 1977. Vermiculites. In Dixon, J.B. and Weed, S.B. (eds.). Minerals in soil environment. Soil Sci. Soc. Am., Wisconsin, USA, pp. 259-292.
- Douglas, L.A. and Fiessinger, T., 1971. Degradation of clay minerals by H₂O₂ treatment to oxidize organic matter. Clays Clay Min. 19, 67-68.
- Drennan, J.A., 1964. An unusual occurrence of chamosite. Clay Min. Bull. 5, 382-391.
- Drits, V.A., Plancon, A., Sakharov, B.A., Besson, G., Tsipursky, S.I. and Tchoubar, C., 1984. Diffraction effects calculated for structural models of K-saturated montmorillonite containing different types of defects. Clay Min. 19, 541-561.
- Duchaufour, P., 1982. Pedology. George Allen & Unwin, London.
- Duncan, N., 1969. Engineering geology and rock mechanics. Leonard Hill, London.
- Eberl, D.D., 1980. Alkali cation selectivity and fixation by clay minerals. Clays Clay Min. 28, 161-172.
- Egashira, K., Dixon, J.B. and Hossner, L.R., 1982. High charge smectite from lignite overburden of East Texas. In van Olphen, H. and Veniale, F. (eds.). Proc. Int. Clay Conf. Bologna; Elsevier, New York, pp.335-345.
- Egashira, K. and Ohtsubo, M., 1983. Swelling and mineralogy of smectites in paddy soils derived from marine alluvium, Japan. Geoderma 29, 119-127.
- Eggleton, R.A. and Buseck, P.R., 1980. High resolution electron microscopy of feldspar weathering. Clays Clay Min. 28, 173-178.
- Eggleton, R.A. and Boland, J.N., 1982. Weathering of enstatite to talc through a sequence of transitional phases. Clays Clay Min. 30, 11-20.

- Emerson, W.W. and Bakker, A.C., 1973. The comparative effects of exchangeable calcium, magnesium and sodium on some physical properties of red-brown earth subsoils. II. The spontaneous dispersion of aggregates in water. *Austr. J. Soil Res.* 11, 2, 151-158.
- Ergun, S., 1970. X-ray scattering by very defective lattices. *Phys. Rev. B.* 131, 3371-3380.
- Eswaran, H., 1979. The alteration of plagioclases and augites under differing pedo-environmental conditions. *J. Soil Sci.* 30, 547-550.
- Eswaran H., Stoops, G. and Sys, C., 1977. The micromorphology of gibbsite forms in soils. *J. Soil Sci.* 28, 136-143.
- Fanning, D.S. and Keramidas, V.Z., 1977. Micas. In Dixon, J.B. and Weed, S.B. (eds.) *Minerals in soil environments.* Soil Sci. Soc. Am., Madison, Wisconsin, pp.195-258.
- Farmer, V.C., (ed.) 1974. *The infrared spectra of minerals.* Mineralogical Soc., London.
- Farmer, V.C., Russell, J.D., McHardy, W.J., Newman, A.C.D., Ahlrichs, J.L. and Rimsaite, J.Y.H., 1971. Evidence for loss of protons and octahedral iron from oxidized biotites and vermiculites. *Min. Mag.* 38, 221-237.
- Fey, M.V., 1974. Characteristics of sesquioxidic soils. Ph.D. thesis, Univ. of Natal.
- Fey, M.V. and Cass, A., 1983. Soil inventory and land capability classification of the Tutuka power station ash dump site. Department of Soil Science and Agrometeorology, University of Natal, Pietermaritzburg.
- Fey, M.V., Böhmann, C., Snyman, K. and Cass, A., 1984. An intensive soil survey of the Tutuka power station fly ash site. 12th Congr. Soil Sci. Soc. S.A. Bloemfontein (unpublished).

- Fitzpatrick, R.W., 1974. Mineralo-chemical studies on soils and related material from pedosystems in the South Eastern Transvaal. M.Sc.Agric. thesis. University of Natal.
- Fitzpatrick, R.W., 1978. Occurrence and properties of iron and titanium oxides in soils along the eastern seaboard of South Africa. Ph.D. thesis, University of Natal.
- Fitzpatrick, R.W. and le Roux, J., 1977. Mineralogy and chemistry of a Transvaal black clay toposequence. J. Soil Sci. 28, 165-179.
- Flaig, W., Beutelspacher, H. and Rietz, E., 1975. Chemical composition and physical properties of humic substances. In Giesekeing, J.E. (ed.) Soil components, Vol.1, Organic compounds. Springer Verlag, New York, pp. 1-212.
- Foscolos, A.E. and Kodama, H., 1974. Diagenesis of clay minerals from lower Cretaceous shales of North Eastern British Columbia. Clays Clay Min. 22, 319-335.
- Frank-Kamenetzkiy, V.A.I., Kotov, N.V. and Rjumin, A.A., 1980. The transformation of feldspars and muscovite to clay minerals in (Ca,Mg)-carbonate bearing hydrothermal media. Clay Min. 15, 263-274.
- Gaultier, J.P. and Mamy, J., 1979. Evaluation of exchange properties and crystallographic characteristics of bi-ionic K-Ca montmorillonite submitted to alternate wetting and drying. Proc. Int. Clay Conf. Oxford, Mortland, M.M. and Farmer, V.C. (eds.). Elsevier, Amsterdam, pp.167-175.
- Gibbs, R.J., 1965. Error due to segregation in quantitative clay mineral X-ray diffraction mounting techniques. Am. Min. 50, 741-751.
- Giese, R.F., 1979. Hydroxyl orientation in 2:1 phyllosilicates. Clays Clay Min. 27,3, 213-223.

- Gilkes, R.J., Suddhiprakarn, A., and Armitage, T.M., 1980. Scanning electron microscope morphology of deeply weathered granite. *Clays Clay Min.* 28, 27-34.
- Gillman, G.P., 1979. A proposed method for the measurement of exchange properties of highly weathered soils. *Austr. J. Soil Res.* 17, 129-139.
- Goodman, B.J. and Bain, D.C., 1979. Mössbauer spectra of chlorite and their decomposition products. *Proc. Int. Clay Conf. Oxford.* Mortland, M.M. and Farmer, V.C. (eds.) Elsevier, Amsterdam, pp.64-74.
- Goulding, V.W.T. and Talibudeen, O., 1984a. Thermodynamics of K-Ca exchange in soils. I. Effects of potassium and organic matter residues in soils from the Broadbalk and Saxmundham rotation I experiments. *J. Soil Sci.* 35, 397-408.
- Goulding, V.W.T. and Talibudeen, O., 1984b. Thermodynamics of K-Ca exchange in soils. II. Effects of mineralogy, residual K and pH in soils from long-term ADAS experiments. *J. Soil Sci.* 35, 409-428.
- Grahame, D.C., 1947. The electrical double layer and the theory of electrocapillarity. *Chem. Rev.* 41, 441-501.
- Greene-Kelly, R., 1953. The identification of montmorillonoids in clays. *J. Soil Sci.* 4, 233-237.
- Greenland, D.J., 1971. Interaction between humic and fulvic acids and clays. *Soil Sci.* 111, 34-41.
- Grim, R.E. and Bradley, W.F., 1955. Structural implications in diagenesis. *Geol. Rundschau* 43, 469-474.
- Gruner, J.W., 1944. The composition and structure of minnesotaite, a common iron silicate in iron formations. *Am. Min.* 29, 363-372.
- Guenot, J., 1970. Etude mineralogique d'une formation argileuse de dolomite. *Bull. du Groupe Francais des Argiles Tome XXII*, pp.137-151.

- Güven, N., Hower, S. and Davies, A., 1980. Nature of authigenic illites in sandstone reservoirs. *J. Sed. Petr.* 50, 761-766.
- Hahne, H.C.H. and Fitzpatrick, R.W., 1984. Soil mineralogy. In land types of maps 2522 Bray, 2622 Morokweng, 2524 Mafeking, 2624 Vryburg. MacVicar, N. (ed.). *Mem. Agric. Nat. Resour. S. Afr.* No. 1.
- Haider, K., Martin, J.P. and Filip, Z., 1975. Humus biochemistry. In Paul, E.A. and McLaren, A.D. (eds.). *Soil biochemistry*, Vol.4, Dekker, New York.
- Harder, H. and Menschel, G., 1967. Quarzbildung am Meeresboden. *Naturwissenschaften* 54, 21, 561.
- Harder, H. and Fleming, W., 1970. Quarzsynthese bei tiefen Temperaturen. *Geochim. Cosmochim. Acta* 34, 294-305.
- Harmse, H.J. von M., 1967. Soil genesis in the Highveld Region of South Africa. D.Sc. thesis. Rijks University, Utrecht, Netherlands.
- Harward, M.E., Carstea, D.D. and Sayegh, A.H., 1969. Properties of vermiculites and smectites : expansion and collapse. *Clays Clay Min.* 16, 437-447.
- Harward, M.E. and Brindley, G.W., 1965. Swelling properties of synthetic smectites in relation to lattice substitutions. *Clays Clay Min.* 13, 209-222.
- Helgeson, H.G., Garrels, R.M. and MacKenzie, F.T., 1969. Evaluation of irreversible reactions in geochemical processes involving minerals and aqueous solutions. II. Applications. *Geochim. Cosmochim. Acta* 33, 455-481.
- Heller-Kallai, L., 1975. Interaction of montmorillonite with alkali halides. *Proc. Int. Clay Conf.*, Mexico City, Bailey (ed.). Wilmette, Illinois, USA, pp.361-372.

- Heller-Kallai, L., 1982. Clay-salt interaction. Proc. VII Int. Clay Conf. 1981, van Olphen, H. and Veniale, F. (eds.). Elsevier, Amsterdam, pp.127-132.
- Herbillon, A.J. and Makumbi, M.H., 1975. Weathering of chlorite in a soil derived from a chlorite schist under humid tropical conditions. *Geoderma* 13, 84-104.
- Heystek, H., 1954. Hydrous mica clay minerals in South African clays, shales and soils. D.Sc. thesis. University of Pretoria.
- Heystek, H., 1955. Some hydrous micas in South African clays and shales. *Clays Clay Min.* 3, 337-355.
- Hoffmann, J. and Klemen, R., 1950. Verlust der Austauschfähigkeit von Lithiumionen an Bentonit durch Erhitzen. *Z. Anorg. Chem.* 262, 95-99.
- Horvath, J.S. and Novak, J., 1975. Potassium fixation and the charge of montmorillonite layer. Proc. Int. Clay Conf. Mexico City, Bailey, S.W. (ed.). Wilmette, Illinois, pp.185-189.
- Hower, J. and Mowatt, T.C., 1966. Mineralogy of the illite-illite/montmorillonite group. *Am. Min.* 51, 821-854.
- Huff, W.D. and Turkmenoglu, A.G., 1981. Chemical characteristics and origin of Ordovician K-bentonites along the Cincinnati arc. *Clays Clay Min.* 29, 113-123.
- Ildefonse, P., Copin, E. and Velde, B., 1979. A soil vermiculite formed from a meta-gabbro, Loire-Atlantique, France. *Clay Min.* 3, 201-210.
- Isphording, W.C., 1973. Discussion of the occurrence and origin of sedimentary palygorskite-sepiolite deposits. *Clays Clay Min.* 21, 391-401.
- Isphording, W.C., 1975. Primary nontronite from Venezuelan Guayana. *Am. Min.* 60, 840-848.
- Jackson, M.L., 1968. Soil chemical analysis - advanced course; sec. ed.; 10th printing. Dept. of Soil Sci., Wisconsin, Madison, USA.

- Jenkins, H.D.B. and Hartman, P., 1982. A new approach to electrostatic calculations for complex silicate structures and their application to vermiculite containing a single layer of water molecules. Proc. Int. Clay Conf. 1981, van Olphen, H. and Veniale, F. (eds.). Elsevier, Amsterdam, pp.87-95.
- Jenny, H., 1941. Factors of soil formation. McGraw-Hill, New York.
- Johnson, L.J., 1964. Occurrence of a regularly interstratified chlorite/vermiculite as a weathering product of chlorite in soils. Am. Min. 49, 556-572.
- Kager, P.C.A. and Oen, I.S., 1983. Iron-rich talc - opal - minnesotaite spherulites and crystallochemical relations of talc and minnesotaite. Min. Mag. 47, 229-231.
- Karathanasis, A.D. and Hajek, B.F., 1983. Transformation of smectite to kaolinite in naturally acid soil systems : Structural and thermodynamic considerations. Soil Sci. Soc. Am. J. 47, 158-163.
- Karickhoff, S.W. and Bailey, G.W., 1976. Protonation of organic bases in clay-water systems. Clays Clay Min. 24, 170-176.
- Keller, W.D., 1976. Scan electron micrographs of kaolins collected from diverse environments of origin. Clays Clay Min. 24, 107-113.
- Keller, W.D., 1978. Classification of kaolins exemplified by their textures in scan electron micrographs. Clays Clay Min. 26, 1-20.
- Kim, Y.K., Gurney, E.L. and Hatfield, J.D., 1983a. Fixation kinetics in potassium-aluminium-orthophosphate systems. Soil Sci. Soc. Am. J. 47, 448-454.
- Kim, Y.K., Gurney, E.L. and Hatfield, J.D., 1983b. Fixation kinetics in potassium-iron-orthophosphate systems. Soil Sci. Soc. Am. J. 47, 455-462.

- Kittrick, J.A., 1973. Mica-derived vermiculites as unstable intermediates. *Clays Clay Min.* 21, 479-488.
- Klug, H.P. and Alexander, L.E., 1974. X-ray diffraction procedures : for polycrystalline and amorphous materials. J. Wiley and Sons, New York, 2nd edition.
- Kodama, H. and Brydon, J.E., 1968. A study of clay minerals in Podzol soils in New Brunswick, eastern Canada. *Clay Min.* 7, 295-309.
- Kononova, M.M., 1975. Humus in virgin and cultivated soils. In Gieseking, J.E. (ed.) *Soil Components*, Vol. 1. Springer Verlag, New York, pp. 475-526.
- Kozak, L.M. and Huang, P.M., 1971. Adsorption of hydroxy-Al by certain phyllosilicates and its relation to K/Ca cation exchange selectivity. *Clays Clay Min.* 19, 95-102
- Kyuma, K. and Kawaguchi, K., 1964. Oxidative changes of polyphenols as influenced by allophane. *Proc. Soil Sci. Soc. Am.* 28, 371-374.
- Laboratory report 71/1. Study of fissured clays. Report on a field visit to a site in Three Rivers, Vereeniging. Soil Mech. Div. Nat. Building Res. Inst., Pretoria.
- Lagaly, G., 1979. The "layer charge" of regular interstratified 2:1 clay minerals. *Clays Clay Min.* 27, 1, 1-10.
- Lagaly, G., 1982. Layer charge heterogeneity in vermiculites. *Clays Clay Min.* 30, 215-222.
- Lagaly, G. and Weiss, A., 1969. Determination of the layer charge in mica-type layer silicates. *Proc. Int. Clay Conf.*, Vol. 1, Tokyo. Heller, L. (ed.) Israel Univ. Press, Jerusalem, pp.61-80.

- Lagaly, G., Schön, G. and Weiss, A., 1972. Über den Einfluss einer unsymmetrischen Ladungsverteilung auf die Wechselwirkung zwischen plättchenförmigen Kolloidteilchen. *Kolloid Z.Z. Polymere* 250, 667-674.
- Lagaly, G., Gonzales, M.F. and Weiss, A., 1976. Problems in the layer-charge determination of montmorillonites. *Clay Min.* 11, 173-187.
- le Roux, J., 1972. Quantitative clay mineralogical analysis of highly weathered Natal soils. *Proc. S. Afr. Sugar Technol. Ass.* 46, 201-203.
- le Roux, J., 1978. Advances in soil mineralogy in southern Africa, 1953-1978. *Proc. VIII Nat. Con., Pietermaritzburg*, pp.88-93.
- le Roux, J. and Sumner, M.E., 1969. The assessment of the potassium status of Natal soils. *Agrochemophytica* 1, 31-42.
- le Roux, J. and Rich, C.I., 1969. Ion selectivity of micas as influenced by degree of K depletion. *Proc. Soil Sci. Soc. Am.* 33, 684-690.
- le Roux, J., Rich, C.I. and Ribbe, P.H., 1970. Ion selectivity by weathered micas as determined by electron microprobe analysis. *Clays Clay Min.* 18, 333-338.
- Loughnan, F.C., 1981. Genesis and synthesis : kaolins in sediments. *Proc. Int. Clay Conf., Bologna*. van Olphen, H. and Veniale, F. (eds.). Elsevier, New York, pp.335-345.
- Lucas, J. and Ataman, G., 1968. Mineralogical and geochemical study of clay mineral transformations in the sedimentary Triassic Jura basin (France). *Clays Clay Min.* 5, 365-372.
- MacEwan, D.M.C., 1958. Fourier transform methods for studying scattering from lamellar systems. 2. The calculation of X-ray diffraction effects for various types of interstratifications. *Kolloid Z* 156, 61-67.

- MacEwan D.M.C. and Wilson, M.J., 1980. Interlayer and intercalation complexes of clay minerals. In Brindley, G.W. and Brown, G. (eds.) Crystal structures of clay minerals and their X-ray identification. Min. Soc., London, pp.197-248.
- Mackenzie, R.C., 1963. Retention of exchangeable ions by montmorillonite. Proc. Int. Clay Conf. Stockholm, pp.183-193.
- MacVicar, C.N., 1962. Soil studies in the Tugela Basin. Ph.D. thesis. University of Natal.
- MacVicar, C.N., 1965a. The climatic factor in soil genesis illustrated by climosequences in the Natal Midlands. S. Afr. J. Agric. Sci. 8, 681-690.
- MacVicar, C.N., 1965b. The constitution and genesis of four soil series from dolerite in the Natal Midlands. S. Afr. J. Agric. Sci. 8, 979-990.
- MacVicar, C.N., 1978. Advances in soil classification and genesis in southern Africa. Proc. VIII Nat. Conf., Pietermaritzburg, pp.22-40.
- MacVicar, C.,N., de Villiers, J.M., Loxton, R.F., Verster, E., Lambrechts, J.J.N., Merryweather, F.R., le Roux, J., van Rooyen, T.H. and Harmse, H.J. von M., 1977. Soil classification : a binomial system for South Africa. Sci. Bull. No. 390, Dept. Agric. Tech. Services, Pretoria.
- Machajdik, D. and Cicel, B., 1981. Potassium-and ammonium-treated montmorillonites. II Calculation of characteristic layer charges. Clays Clay Min. 29, 47-52.
- Maes, A. and Cremers, A., 1979. Cation exchange in clay minerals : some recent developments. In Bolt, G.H. (ed.) Soil Chemistry. Elsevier, Amsterdam, pp.205-232.
- Malla, P.B. and Douglas, L.A., 1984. Charge density of some smectite-like soil clays. Agronomy abstracts, Nov. 25-30, p.274.

- Marchand, B.C., 1925. The original black turf soils in the Transvaal. S. Afr. J. Sci. 21, 162-181.
- McBride, M.B., 1980. Interpretation of the variability of selectivity coefficients for exchange between ions of unequal charge on smectites. Clays Clay Min. 28, 255-261.
- McKeague, J.A., 1978. Manual on soil sampling and methods of analysis. 2nd edition. Can. Soc. Soil Sci., Can. Soil Survey Comm., Ottawa.
- Mehra, O.P. and Jackson, M.J., 1960. Iron oxide removal from soils and clays by a dithionite-citrate system buffered with sodium bicarbonate. Clays Clay Min. 7, 317-327.
- Meunier, A. and Velde, B., 1976. Mineral reactions at grain contacts in early stages of granite weathering. Clay Min. 11, 235-240.
- Millot, G., 1970. Geology of clays. Masson and Ciss, Paris.
- Mills, J.G. and Zwarich, J., 1972. Recognition of interstratified clays. Clays Clay Min. 20, 169-174.
- Mortland, M.M., 1970. Clay-organic complexes and interactions. Advances Agron. 22, 75-117.
- Muravyev, V.J. and Sakharov, B.A., 1970. Experimental study of the sorption of potassium by montmorillonite. Sedimentology 15, 103-113.
- Nadeau, P.H., Wilson, M.J., McHardy, W.J. and Tait, J.M., 1984. Interparticle diffraction : a new concept for interstratification of clay minerals. Clay Min. 19, 757-770.
- Nahon, D., Colin, F. and Tardy, Y., 1982. Formation and distribution of Mg, Fe, Mn-smectites in the first stages of the lateritic weathering of forsterite and tephroite. Clay Min. 17, 339-348.
- Nemeth, K. and Forster, H., 1976. Beziehungen zwischen Ertrag und K-Entzug von Ackerbohnen (*vicia faba*) sowie verschiedenen K-Fractionen von Böden. Die Bodenkultur 27, 111-119.

- Niederbudde, E.A. and Fischer, W.R., 1980. Clay mineral transformations in soils as influenced by potassium release from biotite. *Soil Sci.* 130, 225-231.
- Norrish, K., 1954. The swelling of montmorillonite. *Trans. Faraday Soc.* 18, 120-134.
- Norrish, K., 1972. Forces between clay particles. *Proc. Int. Clay Conf.*, Madrid, pp.375-383.
- Novich, B.E. and Martin, R.T., 1983. Solvation methods for expandable layers. *Clays Clay Min.* 31, 235-238.
- Oberholster, R.E., 1969a. Genesis of two different soils on basalt. I. Mineralogical characteristics. *Agrochemophysica* 1 : 53-62
- Oberholster, R.E., 1969b. Genesis of two different soils on basalt. II. Contribution of transported material. *Agrochemophysica* 1, 73-78.
- Orr, E.M., 1979. Rapid weathering dolerites. *Civ. Engr. S. Afr.* 21, 161-167.
- Page, C. and Wenk, H.R., 1979. Phyllosilicate alteration of plagioclase studied by TEM. *Geology* 7, 393-397.
- Paquet, H., Duplay, J. and Nahon, D., 1982. Variations in the composition of phyllosilicate monoparticles in a weathering profile of ultrabasic rocks. *Proc. Int. Clay Conf.*, Bologna, van Olphen, H. and Veniale, V. (eds.). Elsevier, Amsterdam, pp.595-604.
- Petrovic, R., 1976. Rate control in feldspar dissolution. II. The protective effect of precipitates. *Geochim. Cosmochim. Acta* 40, 1509-1521.
- Phillips, J., 1973. The agricultural and related development of the Tugela basin and its influent surrounds. *Natal Town and Regional Planning Report*, Vol. 19.

- Pion, J.-C., 1979. Alteration des Massifs Cristallins Basiques en Zone Tropical Seche. Etude de quelques Toposequences en Haute Volta. Sciences Geologiques, Memoire No. 57, ULP Strasbourg.
- Plancon, A. and Tchoubar, C., 1977. Determination of structural defects in phyllosilicates by X-ray powder diffraction. 1: Principle of calculation of the diffraction phenomenon. Clays Clay Min. 25, 430-435.
- Plancon, A., Besson, G., Gaultier, J.P., Mamy, J. and Tchoubar, C., 1979. Qualitative and quantitative study of a structural reorganization in montmorillonite after potassium fixation. Proc. VI Int. Clay Conf. Oxford, Mortland, M.M. and Farmer, V.C. (eds.). Elsevier, Amsterdam. Pp. 45-54.
- Proust, D. and Velde, B., 1978. Beidellite crystallization from plagioclase and amphibole precursors : local and long-range equilibrium during weathering. Clay Min. 13, 199-209.
- Quirk, J.P., 1968. Particle interaction and soil swelling. Isr. J. Chem. 6, 213-234.
- Rabenhorst, M.C., Fanning, D.S. and Foss, J.E., 1982. Regularly interstratified chlorite/vermiculite in soils over meta-igneous mafic rocks in Maryland. Clays Clay Min. 30, 156-158.
- Range, K.I., Range, A. and Weiss, A., 1969. Fire-clay type kaolinite or fire clay mineral? Experimental classification of kaolinite-halloysite minerals. Proc. Int. Clay Conf., Tokyo, Vol. 1, Heller, L. (ed.). Israel Univ. Press, Jerusalem, pp.3-13.
- Ray, B.K., De, A.K. and Bachatterjee, S., 1980. X-ray diffraction from partially disordered layer structures : general case. Clay Min. 15, 393-398.
- Reerink, F.O., 1961. Clay mineralogical studies in the Tugela Basin. M.Sc.Agric. thesis. University of Natal.

- Reynolds, R., 1968. The effect of particle size on apparent lattice spacings. *Acta Cryst.* A24, 319-320.
- Reynolds, R.C., 1980. Interstratified clay minerals. In Brindley, G.W. and Brown, G., (eds.). *Crystal structures of clay minerals and their X-ray identification.* Min. Soc., London, pp. 249-303.
- Reynolds, R.C. and Hower, J., 1970. The nature of interlayering in mixed-layer illite-montmorillonites. *Clays Clay Min.* 18, 25-36.
- Rich, C.I., 1960. Aluminium in interlayers of vermiculite. *Soil Sci. Soc. Am. Proc.* 24, 26-32.
- Rich, C.I., 1975. Determination of the amount of clay needed for X-ray diffraction analysis. *Proc. Soil Sci. Soc. Am.* 39, 161-162.
- Roberson, H.E. and Lahann, R.W., 1981. Smectite to illite conversion rates : effects of solution chemistry. *Clays Clay Min.* 29,2, 129-135.
- Rodriguez, A.M.J., 1982. Basaltic and rhyolitic rocks as parent material of halloysite in Argentine deposits. *Proc. Int. Clay Conf. Pavia.* van Olphen, H. and Veniale, F, (eds.). Elsevier, Amsterdam, pp.605-612.
- Ross, M., Smith, W.L. and Ashton, W.H., 1968. Triclinic talc and associated amphiboles from Gouverneur Mining District, New York. *Am. Min.* 53, 751-769.
- Ross, G.J., 1971. Evidence for loss of protons and octahedral iron from oxidized biotites and vermiculites. *Min. Mag.* 38, 121-137.
- Ross, G.J. and Rich, C.I., 1974. Effect of oxidation and reduction on potassium exchange of biotite. *Clays Clay Min.* 22, 355-360.
- Ross, G.J. and Kodama, H., 1976. Experimental alteration of a chlorite into a regularly interstratified chlorite/vermiculite by chemical oxidation. *Clays Clay Min.* 24, 183-190.

- Ross, G.J., Kodama, H., Wang, C., Gray, J.T. and Lafreniere, L.B., 1983. Halloysite from a strongly weathered soil at Mont Jacques Cartier, Quebec. Soil Sci. Soc. Am. J. 47, 327-332.
- Sachan, R.S. and Sharma, R.B., 1980. Humic to fulvic acid ratio in relation to depth of cracking in some Vertisols of India. Pedologie 30, 3, 335-339.
- Sawhney, B.L., 1970. Potassium and cesium ion selectivity in relation to clay mineral structures. Clays Clay Min. 18, 47-52.
- Sawhney, B.L., 1972. Selective sorption and fixation of cations by clay minerals : a review. Clays Clay Min. 20, 93-100.
- Schönau, A.P.G. and Boden, D.I., 1981. Soil survey, suitability for afforestation and selection of tree species for the farm Melody Ranch in the Ixopo district, Natal. Pietermaritzburg.
- Schroeder, D., 1979. Structure and weathering of potassium containing minerals. In Potassium Research : Review and Trends. Proc. 11 Cong. Int. Pot. Inst., Bern. "The Bund", AG Bern, Switzerland. Pp.43-64.
- Schuffelen, A.C. and van der Marel, H.W., 1955. Potassium fixation in soils. Proc. 2nd Symp. Int. Potash Inst., Berne, pp.157-201.
- Schultz, L.G., 1969. Lithium and potassium absorption, dehydroxylation temperature and structural water content of aluminous smectites. Clays Clay Min. 17, 115-137.
- Schultz, L.G., Shepard, A.D., Blackman, P.O. and Starkey, H.C., 1971. Mixed-layer kaolinite-montmorillonite from the Yukatan Peninsula, Mexico. Clays Clay Min. 19, 137-150.
- Sieffermann, B. and Millot, G., 1969. Equatorial and tropical weathering of recent basalts from Cameroon : Allophanes, Halloysite, Metahalloysite, Kaolinite and Gibbsite. Proc. Int. Clay Conf., Tokyo, Vol. 1, Heller, L. (ed.). Israel Univ. Press, Jerusalem, pp.417-430.

- Simons, N.E. and Williams, A.A.B., 1963. Preliminary report on moisture studies at the Onderstepoort site near Pretoria. Nat. Inst. Road Res., Pretoria, S.A., pp.41-45.
- Singh, S., 1956. The formation of dark colored clay-organic complexes in black soils. J. Soil Sci. 7, 43-58.
- Snyman, K., Fey, M.V. and Cass, A., 1985. Physical properties of some highveld Vertisols. S. Afr. J. Plant Soil 2, 18-20.
- Soil Survey Staff, 1975. Soil taxonomy : a basic system of soil classification for making and interpreting soil surveys. USDA Handbook, US Gov. Print. Off.
- Srodon, J., 1984. X-ray powder diffraction identification of illitic material. Clays Clay Min. 32, 337-349.
- Srodon, J. and Eberl, D.D., 1980. The presentation of X-ray data for clay minerals. Clay Min. 15, 317-320.
- Srodon, J. and Eberl, D.D., 1984. Illite. In Bailey, S.W. (ed.) Micas : review in mineralogy, Vol.13. Min. Soc. Am., Washington, DC, pp.495-544.
- Stern, O., 1924. Zur Theorie der electrolytischen Doppelschicht. Cited by Theng, B.K.G., 1979.
- Sticher, H., 1972. Potassium in allophane and zeolites. Proc. 9th Colloq. Int. Potash Inst., Berne, pp.43-51.
- Suquet, H., de la Call, C. and Pezerat, H., 1975. Swelling and structural organization of saponite. Clays Clay Min. 23, 1-9.
- Suttner, R.B., Malpas, J., Rona, O.A. and Udintsev, G., 1976. A comparative study of simulated and natural weathering. Geology 4, 233-236.

- Tardy, Y., Duplay, J. and Fritz, B., 1981. Chemical composition of individual clay particles : an ideal solid solution model. Proc. Int. Clay Conf., Bologna and Pavia, van Olphen, H.S. and Veniale, F. (eds.). Elsevier, New York, pp.441-450.
- Taylor, K.P., 1972. An investigation of the clay fraction of soils from the Springbok flats, Transvaal. M.Sci. thesis, Dept. Soil Sci., Univ. Natal, Pietermaritzburg.
- Taylor, R.M. and Schwertmann, U., 1980. The influence of aluminium on the iron oxides. VII Substitution of Al for Fe in synthetic lepidocrocite. Clays Clay Min. 28, 267-274.
- Tettenhorst, R. and Grim, R.E., 1975. Interstratified clays. I Theoretical. Am. Min. 60, 49-59.
- Theng, B.K.G., 1979. Formation and properties of clay-polymer complexes. Elsevier, Amsterdam.
- Theng, B.K.G., 1982. Clay-activated organic reactions. Proc. Int. Clay Conf., Bologna and Pavia, van Olphen, H.S. and Veniale, F. (eds.). Elsevier, New York, pp.197-238.
- Theng, B.T.G. and Churchman, G.J., 1982. Intercalation of some amide into halloysite. Abstr. Vol. of Circum-Pacific Clay Min. Soc., 19th annual meeting. Hawaii Inst. of Geophysics. P.20.
- Theron, J.J. and van Niekerk, P., 1934. The nature and origin of black turf soils. S. Afr. J. Sci. 31, 320-346.
- Thompson, G.D., 1981. The need for further research into sugarcane nutrition in South Africa during the 1980s. Fertilizer Soc. S.A. J. 2, 37-39.
- Townsend, W.N., 1972. An introduction to the scientific study of the soil. 5. Soil organic matter. Butler and Tanner Ltd., London, pp.55-66.

- Trunz, V., 1976. The influence of crystallite size on the apparent basal spacings of kaolinite. *Clays Clay Min.* 24, 84-87.
- Tsipursky, S.I. and Drits, V.A., 1984. The distribution of octahedral cations in the 2:1 layers of dioctahedral smectites studied by oblique-texture electron diffraction. *Clay Min.* 19, 177-194.
- Van der Marel, H.W. and Beutelspacher, H., 1976. *Atlas of infrared spectroscopy of clay minerals and their admixtures.* Elsevier, New York.
- van der Merwe, C.R., 1924. On the formation of soil from diabase in the Central Transvaal. *S. Afr. J. Sci.* 21, 235-242.
- van der Merwe, C.R., 1962. Soil groups and subgroups of South Africa. *Science Bull.* 356. Chemistry Series No. 165. Dept. Agric. Tech. Serv., Pretoria
- van der Merwe, C.R. and Heystek, H., 1952. Clay minerals of South African Soil Groups. I. Laterites and related soils. *Soil Sci.* 74, 383-401.
- van der Merwe, C.R. and Heystek, H., 1955. Clay minerals in South African soil groups. II. Subtropical black clays and related soils. *Soil Sci.* 79, 146-158.
- van der Merwe, C.R. and Weber, H.W., 1965. The clay minerals of South African soils developed from dolerite under different climatic conditions. *S. Afr. J. Agric. Sci.* 8, 111-142.
- van Olphen, H., 1963. *An introduction to clay colloid chemistry.* Interscience, New York.
- van Olphen, H., 1966. Collapse of potassium montmorillonite clays upon heating -- "potassium fixation". *Clays Clay Min.* 14, 393-405.
- van Reeuwijk, L.P. and de Villiers, J.M., 1968. Potassium fixation by amorphous aluminosilica gels. *Soil Sci. Soc. Am. Proc.* 32, 238-240.

- Veith, J.A. and Jackson, M.L., 1974. Iron oxidation and reduction effects on structural hydroxyl and layer charge in aqueous suspensions of micaceous vermiculites. *Clays Clay Min.* 22, 345-353.
- Verwey, E.J.W. and Overbeek, J.T.G., 1948. Theory of the stability of lyophobic colloids. Elsevier, Amsterdam.
- Vogt, K. and Köster, H.M., 1978. Zur Mineralogie, Kristallchemie und Geochemie einiger Montmorillonite aus Bentoniten. *Clay Min.* 131, 25-42.
- Wada, K. and Kakuto, Y., 1983. Intergradient vermiculite-kaolin mineral in a Korean Ultisol. *Clays Clay Min.* 31, 183-190.
- Walker, G.F., 1975. Vermiculites. In Gieseking, J.E. (ed.) *Soil Components, Vol. 2, Inorganic components.* Springer, Berlin, pp.155-189.
- Wang, T.S.C., Min Chao Wang, Yue Lang Ferng and Huang, P.M., 1983. Catalytic synthesis of humic substances by natural clays, silts and soils. *Soil Sci.* 135, 6, 350-360.
- Weast, R.C. and Astle, M.J., 1978. Handbook of chemistry and physics, 59th ed. CRC Press, Inc., Florida, USA.
- Weaver, C.E., 1958. The effects and geological significance of K⁺ fixation by expandable clay minerals derived from muscovite, biotite, chlorite and volcanic material. *Am. Min.* 43, 839-861.
- Weaver, C.E., 1960. Possible uses of clay minerals in search for oil. *Am. Ass. Pet. Geol. Bull.* 44 P, 1505-1518.
- Weaver, C.E. and Pollard, L.D., 1973. The chemistry of clay minerals. Elsevier, Amsterdam.
- Weir, A.H., 1960. Relationship between physical properties, structure and composition of smectite. Cited by Suquet et al, 1975.

- Weir, A.H., 1965. Potassium retention in montmorillonite. Clay Min. 6, 17-22.
- Wilkins, R.W.T. and Ito, J., 1967. Infrared spectra of some synthetic talcs. Am. Min. 52, 1649-1661.
- Williams, A.A.B. and Donaldson, G.W., 1980. Developments relating to building on expansive soils in South Africa : 1973 - 1980. 4th Int. Conf. Expans. Soils, Denver, USA, pp.511-520.
- Williams, A.A.B. and Jennings, J.E., 1977. The in situ shear behaviour of fissured soils. Proc. 9th Int. Conf. Soil Mech. Found. Eng., Tokyo, Vol. 2; pp.169-176.
- Wilson, M.J., 1975. Chemical weathering of some primary rock-forming minerals. Soil Sci. 119, 349-355.
- Wood, R.A., 1980. The role of potassium in the production of sugarcane in South Africa. Fert. Soc. S. Afr. Proc. Intern. Seminar 1979, pp.109-114.

Appendix 1

Exchangeable Ca and Mg values, exchangeable acidity and grain size distribution of Melody Ranch samples.

Soil form	Horizon	Ca	Mg	Exchan. acidity	Grain size distribution			% of < 0,2 um in < 2 um
					Sand	Silt %	Clay	
----- (mmol(+)/kg) -----								
Rensburg	A ₁	146,3	149,2	0,8	17	17	66	72
	A ₂	143,8	136,5	0,4	20	19	61	70
	G ₁	130	145,7	0,6	25	11	64	82
	G ₂	121,3	8,31	0,5	39	16	45	80
	C	130	80,2	0,9	59	16	25	75
Mayo	A ₁	135	73,1	0,6	19	28	53	58
	A ₂	125	102,1	0,7	17	25	58	52
	A ₂ -B	122,5	104,2	0,6	37	19	44	48
	B	24,6	97,9	0,4	49	21	30	58
	C	24,4	65,9	1,8	64	20	16	60
Arcadia	A	133,8	73,1	0,2	21	19	60	
	B	22,4	31,9	0,4	22	22	56	
Shortlands	A	22,3	39,3	0,4	18	20	62	
	B ₁	18,1	37,0	0,5	24	17	59	
	B ₂	8,4	27,3	0,4	18	19	63	
	C ₁	1,5	2,5	0,3	27	26	47	
	C ₂	2,2	2,4	0,3	27	31	42	

- continued -

Appendix 1 (contd.)

Soil form	Horizon	Ca	Mg	Exchan. acidity	Grain size distribution			% of < 0,2 um in < 2 um
					Sand	Silt %	Clay	
----- (mmol(+)/kg) -----								
Bonheim	A	20,1	56,3	0,5	29	16	55	
	B	12,8	33,6	0,4	22	19	59	
Bonheim	A	128,8	61,7	1,2	25	18	57	
	B	20,5	60,1	0,3	25	20	55	
Hutton	A	13,0	31,2	1,0	19	19	62	
	B ₁	1,4	10,9	1,6	22	19	59	
	B ₂	2,0	10,0	0,6	25	15	60	
Hutton	A	20,1	36,1	1,4	23	21	56	
	B	10,5	36,8	0,5	18	17	65	

<u>Depth</u> <u>cm</u>	<u>Horizon</u>	<u>Description</u>
---------------------------	----------------	--------------------

95-140	G2ca	Moist, variegated greyish brown to light olive brown (2,5Y 5/2-4) stony silty clay/silty clay loam; moderate coarse blocky, cleaving along saprolite particles; very firm; common soft CaCO ₃ concretions; common dark cutans on peds and shale fragments; common, becoming abundant with depth, fragments of firm weathered shale.
--------	------	--

Remarks : Ecce shale/mudstone parent material (fragments of weathered saprolite sampled as horizon C for analysis); 1% slope; virgin soil under Themeda grassland; upland. Intergrade between a vertic phase of Valsrivier form or a duplex phase of Rensburg form.

Appendix 3

<u>Profile 2</u>	<u>Soil form</u> : Rensburg	<u>Soil series</u> : Rensburg
		<u>Phase</u> : upland mudstone

<u>Depth</u> <u>cm</u>	<u>Horizon</u>	<u>Description</u>
---------------------------	----------------	--------------------

0-20	A1p	Moist, very dark brown (10YR 2/2) clay loam very weak coarse subangular blocky; friable; abundant roots (old maize land); abrupt smooth transition.
------	-----	---

20-40	A2	Slightly moist; very dark grey (10YR 3/1) clay; strong, coarse subangular blocky with weak prismatic tendency; very firm; common roots mostly compressed against ped faces; few slickensides at base; gradual smooth transition.
-------	----	--

<u>Depth</u> <u>cm</u>	<u>Horizon</u>	<u>Description</u>
40-90	G1	Moist; greyish brown (2,5Y 5/2) clay; moderate to strong coarse angular blocky to wedge; very firm; very plastic; few fine CaCO ₃ concretions; very few, fine ferruginised shale fragments; very few roots; abundant shiny, grooved slickensides; gradual, irregular transition.
90-120	G2	Moist; light brownish grey to greyish brown (2,5Y 2/6 to 5/2) with orange mottles; clay loam; weak coarse angular blocky; firm; very plastic; no observable roots; common, fine, hard, manganese concretions, common, orange-brown, firm, weathered shale fragments increasing with depth; hard, partly weathered mudstone or shale at base.
Remarks		As with P1 this is an intergrade between a vertic phase of Valsrivier form or a duplex phase of Rensburg form.

Appendix 4

Profile 3 Soil form : Rensburg Soil series : Rensburg
Phase : upland mudstone

<u>Depth</u> <u>cm</u>	<u>Horizon</u>	<u>Description</u>
0-20	A1p	As for P2
20-45	A2	Common coarse, medium to large, ferruginised shale fragments.
45-85	G1	Slickensides very prominent in A2/G1.

<u>Depth</u> <u>cm</u>	<u>Horizon</u>	<u>Description</u>
---------------------------	----------------	--------------------

85-120	G2	Hard mudstone at base of G2.
--------	----	------------------------------

Remarks : Very similar to P1 and P2, but common, coarse, medium to large ferruginised shale fragments in A2. Slickensides very prominent in A2/G1.

Appendix 5

<u>Profile 4</u>	<u>Soil form</u> : Arcadia	<u>Soil series</u> : Arcadia
------------------	----------------------------	------------------------------

<u>Depth</u> <u>cm</u>	<u>Horizon</u>	<u>Description</u>
---------------------------	----------------	--------------------

0-25	A1p	As for P3
------	-----	-----------

25-60	A2	Hard mudstone at base of A2, weak gleying at 50-60 cm. Slickensides still prominent in the lower half of A2.
-------	----	--

Remarks : Essentially similar to P1 to P3 but shallow. Lacks a proper G horizon although lower A2 shows weak subordinate gley characteristics (50 to 60 cm) and prominent slickensides in lower half of the A2 horizon.

Appendix 6

<u>Profile 8</u>	<u>Soil form</u> : Arcadia	<u>Soil series</u> : Gelykvlakte
------------------	----------------------------	----------------------------------

<u>Depth</u> <u>cm</u>	<u>Horizon</u>	<u>Description</u>
---------------------------	----------------	--------------------

0-20	A1p	Vertic A.
------	-----	-----------

20-60	A2	Vertic A.
-------	----	-----------

<u>Depth</u> <u>cm</u>	<u>Horizon</u>	<u>Description</u>
---------------------------	----------------	--------------------

60-80	G	Mudstone saprolite.
-------	---	---------------------

Remarks : Transitional between mudstone and dolerite derived soils. Mudstone appears to be baked, fragments of dolerite at surface.

Appendix 7

Profile 12 Soil form : Arcadia Soil series : Arcadia

<u>Depth</u> <u>cm</u>	<u>Horizon</u>	<u>Description</u>
---------------------------	----------------	--------------------

0-20	A1p	Black, strong blocky structure.
------	-----	---------------------------------

20-80	A2ca	Black, strong blocky structure.
-------	------	---------------------------------

80-90+	Cca	Dolerite saprolite, yellow crumbly, with dark clay skins.
--------	-----	---

Remarks : A very black, very strongly structured, very slickensided profile; surface more self mulching than crusting. See profile 13 for typical description.

Appendix 8

Profile 13 Soil form : Arcadia Soil series : Arcadia

<u>Depth</u> <u>cm</u>	<u>Horizon</u>	<u>Description</u>
---------------------------	----------------	--------------------

0-20	A1p	Slightly moist; black (5Y 2,5/1) clay, weak, coarse subangular blocky; friable to firm; many roots; clear wavy transition.
------	-----	--

<u>Depth</u> <u>cm</u>	<u>Horizon</u>	<u>Description</u>
20-55	A2	Slightly moist; black (5Y 2,5/2) clay; extremely firm; very strong medium to coarse angular blocky to wedge; abundant shiny slickensides; many fine to medium CaCO ₃ concretions in lower horizon; few fine saprolite fragments; very few roots; clear smooth transition.
55-70+ C		Moist; firm, gritty dolerite saprolite containing black clay skins and some powdery CaCO ₃ .
Remarks :		Surface moderately self-mulching. Old sorghum land.

Appendix 9

Profile 14 Soil form : Arcadia Soil series : Arcadia

<u>Depth</u> <u>cm</u>	<u>Horizon</u>	<u>Description</u>
0-20	A1p	
20-65	A2	As pit 13.
65-100+ C		
Remarks :		Strongly calcareous in lower A2 and upper C. Very similar to pit 13.

Appendix 10

<u>Profile 17</u>			<u>Soil form</u> : Arcadia	<u>Soil series</u> : Arcadia
<u>Depth</u> <u>cm</u>	<u>Horizon</u>	<u>Description</u>		
0-20	A1	Very strong medium, subangular blocky, abundant roots diffuse smooth transition.		
30-65	A2	Strongly slickensided, weakly calcareous at base.		
65-70	C	Brownish grey dolerite saprolite.		
Remarks :		Virgin veld, weak gilgai present on the surface.		

Appendix 11

<u>Profile 22</u>			<u>Soil form</u> : Arcadia	<u>Soil series</u> : Arcadia
<u>Depth</u> <u>cm</u>	<u>Horizon</u>	<u>Description</u>		
0-30	A1	Cracks 2-3 cm wide, black, very strong blocky.		
30-60	A2	Black, strongly slickensided, calcareous at base.		
60-90+	C	Crumbly, calcareous, yellow brown dolerite saprolite.		
Remarks :		Clear slickensides, CaCO_3 concentrated near top of C. Topography suggests the site may be wetter than other sites; possible very weak gilgai.		

Appendix 12

Profile 25 Soil form : Rensburg Soil series : Rensburg

<u>Depth</u> <u>cm</u>	<u>Horizon</u>	<u>Description</u>
0-30	A1	Moist; black (5Y 2,5/1) clay; strong, coarse, subangular blocky; extremely firm; common roots; few wide (2+ cm) vertical cracks, diffuse smooth transition.
30-70	A2	Moist; black (5Y 2,5/2) clay; strong medium to coarse subangular blocky, common shiny pressure faces on peds; few slickensides at lower boundary; very few roots; diffuse smooth transition.
70-110	G1	Moist; very dark grey (5Y 3/1) clay; strong coarse angular blocky to wedge, extremely firm and plastic; few fine CaCO ₃ concretions; very few roots; common prominent shiny grooved slickensides; diffuse smooth transition.

Appendix 13

Profile 26 Soil form : Arcadia Soil series : Arcadia

<u>Depth</u> <u>cm</u>	<u>Horizon</u>	<u>Description</u>
0-15	A1	Moderate medium subangular blocky; dark greyish brown loamy clay; gradual smooth transition.

<u>Depth</u> <u>cm</u>	<u>Horizon</u>	<u>Description</u>
15-75	A2	Very dark greyish brown clay; strong coarse subangular blocky, tending to prismatic; few roots; extremely firm; slight pedocutanic character; clear smooth transition.
75-90+	C	Crumbly yellow-brown calcareous dolerite saprolite.
Remarks :		Suspect Ecca shale drift on dolerite; colour is more greyish than black; no slickensides; no wide cracks.

Appendix 14

Profile 27 Soil form : Rensburg Soil series : Rensburg

<u>Depth</u> <u>cm</u>	<u>Horizon</u>	<u>Description</u>
0-25	A1	Slightly moist; dark grey-brown; loamy clay; strong, medium subangular blocky; friable to firm; gradual, smooth transition.
25-70	A2	Slightly moist; very dark grey brown clay; strong coarse subangular blocky, tending to prismatic; extremely firm; diffuse smooth transition.
70-100	G	Slightly moist; dark grey clay; strong angular blocky to wedge, clear slickensides; few fine CaCO ₃ concretions; diffuse irregular transition.
100-150	C	Moist yellow-brown saprolite; clay skins with appearance of baked mudstone, but may still be doleritic.

Appendix 15

Profile 28 Soil form : Rensburg Soil series : Rensburg

<u>Depth</u> <u>cm</u>	<u>Horizon</u>	<u>Description</u>
0-20	A1p	Slightly moist; dark brown (10YR 5/3) but (10YR 4/4) when dry, clay loam; friable to firm but hard at surface; weak, very coarse, blocky with massive crusting tendency on surface; very few roots; clear smooth wavy transition.
20-55	A2	Slightly moist; very dark greyish brown (10YR 3/2) clay; strong coarse subangular blocky, tending to prismatic; extremely firm; few clear slickensides as base; diffuse smooth transition.
55-95	G1	Moist; greyish brown (10YR 5/2) clay; strong medium angular blocky to wedge; extremely firm and plastic; many intersecting slickensides; no CaCO_3 reaction; diffuse smooth transition.
95-150	G2	Moist; light brownish-grey (2,5Y 6/2) clay; strong medium angular blocky to wedge; abundant closely intersecting slickensides; common fine Fe-Mn concretions, tendency to many on base; lower limit not reached.

Appendix 16

Profile 29 Soil form : Rensburg Soil series : Rensburg

<u>Depth</u> <u>cm</u>	<u>Horizon</u>	<u>Description</u>
---------------------------	----------------	--------------------

0-20	Ap	Very coarse blocky to massive.
------	----	--------------------------------

20-100	A2	
--------	----	--

100-160	G1	
---------	----	--

160-220	G2	
---------	----	--

Remarks : Similar in all characteristics to previous pit, non-calcareous, extremely slickensided, well structured in last 0,5 m. Lower limit not reached.

Appendix 17

Profile 30 Soil form : Rensburg Soil series : Rensburg

<u>Depth</u> <u>cm</u>	<u>Horizon</u>	<u>Description</u>
---------------------------	----------------	--------------------

0-20	Ap	Abrupt transition to B, weak blocky structure.
------	----	--

20-80	B	Roots present on external ped faces, large blocky structure, minor slickensides; clay greater than 55%, dark grey brown, moist, diffuse transition to G.
-------	---	--

80-110	G1	Fine blocky structure, greater degree of slickensides, blue-grey in colour, diffuse transition to G2.
--------	----	---

110-170	G2	Angular slickensides, Mn coatings on to weathered dolerite.
---------	----	---

170+	C	Weathered dolerite saprolite.
------	---	-------------------------------

Remarks : Similar to profile 29.

Appendix 18

Analytical data for ten profiles selected from the T1 sampling transect

Profile No.	Soil form	Soil series	Hori- zon	Depth cm	Particle size distribution			Exchangeable cations					Organic carbon %	pH CaCl ₂
					Clay	Silt	Sand	Ca	Mg	K	Na	Total		
1	Rensburg	Rensburg (upland, mudstone)	A1	20	29	23	48	6,5	4,4	2,84	0,22	13,96	3,79	4,8
			A2	60	48	16	36	15,1	7,1	0,63	0,91	23,74	1,60	6,3
			G1	95	42	23	35	16,0	9,2	0,71	2,13	28,04	0,48	7,2
			G2	140	40	40	20	18,6	10,8	0,53	1,04	30,97	0,48	7,3
			C	150	32	47	21	17,1	10,4	0,56	0,80	28,86	0,52	7,1
2	Rensburg	Rensburg (upland, mudstone)	A1p	20	35	22	43	10,6	5,6	1,05	0,27	17,52	1,92	5,1
			A2	40	38	26	36	17,3	9,2	0,74	0,78	28,02	1,28	6,2
			G1	90	39	25	36	17,9	11,0	0,71	0,85	30,46	0,48	7,3
			G2	120	44	29	28	23,9	14,6	0,71	1,09	40,30	0,68	7,2
			C	130	15	24	61	16,4	8,1	0,38	1,07	25,95	0,88	7,2
8	Arcadia	Gelykvlakte	A1p	20	36	22	42	17,5	7,3	0,90	0,28	25,98	2,31	5,4
			A2	60	37	15	48	25,1	12,7	0,78	0,73	39,31	1,48	6,5
			G	80	40	21	39	30,9	19,0	0,71	0,68	51,29	0,72	7,3
12	Arcadia	Arcadia	A1p	20	46	22	32	24,0	16,0	0,78	0,36	41,14	1,68	5,7
			A2	80	50	20	30	21,0	18,8	0,42	0,78	41,00	1,48	6,6
			C	90	38	19	43	21,5	22,1	0,37	0,80	44,77	0,60	7,5
13	Arcadia	Arcadia	A1p	20	46	18	36	22,1	19,0	0,77	0,26	42,13	1,36	5,8
			A2	55	47	19	34	25,6	13,5	0,47	0,60	50,17	1,20	6,4
			C	70	35	16	49	16,9	22,2	0,35	0,83	40,28	0,80	7,5
17	Arcadia	Arcadia	A1	20	51	19	30	27,5	20,6	0,37	0,73	49,20	1,36	6,0
			A2	65	49	16	35	27,1	23,9	0,31	1,07	52,38	1,92	6,9
25	Rensburg	Rensburg (bottomland)	A1	30	45	22	34	29,0	12,9	0,56	1,26	43,72	1,88	6,3
			A2	70	40	25	35	28,6	15,0	0,44	1,98	46,02	1,00	7,3
			G1	110	49	17	34	33,8	16,6	0,44	2,22	53,06	0,72	7,5
			G2	150	45	16	39	31,9	15,0	0,46	1,91	49,27	0,68	7,5
26	Arcadia	Arcadia	A	15	22	15	63	11,4	5,2	0,63	0,16	17,39	2,59	5,1
			A2	75	33	14	54	19,9	10,6	0,54	0,67	31,71	1,16	6,5
			C	90	23	6	71	24,8	14,6	0,50	0,76	55,46	0,48	6,4
27	Rensburg	Rensburg	A1	25	27	15	59	10,1	5,6	0,62	0,23	16,55	2,19	5,0
			A2	70	41	12	48	18,5	8,7	0,50	0,59	28,29	0,88	6,6
			G	100	44	10	46	22,8	11,9	0,71	0,80	32,59	0,32	7,2
			C	150	11	7	83	27,3	15,8	0,49	0,77	44,36	0,16	6,9
28	Rensburg	Rensburg	A1p	20	43	28	29	7,4	4,0	0,71	0,11	11,61	1,72	4,5
			A2	55	38	15	48	17,8	8,1	0,44	0,47	26,81	0,80	5,9
			G1	95	34	19	47	23,5	11,0	0,64	0,80	35,94	0,52	6,7
			G2	150	40	12	48	21,3	10,2	0,55	0,85	32,90	0,32	6,9

Appendix 19

(a) Exchangeable cations, iron and manganese oxides and/or oxyhydroxides (Na-DCB extract)

	Ca	Mg	K	Na	Fe%	Mn%	Fe/Mn
	Meq/100 g soil						
Onderstepoort A ₁	32,4	15,3	0,42	0,98	1,575	0,21	7,5:1
A ₂	33,7	17,2	0,47	1,02	1,375	0,23	5,8:1
G ₁	27,1	23,4	0,32	0,98	0,275	0,042	6,5:1
G ₂	33,8	22,2	0,35	0,78	0,213	0,031	6,9:1
C	31,4	23,5	0,51	0,87	0,185	0,055	3,36:1
Vereeniging CC ₂	23,8	12,3	0,65	0,76	0,413	0,063	16,5:1
BMD	18,5	11,2	0,45	1,08	0,444	0,125	3,5:1
Vredefort	34,8	19,2	0,45	1,34	0,253	0,023	10,7:1
Kimberley varv _{red}	18,4	10,2	1,04	0,53	3,78	0,009	444:1
Kriel	17,7	10,4	0,80	0,98	0,15	0,009	17:1
Cape Town	10,2	5,8	0,62	0,24	0,67	0,0035	189:1

- continued -

Appendix 19 (continued)

(b) Grain size analysis

Locality	>200um	20-200um	<20um	<2um	<0,2um	% of < 0,2 um in < 2 um
----- % -----						
<hr/>						
Onderstepoort						
A ₁	1,74	17,76	80,5	65,28	48,66	76,1
A ₂	3,86	15,09	81,05	69,6	61,06	87,73
G ₁	1,13	20,62	78,25	75,96	71,1	93,6
G ₂	4,27	34,08	61,65	43,72	29,38	67,21
C	2,80	13,25	83,95	76,28	62,17	81,5
Vereeniging						
CC ₂	22,03	34,52	43,45	35,8	32,25	90,1
BMD	6,22	23,68	70,1	57,08	54,8	96,0
Vredefort	0,4	6,71	92,9	79,08	49,98	63,2
Kimberley						
varv _{red}	0,84	16,21	82,95	52,6	38,46	73,1
10,5-10,75	0,35	22,3	77,35	49,72	28,62	57,5
Kriel	57,02	10,58	32,4	30,64	28,28	92,3
Cape Town	0,47	20,63	78,9	24,36	15,3	63
<hr/>						